Conditional and transgenic mouse models as tools to study the role of TGFß/BMP signaling in skeletal development

Ph.D. Thesis
to accomplish
Doctorate Degree in Science

at the Faculty of Biology
Johannes Gutenberg University
in Mainz

Bettina Keller
born January12th 1974 in Bad Kreuznach

Mainz 2007

Dean of the faculty:

1. Referee:

2. Referee:

Day of oral examination: 20. September 2007

Table of contents

Index of figures

Index of tables

1 Introduction

1.1 Skeletal development

The skeleton plays a major part in the support and movement of the body, and serves as a storage organ for the whole organism. It is derived from different embryonic tissues and can be divided into three basic groups: the craniofacial skeleton, the majority of which results from cells of the neural tube (a minority originating from the mesoderm of the cephalon), the axial skeleton derived from the sclerotom of the somites, and the extremities developed from lateral-plate mesoderm. Although three different embryonic tissues are involved in the development of the skeleton, only three cell types are responsible for its growth and maintenance: 1) chondrocytes that differentiate from mesenchymal cells forming cartilage, 2) osteoblasts deriving from the neural tube and mesoderm building bone and 3) osteoclasts, responsible for bone resorption, originating from precursors of the macrophage-monocyte lineage (Karsenty and Wagner 2002).

The development of the skeleton is a highly complex process including patterning and differentiation during embryonic and fetal development as well as later inclusion of all processes of physiology and is subject to postnatal pathology. Additionally, it is a highly diverse collection of over 220 components of different sizes and shapes distributed throughout the entire body. The first phase involves patterning, where mesenchymal cells migrate to the sites of future skeletogenesis. In the second phase, morphogenesis, mesenchymal cells differentiate, in most cases, into chondrocytes, the cartilage specific cell type (Riddle et al. 1993). The cartilage is then eventually replaced by bone; this process is termed endochondral ossification. In some skeletal elements, the mesenchymal cells differentiate directly into osteoblasts. This alternative process is known as intramembranous ossification (Karsenty 2003).
In the third and subsequent growth phase, the length of the bones and the proportion of the skeleton are determined. The fourth and final phase is characterized by homeostasis in which the bone mass undergoes a continuous resorption and renewal process.

1.1.1 Patterning

The process by which skeletal pattering is established is one of the most intensively studied biological processes, and yet not fully understood. Studies on chick and mouse limbs first provided insight into this process, constituting probably the most critical step in the development of the skeleton (Mariani and Martin 2003; Goldring et al. 2006). Embryological studies have demonstrated that limb development is controlled by three signaling centers. The apical ectodermal ridge (AER) directs proximal-distal (P-D, shoulder-to-digit) patterning and removal of this ridge leads to decreased proliferation of the mesenchyme and to a P-D limb truncation (Saunders 1948; Summerbell 1974). The posterior polarizing mesenchyme (zone of polarizing activity, ZPA) directs anterior-posterior (A-P, thump-to-little-finger) patterning. Mirror-image duplication can be achieved when posterior polarizing mesenchyme is grafted to the anterior side of the limb. The dorsal-ventral axis (D-V, back of hand to palm) is directed by the non-ridge ectoderm. Reversal of the ectoderm (180 degrees relative to the mesenchyme) results in the formation of dorsal structures ventrally to the limb (Niswander 1996).

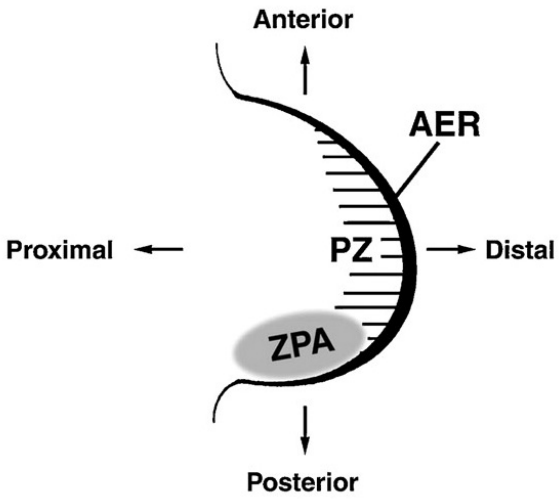

Figure 1: Schematic of the patterning of a limb bud.

Dorsal view of the limb bud, consisting of undifferentiated mesenchymal cells and containing specific regions that initiate the pattering of the bud. The AER (apical ectodermal ridge) contains fast dividing cells and maintains outgrowth of the limb. Cells of the underlying PZ (progress zone) are kept in an undifferentiated state. The ZPA (zone of polarizing activity) is the posterior organization center (Capdevila and Izpisua Belmonte 2001).

The formation of the limb bud begins with the condensation of undifferentiated mesenchymal cells. Two signaling centers are responsible for the correct three-dimensional patterning and outgrowth of the extremities. The apical ectodermal ridge (AER) and the zone of polarizing activity (ZPA) regulate proximal-distal outgrowth and anterior-posterior patterning, respectively (Olsen et al. 2000).

Many genes are involved in mesenchymal condensations of the future skeletal elements that have been described thus far. Fibroblast growth factors (FGF), hedgehog genes, BMPs, genes of the Wnt pathway and homeobox transcription factors coordinate the pattering along the three axes during limb development (Capdevila and Izpisua Belmonte 2001; Tickle 2003; Kmita et al. 2005).

Growth and patterning along the proximo-distal axis is AER dependent, *Fgf4* and *Fgf8* regulating the outgrowth of the limb bud. Removal of the AER leads to a shortening of the limbs, the extent of which is dependent upon when the AER is removed. Genes of the FGF family (*Fgf-2, -4, -8*) can compensate for the loss of AER function leading to normal outgrowth of the limb bud (Crossley et al. 1996; Capdevila and Izpisua Belmonte 2001). Wnt signals (e.g. *Wnt2a* and *Wnt2c*) are required to induce the expression of members of the FGF family and act in positive feedback loops (Niswander 2003). For example, *Fgf-10* induces *Wnt3a*, which increases *Fgf-8* via β-catenin, which then maintains *Fgf-10* expression (Tickle and Munsterberg 2001).

The growth of the limb along the anterior-posterior axis is dependent upon the expression of *Sonic hedgehog* (*Shh*), in a population of mesenchymal cells, on the posterior end of the zone of polarizing activity (ZPA) (Saunders and Gasseling 1968). Shh is a secreted factor, whose signaling is mediated by the receptor Patched (Ptc1), which activates a transmembrane protein, Smoothened (Smo). In the absence of Shh signaling, another transcription factor, Gli3 is proteolytically cleaved to generate a transcriptional repressor. Activation of Shh signaling represses this cleavage, generating transcriptionally active forms (Niswander 2003; Barna et al. 2005). *Shh* is also involved in a feedback loop between the ZPA and AER (Laufer et al. 1994; Niswander et al. 1994). Experiments in chick showed that Shh expression in the ZPA is necessary for the maintenance of the expression of *Fgf9* and *Fgf17* in the AER (Sun et al. 2000), and more recent experiments with knockout mice models have shown, that the expression of Shh in the ZPA is also dependent on the expression of *Fgf8* and *Fgf4* (Boulet et al. 2004). Misexpression of *Shh* in the anterior axis of the limb bud results in a mirror image like duplication of the distal extremities in mouse and chick (Riddle et al. 1993); *Shh* knockout mice also completely lack distal extremities (Chiang et al. 1996). Homeobox (Hox) transcription factors encoded by *HoxA* and *HoxD* gene clusters are also required for the expression of *Fgf8* as well as *Shh*, and therefore both are critical in the early events of limb patterning. In *HoxA* and *HoxD* conditional double knockout mice, the limbs are severely truncated distally, due to an early arrest in developmental patterning, partly attributable to the absence of *Shh* (Kmita et al. 2005).

The dorsal-ventral patterning is dependent, at least in part, on the expression of *Wnt7a*, a secreted glycoprotein that is only expressed in the dorsal ectoderm. Functional inactivation of *Wnt7a* leads to a double-ventral pattern of the limbs in mice (Parr and McMahon 1995). The homoebox protein Engrailed-1 (En1) (expressed in the ventral ectoderm) as well as the transcription factor *Lmx1b* (expressed in the dorsal mesoderm) are important for the correct pattering of the dorsal-ventral axis of the limbs. Mice lacking *Lmx1b,* phenocopy mice lacking *Wnt7a* (Chen et al. 1998), their limbs being distally ventralized, whereas *En-1* knockout mice exhibit a double-dorsal pattern (Loomis et al. 1996; Tickle 2000).

1.1.2 Morphogenesis and Growth

Following the completion of skeletal element patterning, mesenchymal cells differentiate into chondrocytes and osteoblasts. The ossification can occur via two independent processes. During endochondral bone formation (ossification) of the long bones, the mesenchymal cells differentiate into chondrocytes, forming cartilage, which is then gradually replaced by bone. The flat bones of the skull, the mandible and parts of the claviculae are formed by intramembranous ossification, the direct formation of bone without a cartilaginous precursor.

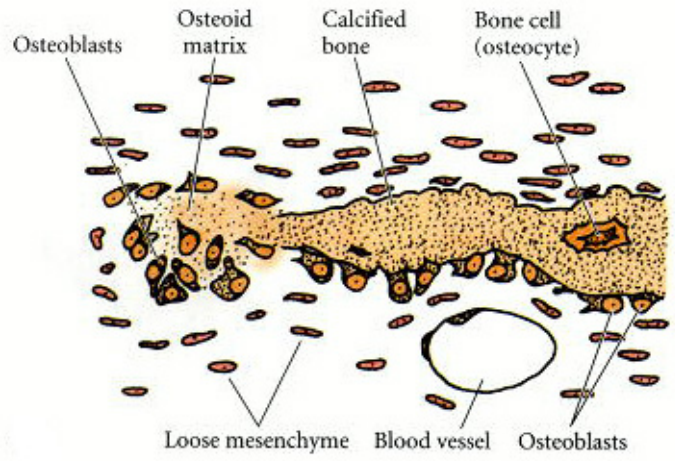

Figure 2: Schematic of intra-membranous ossification.

Mesenchymal cells condense and differentiate into osteoblasts, which produce the osteoid matrix. Osteoblasts, which are trapped within this matrix, differentiate into bone cells (osteocytes). From: Gilbert, Developmental Biology 6. Edition @ NCBI http://www.ncbi.nlm.nih.gov/books/bv.fcgi?call=bv.View..ShowSection&rid=dbio.figgrp.3481

The intramembranous or desmal ossification (figure 2) begins with the condensation of mesenchymal cells that directly differentiate into osteoblasts, followed by the formation of ossification centers, which are invaded by blood vessels. Osteoids, consisting of glycoproteins, collagens and proteoglycans are formed. This protein mixture is able to bind calcium salts, ultimately leading to the calcification of these structures. When the osteoblasts become trapped in the matrix they produce, they terminally differentiate into osteocytes.

More layers of mesenchymal cells, which differentiate into matrix-producing osteoblasts, are added on top of the newly forming bone. The mechanism of intramembranous ossification involves bone morphogenetic proteins (BMPs) and the transcription factor *Runx2/Cbfa1*. *BMP2*, *BMP4* as well as *BMP7* are expressed from the epidermis of the head. These are thought to instruct the neural crest-derived mesenchymal cells to become bone cells directly by activating the expression of *Runx2/Cbfa1* in the mesenchymal cells (Hall 1988).

Endochondral ossification (figure 3) commences with the migration of mesenchymal cells to the site of the future skeletal structures where they then undergo condensation. These cells initially express type I collagen and differentiate during chondrogenesis from resting chondrocytes to proliferating chondrocytes then are seen to express chondrocyte-specific markers such as type II, type IX, type XI collagens, the proteoglycans and aggrecans.

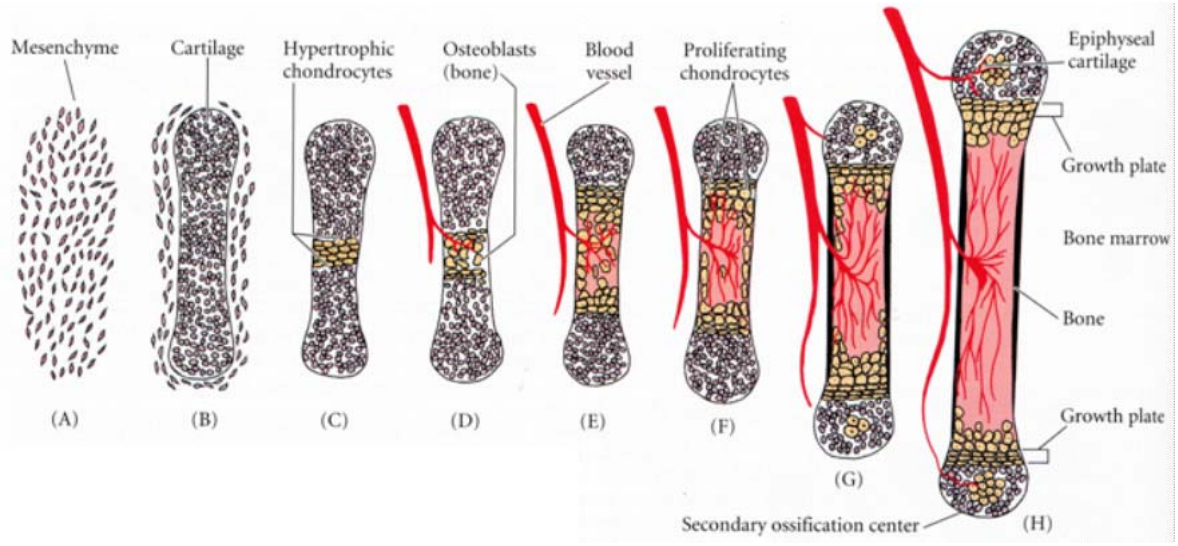

Figure 3: Schematic of endochondral bone formation.

The formation of the bone begins with the migration and condensation of mesenchymal cells, which then differentiate into chondrocytes to form the cartilaginous model of the developing bone. The chondrocytes in the center of the bone undergo hypertrophy and apoptosis. During primary ossification their extracellular matrix mineralizes and blood vessels invade. During the growth phase of the bone resting chondrocytes in the secondary ossification centers undergo a similar process. They differentiate into proliferating chondrocytes and undergo hypertrophy and apoptosis. Finally they are replaced by bone. From: Developmental Biology 5th ed. Gilbert 1997, pg. 354.

Four major signaling cascades are important for morphogenesis and growth of bones. The Ihh/PTHrP negative feedback loop, the FGF pathways, the Wnt pathways and the TGFβ/BMP signaling cascade regulate the survival and control the balance of proliferation and differentiation of chondrocytes within the growth plate.

Ihh/PTHrP feedback loop

PTHrP and PTHrPR promote chondrogenic differentiation via Indian hedgehog (Ihh), which is expressed exclusively in prehypertrophic chondrocytes. Ihh stimulates expression of *PTHrP* in periarticular cells and regulates the onset of hypertrophic differentiation. In turn PTHrP signals back to proliferating chondrocytes by binding its receptor. It prevents their apoptosis as well as their differentiation into prehypertrophic cells. Independently of PTHrP, Ihh can stimulate differentiation of resting chondrocytes and is able to induce the ossification of the perichondrium (figure 4) (Minina et al. 2001; Minina et al. 2002; Kronenberg 2003; Kobayashi et al. 2005).

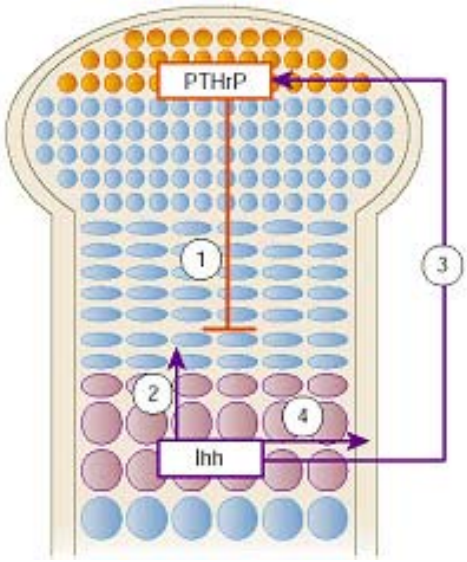

Figure 4: Indian hedgehog (Ihh)/ /parathyroid hormone-related protein (PTHrP) negative feedback loop.

PTHrP is expressed in perichondrial cells and in chondrocytes at the termini of long bones. It acts at receptors on proliferating chondrocytes to maintain them in a proliferating state and thereby to delay the production of Ihh (1). Ihh is expressed in prehypertrophic chondrocytes and acts upon its receptor on chondrocytes to increase the rate of proliferation (2) and to stimulate the expression of PTHrP at the ends of the bones (3). Ihh also stimulates perichondrial cells to differentiate into osteoblasts forming the bone collar (4). (Kronenberg 2003)

FGF pathways

The importance of the FGF signaling pathway in skeletal development was revealed by the discovery that achondroplasia (ACH) is caused by an activating mutation in the FGF receptor gene *Fgfr3* (Ornitz and Marie 2002; Wilkie et al. 2002). FGFs provide potent inhibitory signals; both *Fgfr3* gain-of-function and loss-of-function mouse models have shown that the predominant role of Fgfr3 is to limit chondrocyte proliferation and differentiation (Colvin et al. 1996; Deng et al. 1996; Naski et al. 1998). This effect is mediated in part by direct signaling (Rozenblatt-Rosen et al. 2002) and indirectly by regulating the expression of IHH/PTHrP/BMP signaling (Naski et al. 1998; Li et al. 1999; Chen et al. 2001). The signals are transduced via multiple pathways. The signal transducer and activator of transcription

(STAT), as well as the mitogen-activated protein kinase (MAPK) are components of two of these pathways and they are known to play a role in the signaling cascade affecting chondrocytes (Sahni et al. 1999; Ornitz and Marie 2002; Murakami et al. 2004). STAT1 null mice are protected from chondrodysplasias resulting from overexpression of FGF2, supporting the hypothesis that STAT1 has an important role in the FGF-mediated inhibition of proliferation (Sahni et al. 2001). Besides the role of delaying chondrocyte proliferation and differentiation, FGFs might regulate some aspects of terminal hypertrophic differentiation as well. Microarray experiments performed with RNA from chondrocyte cell lines have shown that FGFs promote the expression of some of the hypertrophic makers (Dailey et al. 2003).

Wnt pathway

Multiple Wnt pathways are involved in chondrogenesis. Expression studies suggest that numerous Wnt proteins signal to mesenchymal condensations and regulate chondrocyte and osteoblast differentiation (Parr et al. 1993; Kato et al. 2002; Guo et al. 2004).

Wnt proteins signal by binding to the Frizzled (Fz)/low density lipoprotein (LDL) receptor-related protein (LRP). These receptors transduce a signal to stabilize β-catenin via several intracellular proteins like Dishevelled (Dsh), glycogen synthase kinase-3β (GSK-3), Axin, and Adenomatous Polyposis Coli (APC). Normally cytoplasmic β-catenin levels are kept low through proteasome-mediated degradation; this process is controlled by a complex containing GSK-3/APC/Axin. Wnt signals inhibit the degradation pathway and β-catenin thereby accumulates in the cytoplasm and nucleus. Nuclear β-catenin interacts with transcription factors such as lymphoid enhancer-binding factor 1/T cell-specific transcription factor (LEF/TCF) to affect downstream gene transcription (Logan and Nusse 2004). Wnt signaling through β-catenin seems to inhibit prechondrogenic cells from acquiring or maintaining a chondrogenic fate and Wnt signals are also required to allow exit of proliferating chondrocytes from the cell cycle in order to promote hypertrophy (Pogue and Lyons 2006).

The Bone morphogenetic proteins (BMPs) also influence the proliferation and maturation of chondrocytes during endochondral ossification. The multitude of functions that they perform during skeletal development will be described in forthcoming chapters.

In long bones of mammals, endochondral ossification spreads outward, bi-directionally from the center of the bone. The cartilaginous areas at the ends of the bone are referred to as

epiphyseal growth plates. They are essential for the longitudinal growth of the bone. The resting chondrocytes differentiate to hypertrophic chondrocytes, undergo apoptosis and are replaced by osteoblasts, to form bone in the same temporal and spatial fashion as previously described (see figure 3). Following puberty, the growth plate closes and is replaced by spongy bone (Kronenberg 2003). Many growth and transcription factors are involved in the ossification process and the growth of long bones (figure 5) (Goldring et al. 2006).

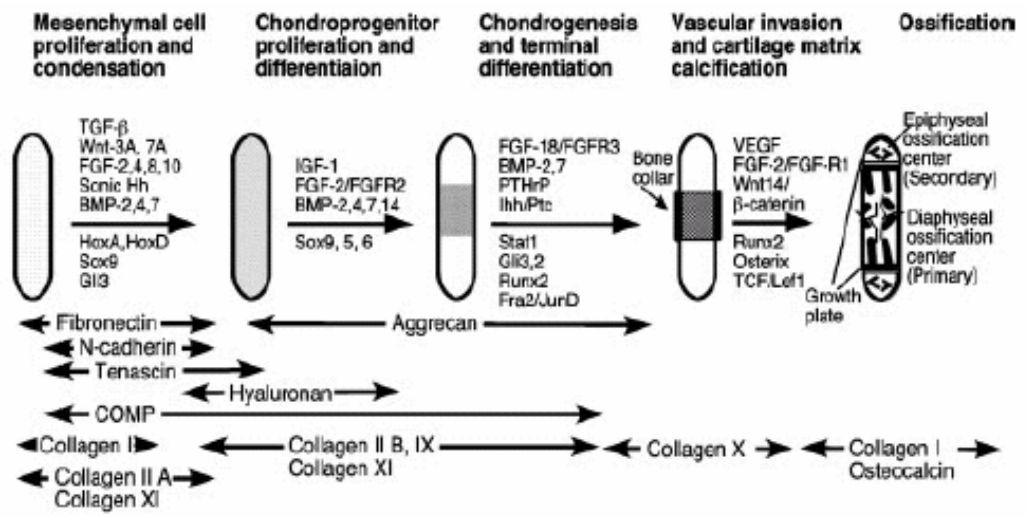

Figure 5: Overview of the key regulatory factors involved in the endochondral ossification.

The upper panel schematically shows the steps of skeletal development. The temporal expression of the growth and differentiation factors, as well as the transcription factors are shown above and below the arrows, respectively. The lower panel identifies the extracellular matrix proteins (Goldring et al. 2006).

Osteoblasts are specialized stromal cells, and are essential for the formation, deposition and mineralization of bone tissue. Two transcription factors are known to be important for the differentiation of mesenchymal cells into osteoblasts, Runx2 (Cbfa1) and Osterix. Homozygous *Runx2* deficient mice (Runx2-/-) develop the cartilaginous skeleton, but they are unable to differentiate mesenchymal cells to osteoblasts (Komori et al. 1997; Otto et al. 1997). *Osterix* knockout mice are also unable to form bone (Nakashima et al. 2002). The expression of *Osterix* is induced by BMP-2 and although it has been proposed that *Osterix* acts downstream of *Runx2*, the induction of *Osterix* is *Runx2* independent (Nakashima et al. 2002; Lee et al. 2003a; Lee et al. 2003b).

Osteoclasts are large, terminally differentiated cells that have large multiple nuclei per cell. They are normally located in the tissue layer lining the medulla of the bone (Suda et al. 1996).

Osteoclasts derive from the macrophage/monocyte lineage (hematopoietic cell line) (Walker 1975a; Walker 1975b). Two factors are important for the differentiation of osteoclasts. The Macrophage colony-stimulating factor (M-CSF) is essential for the maturation of macrophages. It binds to its receptor c-Fms, which is presented on the surface of early osteoclast precursors and is imperative for the survival and proliferation of these cells. The second important factor is the receptor activator of NF-κB ligand (RANKL), which stimulates the pool of M-CSF-expanded precursors to commit to the osteoclast cell line (Rodan and Martin 2000).

1.1.3 Homeostasis

The long bones undergo constant remodeling during their lifetime. Two processes are very important for healthy bone: the resorption of bone through osteoclastic activity and new bone formation by osteoblasts both ensuring constant bone mass through life. Many different factors are involved in the maintenance of the bone. Hormones like estrogens and parathyroid hormone, Vitamin D, calcitonin, the interleukins IL4 and IL6 and tumor necrosis factor (TNF) are responsible for maintaining bone mass. Disruption of the balance of resorption and renewal of the bone can result in osteoporosis (loss of bone mass), which is most often due to an increase in osteoclast activity. Defects in osteoclast differentiation on the other hand lead to osteopetrosis (increased bone mass). An increased activity of osteoblasts can cause osteosclerosis, an increase of bone mass due to an increased production of bone matrix (Phan et al. 2004).

1.2 TGF superfamily and TGFβ/BMP signaling cascades, interactions between the pathways

1.2.1 TGFβ superfamily

TGFβ is a very large family of secreted polypeptides vitally important at almost every stage and in every tissue or cell type during embryogenesis, as well as in the maintenance of homeostasis in adults. TGF-β1-3, activins, inhibins and nodal, as well as the bone morphogenetic proteins (BMPs) and growth differentiation factors (GDFs) belong to this group (table 1) and these molecules are involved in the regulation of cellular processes like proliferation, differentiation, morphogenesis and apoptosis.

The Bone morphogenetic protein (BMPs) family of secreted growth factors is a subgroup of the transforming growth factor β (TGFβ) superfamily. This family was first described as molecules that are able to induce ectopic bone formation (Urist 1965). To date, 20 members of this family have been identified. Most of these proteins are involved in bone, cartilage and tendon/ligament development. The BMPs consist of a signal peptide, a pro-domain and a mature peptide. After cleavage of the signal peptide the protein undergoes glycosylation and dimeriziation. Only after secretion of the active dimeric BMP, is the pro-domain cleaved (ten Dijke 2006).

Table 1: Partial list of members of the TGFβ superfamily present in mammals and Drosophila. BMP, Bone morphogenetic proteins; GDF, Growth differentiation factor; MIS, Muellerin inhibiting substance. Adapted from (Moses and Serra 1996).

Transforming growth factor β (TGFβ) superfamily

TGFβ	BMP	MIS/Inhibins/Activins
TGFβ1	BMP2	MIS
TGFβ2	BMP3	n-inhibin
TGFβ3	BMP4	Inhibin-βA
	BMP5	Inhibin-βB
	BMP6	Inhibin-βC
	BMP7	GDF-9
	BMP8/OP-2	Activin-βA
	GDF-1	Activin-βB
	GDF-3	Activin-βC
	Nodal	Activin-βD
	Dpp	

Upon activation and dimerization, TGFβ/BMPs bind to their respective, specific receptors. The signals can be mediated through canonical and non-Smad pathways. The importance of these two pathways in the regulation of chondrogenesis has been established, but the roles of the signals in regulating specific aspects of chondrogenesis remain unclear. The canonical pathway via Smad proteins is described in detail in chapter 1.4. The most extensively studied non-canonical pathway active in chondrocytes is the p38 pathway. BMP is able to affect chondrocytes by activation of p38 MAPK through the TGFβ-activated kinase 1 (TAK1) (Nakamura et al. 1999; Hatakeyama et al. 2003; Seto et al. 2004; Qiao et al. 2005). The overexpression of MKK6, which activates p38, results in dwarfism, characterized by delayed endochondral ossification, reduced chondrocyte proliferation, as well as inhibition of hypertrophy (Zhang et al. 2006). *In vitro* data from ATDC5 cell experiments, showed that BMP treatment led, to an increased phosphorylation of p38, while the inhibition of p38 in

turn suppresses the production of type II collagen and chondrogenic differentiation (Nakamura et al. 1999; Zuzarte-Luis et al. 2004). Additionally, it seems that BMP influences terminal differentiation; p38 together with Smads acts as a coactivator of the *Col10a1* promoter (Reilly et al. 2005).

1.2.2 Interactions between the signaling pathways

The control of proliferation and differentiation of chondrocytes is subjected to interactions between the previously described signaling pathways. These interactions promote or inhibit proliferation, hypertrophic differentiation and apoptosis (Kronenberg 2003; Yoon and Lyons 2004; Goldring et al. 2006). BMPs interact with IHH/PTHrP pathway. They promote the expression of Ihh most probably directly, since the Ihh promoter contains multiple BMP binding sites (Seki and Hata 2004). IHH in turn is able to maintain BMP levels, suggesting the existence of a positive feedback loop between those two signaling pathways (Pathi et al. 1999; Minina et al. 2001). Additionally there is a synergy between the BMP and IHH signaling pathways. Blocking of Ihh in a limb bud cell line, leads to an inhibition of BMP-induced expression of *Runx2* and *osteocalcin*, while Ihh alone is unable to induce the expression of these genes (Long et al. 2004).

In contrast to the synergy of Ihh and BMP pathways in the chondrogenic proliferation and differentiation, the FGF and BMP pathways seem to have antagonistic effects in the growth plate. As previously discussed, FGF signaling provides important inhibitory effects on proliferation and terminal differentiation (Kronenberg 2003). The antagonistic functions of these two pathways have been confirmed in cell culture studies. While BMP treatment is able to rescue the phenotype of FGF-treated growth plates, FGF in turn can neutralize the effects of BMPs (Minina et al. 2002). BMPs are able to induce expression of *Ihh*, whereas FGF can inhibit its induction in the growth plate (Naski et al. 1998; Minina et al. 2002). The mechanism by which the FGF pathway antagonizes the BMP-induced *Ihh* expression is still unclear. One explanation could be that the linker region of the Smad proteins contains multiple sites for phosphorylation by ERK1/2 MAP kinases (compare chapter 1.4), which are components of the FGF-induced growth arrest in cartilage (Kretzschmar et al. 1997; Aikawa et al. 2001; Murakami et al. 2004). Phosphorylation of these sites inactivates Smad activity and thus inhibits the BMP-induced *Ihh* expression. Additionally the inhibition of ERK1/2 increases the BMP-stimulated activation of the *Col10a1* promoter (Reilly et al. 2005; Pogue and Lyons 2006).

1.3 The role of TGFβ and BMPs in skeletal development

The importance of TGFβ during skeletal development has been demonstrated by *in vitro* studies, in transgenic mice and human diseases, e.g. Marfan syndrome, Camurati-Engelmann disease and osteoarthritis (Kinoshita et al. 2000; Neptune et al. 2003; Serra and Chang 2003). These studies together with the expression pattern of proteins of this signaling pathway support the assumption that TGFβ proteins play an important role in the development of cartilage and bone. TGFβ 1, 2 and 3 are expressed in the mouse perichondrium and periosteum from 13.5 dpc until postnatally (Sandberg et al. 1988; Gatherer et al. 1990; Pelton et al. 1990; Millan et al. 1991; Pelton et al. 1991). Also TGF-β receptors are expressed in perichondrium and chondrocytes (Serra et al. 1999).

TGFβ proteins are synthesized as inactive precursor proteins, referred to as latency associated peptide or LAP, including a signal sequence and a large N-terminal pro-domain (Pircher et al. 1986; Wakefield et al. 1988). The peptides are activated by cleavage of the pro-domain with a furin peptidase (Dubois et al. 1995); this process is in all probability a major regulatory step of TGFβ signaling *in vivo*. This pathway is additionally regulated by association of a family of latent TGFβ binding proteins (LTBP) to the latent TGF-β peptide, which results in a large latency complex (Annes et al. 2003).

E-selectin ligand 1 (Esl-1) is as a putative inhibitor of TGFβ signaling. It is a highly conserved type I transmembrane sialoglycoprotein, which was originally identified as a cell adhesion ligand of E-selectin in myeolid cells, and its role in the regulation of leukocyte rolling was predicted (Steegmaier et al. 1995); but the loss of Esl-1 caused distinctive skeletal and growth defects. While Esl-1 heterozygous null mice appear normal, the homozygous littermates are 30 to 50% smaller from E15.5 until adulthood. Skeletal preparations have shown a generalized shortening and thinning of the long bones, ribs and spine. Histological analyses have revealed a shortening of the growth plate in both the proliferating and hypertrophic zone (Yang et al., unpublished data). The fact that Esl-1 could be experimentally co-purified with TGFβ1 suggests a role of Esl-1 in the regulation of TGFβ signaling during skeletal development (Olofsson et al. 1997).

Overlapping expression of multiple BMP ligands is characteristic of every region in the growth plate (Pogue and Lyons 2006). BMP7 is highly expressed in the proliferating chondrocytes, particularly in regions close to the perichondrium (Lyons et al. 1995; Minina et al. 2005). BMP2 and BMP6 are expressed in hypertrophic chondrocytes (Lyons et al. 1990;

Minina et al. 2005). Multiple BMPs are expressed at high levels in the perichondrium (Lyons et al. 1990; Chang et al. 1994; Macias et al. 1997; Minina et al. 2005).
Three type I and three type II receptors have been described to date: BMP receptors type IA (BMPR-IA, ALK-3), type IB (BMPR-IB, ALK-6) and activin type I receptor (ActR-I, ALK-2) as well as BMP receptor type II (BMPR-II), ActR-II and ActR-IIB (ten Dijke et al. 1994; Rosenzweig et al. 1995). A group of different BMP ligands are able to bind to different type I receptors dependent on the cell type. BMPR-II for example activates BMP2, BMP4, BMP6, BMP7 as well as growth differentiation factor-5 (GDF-5) and GDF-9 (Wan and Cao 2005). The diversity of the BMP signaling pathway is also characterized by the expression pattern of the different receptors. BMPR-1A is expressed in several tissues, whereas BMPR-1B is the only receptor expressed in all types of cartilage (Ikeda et al. 1996; Ashique et al. 2002).

TGFβ/BMP pathways in the growth plate are under tight regulation of different extra- and intra-cellular modulators. Secreted extra-cellular antagonists like noggin, chordin, follistatin and gremlin form complexes with BMPs to inhibit the signal transduction (Balemans and Van Hul 2002). The modulation of the intracellular signal is subject to multiple independent influences, e.g. the pseudoreceptor BAMBI, and can occur through proteasomal degradation mediated by Smad ubiquitination regulatory factors (Smurf, described in detail in chapter 1.4). Smads are also able to interact with filamins (Sasaki et al. 2001; Tang et al. 2003). Filamins are actin cross-linking proteins important for the regulation of the cytoskeleton; mutations in *filamin*-b are responsible for various skeletal phenotypes (Krakow et al. 2004; Bicknell et al. 2005; Pogue and Lyons 2006).

1.4 The *Smad* gene family as mediators of the TGFβ signaling pathway

1.4.1 Structure of SMAD proteins

SMAD proteins are mediators of the TGFβ signaling pathway. They were first discovered through genetic studies in *Caenorhabditis elegans* and *Drosophila.* The name originates from the fusion of *Drosophila mother against dpp* (*Mad*) and C. elegans *Sma* (Derynck et al. 1996; Derynck and Zhang 1996). The SMADs can be divided into three groups: the "receptor related" (R-) SMADs, the "common partner" (Co-) SMADs (SMAD4) and the "inhibitory" (I-) SMADs.

Their structure is highly conserved in all species and varies only slightly relevant to the function of the protein. SMAD proteins are approximately 500 amino acids in length and consist of two globular domains coupled by a linker. The MH1 (Mad-Homology 1) domain at the N-terminal end of the protein is conserved in all R-Smads and in Smad4. This domain has DNA-binding properties. The interaction of the protein and DNA is established by a highly conserved β-hairpin structure, which inserts into the major groove of the DNA and builds hydrogen bonds with nucleotides (base triplets) of the SBE (Smad binding element) (Shi et al. 1998). The carboxy-terminal MH2 domain contains structures for protein-protein interactions. A set of hydrophobic patches in the R-SMADs ("hydrophobic corridor", see figure 6) mediates interaction with cytoplasmatic retention proteins, with components of the nuclear pore complex and with DNA binding cofactors.

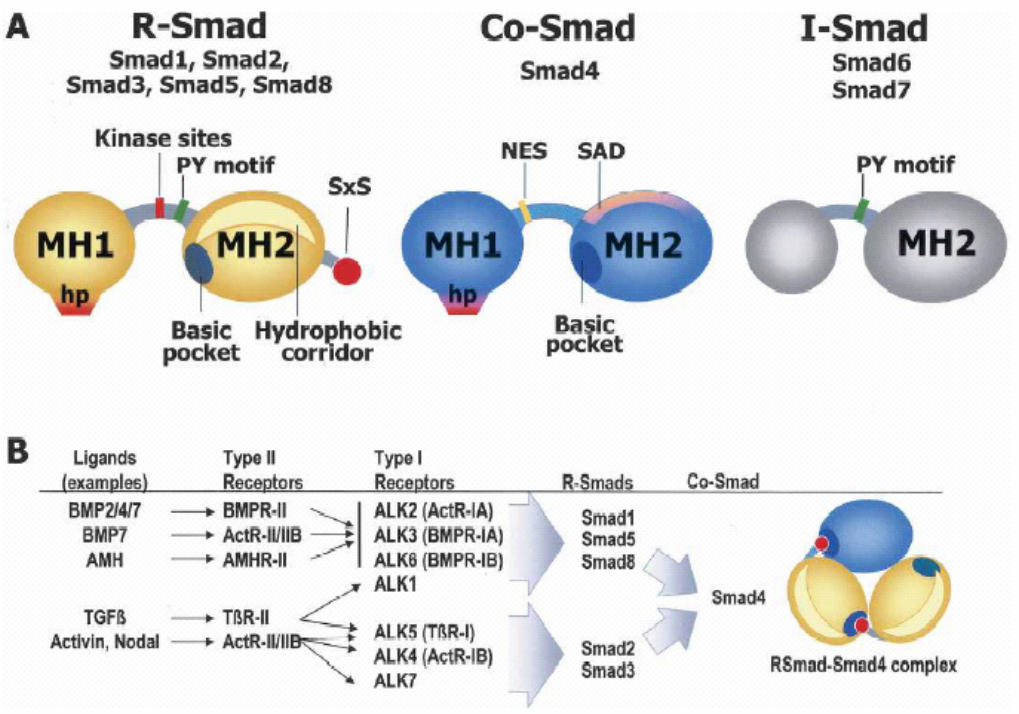

Figure 6: Structural elements of the SMAD proteins.

(A) SMAD proteins have two domains, which are connected by a variable linker. The MH1 domain has a β-hairpin structure, responsible for the DNA binding properties of the protein. The MH2 domain contains various structures, which allow binding to other proteins.
(B) SMADs and their receptors. SMAD 1, 5 and 8 recognize and bind specifically to BMP-, activin- and Anti-Muellerian receptors, whereas SMAD2 and SMAD3 mediate the signals from the TGFβ- and activin receptors. AMH, Anti-Muellerian Hormone; Co-Smad, Common Partner Smad; hp, hairpin; I-Smad, Inhibitory Smad; MH, Mad Homology; NES, nuclear export signal; R-Smad, Receptor-related Smad; SAD, Smad4 activation domain; (Massague et al. 2005).

A region in the Co-SMAD (SMAD4) that is the overlapping part of the linker and the MH2 domain is referred to as the SMAD4 activation domain (SAD). It mediates interactions with transcriptional activators as well as repressors (Massague et al. 2005).
The linker region of the R-Smads also contains multiple specific phosphorylation sites for different kinases, like ERK, MAP kinases and the G1 cyclin dependent kinases (CDKs). Phosphorylation attenuates the activity of the R-Smads (Kretzschmar et al. 1997; Kretzschmar et al. 1999; Matsuura et al. 2004).
The PY-motif in R- and I-Smads is recognized by the WW domain of Smurf ubiquitin ligases. Smad1 and Smad2 were the first Smads reported to be ubiquitinated, resulting in targeting to the 26S proteasome for degradation (Lo and Massague 1999; Zhu et al. 1999).
The linker of Smad4 contains a leucine-rich nuclear export signal (NES), that plays an important role in the subcellular localization of Smad4 and thus in the maintenance of optimal responsiveness to TGFβ/BMP signaling (Watanabe et al. 2000).

1.4.2 The SMAD signal transduction

SMAD proteins accumulate in the nucleus in response to TGFβ or BMP signaling (Hoodless et al. 1996; Liu et al. 1996). During the constant process of nucleocytoplasmatic shuttling, their accumulation, in the nucleus, results from receptor-mediated phosphorylation. This phosphorylation decreases the affinity of the R-Smads to their cytoplasmatic anchors and increases their affinity for nuclear factors (Massague et al. 2005). Dephosphorylation of R-Smads leads to their return to the cytoplasm, where they can be again phosphorylated and translocated into the nucleus (Inman and Hill 2002).
Initiation of the phosphorylation of Smad proteins requires that the ligand bind to its specific type II receptor (with serine/threonine kinase activity), which is constitutively activated, by means of phosphorylation (figure 7).
This complex is now able to recruit the type I receptor, which is then phosphorylated in a serine/threonine rich region, called the GS region, located N-terminally to the canonical kinase domain of the type I receptor (Shi and Massague 2003; Massague et al. 2005). The GS region acts as an auto-inhibitory element. In the absence of the ligand, FKBP12 or FKBP12.6 can bind instead and occlude the phosphorylation site (Chen et al. 1997b; Datta et al. 1998). Another regulatory mechanism is provided by the pseudoreceptor BAMBI, which interacts with the receptor complex and inhibits the phosphorylation of the type I receptor through the type II receptor (Onichtchouk et al. 1999). The R-Smad protein now binds to the activated receptor complex to become itself phosphorylated. The binding affinity of Smads to their

receptors is weak and demands support from other proteins within the cytoplasm. The Smad anchor for receptor activation (SARA) is a FYVE domain containing protein, which consists of two zinc finger motifs; it may bind to phophoinositol-3-phosphate and thereby tether SARA to endosomal membranes. SARA binds to both, R-Smad and the receptor, by its Smad binding domain and the c-terminal portion of SARA, respectively. After phosphorylation the affinity of Smad to the receptor, as well as the affinity of SARA to the Smad protein, decreases resulting in the dissociation of the protein complex. The presentation of the Smad protein to the receptor by SARA is crucial, since overexpression of mutant SARA, lacking the FYVE domain leads to a decreased TGFβ signaling (Tsukazaki et al. 1998).

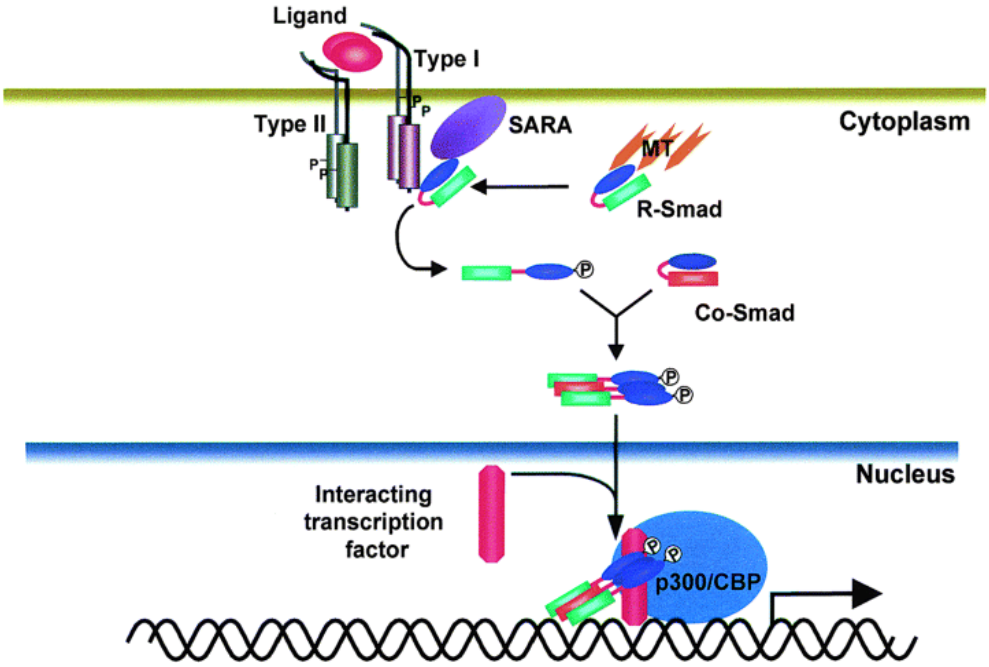

Figure 7: Schematic of the Smad-mediated signal transduction.

The binding of the ligand to the type II serine/threonine receptor recruits the type I receptor, which is phosphorylated at the GS domain in the cytoplasmatic region of the receptor. This phosphorylation leads to binding and phosphorylation of a R-Smad protein, which undergoes a conformational change and then able to bind to the Co-Smad, Smad4. This complex is able to translocate into the nucleus and to activate or repress the expression of the target genes. Co-Smad, Common partner-Smad; MT, Microtubuli; R-Smad, Receptor-related Smad; SARA, Smad anchor for receptor activation (Itoh et al. 2000)

Microtubules have been found to be subcellular regulators of Smad signaling. Smad 2, Smad3 and Smad4 are shown to co-localize and interact with β-tubulin. Following phosphorylation, the Smad protein dissociates from β-tubulin. Treatment with microtubule disrupting agents prevents non-phosphorylated Smad2 from associating with β-tubulin and

promotes the phosphorylation of Smad2 (Dong et al. 2000; Wrana 2000). To date, little is known about the subcellular regulatory mechanisms for Smad1, Smad5 and Smad8, which mediate signals from the BMP pathway. Regarding the similarities of BMP and TGFβ pathway, the existence of SARA-like proteins is highly likely (Massague et al. 2005).

The specificity of the interaction between the receptors and their Smad protein is determined by a region termed the L45 loop in the kinase region of the receptor and a complementary region on the MH2 domain of the Smad protein, the L3 loop. ALK5 (TβR-I) and the nodal/activin type I receptors ALK2 and ALK7 recognize and bind Smad2 and 3 while Smad1, 5 and 8 are bound specifically by ALK 1, ALK3 and ALK6 (Itoh et al. 2000; Massague et al. 2005). The receptor complex mediated R-Smad phosphorylation affects both serine residues of the extreme C-terminal SXS-region of the protein and leads to a conformational change, enabling it to bind the basic pocket in the MH2 domain of the common partner Smad4 (Wu et al. 2001; Chacko et al. 2004). This heterocomplex (R-Smad-Smad4 oligomer) is now able to translocate into the nucleus and either activate or repress the expression of the target genes by interacting with other transcription factors.

The inhibitory Smads (I-Smads), Smad6 and Smad7, can function to block the signaling pathway. Smad7 inhibits TGFβ/activin as well as BMP signaling (Hayashi et al. 1997; Nakao et al. 1997), whereas Smad6 interferes with signals mediated by BMP receptors (Imamura et al. 1997; Hata et al. 1998). Smad7 binds to activated TGFβ and BMP receptors thus preventing binding and phosphorylation of the R-Smads (Hayashi et al. 1997; Nakao et al. 1997). Probably its more important role is to form a complex with Smurf ubiquitin ligases in the nucleus, leading to export to the cytoplasm, binding and ubiquitination of activated TGFβ receptor complexes and consequently the downregulation of signaling. BMP receptors are subject to the same regulatory mechanism; Smurf1 in conjunction with Smad6 and Smad7 can lead to the degradation of activated BMP complexes (Kavsak et al. 2000; Murakami et al. 2003). Smad6 can also compete with R-Smads for heteromeric complex formation with activated Smad1 (Hata et al. 1998). Smad 6 displays a potential role as transcriptional corepressor by binding to the homeodomain transcription factor Hoxc-8 (Bai et al. 2000), and can interfere together with TGFβ activated kinase (TAK) 1 toward BMP-induced p38 activation (Itoh et al. 2000; Kimura et al. 2000). Thus Smad6 and Smad7 are able to interfere with TGFβ/BMP signaling in many different ways (Itoh et al. 2000; Massague et al. 2005).

The R- SMAD/ SMAD4 complex translocates into the nucleus and is able to bind (together with different transcriptional coactivators or repressors) to the DNA of target genes, affecting their transcription. Many different binding partners for the Smads are thus far known and

only a few well-studied proteins will be described here as further examples. The histone acetyltransferases p300 and CBP are coactivators for TGFβ and BMP signaling. They have been shown to interact with Smad1 (Pearson et al. 1999) as well as with SMAD3 and SMAD2 in a complex with SMAD4 (Janknecht et al. 1998) and enhance transcriptional activity by facilitating the interaction of Smads with the basal transcription machinery and by loosening the chromatin structure with their histone acetyltransferase activity (Massague and Wotton 2000; Massague et al. 2005). Transcriptional corepressors for Smads include the Smad interacting protein (SIP) 1, a zinc finger containing protein (Verschueren et al. 1999), the nuclear proto-oncogenes Ski and SnoN as well as TGIF, which contains a homeodomain. TGIF interacts specifically with Smad2 and Smad3 and recruits other transcriptional repressors, such as CtBP and mSin3/HDAC, preventing the interaction of Smads with coactivators thus reducing the activation of target genes (Wotton et al. 1999; Hyman et al. 2003). Like TGIF, Ski and SnoN are able to recruit corepressors to Smad3, but they can also compete with the coactivator p300 for binding to Smad2 and compete with Smad2 for binding to Smad4 (Luo et al. 1999; Stroschein et al. 1999; Wu et al. 2002).

Smads can bind to many different transcription factors, thereby providing specificity for target genes. One of the first identified transcription factors was the *Xenopus* forkhead activin signal transducer (FAST)-1. It is able to bind to the activin response element (ARE) in the *Mix.2* promoter, but it requires Smad2 for binding and activation of Mix.2 gene transcription (Chen et al. 1996; Chen et al. 1997a). Many other transcription factors have been found to be associated to Smads and thus regulate the TGFβ and BMP signaling pathway by affecting the transcription of their target genes in a positive or negative manner (Massague et al. 2005; Massague and Gomis 2006)

1.5 TGFβ/BMP in the growth plate – in vivo and in-vitro data in skeletogenesis

BMPs play an important role in the earliest stages of chondrogenesis, condensation and determination. *In vitro* experiments on mesenchymal cell lines have shown that under the influence of BMPs these cells differentiate into chondrocytes in high-density cultures (Yoon and Lyons 2004). BMPs appear to promote cell-cell interactions, since they act through the up-regulation of N-Cadherin (N-Cad), and N-Cad inhibitors are able to neutralize BMP mediated effects (Haas and Tuan 1999). Experiments on chick limbs showed that overexpression of noggin, an inhibitor of the BMP signaling pathway (which binds directly to

BMP thus preventing the binding of the ligand to its receptor), blocks condensation, whereas overexpression of constitutively active BMP receptors results in an expansion of cartilaginous tissue (Capdevila and Johnson 1998; Pizette and Niswander 2000; Yoon and Lyons 2004).

BMPs also induce *Sox* gene expression via BMPR-1A and BMPR-1B, both of which are functionally redundant and active during condensation (Yoon et al. 2005). Sox proteins are Sry-related high-mobility group (HMG) box transcription factors. *Sox9* is the earliest known marker for chondrocytes and loss of *Sox9* leads to the loss of most of the skeletal elements, due to an inability to form chondrogenic condensations (Bi et al. 1999). *Sox9* as well as *L-Sox5* and *Sox6* (Smits et al. 2001) are expressed continuously during all stages of chondrogenesis and are required for maintaining the chondrocyte phenotype.

In addition to BMP function in early stages of skeletal development, they also play an important role in the growth plate. *Bmp2*, *-4* and *-5* are expressed in the perichondrium, *Bmp7* is expressed in the perichondrium as well as in proliferating and *Bmp6* is expressed in prehypertrophic and hypertrophic chondrocytes (Lyons et al. 1995; Pathi et al. 1999; Minina et al. 2001). The type I receptors have distinct and overlapping expression in the growth plate; *Bmpr-1a* is expressed only in prehypertrophic and hypertrophic chondrocytes, while *Bmpr-1b* is present throughout the whole growth plate. The activin receptor *ActR-I*, which can signal through both, TGFβ and activin, can be found in resting and proliferating chondrocytes (Zou et al. 1997; Zhang et al. 2003; Yoon and Lyons 2004).

BMPs influence proliferation and differentiation in the growth plate. They promote proliferation, which was observed in *noggin* null mice. Noggin is a BMP antagonist and the loss of function of *noggin* leads to an overexpression of BMPs and to an overgrowth of skeletal elements in these mice (Brunet et al. 1998). On the other hand, misexpression of noggin in chick limbs leads to an extreme reduction in the size of the skeletal elements (Pathi et al. 1999). BMPs also promote the differentiation of proliferating chondrocytes to hypertrophic chondrocytes. Overactivity of BMP signaling through expression of constitutively active *Bmpr-1a* in proliferating chondrocytes (under the control of type II collagen promoter) accelerates the maturation toward hypertrophic differentiation (Kobayashi et al. 2005).

Bmp2 is a potent inducer of osteogenesis. BMP2 treated myoblastic C2C12 cells start expressing osteoblastic markers such as alkaline phosphatase and osteocalcin, indicating that BMP2 is able to direct differentiation of non-osseous cells into an osteoblastic phenotype. (Katagiri et al. 1994).

BMPs are also involved in the regulation of osteoclasts. Overexpression of BMP4 in bone leads to severe osteopenia, which is due to an increased osteoclast number, and overexpression of noggin in bone leads to a decreased bone formation rate and a decreased number of osteoblasts. Cell culture experiments with noggin-transgenic calvaria show a decreased osteoclast formation, which can be rescued by adding recombinant BMP2. Osteoclast precursors are probably stimulated by BMPs. Recently, immunoblot analyses showed an increased phosphorylation of the BMP mediators Smad1, Smad5 and Smad8 after treatment of these cells with BMP2 (Okamoto et al. 2006).

1.6 Conditional mouse model with Cre-*loxP* system as a tool to analyze skeletogenesis and the growth plate

The role of Smad1 and Smad5 in the development of the skeleton will be addressed in this thesis. Loss of function of either of these genes (in conventional mouse models) leads to early embryonic lethality; each die before the onset of skeletal development. *Smad1* null mice (*Smad1*-/-) die around 10.5 days post coitum (dpc), due to defects in morphogenesis and proliferation of extraembryonic tissues. They display an overgrowth of the posterior visceral endoderm, the extraembryonic mesoderm and the chorion, a dramatic reduction in size and pattern of the allantois, are not able to form an umbilical connection, and have a marked reduction in number of primordial germ cells at 8.5 dpc (Tremblay et al. 2001). Homozygous *Smad5* knockout mice die between 9.5 and 11.5 dpc due to variable embryonic and extraembryonic defects. They exhibit defects in amnion, gut and heart, as well as craniofacial and neural tube abnormalities. The embryos also fail to undergo proper turning. Extraembryonic defects in mutant animals include disorganized vasculature of the yolk sac, impaired development of the allantois and the chorion and a mislocation of the allantois tissue, leading to ectopic vasculogenesis and hematopoiesis. Heterozygous animals appear viable and are fertile (Chang et al. 1999).

To study the role of Smad1 and Smad5 in skeletal development, conditional mouse models are useful and necessary. Collagen type II and type X are markers for different developmental stages during chondrogenesis. The gene for collagen type II (proαI(II)) becomes activated during embryonic development with the onset of chondrocyte differentiation. Expression can also be detected in non-cartilaginous tissues e.g. notochord, heart, epidermis, as well as in some parts of the brain (Cheah et al. 1991). Extensive promoter studies with transgenic mouse lines expressing *β-galactosidase* (under the control of

different promoter constructs) revealed *cis*-acting elements that are responsible for the specific and temporally correct expression of collagen type II in chondrocytes (Horton et al. 1987; Zhou et al. 1995; Zhou et al. 1998).

Transgenic mice that express *Cre recombinase* (especially in the developing limb) were utilized in this thesis to disrupt *Smad1* expression in proliferating chondrocytes. In these transgenic mice the *Cre recombinase* is expressed under the control of a *Col2a1* promoter fragment (6kb in length). (Ovchinnikov et al. 2000). *Smad1* and *Smad5* are both expressed in the growth plate, and in similar fashion. Immunostaining of rat limbs, revealed a co-expression of both mediators in proliferating chondrocytes near the zone of maturing cartilage (Sakou et al. 1999). This expression pattern suggests an important role of both proteins during chondrocyte hypertrophy. Additional studies infer that the collagen type X promoter is regulated by the BMP mediated Smad activation by interacting with Runx2/Cbfa1 (Leboy et al. 2001).

Col10a1 is expressed exclusively in and the only known marker of hypertrophic chondrocytes. Collagen type X is a member of the short-chain collagens. It consists of a homotrimer of α1 (X) chains, with a 38 amino acids long non-helical amino terminus, called NC2, a triple helix of 463 amino acids, and a C-terminal highly conserved non-collagenous domain (NC1) of 161 amino acids (Shen 2005). Mutations in *COL10a1* in humans have been associated with metaphyseal chondrodysplasia type Schmid – MCDS (Warman et al. 1993). *Col1a1* null mice partially resemble the phenotype of MCDS, displaying a mild skeletal phenotype, aberrant mineralization, and hematopoiesis as well as disturbances of spongy bone formation (Kwan et al. 1997). *Col10a1* is also up-regulated in osteoarthritis (von der Mark et al. 1992) and is transiently expressed in bone callus during fracture healing (Grant et al. 1987; Topping et al. 1994).

Extensive promoter studies using comparative sequence analyses, as well as transgenic mouse model studies (expressing *β-galactosidase* under the control of different fragments of the *Col10a1* promoter or using *in-vitro* transfection/reporter studies) have been performed to identify the specific regions in hypertrophic chondrocytes responsible for the expression of type X collagen (Beier et al. 1996; Beier et al. 1997; Riemer et al. 2002; Zheng et al. 2003; Gebhard et al. 2004). Specific regions in the *Col10a1* promoter could be identified that enhance or repress the specific expression of type X collagen. Sequence analyses of the 5' promoter region revealed several putative *Runx2* binding sites. Runx2 has been shown to regulate transcription of *Col10a1* directly (Zheng et al. 2003). The human promoter carries a c-fos responsive element that might mediate parathyroid hormone/parathyroid hormone

related peptide regulation of *COL10A1* gene expression (Riemer et al. 2002). Transgenic studies have shown that the 10kb promoter region (including exon1, exon2 and a short fragment of the exon3, endogenous ATG codons in exon2 mutated) drives a strong and specific expression of collagen type X in hypertrophic chondrocytes. This promoter was used to generate a transgenic mouse specifically expressing *Cre recombinase* in hypertrophic chondrocytes. These mouse models enable functional study of candidate genes by targeting genes of interest in hypertrophic chondrocytes following Cre-*LoxP* recombination technologies.

The Cre-*loxP* system

The Cre-*loxP* (Cre: causes recombination) system is a widely used system for mammalian genome modification. This system can be utilized to knockout genes in a time and tissue specific fashion. The prokaryotic enzyme *Cre recombinase* is a 38-kDa cyclization recombination enzyme, naturally expressed in the bacteriophage P1. This enzyme belongs to the integrase family of recombinases and catalyzes the recombination between 34bp long DNA sequences (*loxP*, locus of crossover (x) in P1) by forming a transient DNA-protein covalent linkage to bring the two loxP sites together and mediate a site-specific recombination (Kos 2004).

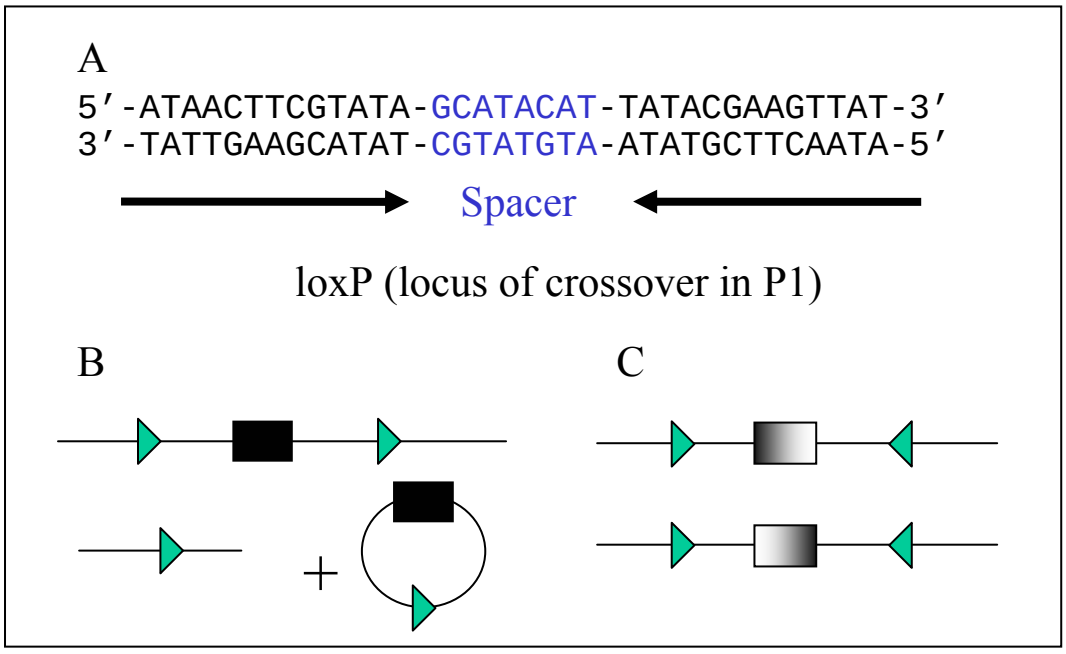

Figure 8: Schematic of the Cre-*loxP* system.

(A) Sequence of the *loxP* site. (B) Excision of a DNA sequence between two *loxP* sites (green arrowheads) orientated in the same direction. C Inversion of the "floxed" DNA sequence.

The *loxP* sites consist of two 13bp long inverted repeats that are connected by an 8bp long non-palindromic spacer sequence (see figure 8A), which determines the orientation of the site and the outcome of the recombination event (Abremski et al. 1983). If two *loxP* sites on a linear DNA molecule are orientated in the same direction, the DNA sequence between these two sites will be excised by intramolecular recombination. One of the two *loxP* sites will remain in the DNA backbone; the excised sequence together with the second loxP site will form a circular molecule. If the *loxP* sites are orientated in opposite direction the "floxed" DNA sequence in between the sites will be inverted (see figure 8 B and C).

Transgenic mice carrying the *Cre recombinase* under the control of tissue-specific promoters are mated to mice carrying the "floxed" alleles for the gene of interest, which results in the conditional knockout of this gene in the specific tissue. This approach is often used, when the conventional gene targeting leads to embryonic lethality (Bockamp et al. 2002; Schipani 2002).

1.7 Specific aims

The role of BMPs and TGFβ in the development of the skeleton is under comprehensive investigation. Different knockout and transgenic mouse models have helped to elucidate the principle mechanisms of these pathways. But thus far the role of the mediators of the BMP pathway in this process is not yet completely understood. *Smad1* as well as *Smad5* null mice are embryonic lethal. Heterozygous *Smad1* null mice are viable and fertile, but homozygous *Smad1* null mice die at 10.5 dpc due to an overgrowth of the posterior visceral endoderm (VE), the extraembryonic mesoderm and the chorion. These mice also display a dramatic reduction in size and pattern of the allantois, they are not able to form an umbilical connection and have a marked reduction in number of primordial germ cells at 8.5 dpc (Tremblay et al. 2001). Homozygous *Smad5* mutant mice die between 9.5 and 11.5 dpc, while heterozygous mice are viable and fertile. The first morphological defects of amnion, heart and guts in the mice can be observed at 8.0 dpc. The embryos fail to undergo proper turning and display craniofacial and neural tube defects. The integrity of the yolk sac as well as the development of the embryonic vasculature is disturbed and they display defects in the development of the allantois and the amnion (Chang et al. 1999).

The primary aim of this thesis was to examine the role of *Smad1* in the development of cartilage with a conditional knockout mouse model. Mice carrying the "floxed" allele for *Smad1* were obtained from E. Robertson's laboratory (Tremblay et al. 2001) and mated with transgenic mice expressing the *Cre recombinase* specifically in proliferating chondrocytes (Ovchinnikov et al. 2000). Alizarin red and Alcian blue staining of whole skeletons, growth studies and histological analyses of growth plates were performed to characterize these mouse models. Since the Smad5 protein shows significant homology to Smad1 and *Smad5* and *Smad1* are expressed in the same region in the growth plate (Sakou et al. 1999) the same studies were performed using mice, which are heterozygous for the *Smad5*-null allele in addition to the complete ablation of Smad1 in the proliferating chondrocytes.

Not only BMPs are crucial for the development of skeletal elements. The expression pattern of TGFβs suggests an important role of these signaling molecules in this process as well. To compare the function of BMPs and TGFβs in the developing growth plate, mice overexpressing *Esl-1* in proliferating chondrocytes and mice overexpressing a dominant negative TGFβ type I receptor (*ΔTbRI*, *ΔALK5*) were generated and characterized. Esl-1 can be co-purified with TGFβ1 in a large protein complex and is a putative inhibitor/repressor of

the TGFβ pathway. Both transgenic mouse models were characterized by histological analyses and staining of whole skeletons and each of the two lines were bred for further characterization.

A secondary aim of this thesis was to design and generate a transgenic mouse expressing *Cre recombinase* (specifically in hypertrophic chondrocytes). As previously stated, *Col10a1* is the only known marker specific for hypertrophic chondrocytes. Preliminary data have demonstrated that a 10 kb promoter fragment of the *Col10a1* gene was able to drive a high-level expression of *β-galactosidase* in transgenic mouse studies. This promoter fragment was used to generate the transgenic mouse lines, which can be further used to study the role of genes during terminal differentiation in the growth plate using the Cre-*loxP* system. The specificity and magnitude of the expression was tested by mating the founder mice with Rosa26R reporter mice (Soriano 1999) with subsequent staining for β-galactosidase.

2 Material and methods

2.1 Animal husbandry and dissection of mice

2.1.1 Animal husbandry

Animals were held in standardized conditions. The cages are stored in ventilated racks. Room temperature is 22ºC, the humidity ranges from 30-70% and the standard light timer is set on a 14 h light cycle (6:00-20:00). The mice were given irradiated low calorie standard feed and acidified water *ad libitum* in autoclaved water bottles.

2.1.2 Isolation of ribcages

To obtain ribcages from the mice (age 1.5 –3.5 dpc), the skins of the mice were removed and stored for genomic DNA isolation for genotyping (2.2.2), and the ribcage part was dissected. The limbs and internal organs were removed and the ribcage was cut open by cutting off the spine. The ribcage was flattened and the soft tissue was removed with a sharp rounded scalpel. The ossified portion of the ribcage close to the spine was cut off and the sternum was removed. Additional connective tissue was removed using KIMTECH Science Kimwipes® (Kimberley-Clark Corporation, Neenah, WI, USA). The separated ribs were stored at -80ºC.

2.2 DNA isolation methods

2.2.1 Isolation of DNA from mouse-tails for genotyping

Each mouse-tail was cut 1 cm from the tip and transferred to a 1.5 ml reaction tube. 700 µl NTES buffer and 100µg/ml proteinase K were added to the reaction tube and incubated overnight in a rocking cylinder at 58ºC. Undigested material was pelleted by centrifugation for 2 min at 14,000 rpm. The clear supernatant was transferred to a 1.5 ml reaction tube and 200 µl of saturated NaCl (~5.2 M) was added. The mixture was vortexed for 30 s and then centrifuged for 10 min at 14,000 rpm. Afterwards, the supernatant was transferred into a 2 ml reaction tube containing 1 ml of 100% ethanol. The forming buffy coat was then transferred

into 1 ml 70% ethanol. After two washes with 70% ethanol the samples were centrifuged, the ethanol was completely removed and the DNA was air dried for approximately 30 min.
The DNA was dissolved in 150-200 µl of water. The concentration as well as the quality of the DNA was determined by measuring the optical density (OD_{260nm}) with a spectrophotometer. The genomic DNA was stored at 4ºC.

2.2.2 Isolation of DNA from skin for genotyping

700 µl NTES buffer and 100 µg/ml proteinase K were added to a piece of the skin, which was then incubated overnight in a rocking cylinder at 58ºC. 700 µl of phenol (saturated, buffered, pH 8.0) was added. The mixture was rocked for 10 min and then centrifuged for 10 min at 20ºC. The upper aqueous phase was transferred into a fresh 1.5 ml reaction tube. Then 700 µl phenol:chloroform:isoamylalcohol (25:24:1) was added, rocked for 10 min and centrifuged for 10 min at 14,000 rpm at 20ºC. The aqueous phase was again transferred into a fresh 1.5 ml reaction tube and the genomic DNA was precipitated by adding 700µl isopropyl alcohol. The DNA was retrieved with a closed end glass Pasteur pipette. The spooled DNA was dipped into 70% ethanol and then dried for 5 min at room temperature. The DNA was dissolved in an appropriate volume of water. The concentration was determined by measuring the optical density (OD_{260nm}) with a spectrophotometer and the quality of the DNA by gel electrophoresis. The genomic DNA was stored at 4ºC.

2.2.3 Isolation of plasmid DNA from bacteria

The Aurum Plasmid Mini Kit (Bio-Rad Laboratories Inc., Hercules, CA, USA) was used to isolate smaller amounts of plasmid DNA for sequencing and cloning. This method is based on the alkaline lysis procedure described by Birnboim and Doly (Birnboim and Doly 1979). A single colony was picked and grown for not longer than 12 h in 4 ml of LB-medium supplemented with 100 µg/ml ampicillin at 37ºC in an incubator. The cells were pelleted by centrifugation at 4,000x g for 5 minutes and resuspended in 250 µl resuspension solution. To lyse the bacteria, 250 µl lysis solution was added and mixed by inverting the tube. This reaction was stopped by adding 350 µl of neutralization solution. The proteins and cells debris were pelleted by centrifugation at 14,000 rpm for 5 min and the supernatant was transferred in a provided column. The DNA was bound to the column by centrifugation for 1 min at 13,000 rpm and washed twice with 500 µl and 750 µl of wash buffer, respectively. The DNA was eluted with 50µl ddH_2O and stored at -20ºC.

2.2.4 Isolation of plasmid DNA for in situ hybridization probes

Two different kits were used to isolate plasmid DNA for the preparation of *in situ* hybridization probes. The High Purity Plasmid Midiprep System (Marligen Biosciences, Ijamsville MD, USA) and QIAGEN® Plasmid Midi Kit (QIAGEN, Valencia CA, USA) are both based on the same principle. Bacterial cells from a 25 ml overnight cell culture were pelleted, resuspended in cell suspension solution (P1) and lysed with cell Lysis Solution (P2). Neutralization Solution (P3) was added and the mixture was centrifuged at 15,000 - 20,000 x g at room temperature for about 10 min. The columns were equilibrated with 10 ml Equilibration Buffer (4 ml QBT) and the supernatant was applied on the columns. DNA binds to the column and was washed afterwards, twice with 10 ml Wash Buffer (QC). The DNA was eluated with 5 ml Elution Buffer (QF). For the precipitation of the DNA, 3.5 ml of isopropanol was added, the mixture was divided into several 1.5 ml tubes and centrifuged in a table top centrifuge at maximum speed for about 30-60 min at 4ºC. The DNA was washed with 70% ethanol, air-dried and dissolved in a suitable volume of TE buffer. The DNA concentration was measured with a spectrophotometer and stored at -20ºC.

2.3 Total RNA isolation

2.3.1 Isolation of total RNA from a ribcage

The ribcage was homogenized in 1 ml of cold Trizol® reagent (Invitrogen Corporation, Carlsbad, CA, USA) for 20 - 30 seconds on ice. The sample was then transferred to a 1.5 ml tube and 250 µl Chloroform was added. After shaking for 15 s and 3 min incubation at room temperature, the samples were centrifuged for 10 min (14,000 rpm, 4ºC). The upper, aqueous phase was carefully transferred into a new tube. To precipitate the RNA, 1 volume of isopropanol was added, incubated at room temperature for 10 minutes and centrifuged with 14,000 rpm at 4ºC. After a wash step with 70% ethanol, the RNA was air dried for approximately 5 minutes and dissolved with 50 µl ddH_2O.

2.3.2 DNaseI treatment

To avoid contamination of the RNA with DNA, the isolated RNA was treated with DNaseI. DNaseI is an unspecific endonuclease that efficiently hydrolyses single- and double stranded

DNA to short oligo- or mononucleotides with a phosphate residue at the 5'end. In the presence of Mg^{2+}, cleavage of each strand of a double stranded DNA substrate proceeds independently.

After adding 1xTE, 10 mM MgCl2, 1 mM DTT, 10-30 Units RNase-Inhibitor and 10-30 Units DNase I (RNase-free) the samples were incubated for 2 h at 37°C. Afterwards, the RNA was purified using the Sigma RNA-Kit to stop the reaction and remove the proteins. The RNA was eluted with 30-40 µl of RNase-free water and the concentration was determined with a spectophotometer. The quality of the RNA was controlled on a non-denaturating gel.

2.4 DNA standard methods

2.4.1 Agarose gel electrophoresis for DNA

Horizontal agarose gels were used to separate plasmid DNA and PCR products. 1 x TBE buffer was the electrophoresis buffer. Dependent upon the size of the expected fragments 0.8% to 1.5% agarose gels containing 100 µg/ml ethidium bromide were used. The gels were run at a maximal voltage of 120 V. The DNA was visualized at 356 nm with either the gel imaging systems Eagle Sight (Stratagene, La Jolla, CA, USA) or AlphaImager (Alpha Innotech Coperation, San Leandro, CA, USA).

To determine the product size of plasmid DNA and PCR products 1 kb Plus DNA Ladder or λ DNA/Hind III Fragments (Invitrogen Corporation, Carlsbad, CA, USA) were loaded on the agarose gels.

2.4.2 PCR Purification of DNA

PCR product as well as digestion reaction were purified with the Promega Wizard® SV Gel and PCR Clean-Up System (Promega Corporation, Madison WI, USA) according to the manufacturer's instructions. 10 µl membrane binding buffer was added to each 10 µl reaction, the mixture was transferred to the provided column and incubated for 1 min. The samples were centrifuged for 1 min at 16.000 x g. Afterwards, the column was washed with 700 µl wash buffer and again centrifuged for 1 min at 16.000 x g. A final wash step with 500 µl wash buffer and a centrifugation step for 5 min at 16.000 x g was followed by incubation

of 30 µl water on the column to eluate the DNA for 2 min. The DNA was finally eluated by centrifugation for 1 min at 16,000 x g and stored at -20°C.

2.4.3 Purification of DNA fragments < 10 kb from agarose gels

After electrophoresis the DNA fragments for cloning purposes were cut out from the agarose gel and purified with the Promega Wizard® SV Gel and PCR Clean-Up System (Promega Corporation, Madison WI, USA) according to the manufacturer's instructions. The gel slice was weighed, 10 µl of the Membrane Binding Solution per 10 µg of gel was added and incubated at 50ºC until the gel slice was completely dissolved. The dissolved gel mixture was transferred onto a provided SV Minicolumn and incubated at room temperature for 1 minute. The following purification steps were performed as described in chapter 2.4.2.

2.4.4 Purification of DNA fragments >10 kb from agarose gels for injections

After restriction enzyme digest, the DNA was separated on an agarose gel. The desired DNA fragment were cut out and purified with the QIAEX II Gel Extraction kit (QIAGEN, Valencia CA, USA). The excised gel slice containing the DNA was weighed, 3 volumes of Buffer QX1 as well as 2 volumes of H_2O and 30µl of QIAEX II were added, then mixed and incubated for 10 min at 50ºC. The samples were mixed by inverting the tube every 2 min. The samples were then centrifuged for 30 s and washed twice with 500 µl QX1 buffer and then three times with 500 µl PE buffer. After air-drying the pellet for at least 30 min, the DNA was eluted two times with 20 µl injection buffer (10mM Tris HCl / 0.1 mM EDTA). The yield of the recovered DNA was measured with a spectrophotometer and the quality was determined by loading different dilutions on an agarose gel.

2.5 PCR techniques

2.5.1 Standard PCR

50-100 ng genomic DNA or 5 ng plasmid DNA were used as a template for the reaction. In the first step, the DNA was denatured at 94ºC for 1 min. The following 30-35 cycles consisted of 1 min denaturing at 94ºC followed by the annealing of the primers at 54 - 62ºC for 1 min and an elongation step of 1 – 2 min at 72ºC depending on the size of the product (1 min / 1 kb) and a final elongation step at 72ºC for 10 min. Lastly, the samples were cooled

down to 4ºC. 5 µl of the PCR reaction was loaded on a 1% agarose gel to control for the specificity and the size of the PCR product.

2.5.2 Reverse-Transcriptase polymerase chain recation (RT-PCR)

To convert RNA into complementary DNA, 4 µg of total RNA isolated as described in chapter 2.3.1 was denaturated for 10 min at 70ºC in a maximal volume of 18 µl and directly afterwards chilled on ice. Then 2 µl of random hexamers (c=50 µM), 1.5 µl dNTPs (25 mM each), 1 µl RNase Inhibitor (40 U/µl), 8 µl of 5 x 1st strand synthesis buffer, 4 µl of 0.1 M DTT, and 1.5 µl Reverse Transcriptase (40U/µl) (Invitrogen Corporation, Carlsbad, CA, USA) were added, mixed and incubated at 37ºC for 90 min. The enzyme was inactivated by heating up the sample to 94ºC for 10 min. The cDNA was stored at –20ºC until further use.
2 µl of cDNA was normally added to a 50 µl PCR reaction containing 50 mM KCl, 10 mM Tris/HCl (pH 8.3), 0.01% gelatin, 1.5 mM $MgCl_2$, 100 nM each of the two primers, 100 µM each of the four dNTPs and 1-2 U Taq polymerase (AmpliTaq Gold, Perkin Elmer, Wellesley, MA, USA). Primer pairs that span at least one intron were used to distinguish cDNA from possible DNA contaminations and annealing temperature for the primers ranged from 52-60ºC. The cycle program is similar to the one described in chapter 2.5.1.

2.5.3 Semiquantitative RT-PCR

The semiquantitative RT-PCR was performed as described in chapter 2.5.2. After cycles 20, 25 and 30 each, 10 µl was obtained from each PCR sample to quantify the transcription rate. A housekeeping gene was amplified as a positive control. The samples were then loaded on an agarose gel.

2.5.4 Quantitative RT-PCR

Quantitative PCR was performed to verify the overexpression of Esl-1 in transgenic mice using ribcage cDNA from transgenics and wild type littermates. In addition, it was used to quantify the different expression patterns for cartilage markers. The LightCycler® 2.0 Instrument and the reagents from Roche Applied Science (Indianapolis, IN, USA) were used for the quantitative PCR and the recommendations of the manufacturer were followed exactly. The amount of generated PCR product in a reaction was detected and quantified with a fluorescent reporter, the intensity of the fluorescence is proportional to the amount of PCR

product generated each PCR cycle which is a function of the quantity of template in each reaction and can be directly monitored. Variations of the amount of template among samples are compensated by using constitutively expressed genes that amplify with efficiencies equal to that of the target (gene of interest). Amplicon homogeneity is verified by a melting curve analyses performed subsequent to the last cycle of amplification. Misspriming events and/or primer dimmers, which can complicate or even preclude evaluations, can be detected because of formation of multiple peaks. Single peak verifications were obtained with each system evaluated in this study. 20 µl reactions are prepared with dNTP concentrations of 1200 mM, $MgCl_2$ of 4 mM buffer and hotstart enzyme that has been part of proprietary mastermix. cDNA samples were assayed by fluorometry on a BMG Fluostar plate reader (BMG LABTECH GmbH, Offenburg, Germany) using Pico green assay (Molecular Probes, Eugen, OR, USA). The template concentration was ascertained over multiple dilutions and normalized to 40 ng/ul of which a 1:8 dilution was used for Lightcycler amplification. 2 µl of the 1:8 dilution (12 ng) was added to each 20 µl reaction and fluorescence was monitored for 40 cycles. Crossing points were determined by a second derivative algorithm intrinsic to the Lightcycler software.

2.6 Competent cells

A single colony of DH5α cells was picked and incubated in 4 ml LB-medium at 37ºC overnight in a bacteria shaker. The pre-culture was measured (OD = 600) and used to adjust 100 ml LB-medium to an OD_{600nm} of approximately 0.05. The cells grew afterwards until the suspension reached an OD_{600nm} of approximately 0.5. The cells were pelleted by centrifugation at 2500 rpm at 4ºC for 10 min and resuspended in 20 ml ice cold 100 mM TbfI. After incubation for 30 min on ice the cells were again pelleted by centrifugation at 2100 rpm at 4ºC for 6 min and resuspended in 2 – 4 ml TbfII and stored at -80ºC in 50 µl aliquots.

2.7 Subcloning of DNA fragments

2.7.1 Alkaline phosphatase treatment

To avoid religation of the vector after digestion, the vector was treated with shrimp alkaline phosphatase (SAP; Roche, Indianapolis IN, USA). The SAP catalyzes the dephosphorylation

of 5' phosphates from DNA. For each µg of DNA, 20 Units of SAP were used and incubated in 1 x dephosphorylation buffer for 10 min at 37°C. After heat inactivation at 65°C at 25°C the sample could be used directly for the following ligation step.

2.7.2 Ligation

The subsequent ligation reaction was performed using T4 DNA Ligase (Invitrogen Corporation, Carlsbad, CA, USA; New England Biolabs, Beverly MA, USA) in the provided buffer. The vector:insert ratio was 1:3 and typically varied in the amount of vector by 50-100 ng between reactions. Blunt end ligations were incubated over night at 16°C, and incubation of 1 h at room temperature was sufficient for sticky end ligations. Half of the ligation reaction was used to transform into DH5α cells.

2.8 Transformation of DNA in bacterial cells

50 µl of competent cells and 25 – 50 ng of plasmid DNA were mixed and incubated on ice for 30 min. The samples were incubated for 1 min in a 42ºC water bath and transferred directly on ice. Then 1 ml of LB-medium was added and incubated at 37ºC for 60 min in a bacteria shaker. 100 - 200 µl was streaked out on LB-agar plates, supplemented with 100 µg/ml Ampicillin and incubated for 12 – 18 hrs at 37ºC. For blue/white selection, 40 µl of 20 mg/ml X-gal and 4 µl of 100 mg/ml IPTG were added to the LB-Ampicillin plates.

2.9 DNA Sequencing

The sequencing was performed by the company SeqWright DNA Technology Services (Houston, TX), after sending them approximately 600 ng plasmid or 80-150 ng PCR product with the suitable primers. Universal primers, like T3 and T7 were provided by SeqWright. The company quantified the samples and performed the sequencing reaction, using fluorescent dye-terminator sequencing. After purification the samples were run on the ABI Prism™ 3730*xl* DNA sequencers. The sequencing files (text files as well as chromatograms) could be downloaded from the Internet the following day.

2.10 Labeling techniques

2.10.1 Random primed oligo labeling

Double stranded DNA was labeled with random primed oligos (Feinberg and Vogelstein 1983). The ALL-IN-ONE™ Random Prime DNA Labeling Mix (Sigma-Aldrich, St. Louis MO, USA) was used and the instructions of the manufacturer were followed. To denature the template 50 ng purified DNA was boiled in a volume of 10 µl for 10 min. The lyophylized random prime labeling mix was dissolved with 35 ml ¼ x TE buffer. The DNA and 5 µl α-^{32}P-dCTP were added, mixed and incubated for 60 min at 37ºC. Afterwards the probe was purified using G-50 sephadex columns (Roche, Indianapolis IN, USA) to remove unincorporated nucleotides. The labeling efficiency was determined using 1 µl labeled DNA probe in 3 ml Scintillation solution and measuring with a Liquid Scintillation Analyzer (Perkin Elmer, Wellesley MA, USA).

2.10.2 Labeling of in situ *probes with S^{35}*

The probes for *in situ* hybridization were amplified by PCR and subcloned into pBSII KS or other plasmids with T3, T7 or SP6 polymerase binding sites. The plasmids were isolated as described in chapter 2.2.4. 20 µg of plasmid DNA was digested overnight with the appropriate restriction enzymes to produce the antisense and sense probes, respectively. Afterwards, the RNases and other proteins were digested with 50 µl/ml Proteinase K and the DNA was purified using phenol/chloroform extraction and precipitation with Na-Acetate and 100% ethanol. The DNA was washed with 70% ethanol, air dried and dissolved in 22 µl of RNase free water. For the *in-vitro* transcription the 0.5-1 µg of the linearized plasmid, 1.5 µl transcription buffer, 1.5 µl RNTP mix (20 µM each RNTP), 2 U RNase Inhibitor, 3.75 µl 0.1 M DTT, 5 µl ^{35}S UTP and 0.5 µl of either T3 or T7 polymerase were mixed and incubated for 45 min at 37ºC. After 45 min another 0.5 µl of polymerase was added and the mix was incubated for additional 45 min. To digest the DNA in the samples, 1.7 µl 0.3 M $MgCl_2$ and 2 U DNase I in a total volume of 50 µl was added and incubated for 15 min at 37ºC. 2 µl out of each sample was used to measure the total counts of the probe. The samples were then purified by using G-50 sephadex columns, following the instructions of the manufacturer and precipitated by adding 10 mg tRNA, 250 µl NH4Ac and 1 ml 100% ethanol. The samples were incubated for 1 h at -80ºC and afterwards centrifuged for 10 min at 4ºC with 14.000 rpm. The ethanol was removed and the samples washed with 70% ethanol, air dried for 45

min to 1 h and resuspended directly in 100 µl hybridization solution. 2 µl of each sample was used to measure the incorporation of the ^{35}S UTP. Using both measurements of unincorporated and incorporated samples, the percentage of incorporation was calculated. The labeled probe was stored at -20ºC.

2.11 Hybridization techniques

2.11.1 Southern Blot

This technique was first described by Southern in 1975 and slightly altered (Southern 1975). 10 to 15 µg of genomic DNA was separated on a 0.8% agarose gel as described in chapter 2.4.1 and then directly transferred to a nylon membrane (Amersham Biosciences, Piscataway, NJ, USA) with 0.5 NaOH for 24 to 48 hrs. The DNA was twice UV crosslinked using the Auto-Crosslink program of the Stratalinker (Stratagene, La Jolla, CA, USA). The nylon membrane was pre-hybridized with Church buffer containing 100 µg/ml salmon sperm DNA for 3 hrs. The pre-hybridization solution was then discarded and replaced with fresh Church buffer containing 10^6 cpm/ml radioactive labeled probe and incubated at 65ºC over night. The unbound and unspecific hybridized probe was washed out with increasing stringency of SSC, 0.1% SDS buffer at 65ºC until the remaining activity measured by a Geiger Müller counter indicated around 50 decompositions/s. The membrane was exposed in a PhosphoImager cassette for 1-2 h and developed with a PhosphoImager (GE Healthcare, Piscataway NJ, USA).

2.11.2 In situ Hybridization

The slides for *in situ* Hybridization were prepared as described in chapter 2.14.1 and serial sections were prepared (compare 2.14.2). Before the hybridization the slides were deparaffinized with 2 incubation steps in xylene for each 15 min and rehydrated in a series by decreasing the ethanol concentration in each step, each 2 times 5 min washes in 100% ethanol, 95% ethanol, one wash with 70% ethanol and then with 50% ethanol, followed by an incubation in PBS for 5 min and afterwards fixed for 15 min in 4% freshly prepared PFA. The slides were then rinsed with proteinase K buffer before proteinase K (final concentration 5 µl/ml) was added. The proteins were digested at 37ºC for 10-20 min depending on the

tissue sample. The slides were then washed with 0.2% glycine in 1 x PBS for 5 min, followed by another fixation step with 4% PFA for additional 5 min and two washing steps with 1 x PBS. The tissue was acetylated in a 10 min incubation step with 200 µl TEA buffer and 500 µl acetic anhydride (after 5 min additional 500 µl acetic anhydride was added). The slides were washed with 1 x PBS for 5 min, afterwards dehydrated with 70%, 95% and 2 times 100% ethanol for 5 min each and air-dried.

The pre-hybridization was performed in a 2 x SSC/50% formamide moistened box. 100 µl of hybridization solution (containing 10 mM DTT and 250 µM α-S-thio-ATP) was added to each slide and was incubated for 2 hours at 55-60ºC, depending on the probe. During the pre-hybridization the probes were denatured by boiling at 95ºC for 5 min. Then the samples were incubated for at least 2 min on ice. The pre-hybridization solution was replaced with 60 µl hybridization solution containing the labeled probe (see chapter 2.10.2) and covered with HybriSlips. The hybridization occurred overnight at the probe specific temperature (55-60ºC).

Unbound probe was removed by post hybridization washes with FSM buffer and STE buffer. All buffers were heated up to the appropriate temperature. The slides were washed 2 times 30 min in FSM. 320 µl β-mercaptoethanol was added to 200 ml of buffer prior to adding of the slides, and then the slides were incubated in STE buffer for at least 10 min, followed by an RNase A digest at 37ºC for 30 min in 200 ml STE buffer plus 400 µl RNase A (10mg/ml, Sigma-Aldrich, St. Louis, MO, USA). The RNases were washed off with STE buffer for at least 10 min at 37ºC, followed by 2 washes for 45 min each with FSM buffer plus 320 µl β-mercaptoethanol added just before the slides. The tissue was then washed with 1 x PBS at room temperature for 2 min and dehydrated with 70%, 95% and 100% ethanol at each step for 2 min at room temperature. The slides were air dried in a hood for about 45 min. The slides were autoradiographed overnight with a blue x-ray film. The slides were afterwards dipped in an emulsion for approximately 5 s at 42ºC, dried in a light proof box overnight and exposed 4-7 days at 4ºC depending on the probe. Afterwards, the slides were incubated in developer for 2 min, washed by dipping in water and fixed for 5 min in fixative. After a 10 min wash in water, the tissue was stained with Hoechst dye for 2 min and rinsed with water for another 2 min. The slides were air dried and mounted with 50-55 µl Canada balsam.

2.12 X-gal staining of lacZ positive newborn mice

Newborn or one day old mice were skinned and all internal organs were carefully removed. After a wash step with 1 x PBS, they were fixed for an hour at room temperature with fixation solution, followed by three washes with rinse solution. The x-gal staining was performed over night in staining solution containing 1 mg x-gal (in N,N-dimethylformamide). After two washes with 1 x PBS the mice were stored in 70% ethanol at -20°C until further analyses.

2.13 Skeletal preparation staining with alcian blue and alizarin red

One-day-old mice were skinned and internal organs were removed. The skeletons were fixed overnight in 95% ethanol on a rotator at room temperature. After staining with Alcian blue solution the skeletons were washed in 95% ethanol for at least 3 hours. Afterwards, they were transferred into 2% KOH for 24 hours. Following this incubation period, the remaining soft tissue was carefully removed with forceps. The skeletons were then stained overnight with Alizarin Red, cleared in 1%KOH/20% glycerol for at least two days and stored in a 1:1 mixture of glycerol and 95% ethanol.

2.14 Histology

2.14.1 Tissue embedding in paraffin

Fore- and hind limbs of one-day-old mice were collected and fixed in 4% PFA (paraformaldehyde in 1 x PBS). The joints of fore- and hind limbs of adult animals of different ages were fixed in 10% formalin w/v. The fixation preserved histological details and avoid tissue degeneration. The embryos were dehydrated with ethanol (30% ethanol/0.9% NaCl, 50% ethanol/0.9% NaCl, 70% ethanol in H_2O overnight, 90% ethanol in H_2O and twice 100% ethanol for one hour each). The joints of the adult mice were decalcified with 10% EDTA, pH 7.2 for two weeks, washed with 1 x PBS and stored in 70% ethanol. The ethanol was replaced with three exchanges of xylene each 30 min at RT on a rocker. The tissue was then embedded in paraffin by replacing the xylene with wax. This was done by incubating in a 50% xylene/50% wax mixture at 58ºC for 30 min followed by

three exchanges of wax for 30 min x at 58ºC each. The tissue was placed in a base mold filled with fresh wax. The paraffin block was stored at room temperature until further use.

2.14.2 Sectioning of paraffin embedded tissue

The tissue was embedded in paraffin as described in 2.15.1. The paraffin block was mounted on the microtome and 5 µm slices were cut. The sections were flattened by floating on the surface of a 50ºC warm water bath and then transferred to a glass slide. The sections were dried on a 37ºC heating bench over night. The slides were stored in a slide holder at RT until further use.

2.14.3 Hematoxylin-Eosin staining

Sectioned tissue was deparaffinized with three washes in xylene for 3 min each, followed by two 1 min incubations in absolute ethanol, then two 1 min rinses in 90% ethanol and 80% ethanol, and a final incubation for 1 min in H_2O. The nuclei were stained red with Mayer's Hematoxylin for 3 min then rinsed in H_2O. For better contrast the slides were incubated in a weakly alkaline $NaHCO_3$ solution to turn the Hematoxylin staining blue. For counterstaining of basic cytoplasmic proteins the slides were washed again in H_2O, then dipped ten times into 80% ethanol and stained for 45 s in Eosin. Afterwards, the slides were dehydrated with successive 1 min incubations in 80% ethanol, 95% ethanol, four times in 100% ethanol and 3 times in xylene. Stained sections were mounted with Cytoseal^{TM}XYL.

2.14.4 Nuclear Fast Red staining

The sectioned tissue was deparaffinized with three washes in xylene for 3 min each, followed by two 1 min incubations in absolute ethanol, then two 1 min rinses in 90% ethanol and 80% ethanol, and a final incubation for 1 min in H_2O. The nuclei were stained red with Nuclear Fast Red for 2 min and 30 s and then rinsed with dH_2O. Afterwards, the slides were dehydrated with successive 1 min incubations in 80% ethanol, 95% ethanol, four times in 100% ethanol and 3 times 2 min in xylene. Stained sections were mounted with Cytoseal^{TM}XYL.

2.14.5 Alcian Blue staining

Alcian blue stains acid mucosubstances and acetic mucins. Strongly acidic mucosubstances will be stained blue, nuclei will be stained pink to red, and cytoplasm will be stained pale pink. The tissue was deparrafinized with three washes in xylene for 3 min each. The hydration occurred with successive incubations in absolute ethanol, 95% ethanol and 80% ethanol for 1 min each followed by incubation in dH_2O. Afterwards, the tissue was stained for 30 min in Alcian blue solution. The slides were washed under running tap water for 2 min and rinsed with dH_2O before the tissue was counterstained with Nuclear Fast Red for 5 min. Residues of the staining solution were removed under running tap water and the tissue was then dehydrated and cleared with successive 1 min incubations in 80% ethanol, 95% ethanol, 2 times in 100% ethanol and finally, 3 times xylene for 3 min each. The slides were mounted with xylene based mounting medium Cytoseal^{TM}XYL.

2.14.6 Safranin O staining

This method is used for the detection of cartilage, mucin, and mast cell granules. Formalin-fixed and paraffin-embedded tissue sections were deparaffinized with 3 times 3 min in xylene and hydrated with successive washes in 100% ethanol, 95% ethanol and 80% ethanol for 1 min each followed by a 1 min incubation in dH_2O. The sections were stained with Weigert's iron Hematoxylin working solution for 10 min and washed in running tap water for 10 minutes. Afterwards, the tissue was stained with 0.001% fast green (FCF) solution for 5 min, rinsed quickly with 1% acetic acid solution for 10 –15 s and stained with 0.1% safranin O solution for 5 min. The tissue was dehydrated with two changes of each 95% ethanol and 100% ethanol, and cleared with two changes of xylene. The slides were mounted afterwards using resinous medium. The cartilage and mucin will be stained orange to red, and the nuclei will be stained black. The background is stained green.

2.14.7 von Kossa staining

This technique is used to detect deposits of calcium or calcium salt by treating tissue sections with a silver nitrate solution. The silver is replacing the calcium reduced by the strong light, and thereby visualized as metallic silver. The sections were deparaffinized with 3 times 3 min in xylene and hydrated with washes in 100% ethanol, 95% ethanol and 80% ethanol for 1 min each and rinsed in several changes of distilled water. The sections were then incubated in

1% silver nitrate solution in a clear glass coplin jar placed under ultraviolet light for 20 minutes. Un-reacted silver was removed by incubating the slides in 5% sodium thiosulfate for 5 min and afterwards the sections were rinsed again in distilled water. The sections were then counterstained with nuclear fast red for 5 min, washed with distilled water, dehydrated with two changes of each 95% ethanol and 100% ethanol, and cleared with two changes of xylene. The slides were mounted using permanent mounting medium.

2.14.8 BrdU Staining

Sectioned tissue was deparaffinized in two changes of xylene for 5 min each, followed by rehydration of the tissue in absolute ethanol, 95% ethanol and 80% ethanol for 2 min each. The slides were transferred into water and washed twice. Formalin-fixed tissues were then incubated in hot 1 x antigen retrieval buffer for 20 min, cooled down at room temperature for another 20 min and washed with water. After one hour incubation in blocking reagent (3% normal goat serum, 3% normal donkey serum, 0,1% BSA, 0,1% TritonX in 1xx PBS) the slides were incubated for 2 hours in blocking reagent containing a 1:40 dilution of the BrdU antibody. Afterwards, the slides were washed 3 times in 1 x PBS for 2 min each and mounted with ProLong® Gold antifade reagent with DAPI (Invitrogen Corporation, Carlsbad, CA, USA).

2.14.9 Type X Collagen Immunostaining

The tissue was deparaffinized in three changes of xylene, first for 10 min and then 2 times for 3 min each, followed by dehydration steps in 100% ethanol two times for 2 min and then for 2 min each in 95% and 80% ethanol. Afterwards the slides were transferred into water and washed twice. Antigen retrieval buffer was preheated in a steamer and the slides were incubated in the antigen retrieval buffer for 20 min and cooled down at room temperature for another 20 min. The tissue was again washed with water and then incubated in blocking reagent (3% normal goat serum, 3% normal donkey serum, 0.1% BSA, 0.1% Triton in 1 x PBS). The Type X collagen antibody was diluted 1:400 in blocking reagent with approximately 100 µl applied to each slide and incubated overnight at room temperature. The tissue was then washed three times with 1 x PBS followed by incubation with a 1:600 dilution of anti-rabbit-antibody DαR Alexa 594 Red (Invitrogen, Carlsbad CA, USA) for 1 h. The slides were mounted with ProLong® Gold antifade reagent containing DAPI (Invitrogen Corporation, Carlsbad, CA, USA).

2.15 x-ray

For x-ray images, mice were skinned and all internal organs were carefully removed. The mice were dried overnight. To clean the skeletons, dermestid beetles (*Dermestes sp.*) (Carolina Biological Supply Company, Burlington, NC, USA) were used. Dermestid beetles can live for 60-70 days. The female beetle lays eggs on a carcass to hatch three days later. The larvae consume the remains, and leave behind tougher meat as well as hair and skin. The beetle colony was maintained in a dark environment with 50-60 % humidity and a temperature of about 26°C.

The clean skeletons were transferred into 95% ethanol to kill attached larvae and then dried. The skeletons were positioned, and pictures were taken using both a Kodak MIN-R 2 Cassette and MIN-R Mammography Films (Eastman Kodak Company, Rochester, NY, USA). The films were developed with an RP X-OMAT Processor, Model M7P developer (Eastman Kodak Company, Rochester, NY, USA).

2.16 Micro-CT

The skulls for Micro-CT analyses were stored in water and scanned using 32 micron resolution with a eXplore Locus SP Micro-CT scanner (GE Medical Systems, London, Ontario, Canada). The results were analyzed using the Microview program, which is freely available at:
http://www.gehealthcare.com/usen/fun_img/pcimaging/products/microview.html.

2.17 Pronuclear injection of transgenes

Superovulated 3-5 week-old female FVB/N mice were used to generate fertilized eggs after mated with males for injection of the DNA. The superovulation is achieved by administration of pregnant mare's serum gonadotropin PMSG followed by human chorionic gonadotropin (hGC) after 42- 46 h. The eggs are harvested at day 0.5 dpc.

20-30 mouse eggs were transferred into the injection chamber and checked for visible pronuclei. The tip of an injection pipette is filled with DNA solution by dipping the blunt end into the DNA solution. In capillaries with internal filament, the DNA solution accumulates in the tip of the pipette. While the egg is being positioned and held by a holding pipette, the

DNA is injected into one of the two pronuclei. The male pronucleus is usually larger and therefore easier to inject. During injection the pronucleus should visibly swell. After the injection the needle has to be removed quickly to avoid pulling out the pronucleus of the egg. The eggs were then incubated at 37°C before transferring them into recipient mothers. The recipient mothers are CD-1 females plugged by vasectomized males the night before.

2.18 Establishing a transgenic mouse line

The founders of a transgenic mouse line are usually mosaic. The degree of mosaicsm depends on the time when the transgene has been integrated into the genome. The earlier it has been integrated the more cells will carry the transgene, while the later this event occurs the fewer cells will contain the transgene. In order to establish a transgenic mouse line, each founder is crossed back to a wild-type mouse of the same strain. The pups resulting from this breeding are called the R1 generation. Each of these pups can differ with respect to transgene expression levels. Some pups of the R1 generation might be negative for the transgene. All R1 carrying the transgene are again crossed back to a wild-type mouse of the same strain. The pups from this breeding are the R2 generation. These pups are now equal (only true for each separate mating) in transgene expression levels, so that the R2 mice can be intercrossed. The resulting F1 generation follows Mendelian distribution of the genotypes. The expected genotypes include wild-type mice not carrying a transgene, mice that are heterozygous for the transgene and mice that are homozygous for the transgene. To identify the mice that are homozygous for the transgene, the F1 are backcrossed to wild-type mice of the same strain. If the F1 mice are homozygous, all offspring will carry the transgene. The F1 mice whose breeding results in offspring that are positive and negative for the transgene are heterozygous for the transgene.

2.19 Material

2.19.1 Solutions

Alcian Blue Solution	0.015% Alcian Blue 20% acetic acid 80% ethanol
Alizarin Red Solution	0.005% Alizarin Red S 1% KOH
5 x 1st strand synthesis buffer	250 mM Tris-Hcl, pH 8.3 375 mM KCl 15 mM $MgCl_2$
Agar plates	15 g Agar-Agar in 1000 ml LB-medium
Blocking solution	3% normal goat serum 3% normal donkey serum 0.1% BSA 0.1% TritonX in PBS
Blue-Dye DNA Loading Buffer	0.25% bromphenolblue 0.25% xylene cyanol 40% sucrose
Denaturation solution	1.5 M NaCl 0.5 M NaOH
Fixation solution	0.05 M Na-phosphate pH7.3 0.2 % glutaraldehyde 2 % paraformaldehyde
2 x FM medium for freezing bacteria	65% glycerin 0.1 M $MgSO_4$ 25 mM Tris-HCl, pH 8.0
Hybridization solution (*in situ*)	50% deionized formamide 0.3 M NaCl 20 mM Tris/HCl 5 mM EDTA 10 % Dextransulfate 0.02% Ficoll 0.02% BSA (RNase free) 0.02% Polyvinylpyrolidone 0.5 mg/ml Bakers yeast RNA

LB- medium	1% tryptone 0.17 M NaCl 0.5% yeast extract dissolve in 1000 ml DW, pH 7.5
Neutralization solution	0.5 M Tris HCl, pH 7 1.5 M NaCl
NTES	100 mM Tris HCl, pH 8 100 mM EDTA, pH 8 100 mM NaCl 10% SDS
Orange G	0.35% Orange G 30% sucrose
1 x PBS	120 mM NaCl 2.7 mM KCl 10 mM potassium buffer, pH 7.4
PBS	120 mM NaCl 2.7 mM KCl 10 mM potassium buffer, pH 7.4
10 x PCR buffer	500 mM KCl 100 mM Tris-Hcl, pH 8.3 0.1% gelatine 15 mM $MgCl_2$
Proteinase K buffer	50 mM Tris/HCl, pH 8.0 5 mM EDTA pH 8.0
Rinse solution	0.1 M Na-Phosphate buffer, pH 7.3 2 mM $MgCl_2$ 0.1% Na-deoxycholate 0.2% NP-40
1 x SSC	0.15 M NaCl 15 mM sodium citrate, pH 7.0
Staining Solution	80 mM Na_2PO_4 20 mM NaH_2PO_4 1.3 mM $MgCl_2$ 3 mM $K_3Fe(CN)_6$ 3 mM$K_4Fe(CN)_6 \bullet 3\ H_2O$ 1 mg X-gal /ml
1 x TBE buffer	90 mM Tris base 90 mM boric acid 1.25 mM EDTA, pH 8.3

1 x TE buffer	10 mM Tris-HCl, pH 8.0 1 mM EDTA
1 x TEA buffer	100 mM Trietanolamine/HCl, pH 8.0
TbfII	30 mM K-Ac 50 mM $MnCl_2$ 100 mM $CaCl_2$ 15% Glycerol, pH 5,8
TbfII	10 mM Na-MOPS, pH 7 75 mM $CaCl_2$ 10 mM KCl 15% Glycerol
Weigert's Iron Hematoxylin Solution Stock Solution A:	1 g Hematoxylin 100 ml 95% Ethanol
Stock Solution B:	4 ml 29% Ferric chloride in water 95 ml distilled water 1ml concentrated hydrochloric acid

2.19.2 Kits

BrdU Staining Kit	ZYMED® Laboratories Inc., San Francisco, CA, USA)
ECL Plus Western Blot Detection	Amersham Biosciences, Piscataway NJ, USA
Gel extraction Kit	QIAGEN, Valencia CA, USA
	Promega Corporation, Madison WI, USA
PCR purification Kit	Mo Bio Laboratories Inc., Solana Beach CA, USA
	Promega Corporation, Madison WI, USA
Plasmid Mini/Midi isolation Kit	Bio-Rad Laboratories Inc., Hercules, CA, USA
	QIAGEN, Valencia CA, USA
RNA isolation kit	Sigma-Aldrich, St. Louis, MO, USA

2.19.3 Enzymes, and isotopes

[α^{32}P] dCTP	Valeant, Costa Mesa CA, USA
[α^{35}S] UTP	Valeant, Costa Mesa CA, USA

Alkaline phosphatase	Roche, Indianapolis IN, USA
Klenow-DNA Polymerase	Roche, Indianapolis IN, USA
Restriction enzymes	Roche, Indianapolis IN, USA, New England Biolabs, Beverly MA, USA
Reverse Transkriptase	Invitrogen, Carlsbad CA, USA
T4 DNA ligase	Invitrogen Corporation, Carlsbad, CA, USA New England Biolabs, Beverly MA, USA
T4-DNA polymerase	Roche, Indianapolis IN, USA
T4-Polynucleotid Kinase	Roche, Indianapolis IN, USA
Taq-DNA Polymerase	Perkin Elmer, Wellesley MA, USA

2.19.4 Molecular Weight Markers

100 bp ladder	New England Biolabs, Beverly MA, USA
λ/Hind III	Roche, Indianapolis IN, USA
1 kb marker	Invitrogen, Carlsbad CA, USA
1 kb Plus marker	Invitrogen, Carlsbad CA, USA
Marker X	Roche, Indianapolis IN, USA

2.19.5 Primer

Genotyping

LacZA	5'-TGG CTG GAG TGC GAT CTT CCT GAG-3'
LacZB	5'-GCC GAG TTA ACG CCA TCA AAA ATA-3'
CreP1	5'-TCC AAT TTA CTG ACC GTA CAC CAA-3'
CreP2	5'-CCT GAT CCT GGC AAT TTC GGC TA-3'
Smad5 gen_F1	5'-GAG ACT AGT GAG ACG TGC TAC TTC C-3'
Smad5 gen_R1	5'-CAT GCA AAT TGG GGA GGT ACA CGT T-3'
S1-hygro-F	5'-GTC ATC TCC TTC TCG TAC AG-3'
S1-hygro-R	5'-GGC CTT TAC TTT CTC GTG AC-3'
Smad1-5'F	5'-CGC AGA CCA AGA AGC TAA G-3'
Smad1-3'R	5'-TCG TGG CTC CTT CGT CAG-3'
Smad1-WTfor	5'-TTG ATC AGG AGC CAT TGC AG-3'

Tyr-F	5’-CCT GCT GTC CAT TCC TTA TTC CAT AG-3’
q PCR	
mCol2a1 F	5’-AAG AAC AGC ATC GCC TAC CT-3’
mCol2a1 R	5’-GGA GTG ACT GCG GTT G-3’
mCol10a1 F	5’-AAA GCT TAC CCA GCA GTA GG-3’
mCol10a1 R	5’-ACG TAC TCA GAG GAG TAG AG-3’
mEsl-1 F	5’-TTC CCG CCT TTG CCA TAC-3’
mEsl-1 R	5’-GCT CCT GCC CAG TCT CCG TCT T-3’
mIhh F	5’-GGA GAC ACC ATT GAG ACT TGA C-3’
mIhh R	5’-TGA AGA ATC GCA GCC AGA G-3’
mPPR F	5’-ACA GCG AGT GCC TCA AGT TC-3’
mPPR R	5’-CGC AGC ATA AAC GAC AGG A-3’
mPthrp F	5’-GCG TTT GAA GAG GGG TTT GAC-3’
mPthrp R	5’-GGG GTG GTT TTT GGT GTT G-3’
mSox9 F	5’AAGCCACACGTCAAGCGACC-3’
mSox9 R	5’GTGCTGCTGATGCCGTAACT-3’
ColXa1	
ColXh-term-F	5’-CAC GTA GGA CTG TTG TGT GAG-3’
ColX-2kb-F1	5’-GTG AGT ACT GGC ACT CTA TTA TG-3’
ColX-2kb-F2	5’-CTT GCA TCT ACA CAG ACA CTG-3’
ColX-2kb-F3	5’-AAG CTC CTT CAT AAA GTC ACA G-3’
NotI-cre-for	5’-ATC AGC GGC CGC CAG TCT TCG AGT CGA GG-3’
NotI-cre-rev	5’-AGA TGC GGC CGC CAA TCA TTT ACG CGT TAA TG-3’
Other	
Sry-F	5’-CAT GAC CAC CAC CAC CAC CAA-3’
Sry-R	5’-TCA TGA GAC TGC CAA CCA CAG-3’
Esl1-1	5’-GAT GCA CAT TCA CAA GGT GAG-3’
Esl1-2	5’-CTG TCT GAT GAA AGT GGT TCG-3’
Esl1-3	5’-TGG AAT GCA GAG ACA TCG TG-3’
Esl1-4	5’-CTA TAC TCT GAT GAG AGA GTC TG-3’
Esl1-5	5’-TGA AGG TCA ACC TGC TCA AG-3’
Esl1-R	5’-GCT GCG ATA ACT GAG GCT GC-3’

col1-GZ	5'-CCA GCC AGT CGT CGG AGC AGA CG-3'
col1-sequencing	5'-CCT CTG CTA ACC ATG TTC ATG-3'
col2-GZ133	5'-ACT CTT CGC GGT CTT TCC AGT G-3'
pcDNA3.1	5'-TAA TAC GAC TCA CTA TAG GG-3'
pcDNA3.1 (=BGH Rev)	5'-TAG AAG GCA CAG TCG AGG-3'
MAKT1	5'-GTG GGC CGC TCT AGG CAC CA-3'
MAKT2	5'-TAG CCC TCG TAG ATG GGC ACA G -3'
T3	5'-AAT TAA CCC TCA CTA AAG GG-3'
T7	5'-TAA TAC GAC TCA CTA TAG GG-3'
M13F	5'-GTA AAA CGA CGG CCA G-3'
M13R	5'-CAG GAA ACA GCT ATG AC-3'

2.19.6 Chemicals

Acitic acid	Fisher Scientific, Fair Lawn NJ, USA
Acrylamide	Biorad, Hercules CA, USA
Agar-agar	USB corporation, Cleveland OH, USA
Agarose	GeneMate, Bioexpress, Kaysville UT, USA
Ethanol	AAPER Alcohol and Chemical Co, Shelbyville KY, USA
Formaldehyde	Fisher Scientific, Fair Lawn NJ, USA
Formamide	Fisher Scientific, Fair Lawn NJ, USA
Hydrochloric acid	J.T. Baker, Phillipsburg NJ, USA
LB Broth	Molecular Biology Laboratories, Solana Beach, CA, USA
Lipofectamine 2000	Invitrogen. Carlsbad CA, USA
Methanol	VWR, West Chaster PA, USA
Potassium ferrocyanide	J.T. Baker, Phillipsburg NJ, USA
Sodium pyrophosphate	Fisher Scientific, Fair Lawn NJ, USA
Tryptone	Becton Dickinson and Co, Spraks MD, USA
Xylene	Fisher Scientific, Fair Lawn NJ, USA
Yeast extract	Difco, Becton Dickinson, Sparks MD, USA

All chemicals not listed here were purchased from Amresco, EM Science or Sigma.

2.19.7 Equipment

Bacteria incubator	ORPITAL Incubator Shaker, Gyromax™737 Amerex Instruments Inc., Lafayette CA, USA
Balances	Sartorius BP121 S, Goettingen, Germany sartorius LP6200, Goettingen, Germany
Centrifuges	Avanti™ J-25 I, Beckman, Fullerton CA, USA eppendorf centrifuge 5415 C Brinkmann Instruments, Hamburg, Germany eppendorf centrifuge 5417R Brinkmann Instruments, Hamburg, Germany eppendorf centrifuge 5810R Brinkmann Instruments, Hamburg, Germany Z233M-2, HERMLE Labortechnik, Wehingen, Germany Z233MK-2, HERMLE Labortechnik, Wehingen, Germany
DNA sequencing machine	ABI PRISM™ 377, Applied Biosystems, Foster City CA, USA
Electrophoretic apparatus	Dual Vertical Slab Gel System, cat#DSG-250-02 CBS Scientific Company, Inc., Del Mar CA, USA
Electroblotter	Panther™ Semidry Electroblotter Model HEP-1, #17494 Owl Separation Systems, Portsmouth NH, USA
Gel imaging system	AlphaImager™2200, Alpha Innotech, San Leandro CA, USA Eagle Sight, Stratagene, La Jolla, CA, USA
Hybridization oven	Hybridiser HB-1D, TECHNE, Duxford Cambridge, U.K.
Liquid Scintillation	Analyzer Tri-Carb 2100 TR, Packard Perkin Elmer, Wellesley MA, USA
Magnetic stirrer	Corning Stirrer/Hot Plate, Corning Incorporated Life Sciences, Acton MA, USA
Micro-CT Scanner	eXplore Locus SP Micro-CT Scanner, GE Medical Systems, London, Ontario, Canada
Microscopes	Axioplan 2, Zeiss, Jena, Germany EXLIPSE TS100, Nikon, Japan SMZ150, Nikon, Japan
PCR machine	MJ Research, PTC-200, Watertown MA, USA

pH meter	Corning pH meter 430, Corning Incorporated Life Sciences, Acton MA, USA
Phosphoimager	Molecular Dynamics Storm 860, GE Healthcare Piscataway NJ, USA
Phosphor Screens	Molecular Dynamics, GE Healthcare Piscataway NJ, USA
Plate reader	BMG FLUOstar OPTIMA Plate reader, BMG LABTECH Gmbh, Offenburg, Germany)
Power supply	Model PowerPac HC, cat.#164-5052 BioRad, Hercules CA, USA
Safety carbinet	NU-437-400 series 2, class II type A/B3 Nuaire™Plymouth MN, USA
Spectrophometer	GeneQuant II, Pharmacia Biotech, Amersham Biosciences, Piscataway NJ, USA
UV-crosslinker	Stratalinker®2400, Stratagene, La Jolla CA, USA
Water bath	Isotemp 215, Fisher Scientific, Fair Lawn NJ, USA HAAKE B3, Karlsruhe, Germany

2.19.8 Miscellaneous materials

Coverslips	Fisher Scientific, Fair Lawn NJ, USA
Nylon membrane (Hybond™-N+)	Amersham Biosciences, Piscataway NJ, USA
Superfrost plus slides	Fisher Scientific, Fair Lawn NJ, USA
X-ray films (Hyperfilm™-MP)	Amersham Biosciences, Piscataway NJ, USA

3 Results

3.1 Conditional knockout mouse models in the growth plate

Knockout mouse models are useful to understand the functional role of genes in developmental processes.

One of the specific aims of this thesis was to elucidate the role of BMP signaling in the growth plate, using a conditional knockout of Smad1, a principal mediator of the signaling pathway. Smad1 belongs to the Smad family of transcription factors. To date, eight proteins of this family have been described and Smad1, together with Smad5 and Smad8, specifically mediate signals from the BMP pathway. Immunostaining of Smad1 in the epiphyseal growth plate has shown a strong expression in proliferating chondrocytes, close to the zone of maturating chondrocytes (Sakou et al. 1999).

Smad1 null mice (*Smad1-/-*) die by 10.5 days post coitum (dpc), from defects in morphogenesis and proliferation of extraembryonic tissue. They display overgrowth of the posterior visceral endoderm, the extraembryonic mesoderm and the chorion, as well as a dramatic reduction of size and pattern of the allantois. Additionally, they are not able to form an umbilical connection and have a marked reduction in number of primordial germ cells at 8.5 dpc (Tremblay et al. 2001).

3.1.1 Verification of the specificity of Cre-expressing mice in proliferating chondrocytes

To knockout *Smad1* specifically in proliferating chondrocytes, mice carrying the floxed *Smad1* allele were crossed with transgenic mice expressing *Cre recombinase* under the control of the type II collagen promoter (Ovchinnikov et al. 2000). These mice were kindly provided by Dr. Richard Behringer (M. D. Anderson Cancer Center, Houston, USA) and were maintained as heterozygotes in the colony. Dr. Behringer's group used a 6kb promoter fragment, containing the first exon (with start codon mutated) and the first intron, to drive the *Cre recombinase* (*Col2-cre*, figure 9). This promoter resulted in a highly specific expression exclusively in proliferating chondrocytes in transgenic mouse experiments using *β-galactosidase* as a reporter (Zhou et al. 1995).

To verify the specificity of the *Cre recombinase* driven by the collagen type II promoter, the *Col2-cre* mice were crossed with *Rosa26 β-galactosidase* reporter (*Rosa26R*) mice, which express *β-galactosidase* following *Cre*-mediated recombination.

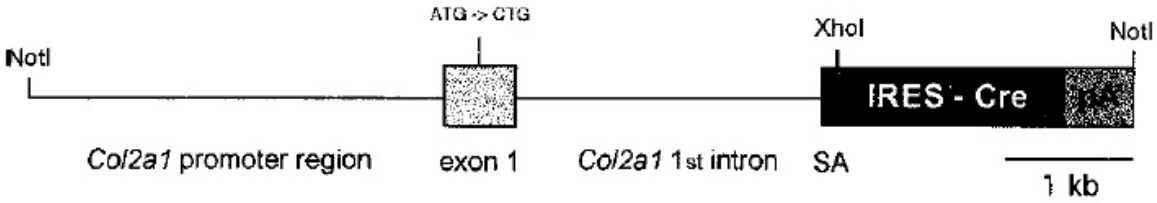

Figure 9: Construct used to generate transgenic mice expressing *Cre recombinase* specifically in proliferating chondrocytes.

The 6kb long promoter fragment containing the first exon (with mutated start codon) drives an *IRES-Cre recombinase* cassette. SA, Spicing acceptor; IRES, internal ribosome entry site (Ovchinnikov et al. 2000).

The skin and the internal organs of the newborn mice from this mating were removed, and the remaining whole body was fixed and stained with x-gal (2.13). All cartilaginous segments were stained in mice carrying both the transgenic allele, *col2-cre* as well as the *Rosa26R* allele (figure 10A). The control animal (figure 10B) was completely negative, showing no direct or non-specific background staining.

Figure 10: Verification of the tissue specific expression of the cre recombinase under the control of the *col2a1* promoter.

Overnight staining with x-gal showed strong *β-galactosidase* expression in all cartilaginous segments of the transgenic *Col2-cre* mouse (A), but none in the control littermate (B).

3.1.2 Conditional knockout of Smad1 in proliferating chondrocytes

A conditional knockout allele for *Smad1* was generated and the strategy is depicted in the following figure (Tremblay et al. 2001).

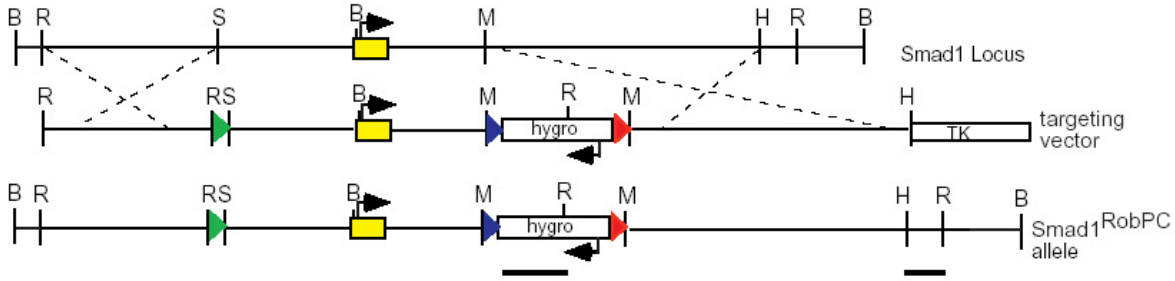

Figure 11: Strategy to generate Smad1 conditional allele.

The *Smad1*^{RobPC} allele introduces a *loxP* site (green triangle) together with EcoR1 (R) 5' of the first coding exon and a, with *loxP* sites and MluI restriction sites (green and red triangles) flanking the *hygromycin* cassette (Tremblay et al. 2001).

The use of a reporter mouse line expressing C*re recombinase* under the control of a *protamine* promoter leads to a germline excision of the hygromycin cassette, leaving an allele bearing only the first coding exon, flanked by two loxP sites (Tremblay et al. 2001).

The mice containing this construct were obtained from Dr. Elizabeth Robertson (Harvard University, Boston, USA). Due to a viral infection detected upon receipt, these animals had to be subjected to an embryo transfer; genotypes were initially verified using a Southern Blot (with the 5' probe) approach as described in the original paper. The heterozygous mice were then crossed among each other to obtain a colony of homozygous animals, necessary to ultimately obtain the conditional *Smad1* allele.

3.1.3 Mating- and PCR genotyping approach for Smad1 and Col2-cre transgenic mice

Homozygous Smad1 conditional knockout mice were crossed with heterozygous *Cre*-expressing mice to obtain double heterozygote mice for both alleles. The double heterozygotes were then crossed among themselves to obtain mice carrying homozygous *Smad1* floxed alleles as well as one allele of the *Cre recombinase.* Mice with the genotype *Smad1*$^{fl/fl}$ x *Col2-cre*$^{+/-}$ (*Smad1* homozygous for floxed allele and heterozygous for the *Cre recombinase* transgene) were compared to *Smad1*$^{fl/fl}$, without the *Cre recombinase* transgene, which are considered as wild type (WT).

The primers used to detect the floxed allele of *Smad1* encompass the second *loxP* site (P1+P2) (figure 12A). The amplicon size of wild type DNA using the primer pair P1 and P2 is 140 bp. The PCR product obtained from mouse DNA carrying the floxed allele for Smad1 is longer (190 bp) due to the additional *loxP* site and two introduced MluI restriction enzyme sites. Amplicons from heterozygous mice DNA result in a three-banded pattern, with an additional product of approximately 220 bp. All products were gel purified and sequenced. The 220 bp product represents a heteroduplex formed between the two smaller PCR products; due to the conformation change its size is altered compared to the two separate products. Using this PCR genotyping approach, it is possible not only to distinguish between wild type and knockout alleles, but also between heterozygous and homozygous mice (figure 12 B(a)). The primers that were used to detect the transgenic *Col2-cre* were specific for the *Cre recombinase* and amplify a region approximately 500 bp in length. The colony was kept in a heterozygous state to generate wild type as well as transgenic animals for *Col2-cre* in every mating (see figure 12 B(b)).

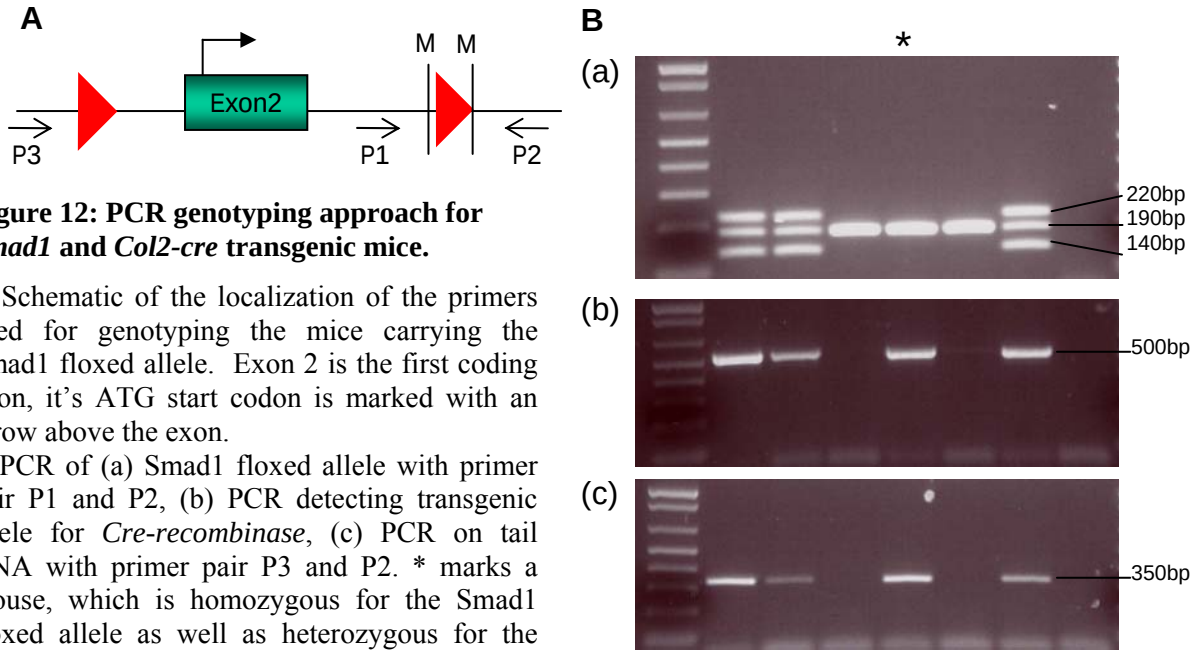

Figure 12: PCR genotyping approach for *Smad1* and *Col2-cre* transgenic mice.

A Schematic of the localization of the primers used for genotyping the mice carrying the Smad1 floxed allele. Exon 2 is the first coding exon, it's ATG start codon is marked with an arrow above the exon.
B PCR of (a) Smad1 floxed allele with primer pair P1 and P2, (b) PCR detecting transgenic allele for *Cre-recombinase*, (c) PCR on tail DNA with primer pair P3 and P2. * marks a mouse, which is homozygous for the Smad1 floxed allele as well as heterozygous for the transgenic *Cre recombinase* allele.

To determine, whether *Smad1* is truly floxed out, DNA extracted from mouse tail or ribcage was used as template in a PCR with the primer pair P3 and P2 (figure 12A). The 350 bp product could only be obtained in mice carrying the floxed allele for *Smad1* (either heterozygous or homozygous) and the *Cre recombinase* (figure 12 B(c)), thus confirming that *Smad1* in the cartilage derived samples is truly floxed out.

This PCR genotyping strategy was used to evaluate the genotypes of all mice that were utilized for subsequent matings and for further phenotype characterizations. DNA from tail was isolated to genotype adult mice (three weeks and older), whereas DNA extracted from skin was used to determine the genotype of P0.5-3.5 old mice.

3.1.4 Verification of the Smad1 knockout in proliferating chondrocytes using semiquantitative RT-PCR

To further verify that the conditional knockout was achieved, a semiquantitative RT-PCR was performed. RNA was isolated (Trizol) exclusively from ribcage cartilage from *Smad1*$^{fl/fl}$/*Col2-cre*$^{+/-}$ mice as well as their wild type littermates (*Smad1*$^{fl/fl}$) as controls (2.1.2). The RNA was transcribed into cDNA and 2 µl were used as template in a 50 µl PCR reaction with *Smad1* specific primers as well as murine *β-actin* specific primers (as control), divided among 4 reaction tubes. Following completion of the 20th, 25th, 30th, and 33rd extension cycle, one tube was removed from the thermocycler. Following removal of the last reaction tube, the PCR products were loaded on an agarose gel (figure 13) with *β-actin* serving as an internal control for the amount of the template cDNA available to each reaction, which directly influences the quantity of amplicon ultimately produced.

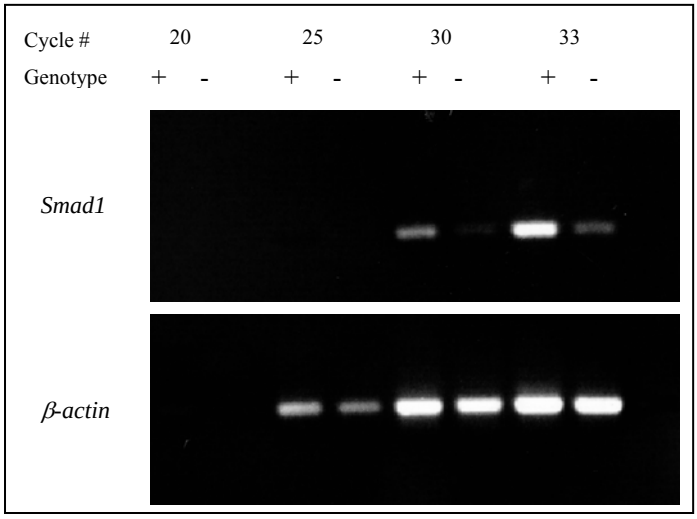

Figure 13: Deprived expression of *Smad1* in proliferating chondrocytes in transgenic mice.

In the upper panel the PCR with the *Smad1*-specific primer is shown. The lower image shows the *β-actin* control.
+ cDNA from wild type littermates
- cDNA from mice, carrying *Smad1*$^{fl/fl}$ and the *col2-cre* transgene.
The total amount of cycles was 33.

The upper image shows the expression of *Smad1*, the lower image the expression level of the murine *β-actin* control PCR. After 20 cycles no products were visible for either reaction. After 25 cycles only products for *β-actin* are visible. The cDNA obtained from the wild type

littermates (+) is apparently of lower concentration than the cDNA from mice carrying the *Cre recombinase* transgene (-). *Smad1* expression cannot be observed until the 30th cycle and it is at this point only visible in the wild type control, suggesting that in fact the conditional knockout of *Smad1* in proliferating chondrocytes has been achieved. The faint *Smad1* product, which is observed in the cDNA of the conditional knockout mouse, is in all probability due to the technically difficult ribcage preparation procedure. The samples could be contaminated with cells of the connective tissue between the ribs or cells at the junction between proliferating and prehypertrophic chondrocytes, not expressing *Cre recombinase*, since the type II collagen promoter is not active in these cells.
In conclusion, the *Smad1* conditional knockout, specifically affecting proliferating chondrocytes functions as designed; *Smad1* expression is effectively down regulated in the target tissue.

3.1.5 Skeletal phenotype of Smad1$^{fl/fl}$ x col2-cre$^{+/-}$

Skeletal preparations, with subsequent Alcian blue and alicarin red staining, of mice lacking *Smad1* in proliferating chondrocytes, reveal that the conditional knockout mice are smaller compared to their wild type littermates. Alcian Blue stains cartilage, while alicarin red stains the bony parts of the skeleton. It was evident during the preparation of the skeletons that the knockout mouse was more fragile; removal of the skin without breaking the bones was considerably more difficult that with wild type mice.

When *Smad1* is dysfunctional in proliferating chondrocytes no pattering defects are observed, but all skeletal elements are seen to be significantly smaller and more fragile compared to those of wild type littermates (figure 14). Hind limbs (B) and forelimbs (C) were disarticulated, (D) shows the digits of the forelimbs. Particularly in frame (D), the size differences of all skeletal elements are clearly noticeable and it is obvious that no patterning defects exist.
To verify that this phenotype is not due to the difference in the sex of these two mice, PCR on the *Sry* gene, a male specific y chromosome locus, was performed. The PCR confirmed that both animals were females. In skeletal preparations of subsequent matings, this phenotype was not seen again, possibly attributable to the genetic background of the mice.

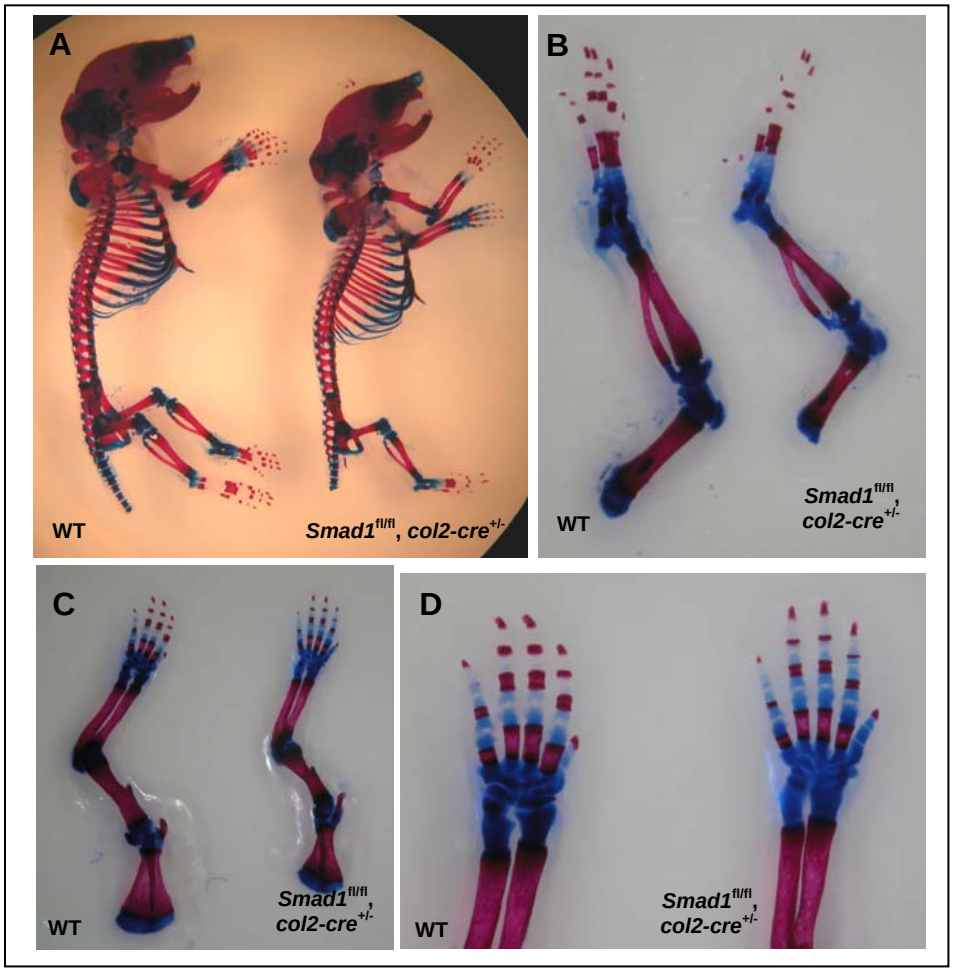

Figure 14: Alcian Blue and Alizarin Red staining of the whole skeleton of a 1.5 dpc old knockout mouse in comparison with a wild type littermate.

Both mice are female. Size difference between wild type and transgenic littermate. Picture B shows the hind limbs, C the forelimb and D only the digits of the forelimb. All parts of the skeleton are shorter and thinner compared the wild type control, but no patterning defects are noticeable.

3.2 Conditional Smad1 knockout in proliferating chondrocytes with Smad5 heterozygous background

Smad1 and Smad5 are both expressed in proliferating chondrocytes close to the zone of maturation (Sakou et al. 1999). Protein similarity (up to 90%) suggests that they may have a redundant function in the growth plate, suggesting that loss of function of one protein could be rescued by the other.

Smad5 and *Smad1* homozygotes are embryonically lethal. Homozygous mutant mice die between 9.5 and 11.5 dpc due to multiple embryonic and extraembryonic defects, but heterozygous animals are viable and fertile (Chang et al. 1999). The conditional knockout model for *Smad5* has been published (Umans et al. 2003) but the group that generated these mice was uncooperative in sharing, so that the line could not be used in these studies. Alternatively, the conditional *Smad1* knockout mice were crossed onto a heterozygous *Smad5* null background, in order to evaluate the impact of a complete loss of *Smad1* in proliferating chondrocytes, in conjunction with haploinsufficiency of *Smad5*. The *Smad5*+/- null mice (on a mixed genetic background) were generously provided by Dr. Martin Matzek (BCM, Houston, USA). To genotype these animals, the PCR protocol described in the original paper was used (Chang et al. 1999).

To study the phenotype of these mice, weight measurements, skeletal preparations and histological analyses, x-ray analyses of two different time points (eight weeks and one year) and Micro-CTs of the head were performed.

3.2.1 Weight measurement and histological analyses of one day old mice

P1 mice were collected for skeletal preparations with subsequent alician blue and alizarin red staining, all of which showed no gross differences. Sex determinations, histological analyses by H & E staining, and weight measurements were also performed.

The weight differences between mice that are deficient for Smad1 in proliferating chondrocytes with (*Smad1*$^{fl/fl}$, *col2-cre*$^{+/-}$, *Smad5*$^{+/-}$) and without a (*Smad1*$^{fl/fl}$, *col2-cre*$^{+/-}$) *Smad5* heterozygous background as well as wild type mice (*Smad1*$^{fl/fl}$) are shown in figure 13; included are data for mice only heterozygous for *Smad5* (*Smad1*$^{fl/fl}$, *Smad5*$^{+/-}$) are also shown (figure 15).

While no significant weight differences among males was observed, weights of females demonstrated an obvious trend, suggesting that mice lacking *Smad1* and/or *Smad5* have a slightly impaired growth rate compared to their wild type littermates. The observed weight difference is close to 0.5 g and this is statistically significant, providing a p-value exceeding 0.006 (figure 15 lower panel, marked with *).

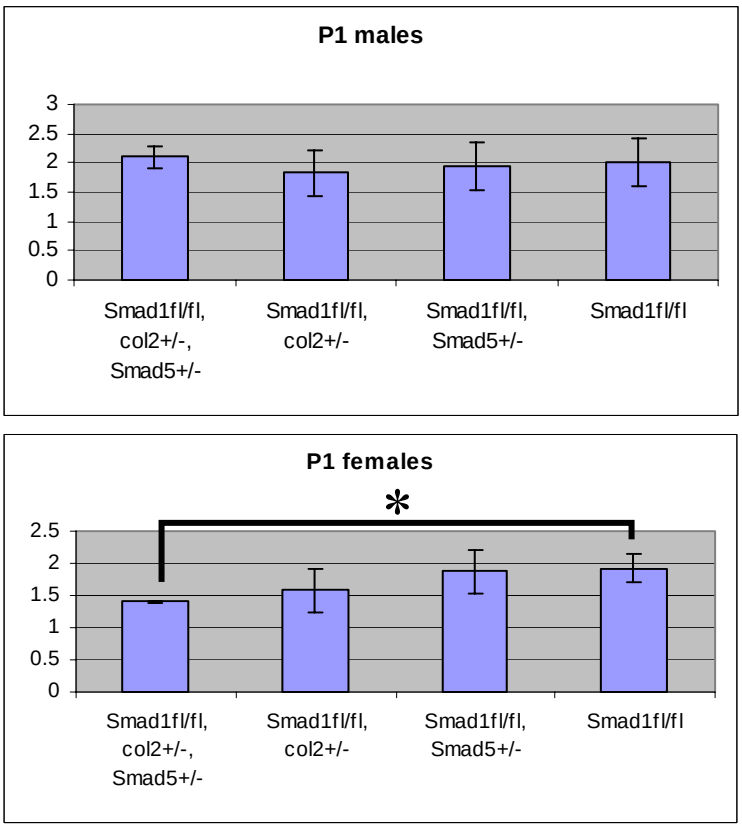

Smad1$^{fl/fl}$, *col2*$^{+/-}$*-cre*, *Smad5*$^{+/-}$ N=4
Smad1$^{fl/fl}$, *col2-cre* $^{+/-}$ N=3
Smad1$^{fl/fl}$, *Smad5*$^{+/-}$ N=9
Control (*Smad1*$^{fl/fl}$) N=10

Smad1$^{fl/fl}$, *col2-cre*$^{+/-}$,Smad5$^{+/-}$ N=4
Smad1$^{fl/fl}$, $^{col2\text{-}cre+/-}$ N=4
Smad1$^{fl/fl}$, *Smad5*$^{+/-}$ N=4
Control (*Smad1*$^{fl/fl}$) N=5

Figure 15: Weighting studies of Smad1 conditional knockout mice, with and without Smad5 heterozygous background.

Weight differences are not statistically significant, (excepting the difference between female *Smad1* knockout mice with *Smad5* heterozygous background compared to the wild type mice marked with *. A trend is however obvious, suggesting that perhaps growth is slightly impaired in mice lacking *Smad1* as well as *Smad5* by affecting proliferating chondrocytes.

Histological findings are more consistent, with both females and males demonstrating a shortened growth plate. The differences among the growth plates for the three mouse phenotypes are exemplified with the distal femur of male mice. Mice lacking *Smad1* in proliferating chondrocytes (on a *Smad5* heterozygous background) have the shortest hypertrophic zone (marked with a green bar) compared to mice that lack only *Smad1* in proliferating chondrocytes (marked with a yellow bar). The wild type control animals (*Smad1*$^{fl/fl}$) display the longest growth plate, which is marked with a red bar.
Comparison of the length of the three bars is shown at the far left in the figure.

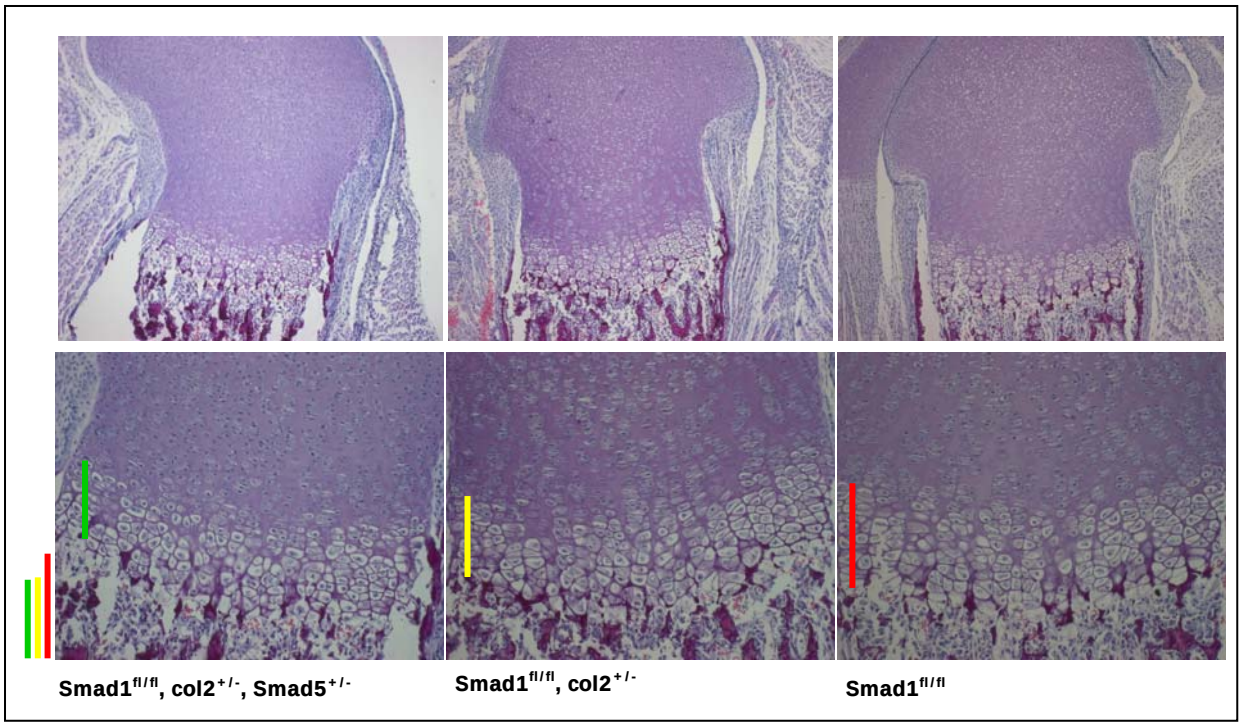

Figure 16: Histological analyses of Smad1 conditional knockout mice, with and without *Smad5* heterozygous background compared to wild type littermates.

In the upper panel 10 x magnification of the distal femurs of mice lacking *Smad1* in proliferating chondrocytes compared with wild type littermates. The lower panel is a 20 x magnification, the length of the growth plate depicted by bars of different colors. Comparison of the length of the bars shows that mice lacking *Smad1* have a shortened growth plate compared to their wild type littermates. A *Smad5* heterozygous background therefore amplifies the phenotype among these mice. No other gross differences could be observed between the knockout and wild type mice.

The weight and histological analyses of P1 mice demonstrated a significant weight difference only in females, but the shortening of the growth plate occurred in both sexes with females and males showing an obvious difference in the length of the growth plate among the three genotypes evaluated.

3.2.2 Weight measurement and histological analyses of adult mice

The weight study of adults was conducted with a total of 67 mice. Breedings produced mice of the three different phenotypes, determined by genotyping at three weeks of age. All weighings of were performed at the same intervals (weekly). The results of the three and seven week old mice are shown in figure 17.

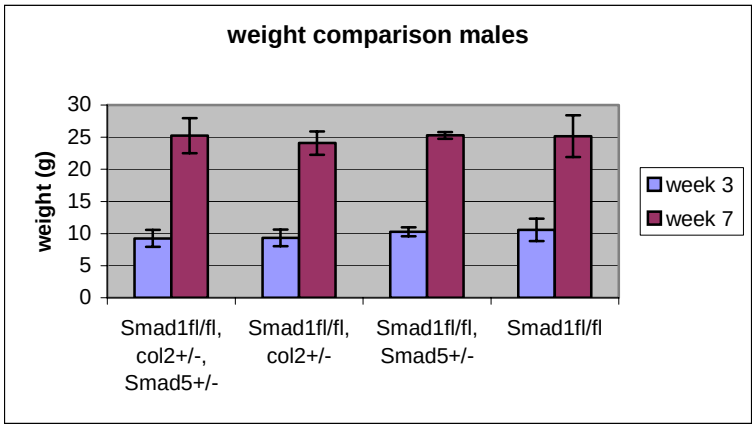

Smad1$^{fl/fl}$, *col2-cre*$^{+/-}$, *Smad5*$^{+/-}$ N=12
Smad1$^{fl/fl}$, *col2-cre*$^{+/-}$ N=8
Smad1$^{fl/fl}$, *Smad5*$^{+/-}$ N=5
Control (*Smad1*$^{fl/fl}$) N=15

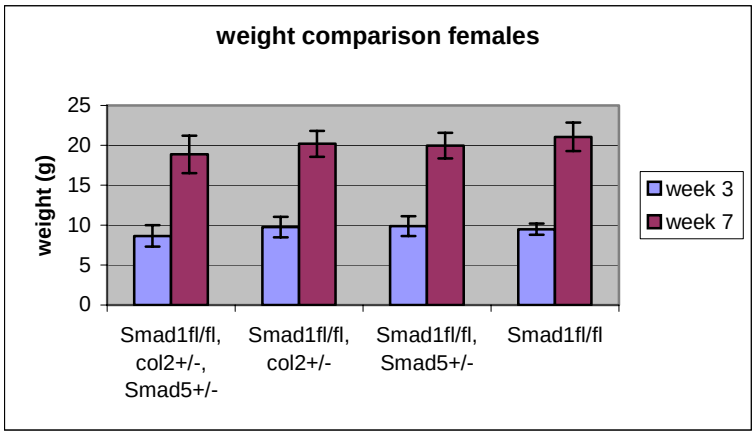

Smad1$^{fl/fl}$, *col2-cre*$^{+/-}$, *Smad5*$^{+/-}$ N=5
Smad1$^{fl/fl}$, *col2-cre*$^{+/-}$ N=9
Smad1$^{fl/fl}$, *Smad5*$^{+/-}$ N=7
Control (*Smad1*$^{fl/fl}$) N=5

Figure 17: Weighting studies of adult *Smad1* conditional knockout mice, with and without a heterozygous background of *Smad5*.

Shown are the weights of mice, aged three and seven weeks, males and females being calculated separately given the substantial weight difference between males and females (especially at seven weeks). Shown are all genotypes. *Smad1*$^{fl/fl}$ serves as a wild type control. There is no big difference observed between wild type and knockout mice and differences are not statistically significant. But there is a trend obvious, which leads to the presumption that there is an impaired growth, which is supported by the histological analyses.

No significant weight difference was observed in either males or females at three and seven weeks of age. Female mice lacking *Smad1* in proliferating chondrocytes with a *Smad5* heterozygous background were slightly lighter in weight then the other three groups.

After completion of the weight studies, the mice were sacrificed at 8 weeks and the limbs were dissected, fixed with formalin for two days and then decalcified with EDTA, pH 7.2 for two weeks. Afterwards the limbs were dehydrated and embedded with paraffin, 7 µm sections were generated and stained with Hematoxylin and Eosin.

Comparison of the growth plates of wild type control animals (*Smad1*$^{fl/fl}$) against *Smad1*$^{fl/fl}$, *Col2-cre*$^{+/-}$ and *Smad1*$^{fl/fl}$, *Col2-cre*$^{+/-}$ with *Smad5* heterozygous background, respectively, demonstrates significant differences (figure 18).

The *Smad1* knockout mice exhibit a shorter growth plate, narrower areas of both the prehypertrophic and hypertrophic zones, with fewer cells present. Additionally the entire growth plate appears somewhat disorganized.

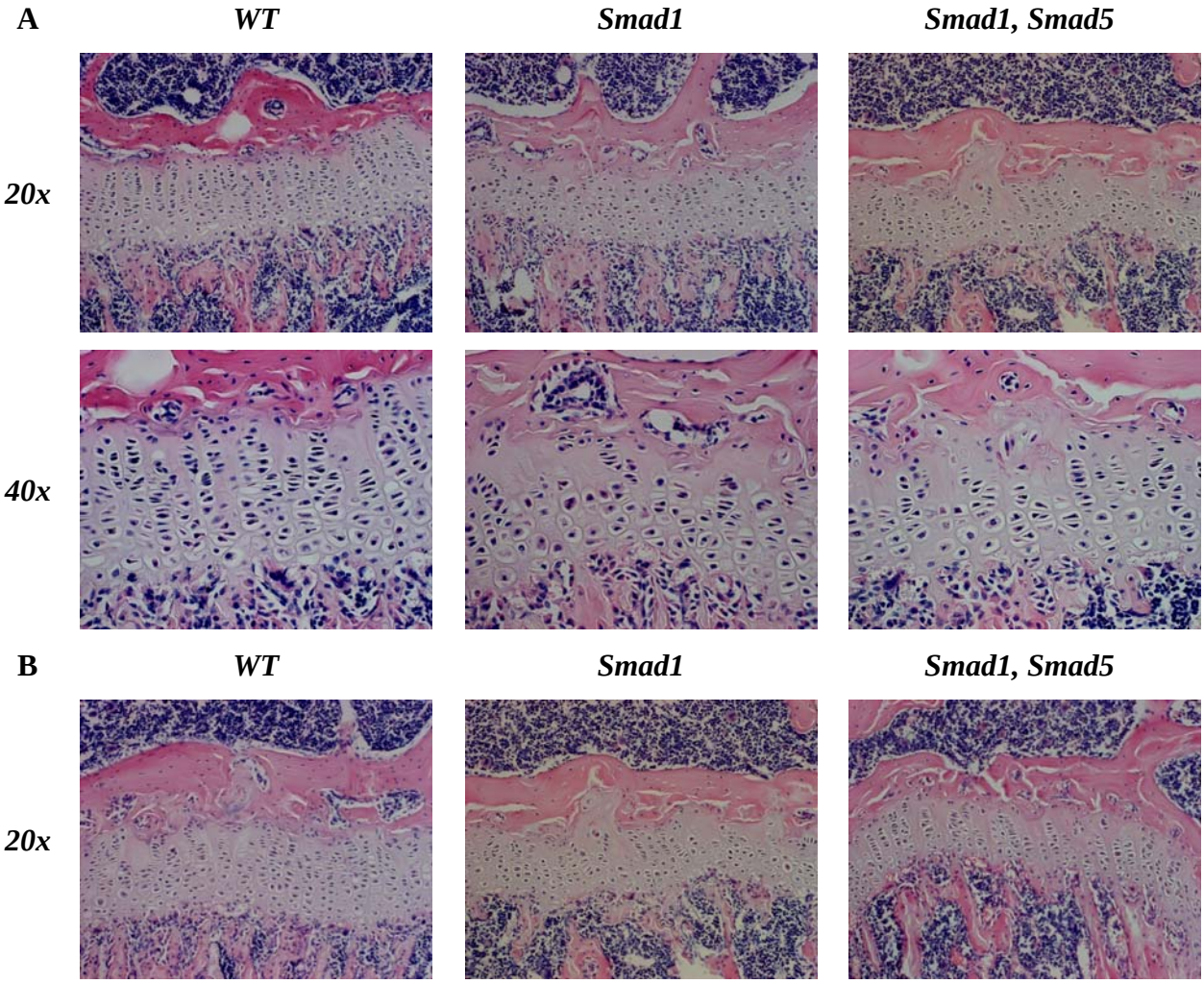

Figure 18: Histological analyses of growth plates in eight week old mice deficient for *Smad1* in proliferating chondrocytes, with and without a *Smad5* heterozygous background.

Upper panels (A): 20 x and 40 x magnifications of the proximal tibia. The left panels are sections of wild type littermates. The middle panel shows the growth plates of mice deficient for *Smad1* in proliferating chondrocytes. The right panel shows shortening and disorganization of the growth plate with fewer cells being detected in *Smad 5* heterozygous background mice. Additionally, the phenotype is slightly reduced in these mice. (B) 20 x magnification of the distal femur of the same mice demonstrating the same phenotypic effects.

The phenotype of mice lacking *Smad1* in proliferating chondrocytes with a heterozygous *Smad5* background is slightly reduced in comparison to *Smad1*deficient mice alone. Fewer cells are also detected in mice where *Smad1* was absent in the proliferating zone (clearly seen in the 40 x magnifications).

3.2.3 Measurement of the proliferation rate with BrdU

It was next necessary to determine, if the shortening of the growth plate was due to a decreased proliferation rate in the knockout animals. The proliferation rate can be measured with Bromodeoxiuridin (5-bromo-2-deoxyuridine, BrdU). BrdU is an analogue of thymidine and it is incorporated into newly synthesized DNA of cells that are replicating (S-phase cells). BrdU was injected into newborn mice of all three genotypes and after 2 hours these mice were sacrificed and the limbs were processed for histological analyses. Sections were prepared and the BrdU was detected by monoclonal antibody, coupled to a fluorescent dye. Proliferating cells can be detected in this way and are counted and compared to the total of all cells counted. To count cells specific regions were demarcated as depicted in figure 19.

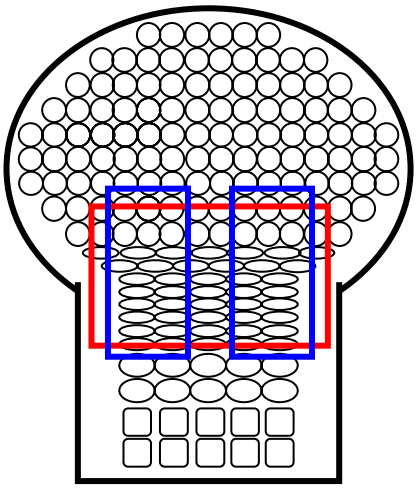

Figure 19: Schematic of a growth plate.

The schematic shows the region of the growth plate used to count BrdU positive cells marked by the red rectangle. This approach was also followed for studies of the tibia.
The two blue rectangles identify the regions that were used for counting BrdU positive cells in femurs.

Histological analyses revealed that mice lacking *Smad1* in proliferating chondrocytes with a *Smad5* heterozygous background had significantly fewer proliferating cells than wild type controls (figure 20, upper panel).

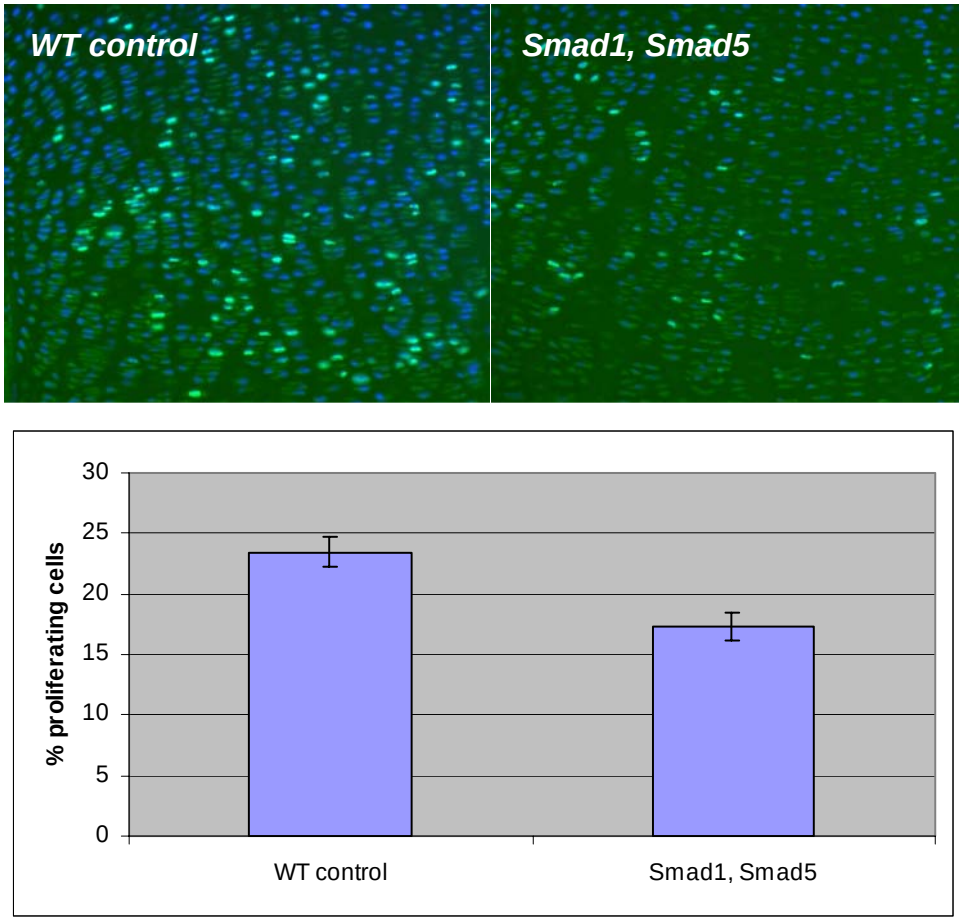

Figure 20: Rates of proliferation in mice lacking *Smad1* with a *Smad5* heterozygous background compared to wild type controls.

In *Smad1* conditional knockout mice with a *Smad5*$^{+/-}$ background, 17.3 % proliferating cells could be detected as compared to wild type mice a frequency of 23.4 %. A p value of 0.006 demonstrates this result to be statistically significant. The upper panel shows BrdU stained sections of P1 distal femurs: a Smad conditional knockout mouse with haploinsufficiency of *Smad5* compared to a wild type control.

Cell counts demonstrated that wild type mice had 23.4% proliferating cells, while the proliferation rate in *Smad1* conditional knockout mice was decreased to 17.3% (figure 20, lower panel). This result is statistically significant (p value = 0.006).

3.2.4 In situ Hybridization with probes specific for Ihh and Col10a1

To corroborate the reduced areas of the prehypertrophic and hypertrophic zones, *in situ* hybridization on hind limb sections was performed with riboprobes specific for *Ihh* and *col10a1*. *Ihh* is a marker specifically expressed in the prehypertrophic zone, while *Col10a1* serves as a marker for the hypertrophic zone.

The hypertrophic zone is slightly shorter in *Smad1* conditional knockout mice and consistently the expression of *Ihh* is visibly decreased in these animals as well. In mice with an additional heterozygous null background for *Smad5,* the expression of *Ihh* seems to be slightly elevated compared to the expression of *Ihh* in the *Smad1* conditional knockout mouse, but the prehypertrophic zone is still shorter compared to the wild type littermates (figure 21).

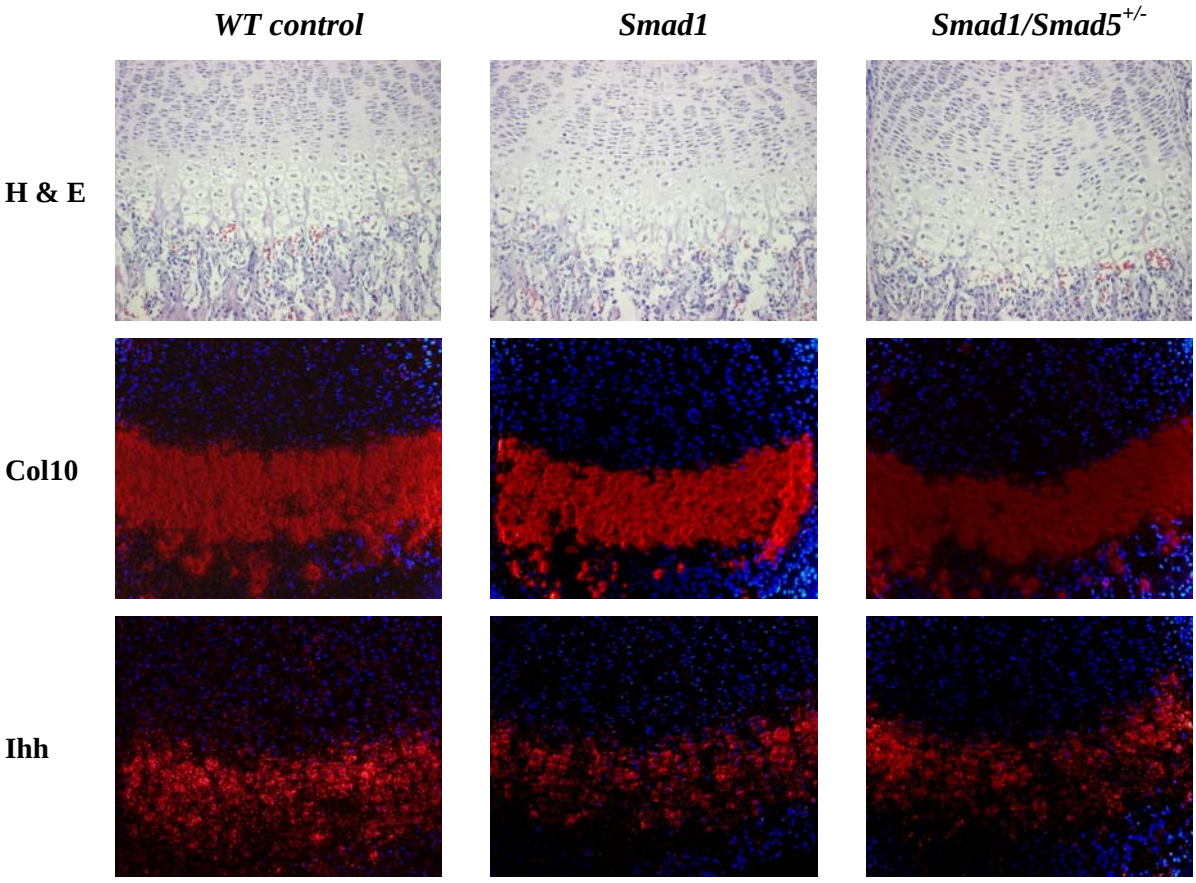

Figure 21: *In situ* Hybridization on hind limb sections of *Smad1* conditional knockout mice with and without *Smad5* heterozygous background.

Both the hypertrophic (*col10a1*) and the prehypertrophic (*Ihh*) zones are shortened in *Smad1* conditional knockout mice. Less *Ihh* is expressed in knockout mice for *Smad1* with and without heterozygous Smad5 background.

As a result of the decreased proliferation rate, fewer cells enter terminal differentiation, leading to a shortening of the prehypertrophic as well as the hypertrophic zone. Differentiation itself is likely not impaired.

3.2.5 Cartilaginous Matrix composition and mineralization

Safranin O staining can reveal changes in the composition of the extracellular matrix (ECM). Proteoglycans are stained; differences in the color of the staining occur when the production of proteoglycans is impaired. The staining of wild type compared to conditional *Smad1* knockout mice with *Smad5* heterozygous background showed no gross differences in the extracellular matrix of either genotype (figure 22A).

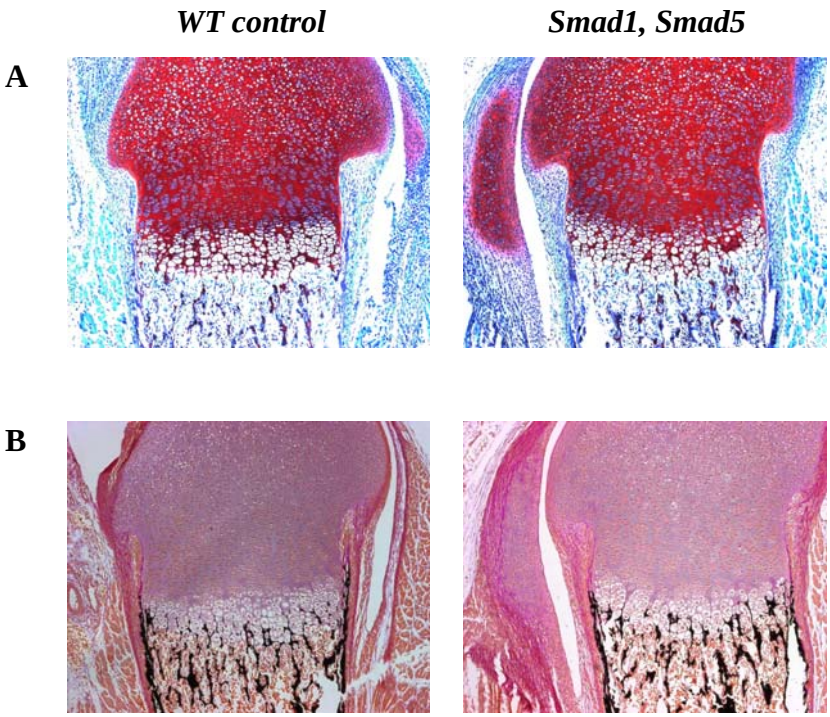

Figure 22: Safranin O and von Kossa Staining of hind limb sections of one day old knockout mice compared to wild type littermates.

10x magnification of the distal femur (A) Safranin O stains proteoglycans in the extracellular matrix. No differences in the matrix composition between knockout (*Smad1* with *Smad5* heterozygous background) and wild type mice can be observed. (B) Mineralization assay with von Kossa staining. No differences in the mineralization in *Smad1* conditional knockout mice with *Smad5* heterozygous background can be detected.

Von Kossa staining was used to examine whether there was a difference in the mineralization of the newly formed bones between the genotypes. In this staining technique, silver replaces calcium and is visualized by a chemical reduction with light.

No mineralization difference was detected between wild type and Smad1 conditional knockout mice with Smad5 heterozygous background (figure 22B). But the Von Kossa staining clearly demonstrates and affirms the shortening of hypertrophic zone in the conditional knockout mice.

Given these data, Smad1 and Smad5 do not seem to play a role either in the production of molecules of the extracellular matrix or in the mineralization of the newly formed bone.

3.2.6 X-ray analyses of eight weeks and one year old knockout mice

X-rays were taken from eight week old mice as described in 2.16 and no differences could be observed in the bones of the appendicular skeleton. The size of all bony elements as well as the bone density was within normal ranges.

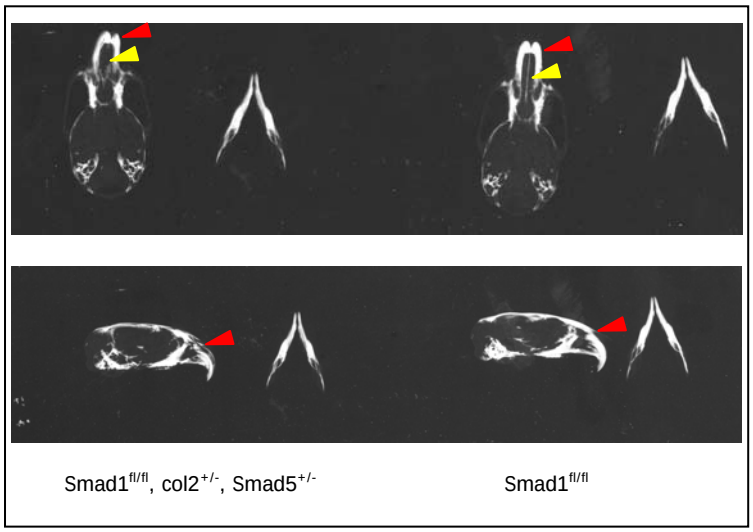

Figure 23: X-ray analyses of heads of one-year-old mice.

The upper panel shows the skull ventrally with the mandible separated from the skull. The mandible appears normal and no gross size difference is noticeable between knockout and wild type animals. The nasal cartilage appears to be disorganized and the nasal septum is absent (yellow triangle). The lower picture shows the lateral view of the same heads and a slight disorganization of the maxilla could be observed (red triangle).

A craniofacial phenotype was observed, when comparing *Smad1* conditional knockout with *Smad5* haploinsufficiency and wild type animals. In one-year-old mice, the nasal cartilage is disorganized and the nasal septum completely absent (figure 23). No striking differences between the mandibles or the heads were seen.

To verify these results, eight-week-old mice were also analyzed and the same phenotype was observed. These mice have no obvious phenotype in the appendicular skeleton, no remarkable size differences, nor lower bone density, but the same craniofacial phenotype was seen in these eight week old mice as was observed in the one-year-old mice (figure 24). The mice also demonstrate a disorganized nasal cartilage and absence of the septum. Between mice on and without a *Smad5* heterozygous, a size difference could be noticed, which leads to the suggestion that *Smad1* and *Smad5* have similar, but not completely redundant functions in the development of the craniofacial skeletal elements.

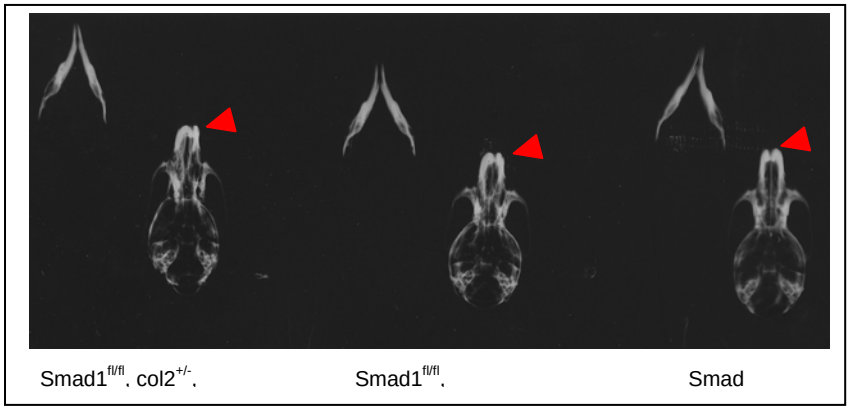

Figure 24: X-ray eight-week-old mice.

X-ray images from heads from eight-week-old mice show a similar phenotype to one-year-old mice. The nasal septum is absent and the cartilaginous part of the nose is disorganized. Comparison of *Smad1* knockout mice in proliferating cartilage, without the *Smad5* heterozygous background, with wild type mice shows that these mice have also a smaller head.

To verify these data, Micro-CT analyses of the heads of these mice was performed, but no gross difference was observed between them (figure 25).

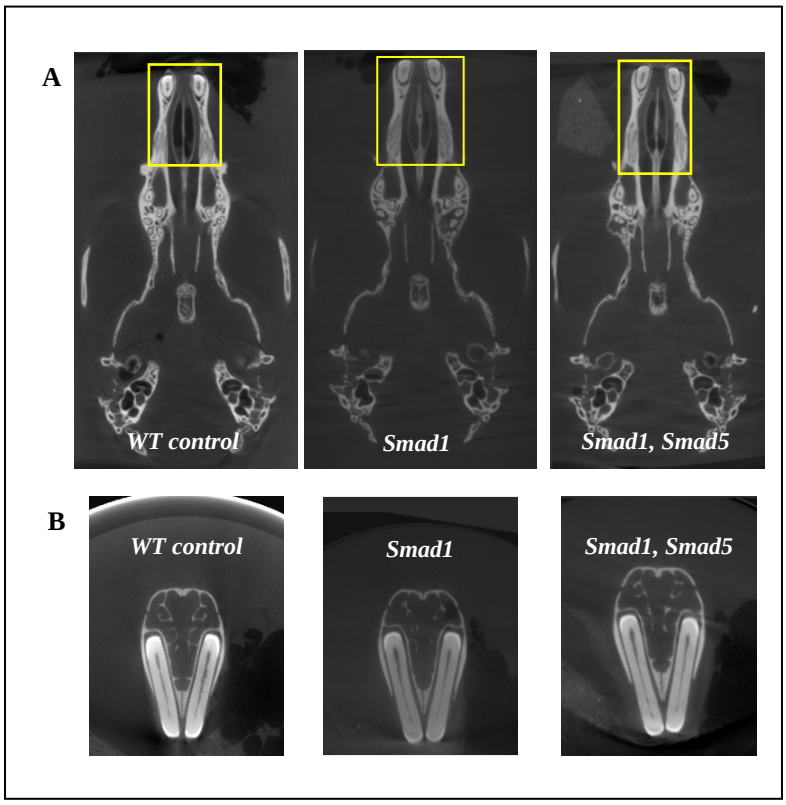

Figure 25: Micro-CT on heads of eight weeks old *Smad1* conditional knockout mice on and without Smad5 heterozygous background.

(A) Transverse section through the head close to the nasal cartilage. In *Smad1* conditional knockout mice the nasal region seems to be slightly disorganized, whereas in mice with *Smad5* heterozygous background the phenotype appears slightly more severe. The entire snout region is disorganized, perhaps asymmetric. (B) Frontal section through the snout region showing no difference between *Smad1* conditional knockout mice and the wild type control. With *Smad5* heterozygous background the incisors are not in an even plane.

Only the obvious size difference (by x-ray) and the clear disorganization of the nasal region (figure 25A) are evident as phenotypic effects among these mice. Frontal sections through

the snout region of the head show no striking differences between mice lacking Smad1 in proliferating chondrocytes compared to wild type controls. The right panel of figure 25A shows sections from a knockout mouse with *Smad5* haploinsufficiency; no difference could be detected, but the nasal region shown in the lower panel of the figure seems to be more disorganized in these mice compared to the *Smad1* conditional knockout. The snout region seems to be slightly asymmetric, which might be a consequence of mechanical stress. These same observations were made in one-year-old mice (data not shown).

BMP signaling is critically important in the development of craniofacial structures. The loss of function of *Smad1* and *Smad5* in proliferating chondrocytes leads to a shortening of the head (*Smad1*) as well as to impaired development of the nasal cartilage (*Smad1* as well as *Smad1* and *Smad5*).

3.3 Transgenic mouse studies

3.3.1 Overexpression of Esl1 in proliferating chondrocytes

As a result of Esl-1 being co-purified in a large complex together with TGFβ1 (Steegmaier et al. 1995) and the knockout mouse model of *Esl-1* showing distinctive skeletal and growth defects, a role for Esl-1 in the negative regulation of the TGFβ signaling pathway was hypothesized. To assess the role of Esl-1 in the regulation of TGFβ and its role in development of the long bones, a transgenic mouse model was created overexpressing *Esl-1* specifically in proliferating chondrocytes.

3.3.1.1 Generation of the transgenic mice and genotyping

Transgenic mice were created by first cloning *Esl-1* cDNA, attached to a myc-tag, under the control of a 6kb *col2a1* promoter (Zhou et al. 1998) (figure 26A). To increase the transcription efficiency, a woodchuck hepatitis virus posttranscriptional regulatory element (WPRE) followed by the human growth hormone polyadenylation signal (hGHpA) was incorporated into the construct. WPRE can posttranscriptionally stimulate the expression of heterologous cDNA up to 10 fold (Donello et al. 1998; Zufferey et al. 1999; Mian et al. 2005). The construct was next cloned into a vector with *Tyrosinase* cDNA under the control of the K14 promoter, allowing for visual genotyping. Mice born carrying the transgene and expressing it at appreciable levels will have black eyes (as a result of the influence of the K14 promoter) and reflect successful integration of the construct into injected pronuclei of mice from FVB/N background (figure 27). The vector also contains also the HS4 chicken β-globin insulator sequences that help to prevent transgene silencing resulting from putative positional silencing effects of the transgene integration site. The construct is released with PacI digestion, and the DNA gel purified using QUIAEXII (2.4.5); concentration is determined by spectrophotometry and the quality of the DNA ascertained by electrophoresis of construct dilutions at diminishing concentrations on an agarose gel.

The first injection of the construct resulted in the delivery of 14 pups, but none with black eyes. A PCR was performed with WPRE specific primers, able to specifically detect the transgene, (marked as a black bar in the schematic of the construct) and revealed that four of the 14 mice born actually carried the transgene (figure 26B).

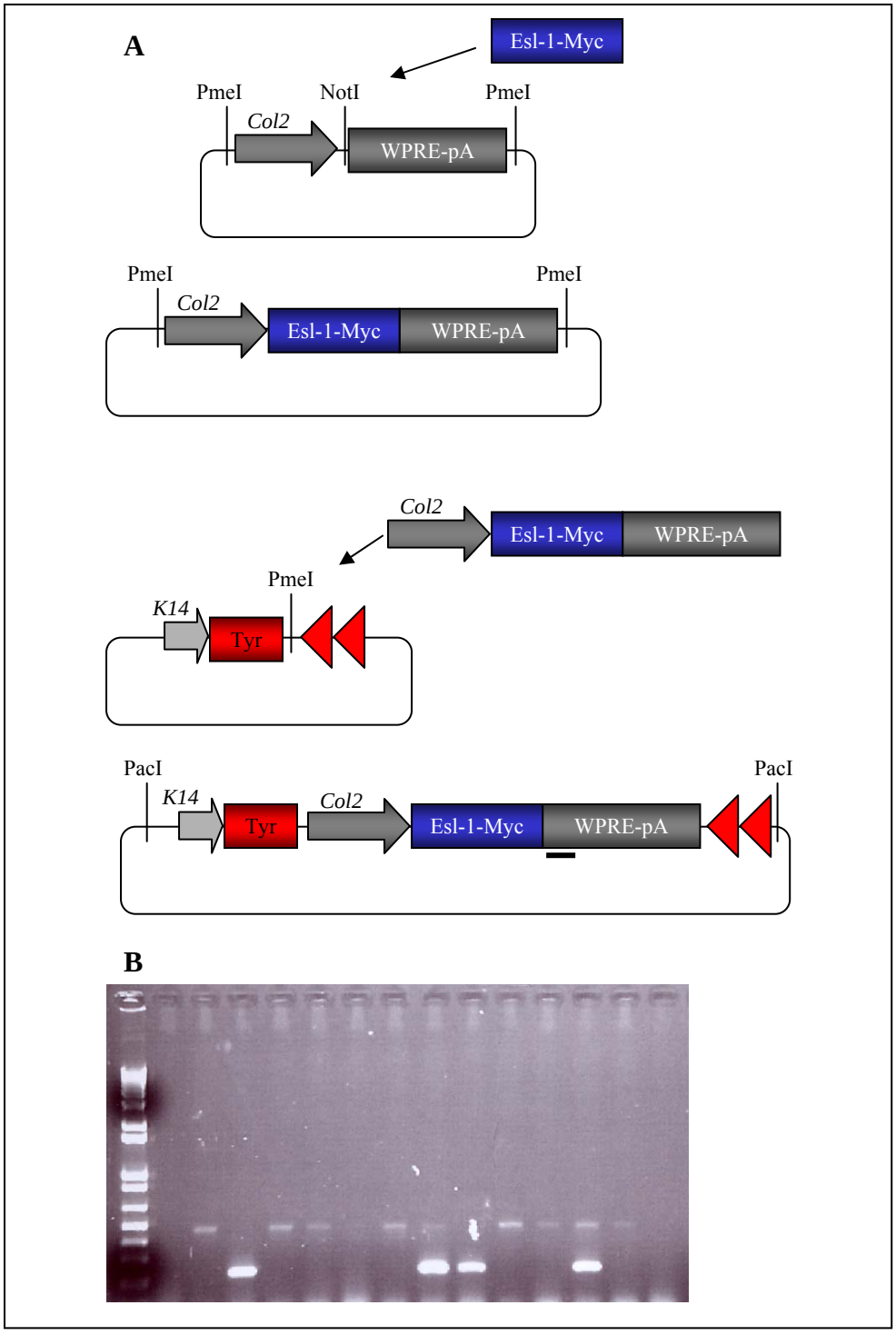

Figure 26: Cloning strategy of *Col2-Esl-1* transgenic mouse construct and PCR genotyping of the received founders.

(A) The *Esl-1* cDNA, containing a myc tag on the 3' end was released from the original plasmid with PmeI and cloned into the blunt ended NotI-restriction site between the *Col2a1*-promoter fragment and the WPRE-polyA cassette. This complete cassette could be released with PmeI and was cloned into the *Tyrosinase* vector, also accessed with PmeI. The construct was cut out with PacI and purified for injection. All junctions were sequenced to verify the correct orientation of the insert. (B) 14 animals from 2 separate female deliveries were obtained none had black eyes as a result of weak *Tyrosinase* expression. Genotyping PCR revealed that 4 out of these 14 animals actually carried the transgenic allele.

The level of expression of the transgene was however insufficient to increase the melanin levels of the eyes, also suggesting poor overall integration of the transgene.

These weakly transgenic mice were crossed with FVB/N wild type mice and from these matings three out of the four founder mice (by PCR genotyping) delivered transgenic littermates with black eyes (BE). Figure 27 shows a wild type and a transgenic mouse differentiable because of the black ring around the eye of the transgenic littermate (as a result of the abundant expression of *Tyrosinase* under the control of the K14 promoter in its eyes).

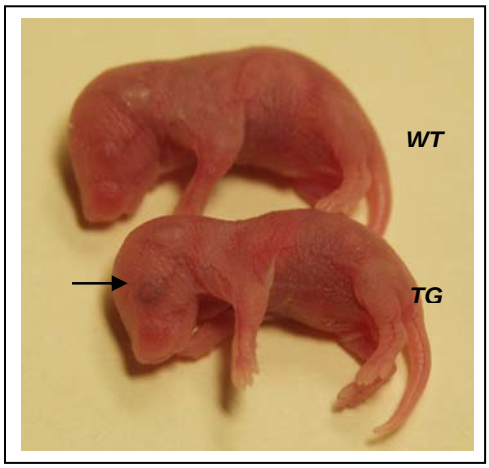

Figure 27: Visual genotyping of transgene mice carrying the *Tyrosinase* cassette.

TG Transgenic animal with the characteristic black ring around the eyes, which confirms the expression of the *Tyrosinase* gene cassette introduced in conjunction with the transgenic allele. *WT* littermate is shown as control.

3.3.1.2 Quantitative PCR on ribcage (cartilage) cDNA

Esl-1 is overexpressed in the transgenic mouse line (14.5 fold). The proliferating and resting chondrocyte markers *Col2a1*, *Sox9* and *PTHrP* are decreased in the transgenic cartilage, whereas terminal differentiation markers, like *Col10a1* and *Ihh*, are increased (see figure 28). These results are in opposition to the qPCR data from the *Esl-1*$^{-/-}$ cartilage, suggesting that the gain of ESL-1 function is sufficient to downregulate TGF-β activity in the cartilage thus leading to increased hypertrophy in the growth plate (unpublished data Tao Yang).

Quantitative PCR (qPCR, 2.5.4) performed on cartilage cDNA isolated from the ribcage, was conducted to confirm the overexpression of the *Esl-1* transgene and to evaluate the expression pattern of select cartilage markers.

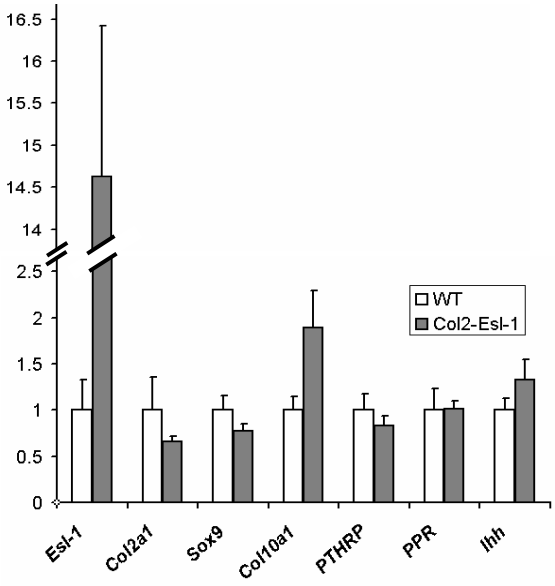

Figure 28: Real-time PCR on cartilage cDNA.

Quantitative PCR (on cartilage cDNA) confirms the overexpression of Esl-1 in proliferating chondrocytes. *Esl-1* is expressed 14.5 x higher than in wild type littermates. The expression of cartilaginous markers is altered in the transgenic mice relative to wild type. *Col2a1* expression is lowered, by almost half the expression normally seen in wild type. The expression of *Sox9* and *PTHRP*, markers for proliferating and resting chondrocytes, is lowered and *Col10a1* expression as well as *Ihh* expression is elevated in transgenic mice, whereas the expression of *PPR* is virtually unchanged.

3.3.1.3 Weight measurements and skeletal findings in *col2-Esl-1* transgenic mice

P2 wild type and transgenic mice (n=11) were weighed and skeletal preparations were evaluated, no obvious size difference was observed (figure 29).

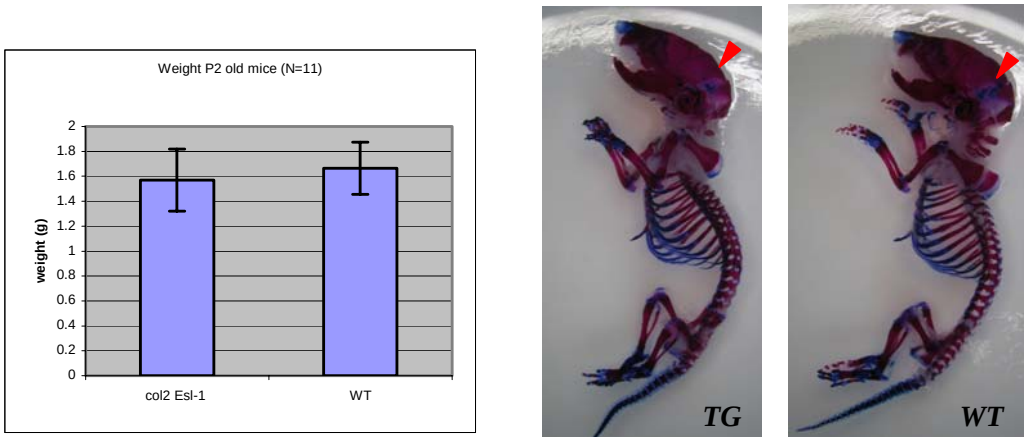

Figure 29: Comparison of the weight and skeletal findings of two-day-old *Col2-Esl-1* transgenic mice.

The weight difference of mice that overexpress *Esl-1* in proliferating chondrocytes compared to their wild type littermates is negligible. The average difference is only 0.1 g and is not statistically significant (left panel). Neither size nor patterning defects could be detected in the skeletal preparation of P2 transgenic mice. But the cartilaginous part of the occipital bone appears to be smaller as compared to the wild type (red triangle). WT, wild type; TG, *Col2-Esl-1* transgenic mouse.

The average weight difference between mice at this time point is only 0.1 g. While transgenic mice are lighter than their wild type littermates the difference is not statistically significant. Skeletal examinations revealed a cartilaginous difference in the occipital region but otherwise unremarkable findings.

Skeletal preparations followed by Alcian Blue and Alizarin Red staining showed no difference between the mice overexpressing *Esl-1* in proliferating chondrocytes when compared to their wild type littermates. There is no obvious patterning defect in these mice. All skeletal elements appear to be normal and no difference in the length of the elements is observed. The head appears to be normal, except for a slight difference in the Alcian blue staining in the cartilaginous area of occipital bone (figure 29, right panel, red arrow).

This result is comparable to the observation that in *Esl-1* null mice the cartilaginous part of the occipital bone is larger (observation T. Yang), suggesting that in *Esl-1* null mice endochondral bone formation is inhibited, while it is accelerated in mice overexpressing *Esl-1* in proliferating chondrocytes enhancing the ossification of the cartilaginous parts of the occipital bone.

3.3.1.4 Histological analyses of hind limb sections of two days old *Col2-Esl-1* transgenic mice

Hind limbs of two-day-old mice were embedded with paraffin (2.15.1), serial sections were generated by microtome (2.15.2) and stained with H & E (figure 28).

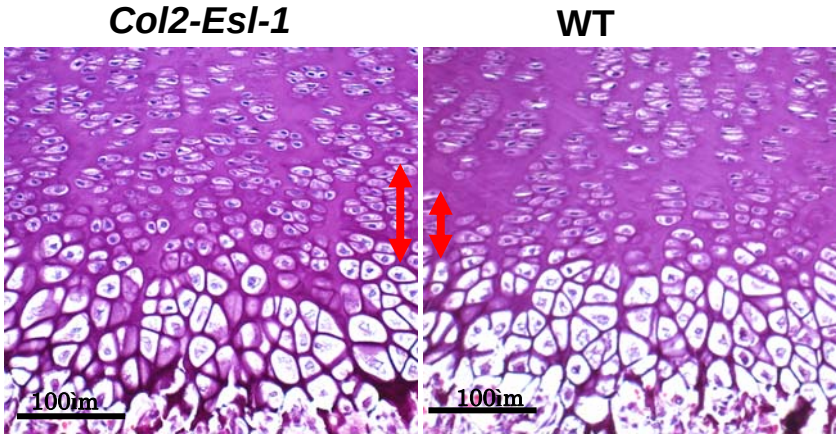

Figure 30: Hind limb sections of the *Col2-Esl1* transgenic mouse and a wild type littermate.

20 x magnification. Hind limb sections following H&E staining show increased numbers of cells and an elongated prehypertrophic zone in the transgenic mouse (red arrow). WT, wild type; *Col2-Esl1* transgenic mouse, overexpression of *Esl1* in proliferating chondrocytes.

The cell density is higher in the transgenic *Col2-Esl-1* mice compared to their wild type littermates. The junction where the proliferating chondrocytes differentiate to hypertrophic chondrocytes is significantly elongated (red arrow), while there is no difference in the overall length of the hypertrophic zone. The proliferation rate seems to be elevated (compare chapter 3.2.2.5) and the hypertrophy of the cells is accelerated. No disorganization of the growth plate is observed.

3.3.1.5 Proliferation assay with BrdU labeling

BrdU is used to assess the proliferation rate of cells (chapter 3.1.3). Since the cell density is elevated in mice overexpressing *Esl-1* in proliferating chondrocytes, an accelerated proliferation rate is anticipated.

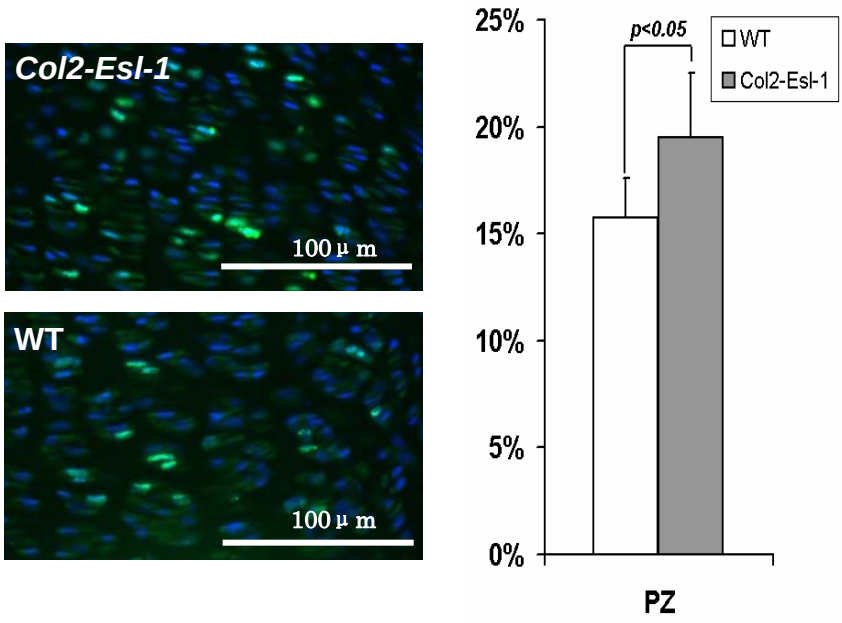

Figure 31: BrdU staining of *Col2-Esl1* transgenic mice and wild type littermates.

The left panel shows sections, which were stained with a BrdU antibody. Proliferating cells are green; all other cells can be counted by DAPI counterstaining. The right panel shows the results of the cell counts. An increase of 4% proliferating cells is seen in the *col2-Esl1* transgenic sections compared to wild type specimens.

BrdU was injected intraperitonally into mice, and 2 hours thereafter newborn animals were sacrificed, limbs skinned, dissected and fixed with formalin. The limbs were embedded (2.15.1), sectioned (2.15.2) and BrdU was detected in an assay using a specific antibody,

coupled to a fluorescent dye. The mounting medium contains DAPI, which stains nuclei blue in contrast to cells, which incorporate BrdU while proliferating, which are stained green. Complete cell counts (DAPI) as well as counts of proliferating cells were conducted, followed by calculation of the percentage of cells proliferating (figure 31). In wild type mice typically 15% of proliferating cells could be counted, whereas the *Col2-Esl-1* transgenic mice demonstrate a 4% increase in proliferating chondrocytes. Inhibition of the TGFβ signaling pathway in proliferating chondrocytes leads to an increased proliferation rate, which suggests, that the antiproliferative function of TGFβ is disrupted in the transgenic mice.

3.3.1.6 *In situ* hybridization of *Ihh* and *col10a1*

To further analyze the apparent lengthening of the prehypertrophic zone, *in situ* hybridization was performed on hind limbs of two-day-old animals. *Ihh* is a marker specific for prehypertrophic chondrocytes. In the transgenic *Col2-Esl-1* mice the expression of *Ihh* is elevated, however this is expected since Esl-1 acts as a repressor for TGFβ signaling that itself promotes terminal differentiation.

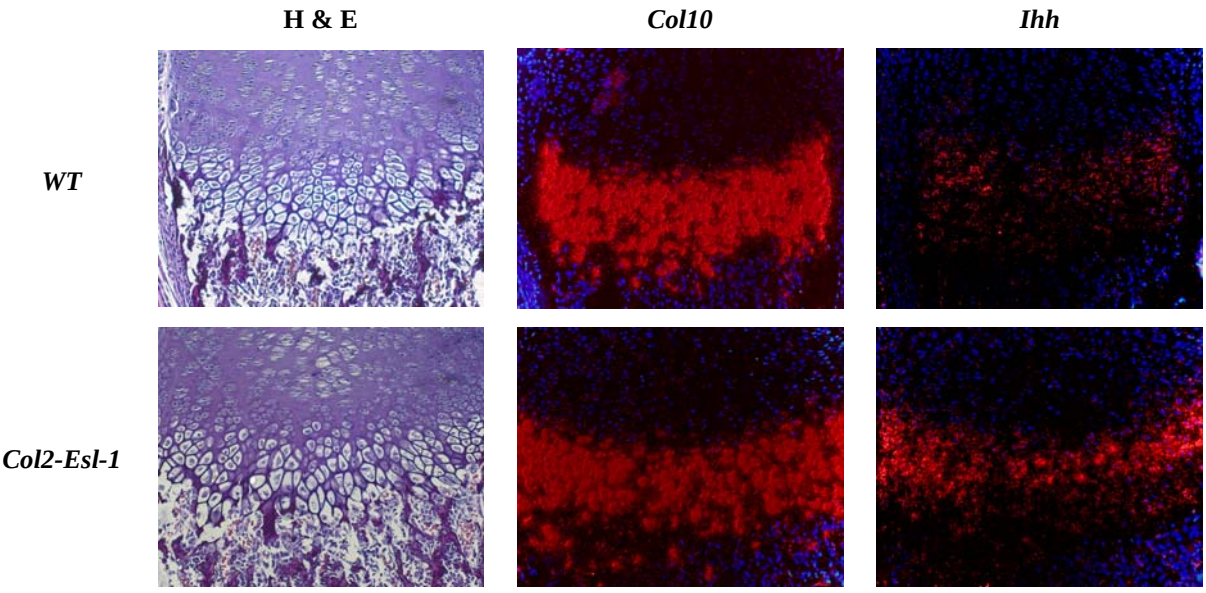

Figure 32: *In situ* hybridizations: hind limb sections of P2 transgenic and wild type mice.

Only a slight elongation of the hypertrophic zone is observed in mice overexpressing *Esl-1* in proliferating chondrocytes, while *Ihh* expression in the transgenic mice is significantly elevated.

Explanation of observations of the hypertrophic zone is difficult. Quantitative real time PCR (compare chapter 3.3.1.2) showed a distinct elevation in the *Col10a1* expression of transgenic

mice, not upheld by the *in situ* hybridization. The higher *Col10a1* expression could be attributed to the elongated prehypertrophic chondrocyte zone (figure 32). Additionally, the cells of the hypertrophic chondrocytes appear to be larger when compared to the wild type littermates; this also could influence for the increased *Col10a1* expression level in transgenics.

3.3.1.7 Histological analyses of 4 week old transgenic mice

Following study of the P2 transgenics, it was decided to analyze four-week-old transgenic mice as well. The weighing study of four week olds suggested that the transgenic *Col2-Esl-1* mice were lighter in weight than their wild type littermates; a difference of 2.3 g was seen in males but the result was not statistically significant, (N equals 7 for each group (figure 33A)). The difference in females could not be studied, given an insufficient number for statistical evaluation.

(A) Weight comparison **(B) H & E staining**

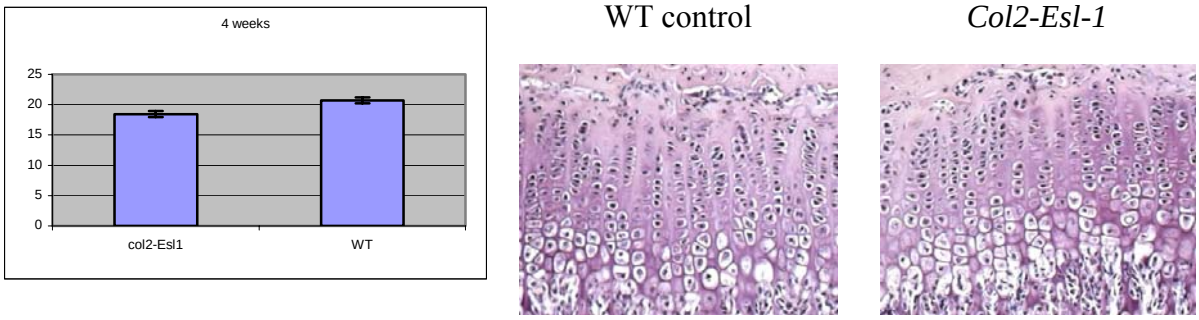

Figure 33: Weight comparison and histological analyses of four-week-old *Col2-Esl-1* transgenic mice.

(A) Weight comparison of four weeks old males. *Col2-Esl-1* transgenic mice are 2.3 g lighter in weight then their wild type littermates. The result (p value of 0.06) is not however statistically significant. The Histological analyses in hind limbs of males is shown in (B). The magnification of the growth plate of the distal femur is 20x. The hypertrophic zone appears only slightly elongated.

The histological analyses suggested that the growth plate is only slightly elongated, and that this elongation results from a longer hypertrophic zone. These histology results are conflicting with those of two-day-old mice, where the proliferating zone showed more cells and the junction of the proliferating to hypertrophic zones appeared elongated (figure 33).

Overexpression of *Esl*-1 in proliferating chondrocytes leads to inhibition of the TGFβ signaling in this tissue, as expected. The antiproliferative effect of TGFβ in the later stages of endochondral ossification is noticeably abolished. The growth plate in the transgenic mice is elongated, more cells can be detected in the proliferating zone, and the prehypertrophic zone as well as hypertrophic zone is enlarged. The markers for these later stages of differentiation (*Ihh* and *Col10a1*) are expressed in higher levels compared to wild type mice.

3.3.2 Overexpression of ΔTβRI in proliferating chondrocytes

An alternate approach to study loss of function or impaired function of TGFβ signaling in the growth plate of transgenics is to overexpress the dominant negative TGFβ receptor type I (TβRI, ALK5) specifically in proliferating chondrocytes. The dominant negative TβRI is a truncated protein, retaining the ligand binding domain and the transmembrane domain, but lacking the activating threonine kinase domain. It can bind TGFβ ligands, but the mediation of the signal is impeded, since the receptor is not able to activate the Smad proteins by phosphorylation. Additionally, by binding the ligand, the ligand itself is not able to bind to a fully working receptor, thus eliminating confounding effects of ligand interaction. The plasmid containing the dominant negative TβR1 (ΔTβR1) was a generous gift of Dr. Rik Derynck (University of California, San Francisco, USA). The protein is coupled to a flag tag at the 3'end.

3.3.2.1 Generation of *Col2-ΔTβR1* transgenic mice and PCR genotyping

The strategy used to generate this transgenic mouse model is similar to the strategy used to clone the transgenic allele for the overexpression of Esl-1 in proliferating chondrocytes (compare chapter 3.3.1.1, figure 26). The dominant negative *TβR1 (ΔTβR1)* cassette was released from its original vector, blunt ended and cloned into a NotI restriction site of the plasmid containing the *Col2a1* promoter fragment and the WPRE-polyA cassette.

Figure 34: Schematic of the *Col2-ΔTβRI* construct.

The truncated cDNA of the protein is coupled to a Flag-tag and followed by a WPRE cassette, which functions to enhance the transcription of the protein. A 6 kb collagen type II promoter fragment leads to a specific expression of the transgene in proliferating chondrocytes. The *Tyrosinase* cassette under the control of the K14 promoter allows visual genotyping of the transgenic animals; the two HS4 chicken insulator sequences (red triangles) protect the transgenic allele against possible positional effects. K14, K14 (keratinocyte) promoter; Tyr, *Tyrosinase*: Col2, collagen type II promoter; WPRE woodchuck hepatitis virus posttranscriptionally regulatory element; hGHpA, human growth hormone polyadenylation signal.

The construct was released using PmeI and cloned between the K14-*Tyrosinase* cassette and the insulators (figure 34).
The correct insertion of the dominant negative protein was verified by sequencing the junctions and the construct was released with PacI and gel purified using QUIAEXII (2.4.5) and the resulting DNA was injected into pronuclei.

Three founder mice (two male and one female), demonstrating a high expression level of the transgenic allele, were generated from three separate surrogate mothers. A very high level of expression was evidenced given the founder mice not only had black eyes due to *Tyrosinase* expression, but gray patched fur. These mice were crossed back to FVB/N wild type mice and the R1 offspring were collected for initial observations of phenotypic effects.

3.3.2.2 Weighting studies of the R1 generation of *Col2-ΔTβR1* transgenic mice

Before the two-day-old mice were dissected for skeletal preparation and limb histology, their weight was measured (N equals 7).

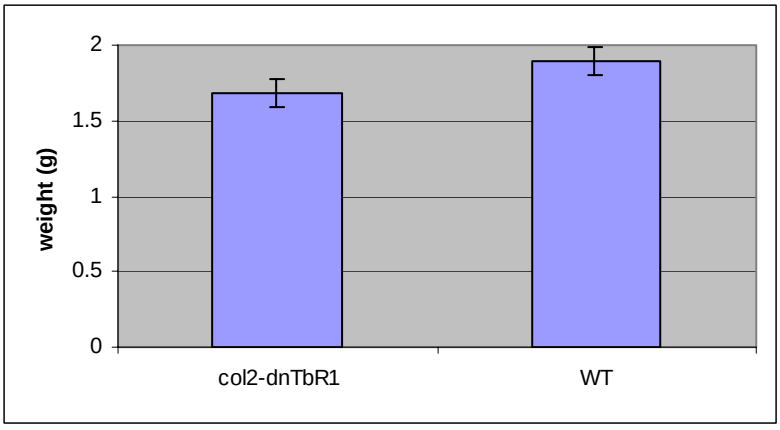

Figure 35: Weight comparison of transgenic *Col2-ΔTβR1* and their wild type littermates.

The weight of two-day-old transgenic mice and their wild type littermates was measured. N equals 6 in both groups. The weight difference in females is 0.22 g and is statistically significant ($p<0.05$).

Two-day-old transgenic mice show a statistically significant weight reduction when compared with their wild type littermates. Skeletal preparation with Alcian blue and Alizarin red staining showed no difference in the patterning and size of the skeleton (data not shown),

consistent with findings of the *Col2-Esl-1* transgenic mice (compare chapter 3.3.1.3). The skeletal elements also appeared to develop normally.

3.3.2.3 Histological analyses of two day and four week old R1 generation Col2-ΔTβR1 transgenic mice.

Staining with Hematoxylin and Eosin revealed an elongated hypertrophic zone in the transgenic mice compared to the wild type controls and larger than normal cells could be observed in proliferating, prehypertrophic as well as the hypertrophic zones of transgenics. It is clearly visible that there are fewer cells in the proliferating and prehypertrophic zones of the *Col2-ΔTβR1* transgenic growth plate in comparison with the growth plate of the wild type control mice. The cells also appear slightly disorganized in the transgenic tissues (figure 36).

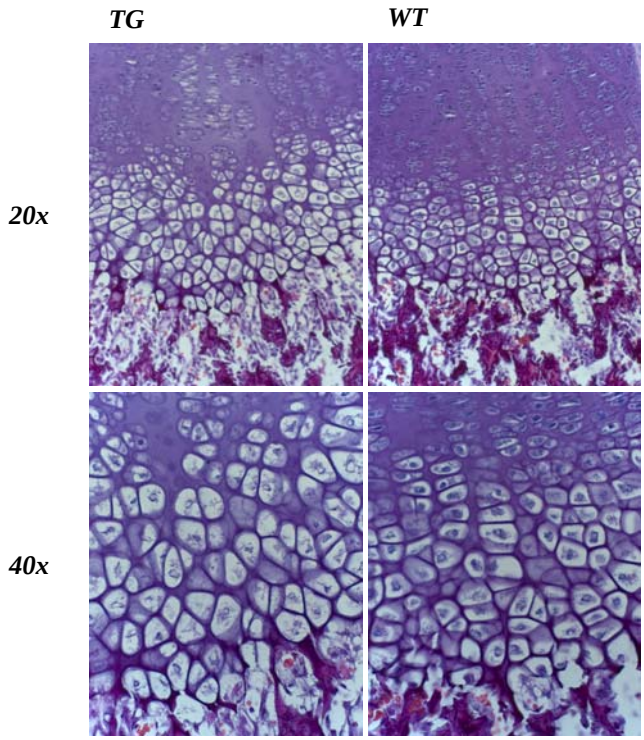

Figure 36: Hematoxylin and Eosin staining of *Col2-ΔTβR1* transgenic mice compared to wild type.

Histological analyses of two-day-old ***TG*** (*Col2-ΔTβR1)* and their wild type littermates (***WT***) revealed an elongated hypertrophic zone. The cells in the transgenic mice are larger and slightly disorganized. The cells in the transgenic prehypertrophic zone are larger than the cells in the corresponding zone of the wild type mice.

Four-week-old mice of the R1 generation were analyzed as well. The weighting study did not show any striking difference either in males or females (figure 37A). The appearance of the mice is indistinguishable from the wild type controls.

Histological analyses of the four-week-old mice demonstrated a phenotypic difference, comparable to the phenotype of the transgenic mice expressing *Esl-1* in proliferating chondrocytes (figure 37B).

A

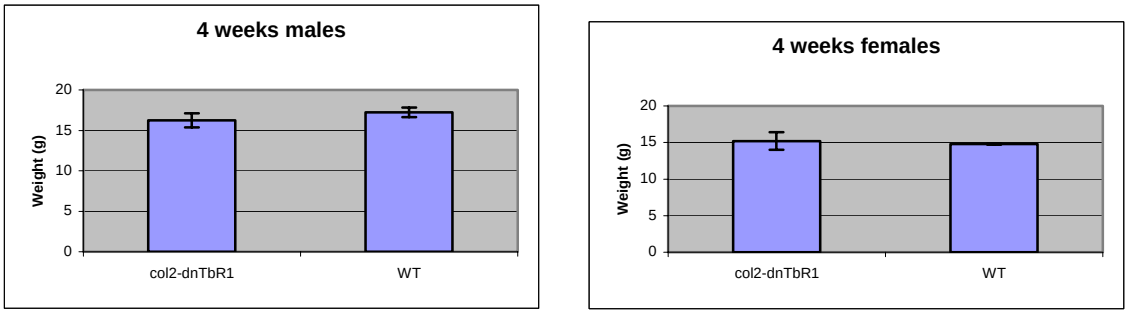

B

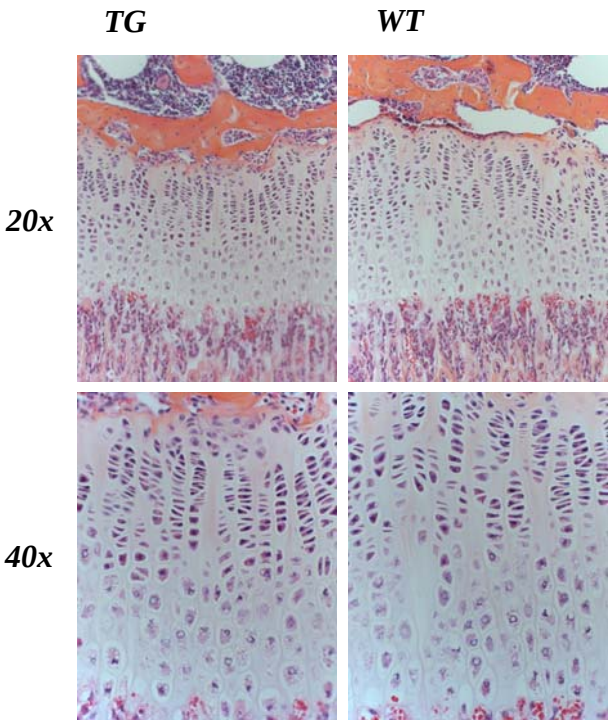

Figure 37: Weighting study and histological analyses of four-week-old *Col2-ΔTβR1* transgenic mice.

(A) Weighting study. The weight difference among males is about 1g, with the transgenic mice being smaller than the wild type controls. In females the difference is only 0.4g less for transgenics compared to wild type mice. N=4 for each group: differences are not statistically significant.
(B) Histological analyses. Sections of transgenic (***TG***) and wild type (***WT***) control animals at three different magnifications. The phenotype is less striking than in two-day-old mice, but the elongation of the hypertrophic zone as well as the prehypertrophic zone is clearly evident.

The prehypertrophic zone of the four-week-old transgenics is elongated and additionally the hypertrophic zone (which could not be observed in the *Col2-Esl-1* transgenic mice) is

enlarged as well. The phenotype is similar, but appears to be strengthened in these mice, and this may be due to variable expression levels of the transgenic allele between lines. Whereas the *Col2-Esl-1* transgenic mice still had white fur and black eyes, mice carrying the *Col2-ΔTβR1* allele had gray fur, suggesting that the transgene in this mouse line is expressed at a very high level.

3.3.2.4 Establishing a transgenic mouse line

The two highest level transgene expressing founder mice (*Col2-ΔTβR1)* were used to establish lines (2.19, figure 38). The founder was then backcrossed with FVB/N wild type and the following R1 generation was used to back cross again with FVB/N wild type.

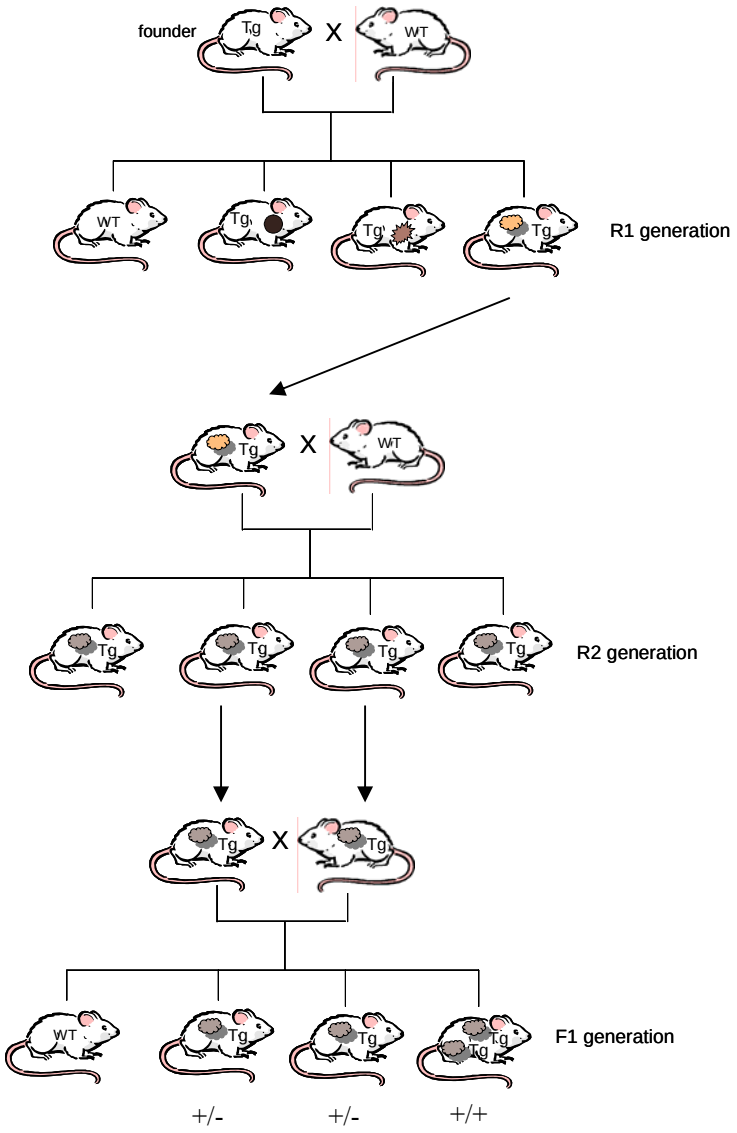

Figure 38: Schematic of establishing a mouse line.

The founder is first backcrossed with a wild type mouse of the same strain and mice of the resultant R1 generation are crossed again with wild type animals of the same strain. The transgenic mice obtained from the R2 generation are then intercrossed. The F1 generation follows the Mendelian distribution of homozygous transgenics, heterozygous transgenics and wild type animals (1:2:1). TG, transgenic; WT, wild type. The pattern in the different mice illustrates the different transgene expression level; +/- heterozygous and +/+ homozygous for the transgene (from Dr. Pia Hermanns, doctoral thesis: "Cartilage Hair Hypoplasia and the *RMRP* gene")

In both generations the black eyes/colored fur was used to visually genotype the mice. R2 x R2 matings produce both homozygous and heterozygous transgenics and wild type mice (F1 generation).

Some offspring produced from these matings of both founders with visibly darker fur, were obviously smaller than their wild type littermates as well as other transgenic littermates (figure 39A). Since these mice were born consistent with expected Mendelian ratios (1:2:1), one explanation would be that the smaller mice are homozygous for the transgenic allele and that the "double" expression of the *ΔTβR1* transgene leads to this extreme expression of the phenotype. All these observations suggest that these mice are homozygous for the transgene and in the following chapters these mice are referred to as homozygous transgenics to distinguish the two different phenotypes.

The smaller size, attributable to the lack of TGFβ signaling in proliferating chondrocytes, is in conflict, with the heterozygous expression of the transgene leading to a severe lengthening in the growth plate (figure 40). The lengthening of the growth plate would infer that the homozygous transgenics would be larger than the controls.

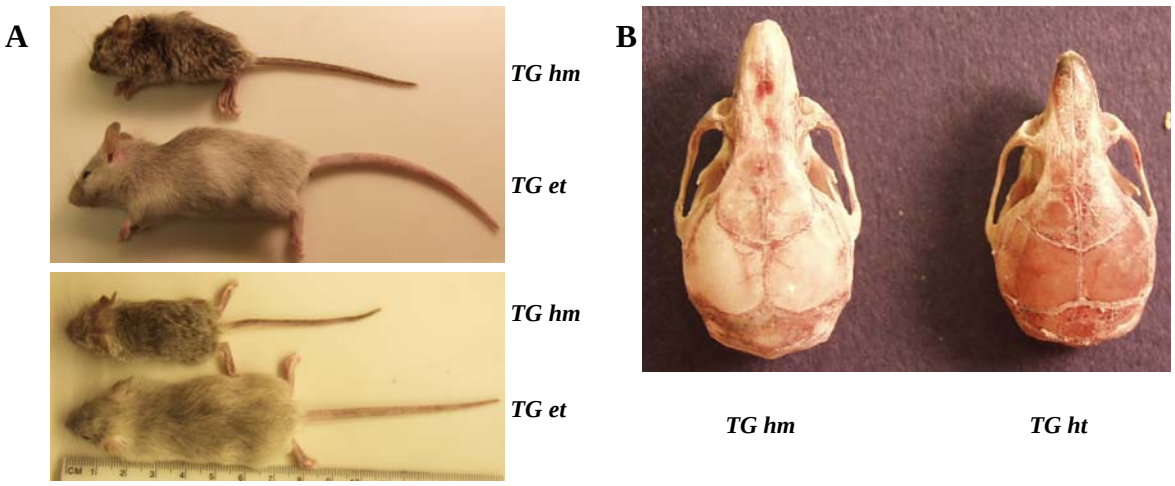

Figure 39: Comparison of homozygous and heterozygous mice of the F1 generation of *Col2-ΔTβR1* transgenic mice.

A. Lateral and dorsal views of a homozygous and heterozygous *Col2-ΔTβR1* transgenic mouse. Homozygous animals are smaller than their heterozygous littermates and they can also be recognized by their darker fur. A wild type animal is not shown. B. The skull preparation reveals that all bony elements of the skull are shorter. The snout of the homozygous mouse is slightly laterally curved. *TG hm*, homozygous transgenic; *TG ht*, heterozygous transgenic.

Heterozygous mice themselves are very similar in appearance to wild type controls, and no visible size difference could be detected when comparing heterozygous transgenic animals

with the wild types. The phenotype of the heterozygous *Col2-ΔTβR1* is restricted to the cellular level.

The size difference might be due to a craniofacial phenotype, hindering normal mastication, and leading to impaired feeding. Homozygous *Col2-ΔTβR1* mice have a shortened snout (figure 39), a finding revealed by simple examination of the skull (figure 39B). The skulls of the homozygous transgenic animals are smaller compared to the heterozygous mouse and the snout region is slightly laterally curved. The mandible is longer compared to the maxilla. The lower teeth are long, the upper incisors are shorter, and appear broken, possibly from an under bite, which may contribute to presumed feeding difficulties.

Three-week-old heterozygous and homozygous mice were prepared for histological analyses of hind limbs and the heads were collected for Micro-CT analyses.

After fixation with formalin and two weeks of decalcification with EDTA, the hind limbs were embedded in paraffin and sectioned. Staining with Hematoxylin and Eosin showed an elongated growth plate in the homozygous animals compared to the heterozygous transgenic animals (figure 40).

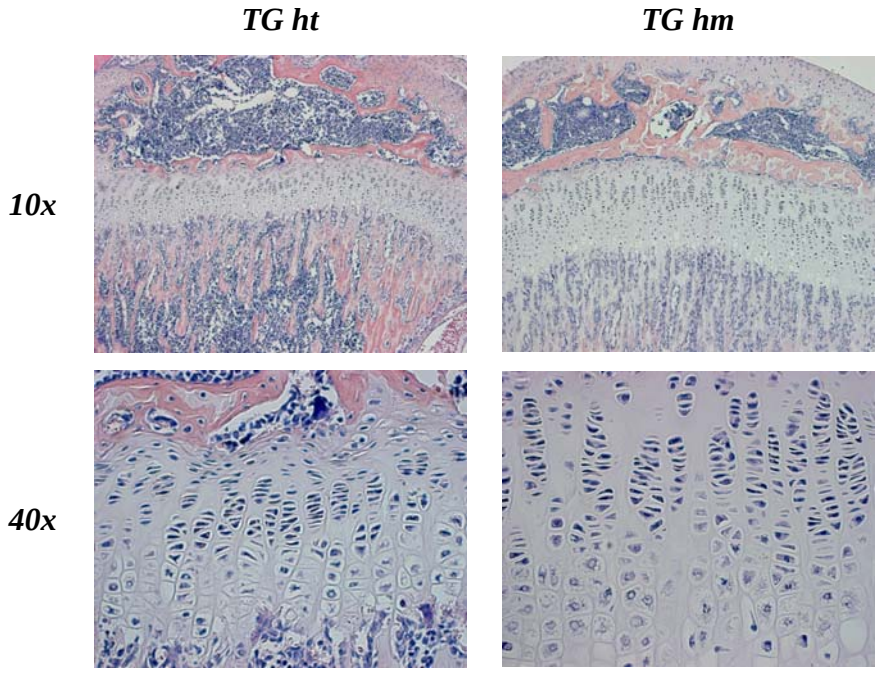

Figure 40: Histological analyses of three-week-old heterozygous and homozygous transgenic *Col2-ΔTβR1* mice.

The growth plate of homozygous mice is elongated compared to heterozygous animals (10 x magnification). The cells of both the prehypertrophic and hypertrophic zones are larger (40 x magnification). The number of cells is unchanged; the elongation of the growth plate is a result of the increase in size of each cell. ***TG ht***, *col2-ΔTβR1* heterozygous transgenics; ***TG hm***, *col2-ΔTβR1* homozygous transgenics.

Both prehypertrophic and hypertrophic zones are significantly elongated compared the heterozygous animals. It does not appear that the elongation of the growth plate is due to an elevated proliferation rate in the transgenic animals. The cells themselves are larger in the growth plate of the homozygous animals and the intracellular spacing is also increased.
Disruption of TGFβ signaling leads to an enlarged growth plate due to an increased proliferation rate. The homozygous mice are significantly smaller than their heterozygous littermates probably attributable to feeding problems as a consequence of the defects in the development of cartilaginous craniofacial elements.

3.3.2.5 Micro-CT evaluation of craniofacial phenotype

To better characterize the apparent shortening of the head (first observed in three week old homozygous transgenic mice), severed heads were first cleaned by Dermestid beetles (*Dermestes sp.*) (2.16). Micro-CT was then performed by Dr. John Hicks (Orthopedics, Baylor College of Medicine, Houston, USA) and colleagues (2.18). Data analyses was performed using Microview (freeware).

While the heads of the heterozygous transgenic animals appear normal, some striking differences were evident in the heads of the homozygous animals: the second molar is missing on both sides (figure 41B) the nasal septum is disorganized and the arrangement of the incisors shows loss of symmetry (figure 41A). To further assess this apparent craniofacial phenotype, the skulls of P2 mice were examined as well (see next chapter). It is possible, that these changes in the skull are due to mechanical stress of the nasal cartilage. If the composition of the cartilaginous matrix is changed in the transgenic mice, resulting in softer cartilage in this region, mechanical stress while feeding could lead to a shifting of the incisors causing problems with feeding, which in turn could explain the dramatic size reduction of these animals. The under-bite seen in these animals is another characteristic suggesting that the size difference of these animals, consistent with the overt overexpression of the *ΔTβR*1, is rather a direct result of a feeding problem.

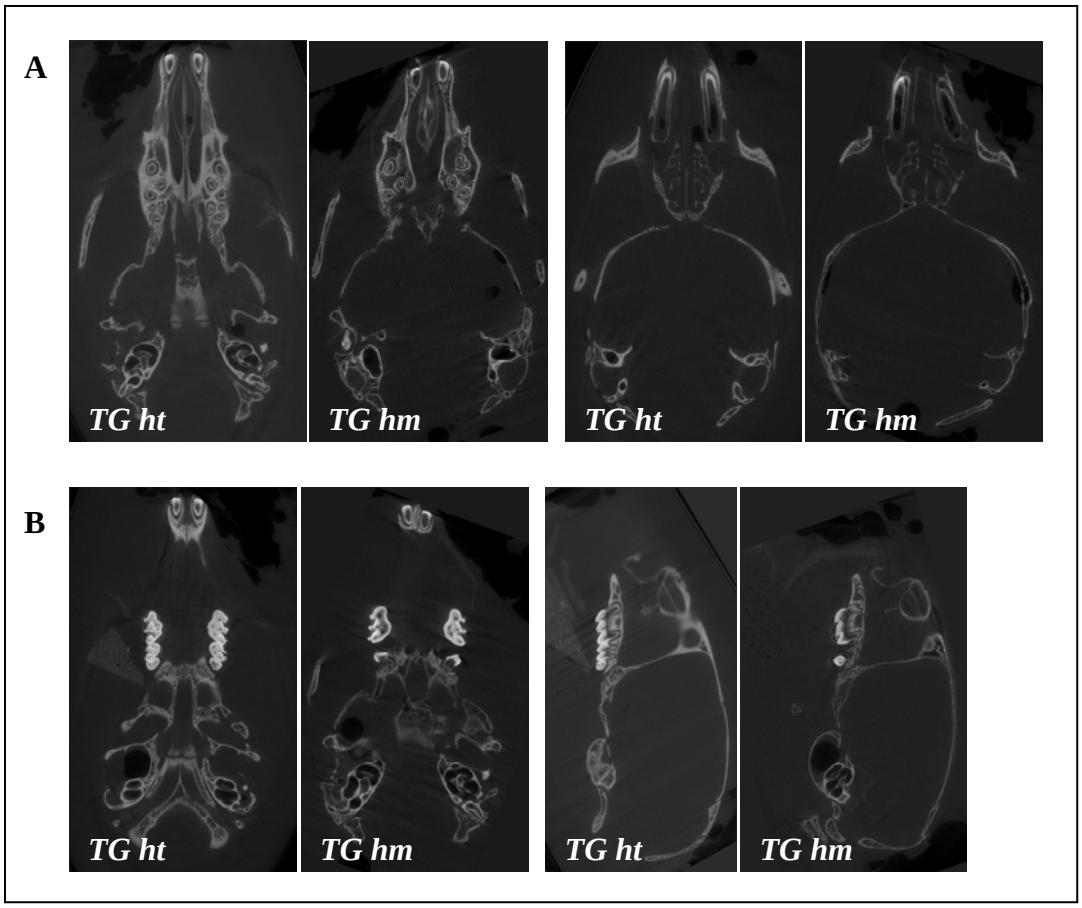

Figure 41: Micro-CT analyses of heads of heterozygous and homozygous transgenic *Col2-ΔTβR1*.

A. Transverse sections through the head to demonstrate the changes of the nasal region in *ΔTβR1* transgenic mice compared to the wild type littermates. The disorganization of the nasal cartilage and bone is more severe compared to mice with disrupted BMP signaling in proliferating chondrocytes (compare figure 25).
B. Transverse and sagittal section of the head shows absence of the second molar. ***TG ht***, *col2-ΔTβR1* heterozygous transgenics; ***TG hm***, *col2-ΔTβR1* homozygous transgenics.

3.3.2.6 Skeletal findings in two days old animals of the F1 generation

To further study the preliminary findings, the F1 generation was obtained by mating R2 littermates. P2 pups were collected and further analyzed beginning with whole skeletal preparation and staining with Alizarin Red /Alcian Blue to assess patterning defects and to see, if an early craniofacial phenotype was present.

The skeletons show no patterning defects, but the transgenic animals are slightly shorter than the wild type littermates, homozygous animals more so then the potential heterozygous

animals (figure 42, upper panel). The P2 skulls demonstrate even greater size reduction, among the transgenics (homozygotes< heterogygotes< wild types) while the mandibles of the transgenics are disproportionately larger relative to their smaller skulls (when compared to wild type mice, figure 42, lower panel).

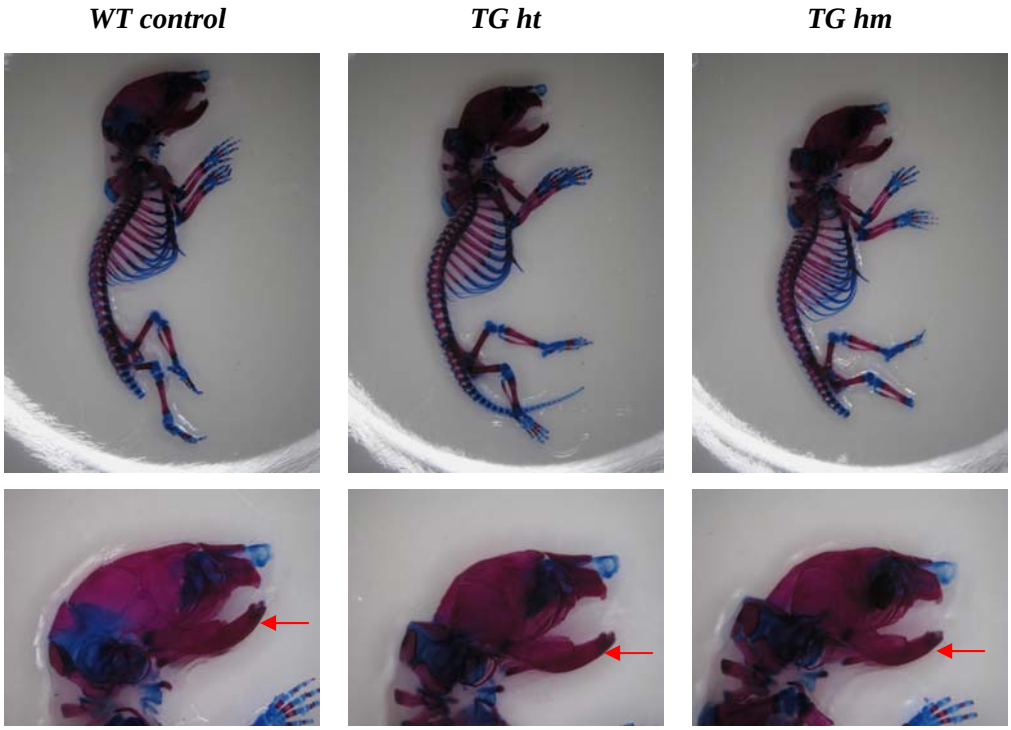

Figure 42: Skeletal preparation of heterozygous and homozygous two-day-old transgenic *Col2-ΔTβR1* mice.

The transgenic mice are slightly smaller then the wild type littermates. No patterning defects are evident (upper panel). The skulls of transgenics are smaller (lower panel), however mandibles in these mice are disproportionately large relative to their skulls and wild types (red arrow). ***WT*** wild type ***TG ht***, *col2-ΔTβR1* heterozygous transgenics; ***TG hm***, *col2-ΔTβR1* homozygous transgenics.

During the skeletal preparation, as the skin was removed from the skulls, cavitation of the occipital region occurred. This technical consequence complicates direct comparison of skull sizes, but this effect notwithstanding, the heads appear smaller, and the transgenic mandibles are relatively larger. These finding are consistent with those where the under-bite was observed earlier in three week old homozygous animals.

3.2.2.6 Histological analyses of heterozygous and homozygous *Col2-ΔTβR1* animals

Given the finding of size differences of transgenics compared to wild types and the observations made from the R1 generation, additional experiments including staining with Hematoxylin and Eosin and *in situ* hybridization with probes detecting *Ihh* and *Col10a1* expression were conducted on littermates of the F1 generation.

The findings from the histological analyses of the R1 generation are as predicted. The growth plate is obviously elongated in the transgenic mice, in both heterozygotes and homozygotes, while the elongation is more severe only in homozygous mice (figure 43). The zone of hypertrophic chondrocytes also appears more disorganized among the homozygotes than was observed in heterozygous littermates.

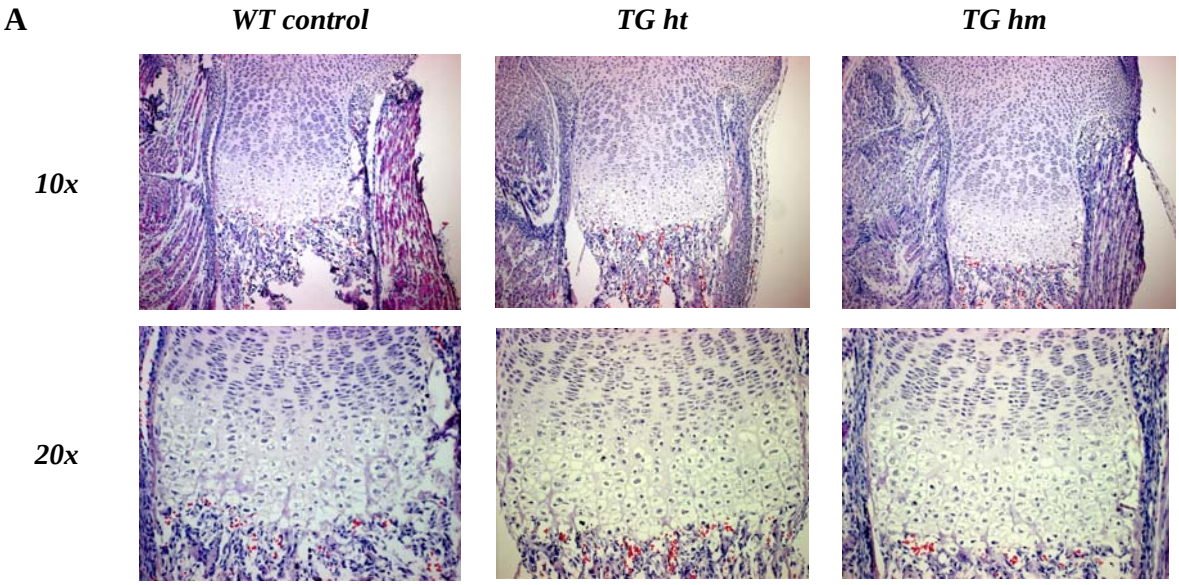

Figure 43: Comparison of tibia sections of F1 mice overexpressing *ΔTβR1* in proliferating chondrocytes.

Histological analyses of the offspring (F1 generation) of mice overexpressing the dominant negative *TβR1* in proliferating chondrocytes. Shown is the proximal tibia from a wild type control, a heterozygous and a homozygous transgenic mouse. The histological findings are comparable to the results obtained in mice of the R1 generation (see figure 34). Heterozygous transgenic mice have an elongated growth plate; the phenotype is even more pronounced in mice that are homozygous for the transgene. ***WT*** wild type ***TG ht***, *col2-ΔTβR1* heterozygous transgenics; ***TG hm***, *col2-ΔTβR1* homozygous transgenics.

In situ hybridization using probes for *Col10a1* (as a marker for hypertrophic chondrocytes) and *Ihh* (as a specific marker for prehypertrophic chondrocytes) shows no difference in the length of the hypertrophic zone and only a slight increase in the length of the prehypertrophic zone. Overall, *Ihh* in transgenics is more strongly expressed than in wild types (figure 44).

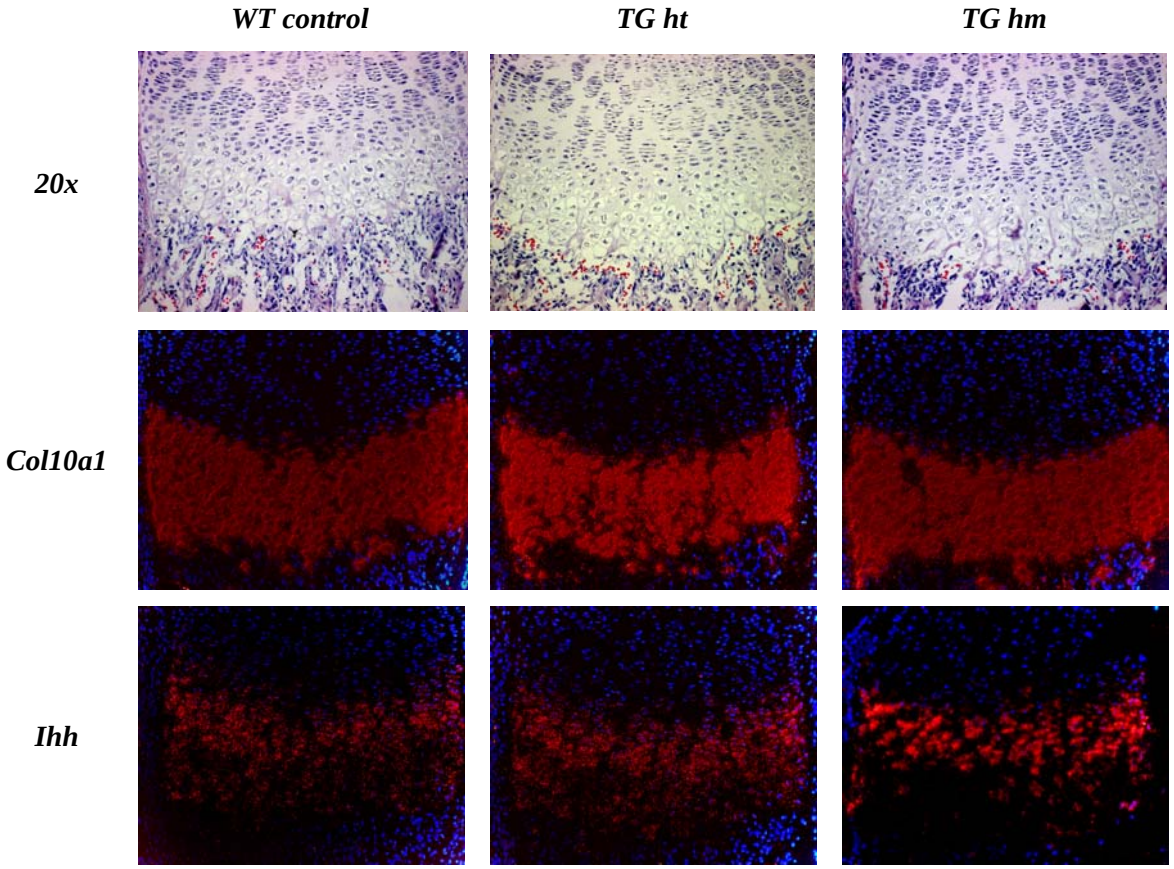

Figure 44: *In situ* hybridization on hind limb sections on *Col2-ΔTβR1* with probes for *Col10a1* and *Ihh*.

In situ hybridization with probes detecting *Col10a1* and *Ihh* on hind limb sections of the offspring (F1 generation) of mice overexpressing the dominant negative *TβR1* in proliferating chondrocytes. Shown is a 20x magnification of the femur of wild type, heterozygous and homozygous mice overexpressing *ΔTβR1* in proliferating chondrocytes. The expression of *Ihh* in the transgenic mice is increased; the prehypertrophic zone is elongated compared to the wild type littermates. ***WT*** wild type ***TG ht***, *col2-ΔTβR1* heterozygous transgenics; ***TG hm***, *col2-ΔTβR1* homozygous transgenics.

A stronger expression of *Ihh* in the transgenic mice is obvious, while a comparison of the hypertrophic chondrocytes is difficult. It appears that the elongation of the growth plate is only due to a longer prehypertrophic zone, not to the elongation of both the prehypertrophic and hypertrophic zones.

The phenotype is stronger in the *Col2-ΔTβR1* transgenic mice but this may be attributable to the increased expression of the transgenic allele in the *Col2-ΔTβR1* mice.

3.2.2.7 Proliferation assay with BrdU staining

Since the growth plate in the transgenic mice is elongated, an increased proliferation rate in these animals was expected and was tested with comparative BrdU staining of transgenic and wild type proliferating chondrocytes (compare chapter 3.2.3 and 3.3.1.5). Four sections each (P2 femurs) from two transgenics and two wild types, were counted and the result are shown in figure 45.

The upper panel shows the BrdU stained section of the proximal femur, clearly demonstrating the increased cell proliferation in the transgenic mouse (figure 45). Statistically, in wild type mice 15.8% of the total cells are proliferating, whereas in the transgenic mice the percentage of proliferating cells is 18.1%. The p value (p = 0.005) is statistically significant.

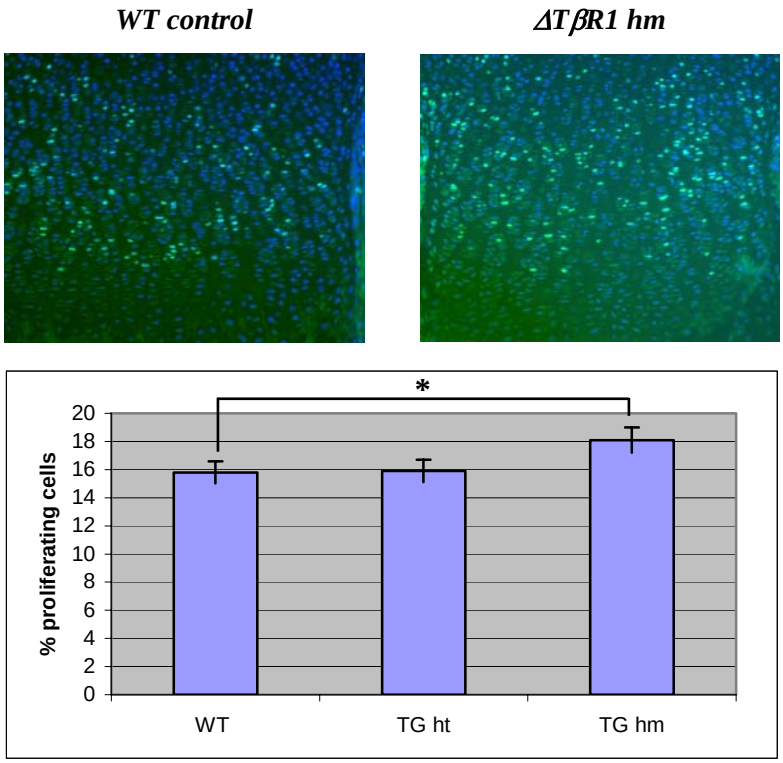

Figure 45: Increased proliferation rate in transgenic mice overexpressing *ΔTβR1*.

The upper panel shows femur sections of a wild type control and a transgenic mouse overexpressing *ΔTβR1* in proliferating chondrocytes. The lower panel shows the percentage of proliferating cells per genotypic class. Differences between wild type (WT) and homozygous transgenic mice (TG hm) are statistically significant with a p value of 0.005.

Cells were counted in sections of the tibia to compare to femur and proliferation rate increases were consistent with those previously seen in the femur. 17.3% of wild type control cells were observed to be proliferating, whereas the proliferation rate was 21.1% in tibial sections of transgenic mice, with a p value of 0.005, a statistically significant finding (data not shown). The percent differences between the cell counts from tibia and femur might be due to the system which was used to count these cells (compare chapter 3.2.3) however this pattern was consistent in all sections across all mice counted.

In distal femur sections of heterozygous animals, 18.1% of the cells were proliferating and in sections of the proximal tibia the rate was 19.9%. These results are as expected with values intermediate to those of wild type and homozygous transgenic animals; neither difference (wild type vs. heterozygous mice nor between heterozygous and homozygous mice) is statistically significant.

It is recognized that TGFβ has antiproliferative activities and these findings (with overexpression of the dominant negative type I receptor for TGFβ) conclusively demonstrate the enhanced proliferation rate in transgenic animals.

3.2.2.8 Cartilage matrix composition and Mineralization

Safranin O staining was performed to examine possible changes in the composition of the extracellular matrix (ECM). Safranin O binds to proteoglycans in the ECM. Changes in the distribution of proteoglycans in the ECM leads to differential staining of the cartilaginous regions.

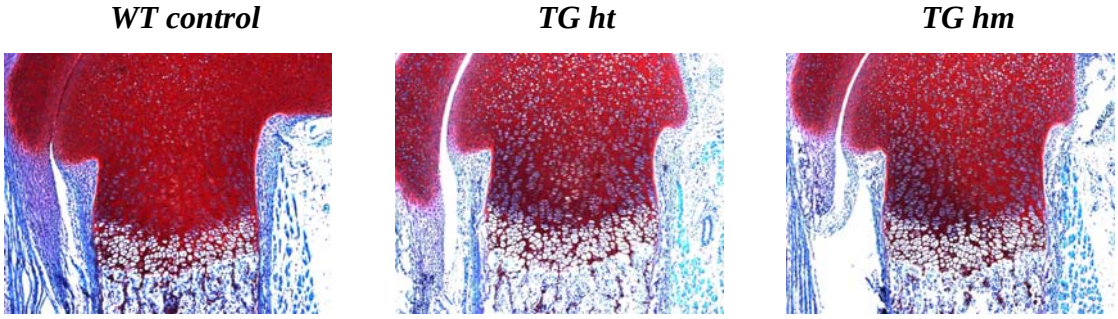

Figure 46: SafraninO staining of two-day-old homozygous and heterozygous transgenic *Col2-ΔTβR1* mice compared to wild type animals.

10x magnification of the distal femur of wild type, heterozygous, and homozygous animals stained with SafraninO. Differences in the strength of staining are apparent by comparison of wild type and the transgenic mouse sections. The staining of the wild type femur is stronger, probably due to a decrease in proteoglycans in the transgenic mice compared to the wild type mice. ***WT*** wild type ***TG ht***, *col2-ΔTβR1* heterozygous transgenics; ***TG hm***, *col2-ΔTβR1* homozygous transgenics.

The SafraninO staining of distal femurs for wild type, heterozygous, and homozygous mice shows that the composition of the extracellular matrix in the wild types is altered compared to the transgenic mice, which infers that a reduction in proteoglycan production occurs in the transgenic mice.

To evaluate possible altered mineralization in the transgenic animals, von Kossa staining was performed on hind limb sections of homozygous and heterozygous mice as well as wild type. The mineralization in the transgenic mice is not obviously impaired or enhanced. Figure 47 shows a 10x magnification of the distal femur of a wild type control, heterozygous and homozygous transgenic mouse.

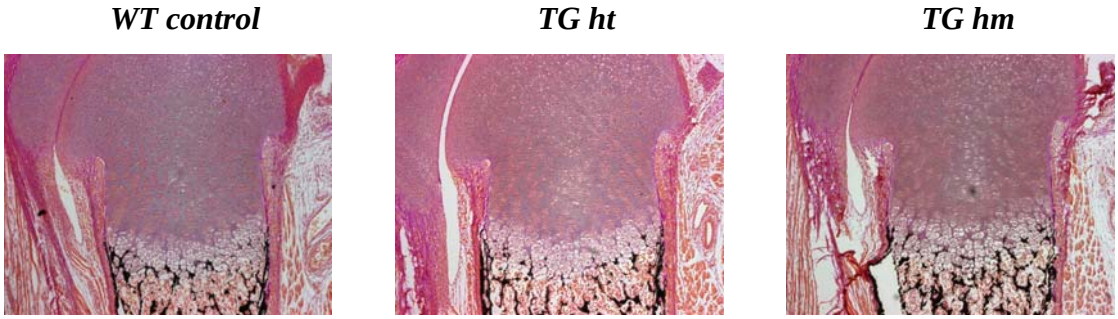

Figure 47: Von Kossa staining of two-day-old homozygous and heterozygous transgenic *Col2-ΔTβR1* mice compared to wild type animals.

Von Kossa staining revealed no differences between wild type and heterozygous animals. With the double overexpression in the potential homozygous mice, the mineralization is slightly enhanced. The elongation of the growth plate is obvious. ***WT*** wild type ***TG ht***, *col2-ΔTβR1* heterozygous transgenics; ***TG hm***, *col2-ΔTβR1* homozygous transgenics.

No substantial difference in mineralization was observed between the heterozygous transgenic animals compared to the wild type controls, although mice homozygous for the transgenic allele appeared to exhibit a slight mineralization increase.

Safranin O and von Kossa staining again demonstrate the elongated growth plate. The TGFβ signaling pathway is important for the formation of the extracellular matrix, but from these data, it does not appear to be essential in the mineralization processes.

3.4 Generation of *Cre recombinase* expressing transgenic mouse line using a 10 kb *Col10a1* regulatory element

Until recently, studies have been limited to either the gain or loss of function of regulatory genes in proliferating chondrocytes during skeletal development. In order to be able to study the function of key regulatory genes in hypertrophic chondrocytes, a mouse expressing the *Cre recombinase* gene under the control of the *Col10a1* promoter would be of obvious value. This would enable spatial / temporal control of the knock out of each candidate gene specifically in hypertrophic chondrocytes. Not all elements of the putative *Col10a1* promoter that are responsible for its tissue specific expression have yet been identified, but currently an intense effort is being directed toward this end in this laboratory. Consequently, an additional aim of this thesis was the generation of a mouse line that expresses the *Cre recombinase* reporter gene under the control of a 10 kb hypertrophic chondrocyte-specific *Col10a1* promoter element.

Promoter studies with transgenic mice, expressing *β-galactosidase* under the control of different collagen type X promoter fragments have shown that a 10 kb long fragment of the promoter can lead to a specific and strong expression of the reporter in hypertrophic chondrocytes (compare chapter 4.4, figure 68). This promoter fragment contains: an approximately 6 kb fragment upstream of exon1 containing the basal promoter, putative Runx2 binding sites, a putative AP1 binding element, as well as exon 1, exon 2 and some initial sequence of exon 3. The three possible start codons (ATGs) in exon 2 have been mutated without altering the open reading frame. The second intron contains a putative CDX element (Zheng et al. 2003). All these elements have been implicated in the modulation of gene expression and may or may not be influential in influencing the tissue specificity of the collagen type X gene.

3.4.1 Cloning strategy of the 10 kb col10a1-Cre

An 8 kb promoter fragment, containing a 4 kb promoter and the large second intron of the collagen type X gene was retrieved by screening a murine BAC library (Zheng et al. 2003). The 10 kb *Col10a1* fragment contains an additional 2 kb promoter fragment upstream. This 2 kb element was generated by PCR amplification with primers that contained XmaI and SalI restriction sites and was cloned into the pBSII KS(-) plasmid (preliminary work of Dr. Qiping

Zheng). A XhoI restriction site downstream of this 2 kb fragment was used to subclone the 8 kb mutated fragment where the three in-frame ATGs in exon 2 had already been mutated.

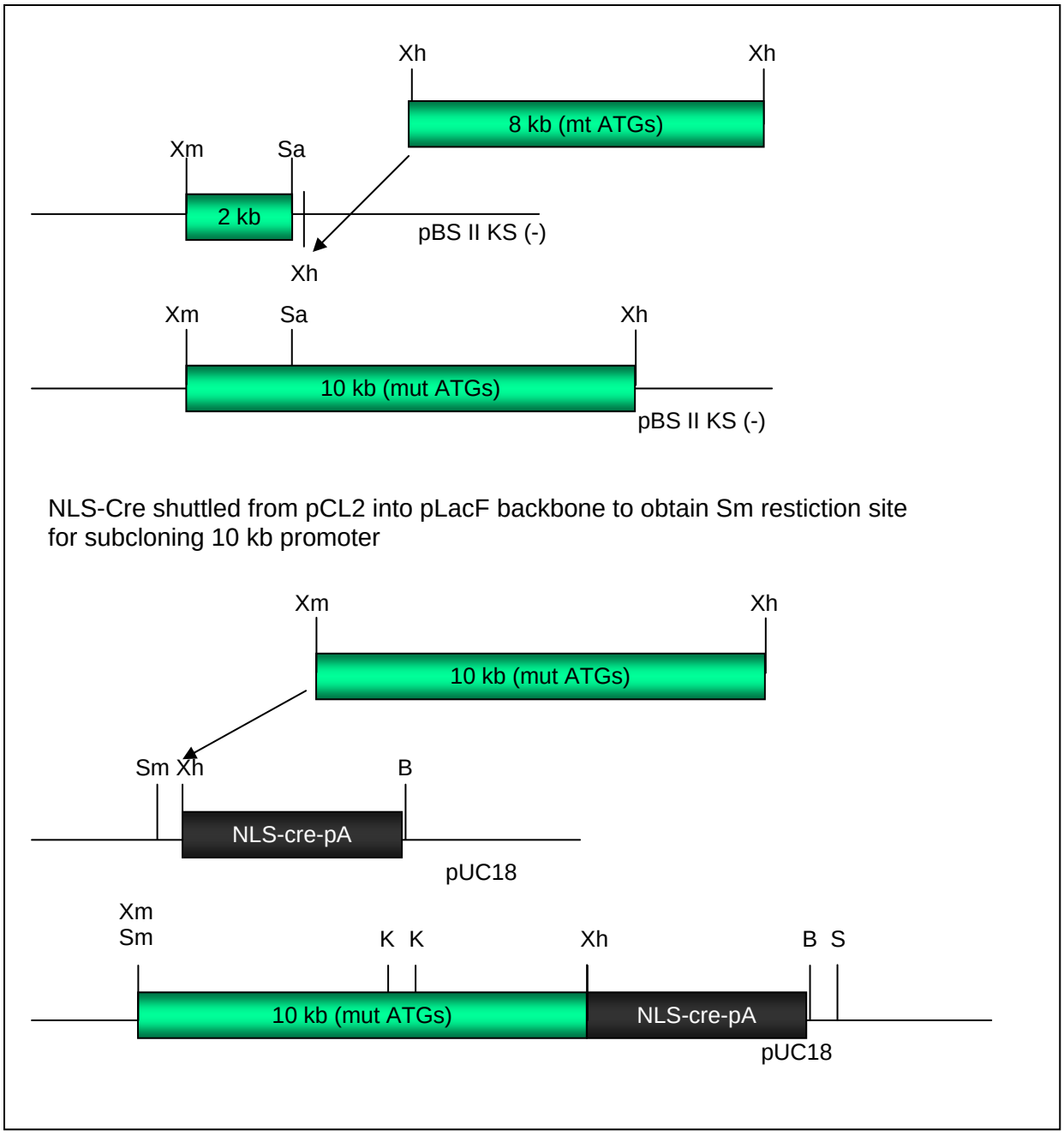

Figure 48: Schematic of the strategy used to clone the *Cre recombinase* under the control of *Col10a1* promoter.

In the first step, the proximal 2 kb region of the col10a1 promoter, which was produced by PCR amplification with XmaI and SalI containing primers was subcloned into s pBSII KS (-) plasmid. The 8 kb long promoter fragment containing exon1 and 2 as well as intron1 and 2 and the mutated endogenous ATGs in exon2 was released from its original plasmid with XhoI and cloned into the XhoI site upstream of the 2 kb promoter part. In the second step the 10 kb promoter fragment was cloned into a XhoI site 5' of the NLS-Cre-pA. After digestion with XmaI and BglI the construct was gel purified and injected in pronuclei.
(K, KpnI; Xm, XmaI; Sm, SmaI; X, XhoI; B, BglI; S, SphI; NLS, nuclear localization signal; cre, *Cre Recombinase* gene; pA, polyadenylation signal)

The 10 kb promoter fragment of the collagen type X gene was cloned upstream of the *Cre recombinase* gene (figure 48). The *Cre recombinase* element contains a nuclear localization signal (NLS), a short amino acid sequence, typically consisting of positively charged lysines or arginines. The sequence is exposed on the surface of the protein and it guides the protein into the nucleus via binding to cytosolic nuclear transport receptors, thus enhancing the transport of the *Cre recombinase* into the nucleus where recombination occurs.
The *Cre recombinase* containing the NLS was released from its original plasmid (pCL2) and shuttled into pUC18. This new backbone contained an additional SmaI restriction site, which was used to place the *Col10a1* promoter fragment in front of the *NLS-cre* cassette.
The junctions of the construct were verified by sequencing and for the subsequent pronuclear injection, the transgenic construct was released with XmaI and BglII and gel purified using the QIAEXII Purification Kit (QIAGEN, Valencia CA, USA) as described in chapter 2.4.5.

After the first injection three mice were obtained and genotyped with primers that amplify the *Cre recombinase* specific product of approximately 500 bp. These same primers had previously been demonstrated in the literature to genotype mice that express *Cre recombinase* in proliferating chondrocytes (Ovchinnikov et al. 2000). No founder mice could be detected among these three pups. A second injection resulted in two pregnant mice and fourteen pups were born. Three different founders (one female and two males) were identified by the PCR genotyping using tail DNA as template. The following figure shows an agarose gel of the PCR genotyping as an example (figure 49).

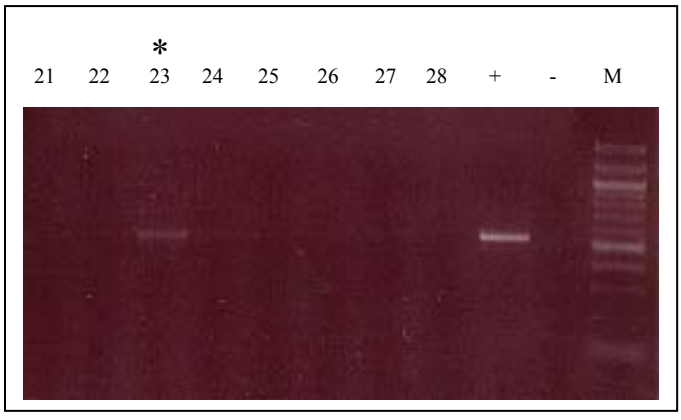

Figure 49: Genotyping of a litter received after injection.

PCR on tail DNA from 8 mice (#7823-7828) was performed. One founder mouse could be detected (#7823). + positive control PCR on plasmid DNA; - negative (H_2O) control; M 100bp marker; * positive founder mouse.

These three founders were mated with Rosa26R reporter mice to test for the specificity of the *Cre recombinase* expression. Newborn mice from these matings were skinned, the internal organs removed and the whole mice stained with x-gal. The skin was used for DNA

extraction and PCR genotyping using both primers for *Cre recombinase* (figure 47) and others for the *lacZ* gene of the Rosa26R mice (data not shown). Double transgenic mice for *Cre recombinase* and lacZ should display a characteristic blue staining in hypertrophic cartilage.

Figure 50 shows the results of the mating of founder mouse #7823. Two transgenic mice as well as one wild type littermate from this mating are depicted. The blue staining in both transgenic littermates is both qualitatively and quantitavely different, possibly due to copy number differences of the transgenic construct. Staining in transgenic mouse 1 (***TG1***, figure 48) seems to be specific; the staining is only detectable in limbs and ribs, whereas ***TG2*** shows blue staining throughout all tissues of the mouse.

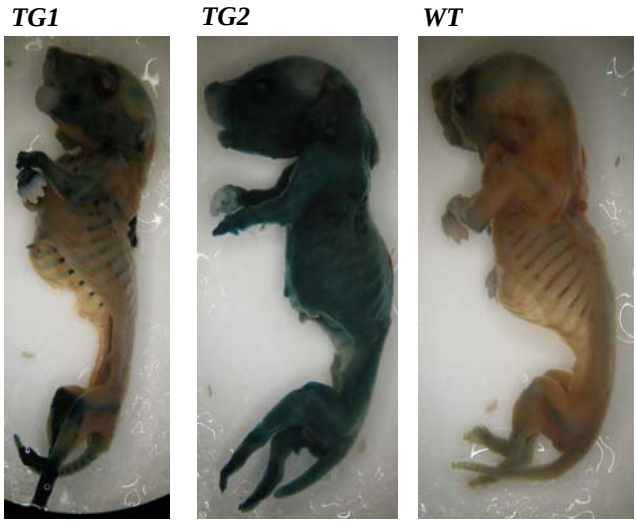

Figure 50: X-gal staining of whole newborn mice of the founder line #7823 after mating with Rosa26R mice.

The WT animal shows no staining. Two different offspring of the same litter are shown, ***TG1*** shows blue staining in cartilaginous elements, whereas ***TG2*** is completely stained.

To evaluate the cellular specificity of the *Cre recombinase*, the limbs and the ribs were dissected, embedded in paraffin (2.15.1), sectioned (2.15.3) and counterstained with Nuclear Fast Red (2.15.4).

Sections of limbs and ribs of transgenic littermates of the offspring of founder mouse #7823 showed a non-specific blue staining, which varied only in the intensity of the staining (figure 51 shows the forelimb sections of ***TG1***). The staining was present not only in the hypertrophic and prehypertrophic zones, but the proliferating chondrocytes and bone marrow as well. The intensity of the staining increased directionally from proximal to distal. While there is nonspecific and weak staining in the proximal humerus (figure 51A), the staining seems to become stronger in the distal humerus and proximal radius (figure 51B). The strong blue staining of the distal ulna as well as cartilaginous parts of the paw supports the

observation that the expression of the *Cre recombinase* is gradually increasing in a proximal to distal direction (figure 51C).

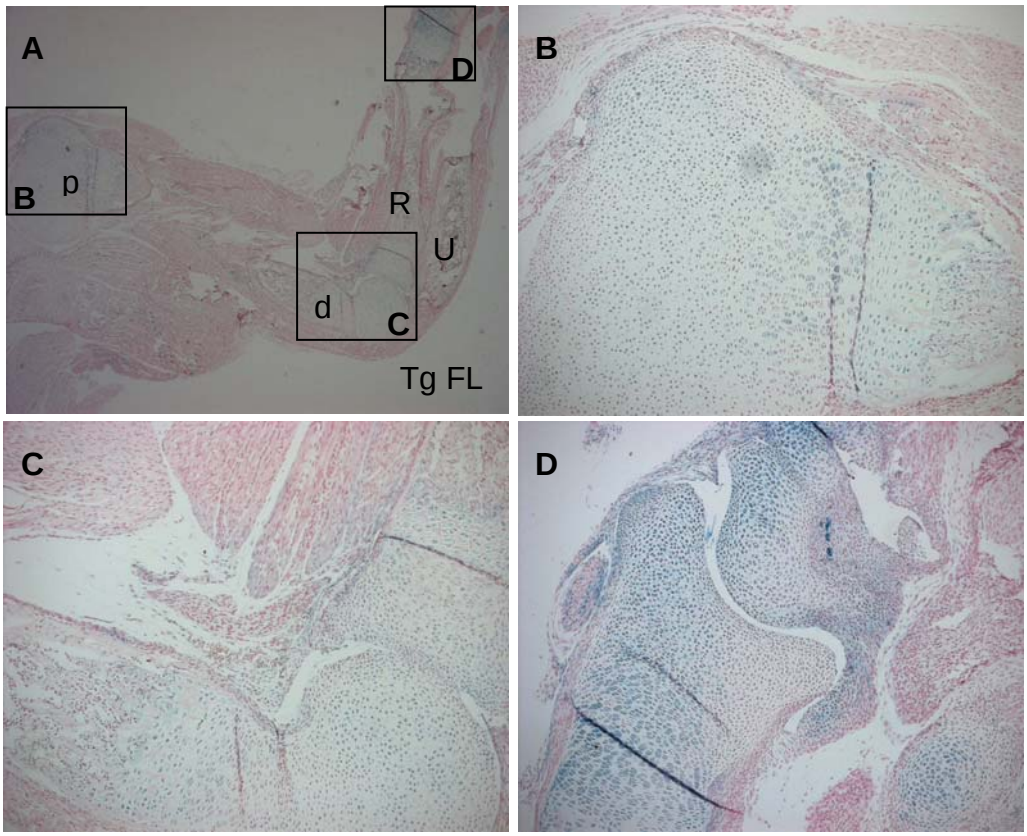

Figure 51: Histological analyses of *Cre recombinase* specificity tested with x-gal staining.

A: Overview of a section of a forelimb (Magnification 2.5x). Boxes B, C, and D lead to each magnification, B: proximal humerus (p H); C: distal humerus (d H) and proximal radius (R); D: distal radius. Staining with x-gal showed an unspecific expression of the *Cre recombinase*. Furthermore, the expression level is not consistent throughout the limb. Proximally, the expression appears significantly weaker than in the distal part of the forelimb. U, Ulna.

The insertion of the *Cre recombinase* gene driven by the 10 kb *Col10a1* promoter in the genome of these transgenic mice did not result in the expected expression pattern of the reporter gene. The different blue staining of the offspring of the founder mouse #7348 after mating with Rosa26R (figure 50) suggests that probably multiple insertions sites are responsible for the non-specific expression of the Cre recombinase. Additionally positional effects, from enhancers or silencers near or far from the insertion site might also affect the expression of the transgene.

3.4.2. Generation and characterization of a 10 kb col10a1-Cre construct with Tyrosinase expression cassette and insulators

Where a transgene inserts into the genome has substantial impact upon its expression. To eliminate or at least minimize the possible position effects of enhancers and/or silencers in the vicinity of the insertion site, the construct was cloned into a plasmid containing two copies of the β-globin HS4 chicken insulator (Hsiao et al. 2004). The chicken insulator sequence should protect the transgene from positional effects; the *Tyrosinase* cDNA is under the control of the K14 (keratocyte) promoter. The successful integration of this transgenic construct leads to changes in the eye and fur color of FVB/N albino mice (from *Tyrosinase* expression) and allows for visual genotyping of the mice (black eyes/mottled fur).

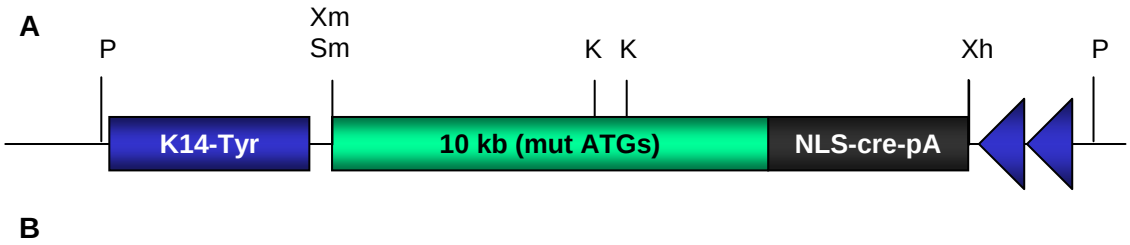

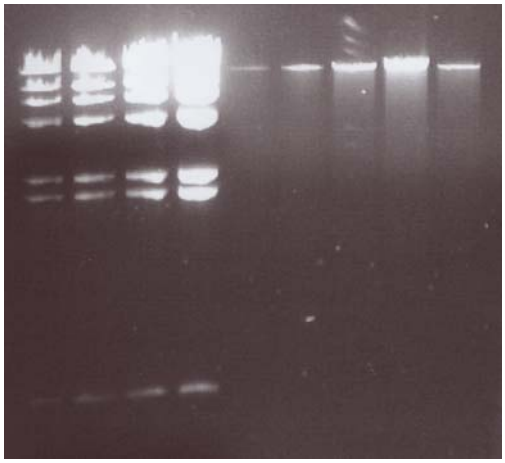

Figure 52: Transgenic *Cre recombinase* construct with *Tyrosinase* expression cassette and insulators (*10 kb-Col10a1-Cre/Tyr*).

(A) Schematic of the construct with restriction sites. (B) Gel image of the construct after its release from the plasmid with PacI and purification with QIAEX II. Four increasing concentrations of the λ/HindIII marker as well as 5 different concentrations of the construct are loaded, to evaluate the quality and to estimate the concentration of the DNA. K, KpnI; P, PacI; Sm, SmaI; Xh, XhoI; Xm, XmaI

Figure 52A shows the construct, which was released from its plasmid with PacI digestion and following gel purification with QIAEX II as described in chapter 2.4.5.

The initial injection into pronuclei resulted in three founder mice out of 26 live born mice (#1341-#1366), which could be identified simply by the visual color change (to black) in the eyes.

To insure insertion of the transgene, all mice were genotyped and the results showed that an additional mouse (which had demonstrated no obvious eye color change) also carried the transgene. Mice #1341, #1354 and #1355 had black eyes; mouse #1345 had no black eyes (figure 53).

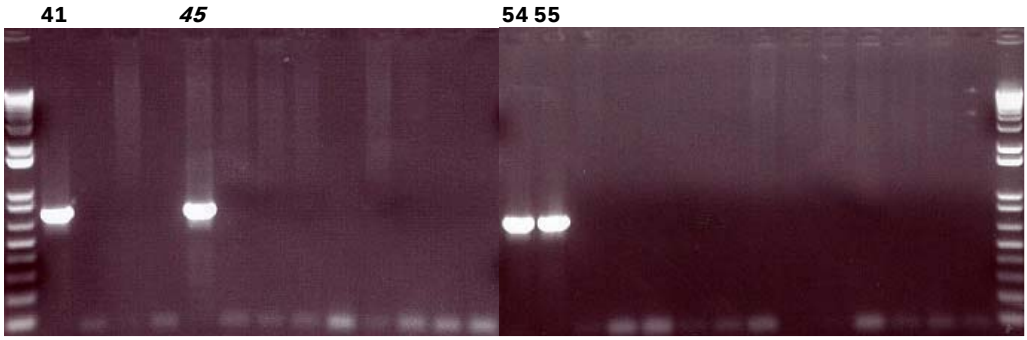

Figure 53: Genotyping of the received founder mice of the injection with Col10-cre/Tyr.

26 mice were obtained in three litters. DNA was isolated from tail and PCR genotyping was performed with primers that are specific for the *Cre recombinase*.

All four founder mice were mated with Rosa26R reporter mice and newborn mice were stained with X-gal. Figure 54 shows the whole embryo staining of the offspring of this mating. No differences between mice from each litter could be observed. The staining seems to be very specific, with variable strength correlating directly with the visible expression levels of the influence of the *Tyrosinase* gene upon the eyes and the fur.

Figure 54: Whole skeleton of transgenic *10 kb-Col10a1-Cre/Tyr* newborn mice stained with x-gal.

All mice were stained overnight with x-gal. Wild type control of all matings did not show any specific staining following overnight incubation.

The staining of the offspring of founder #1345 (which showed no eye color change) is predictably weaker than the staining of the offspring of the other founder mice. Founder mouse #1341 had black eyes, but its fur was still white; the transgene expression level was sufficient to change the color of the eyes, but not strong enough to impact the color of the fur. It follows from this observation that the expression of *Cre recombinase* in #1341 is higher compared to mouse #1345, but it is not as high as the expression of mice #1354 and #1355, which had not only black eyes, but also changes in fur color.

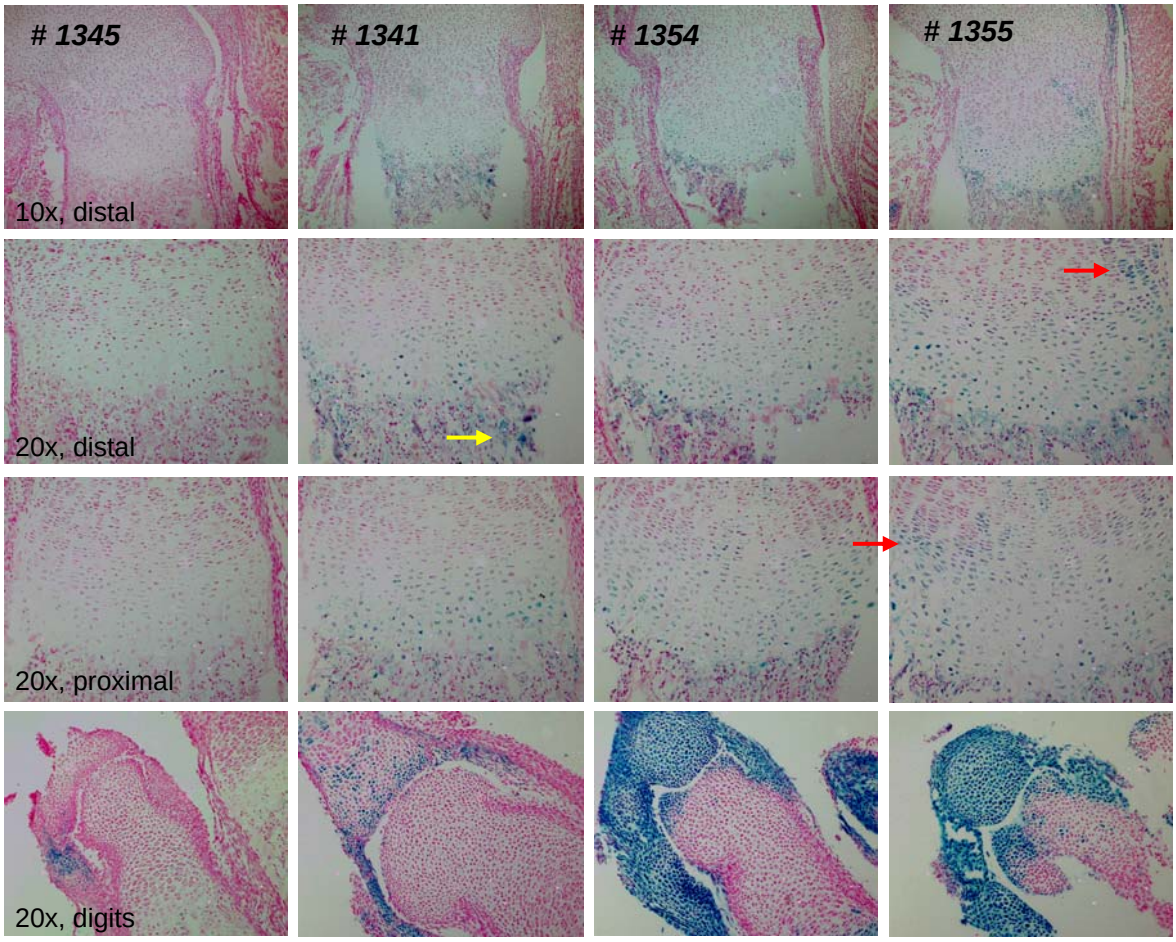

Figure 55: Comparison of x-gal staining in the offspring of the different C*ol10-cre* founder mice with Rosa26R reporter mice.

Offspring of the founder mice #1341, #1354 and #1355, positive for the *Col10-cre* and Rosa26 alleles, demonstrate strong staining throughout the growth plate. In mouse # 1341 no staining can be observed either in resting or proliferating chondrocytes, but some staining can be observed near the junction of the bone marrow (yellow arrow). The mouse most strongly expressing the *Cre recombinase* (#1355) shows nonspecific staining in proliferating chondrocytes (red arrows). The lower panel shows the staining of the digits. Nonspecific staining can be observed in cartilaginous regions of the digits, as well as in soft tissue. Shown are the 10 x and 20 x magnification of the distal femur, 20 x magnification of the proximal tibia and 20 x magnification of the digits, respectively.

All of the founder transgenics were dissected; forelimbs and hind limbs as well as part of the ribs were removed, embedded and counterstained with Nuclear Fast Red (figure 55).

The whole mount staining of founder #1341 with the Rosa26R reporter mouse showed x-gal staining in all cartilaginous regions, but at the cellular level no blue staining could be observed (data not shown). All of the other mice showed variable levels of x-gal staining at the cellular level, consistent with the staining previously observed in whole embryos.

The expression level of the *Cre recombinase* is similar in the offspring of the founder mice #1354 and #1355, both macroscopically and histologically. Figure 55 depicts the levels and patterns of staining of all four founder mice. Shown in the figure are a 10x and 20x magnification of the distal femur and a 20x magnification of the proximal tibia. The lower panel exhibits a 20x magnification of the digits of these same mice.

Littermates positive for both the Rosa26 reporter allele and *Col10-cre* allele from founder #1345 did not show any staining at the cellular level in either the femur or tibia (nor other cartilaginous regions) although such was expected based upon macroscopic evaluation of the staining of the whole mouse. Some staining can be appreciated in the distal regions of the digits, particularly among the resting chondrocytes.

Offspring of the mating of founder #1341 with a Rosa26R reporter mouse demonstrate the most specific staining although not as strong as in the offspring of founder #1354 and #1355. What is interpreted to be leaky expression is noticeable in the bone marrow of all mice. The staining of littermates of founder mice #1354 and #1355 is comparable. Both founders had relatively dark fur, suggesting that the transgene was probably inserted at multiple sites or that it could be (despite the insulator) under the influence of a strong enhancer located in the vicinity of the insertion site.

Figure 56: Comparison of staining of ribs in *col10-cre* founder mice #1341, #1354 and #1355.

The comparison of rib sections show that the founder mouse #1341 expresses *Cre recombinase* in a tissue specific manner, although the expression is very weak. What appears to be leaky expression in the bone marrow is seen as well. Mouse #1354 and #1455 show an overall stronger transgene expression.

LacZ staining comparisons of the ribs of three founders is shown in figure 56. Sections of the ribs from founder #1345 did not show any staining at all and is not presented in this figure.

As in the previously demonstrated sections of the hind limbs, the *Cre recombinase* activity in the ribs is dependent upon the strength of expression of the transgene. At the junction between the cartilage and bone marrow, some non-specific expression of the reporter gene is observed. Only Mouse #1341 shows specific staining of proliferating chondrocytes.
As a consequence of these observations, two additional lines were established using the breeding scheme described in chapter 2.19 (see also figure 38). Founders #1341 and #1354 were bred to wild type FVB/N. Positive offspring of these matings were again mated with wild type FVB/N to produce mice of the R2 generation, and then used for interbreeding. Mice of these matings were bred again to wild type mice as well as mated to Rosa26R reporter mice to re-assess the specificity of the *Cre recombinase* expression.

Cre recombinase expression under the control of the 10 kb *Col10a1* promoter fragment is not as specific as preliminary studies with transgenic mice suggested. In mice with strong reporter gene expression, the *Cre recombinase* activity could be observed not only in the expected hypertrophic zone, but also in some proliferating cells, in cells of the perichondrium as well as in the bone marrow / cartilage junction. These data infer that promoter elements, not absolutely necessary for or restricting the tissue specific expression of collagen type X in hypertrophic chondrocytes, are located in this 10 kb fragment length. These elements might however lead to the non-specific staining that was observed in the reporter mouse lines of these current studies.

3.4.3 Generation of Cre-expressing transgenic mice using a hypertrophic chondrocyte-specific Col10a1 distal promoter element

The preliminary studies with transgenic mice expressing *β-galactosidase* under the 10 kb promoter showed a strong and specific blue x-gal staining in the growth plate of neonatal mice (compare chapter 4.4). The expression of the *Cre recombinase* under the control of the same promoter is however not as specific, since staining can be detected in bone marrow and in tissues surrounding the digits as well and even in proliferating chondrocytes at the most distal regions of the digits.

A detailed histological analyses of the digits of a transgenic mouse line expressing *β-galactosidase* under the 10 kb collagen X promoter fragment was performed in cooperation with Dr. Qiping Zheng to confirm the results detected in the *Cre recombinase* expressing mice. Sections of digits of the mice expressing *β-galact*osidase under the control of the 10 kb promoter were compared with sections of a new transgenic model, in which the *β-galactosidase* was expressed under control of a 4x300 bp element. Delineation of the collagen X promoter showed that this 300 bp fragment, demonstrating high multi-species homology, is most likely responsible for the specificity of the promoter in hypertrophic chondrocytes. The element contains a putative AP1 binding site. Earlier studies showed that a 4 kb long promoter fragment lacking the AP1 binding site does not lead to a specific expression whereas a promoter fragment with this element does (Zheng et al. 2003). To further test this AP1 element, multiples copies were produced by PCR amplification using BamHI and BglII containing primers and cloned, resulting in a 4x tandem AP1 element in conjunction with the basal promoter upstream of the *β-galactosidase* gene (*Tg-4x300*).

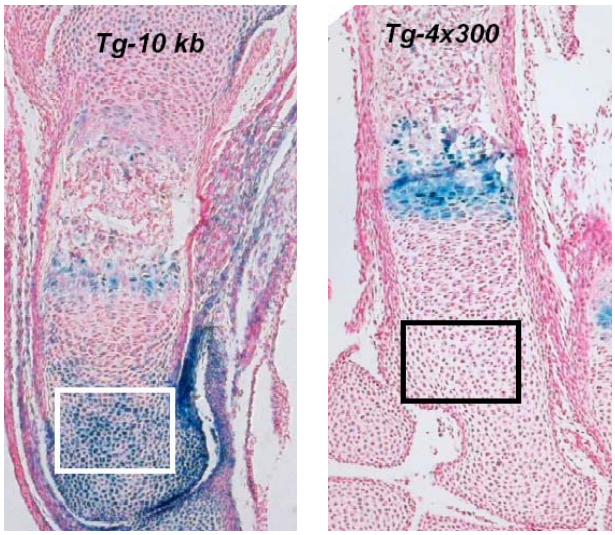

Figure 57: Differential reporter expression in *Tg-10 kb* and *Tg-4x300* mice.

Left panel is a section of an X-gal stained ***Tg-10 kb*** P1 mouse digit. Non-specific blue staining showing LacZ reporter activity can also be seen in the resting chondrocytes, perichondrium and surrounding soft tissues in addition to the hypertrophic zone (white box and vicinity area). The sections from ***Tg-4x300*** show reporter activity in the hypertrophic zone (right panel), but no staining can be observed in the resting chondrocytes or surrounding tissues (right panel, black box and surrounding area).

Figure 57 illustrates a section of a digit of a transgenic mouse expressing the *β-galactosidase* under the control of the 10 kb collagen X promoter. Staining can be detected not only in the hypertrophic chondrocytes but also in the resting chondrocytes of the digits (white box), in

the perichondrium, and in the surrounding soft tissue. In contrast, the sagittal section of a transgenic mouse digit, expressing the reporter gene under the control of the *Tg-4x300* AP1 containing promoter fragment, exhibits staining specific to hypertrophic chondrocytes.

Following the observations from these data, an alternate transgenic strategy was necessarily considered for the expression of *Cre recombinase* in hypertrophic chondrocytes (figure 58).

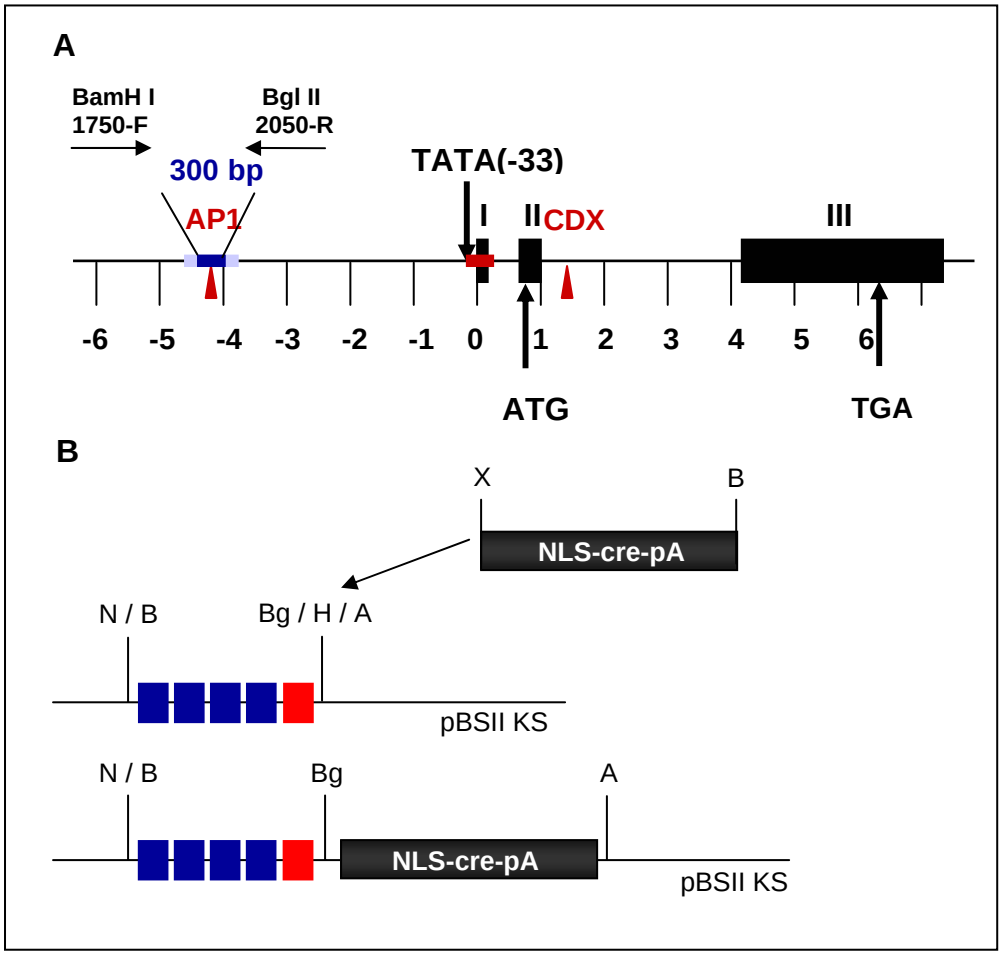

Figure 58: Strategy to generate a *Cre recombinase* expressing transgenic mouse line under the control of a *4x300 bp* element.

(A) Promoter structure of the *Col10a1* gene. The gene consists of three exons, start and stop codons are indicated by arrows. The conserved AP1 element as well as the conserved CDX element in the second intron is depicted with red triangles. The 300 bp element, four copies of which were used to generate the transgenic mouse lines is depicted as blue rectangles. The basal promoter containing the TATA box is indicated in red. (B) Structure of the promoter construct and the strategy, used to generate the *Cre recombinase* expressing transgenic mouse line for evaluation of the tissue specificity of the element to specifically in hypertrophic chondrocytes. A, Asp718I; B, BamHI; Bg, BglII; H, HindIII; N, NotI; X, XhoI.

A NLS-Cre recombinase cassette was cloned downstream of the 4x300 bp element, the construct was later released using the restriction enzymes BamH1 and Asp718I and cloned into the *Tyrosinase* cassette (to allow visual genotyping). As previously described, the construct was released with PacI, gel-purified and injected in pronuclei.

The resulting positive founder mice will be tested for tissue specific expression of the *Cre recombinase* in the future, as it is not possible to do so within the time limitations and in a manner consistent with the scope of this thesis project.

4 Discussion

The TGFβ pathways play an important role in almost all developmental processes. On a cellular level these proteins are involved in many processes such as differentiation, morphogenesis, cell migration and apoptosis. The TGFβ pathways are essential during embryogenesis, and subsequently play vital roles in homeostatic maintenance of adult tissues. TGFβ pathways are also indispensable in the development of cartilage and bone, both in the appendicular skeleton and in the craniofacial structures (Francis-West et al. 1998; Yoon and Lyons 2004; Wan and Cao 2005). The multitude of ligands, receptors and the mediators of this pathway and innumerable variety of associated proteins participating in the regulation of target genes, results in a very complex and highly diverse signal transduction mechanism (figure 59).

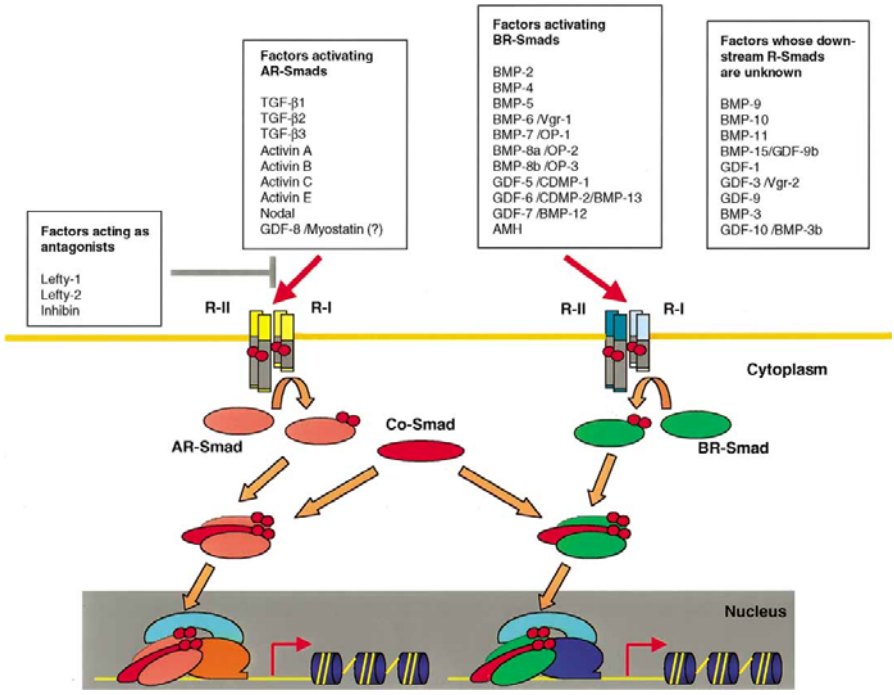

Figure 59: Members of the TGFβ superfamily, their specific receptors and receptor related Smads.

Members of the TGFβ superfamily that bind to their cognate receptors and mediate signaling via two major Smad pathways. TGFβ and activin signals are mediated by Smads2 and 3, while BMP signals are mediated by Smads1, 5, and 8. Both pathways require the Co-Smad, Smad4. Following binding, the heterocomplex is able to translocate into the nucleus and activate or repress the expression of target genes. AMH Anti-Muellerian hormone; AR-Smads, Smads that activated by TGFβs and Activins; BR- Smads, Smads that are activated by BMPs; BMP, Bone morphogenetic proteins; Co-Smad, Common partner Smad; GDF, Growth differentiation factor; OP, Osteogenic protein; Vgr, VG1-related sequence; R-I, type I receptor; R-II, type II receptor (Miyazono et al. 2001).

Two major Smad pathways are responsible for the TGFβ signaling. They include Smads1, 5 and 8, which are receptor-related Smads (R-Smads) that specifically mediate the signals from BMP ligands. Smads2 and 3 are also R-Smads but transduce signals from TGFβ and activin ligands. Smad4 (common partner or Co-Smad) is common to all R-Smads; its activity is essential for translocation of the Smad-protein complex into the nucleus. Smads6 and 7 are inhibitory Smads (I-Smads), which can impede signal transduction by binding to the receptor complex or by binding to Smad4, thereby blocking R-Smads binding. They are also direct target genes of the TGFβ signaling pathway, thereby creating a negative feedback loop (Massague et al. 2005).

Following binding of the ligand to its specific receptor, the receptor with serine/threonine activity phosphorylates the receptor itself and subsequently also phosphorylates a receptor-related Smad (R-Smad) protein. The Smad protein changes conformation upon phosphorylation and forms a heterotrimer with another phosphorylated R-Smad and the common partner Smad4. This complex can now translocate into the nucleus and bind to DNA in conjunction with other proteins, e.g. co-activators, co-repressors, transcription factors and DNA-modifying proteins, leading to the activation or repression of target genes (figure 60).

4.1 The role of BMP signaling in chondrogenesis

It is known that the Bone morphogenetic proteins not only promote chondrogenesis but are also essential for many stages of early chondrogenesis. Three type I receptors (Bmpr1, Bmpr1b and ActR1) as well as three type II receptors (BmprII and ActRII/ActRIIb) mediate signals in the BMP pathway (figure 6B). Differential affinities of the type I receptors to the BMP ligands are thought to contribute to the diversity of this signaling pathway.

Ligands, receptors and mediators of the BMP signaling pathway are expressed throughout the growth plate at various stages during limb development. *Bmps2*, *4*, and *5* are expressed in the perichondrium, *Bmp7* is expressed both in perichondrium and in proliferating chondrocytes and *Bmp6* is expressed in prehypertrophic and hypertrophic chondrocytes (Lyons et al. 1995; Pathi et al. 1999; Minina et al. 2001; Minina et al. 2002). The receptors *Bmpr1a* and *Bmpr1b* demonstrate overlapping expression in prechondrogenic condensations and *Bmpr1a* is also present in prehypertrophic and hypertrophic chondrocytes, while *Bmpr1b* is seen throughout the growth plate (Yoon et al. 2005). Immunostaining in rats revealed that *Smad1* and *Smad5*

are similarly expressed in the growth plate. They both show a strong expression in proliferating chondrocytes near the zone of maturation and a weak expression in proliferating chondrocytes near the zone of resting chondrocytes (Sakou et al. 1999).

A large array of animal models have been generated and studied in an attempt to elucidate the function of TGFβ/BMP signaling in skeletal development (table 1). Constitutively active forms of BMPR1A and BMPR1B in the chick model can promote chondrogenesis in transgenic mouse models, whereas only the overexpression of the dominant negative form of BMPR1B can inhibit chondrogenesis. These findings suggest that BMPR1B is a major receptor for the transduction of signals during chondrogenesis (Zou et al. 1997).
Targeted mice, null for *Bmpr1a,* die during gastrulation (Mishina et al. 1995), but the conditional knockout mouse model showed that loss of function of the receptor in proliferating chondrocytes led to a generalized chondrodysplasia. These mice exhibit shortened long bones, delayed ossification and have a smaller and flattened rib cage, leading to respiratory distress (Yoon et al. 2005). In *Bmpr1b* null mice, the defects are restricted to phalangeal elements and appendicular joints (Baur et al. 2000; Yi et al. 2000). Double knockouts for these two receptors, in proliferating chondrocytes, die due to severe skeletal defects between 17.5 dpc and birth. Most of the skeletal elements, which form through endochondral ossification, are absent or at least truncated and malformed, suggesting that *Bmpr1a* and *Bmpr1b* are functionally redundant at early stages of chondrogenesis. Additionally, chondrocyte differentiation is impaired, cartilage elements are severely disorganized and no cartilage specific extracellular matrix (ECM) is produced. Also, the proliferation rate is reduced and the number of apoptotic cells is increased resulting in the severe truncation of all skeletal elements (Yoon et al. 2005; Yoon et al. 2006).

Bmp2 and *Bmp4* deficient mice are embryonically lethal. Homozygous *Bmp2* null mice die between E7.5 and E10.5 due to defects in cardiac development (Zhang and Bradley 1996), *Bmp4* null mice die even earlier between E6.5 and E9.5 and they show no differentiation of early mesoderm (Winnier et al. 1995). Conditional double mutants for *Bmp2* and *Bmp4* in early mesenchyme condensations (using *Prx 1-Cre*) clarified roles for BMPs through manifestation of severe bone development defects (Cox and Rosen 2004). *Bmp6* is mainly expressed in hypertrophic chondrocytes and mice deficient for *Bmp6* are viable and fertile. Most probably the co-expressed Bmp2 is able to compensate for the loss of function of Bmp6 (Solloway et al. 1998).

Table 2: Bone and cartilage phenotype in different mouse models with alterations in the expression of members of the TGFβ/BMP signaling pathway.

The mouse models studied in this thesis are highlighted in gray.

Gene and mutation (promoter)	Phenotype	Reference
Bmp2/4 cKO (prx-1)	Defects in bone development	(Cox and Rosen 2004)
Bmp3 KO	Increased bone mass	(Daluiski et al. 2001)
Bmp4 cKO (col1a1)	Defects in bone development	(Guo and al. 2004)
Bmp4 KO +/-	preaxial polydactyly of the right hinlimb, craniofacial malformations ("boxer's nose")	(Dunn et al. 1997)
Bmp5 mutation (short ear)	Altered formation and repair of skeletal structures and development of several soft tissues	(Kingsley et al. 1992; Mikic et al. 1995)
Bmp7	Minor bone defects	(Dudley et al. 1995; Luo et al. 1995)
Bmpr1b KO	Impaired development of appendicular skeleton	(Yi et al. 2000)
Bmpr1a cKO (col2a1)/ Bmpr1b KO	Severe generalized chondrodysplasia	(Yoon et al. 2005)
Tgfβ2	Defects in mandibular and maxillary development / cleft palate	(Sanford et al. 1997)
Tgfβ3	Cleft palate	(Sun et al. 1998)
ΔTgfbr1 (col2a1)	Longer growth plate	
Tgfbr2 cKO (col2a1)	Defects in the base of the skull and in the vertebrae	(Baffi et al. 2004)
ΔTgfbr2 (metallothionein)	Longer, disorganized growth plate, elevated Ihh expression	(Serra et al. 1997)
Smad1 cKO	Osteopenia	(Chen and al. 2003)
*Smad1*cKO (col2a1)*/ Smad5+/-*	Shortened growth plate	
Smad3	Smaller, forelimb malformation	(Datto et al. 1999)

So far most attention has been directed toward the BMP ligands and their receptors. The focus of this work has been on the BMP signal mediators Smad1 and Smad5 and their function(s) during skeletogenesis. An additional aim was to compare BMP and TGFβ signaling. Therefore three different mouse models have herein been studied at different levels of the signaling pathways, i.e. on the ligand level (ESL-1), on the receptor level (ΔTβRI) as well as on the signal mediator level (Smad1/Smad5) (figure 61).

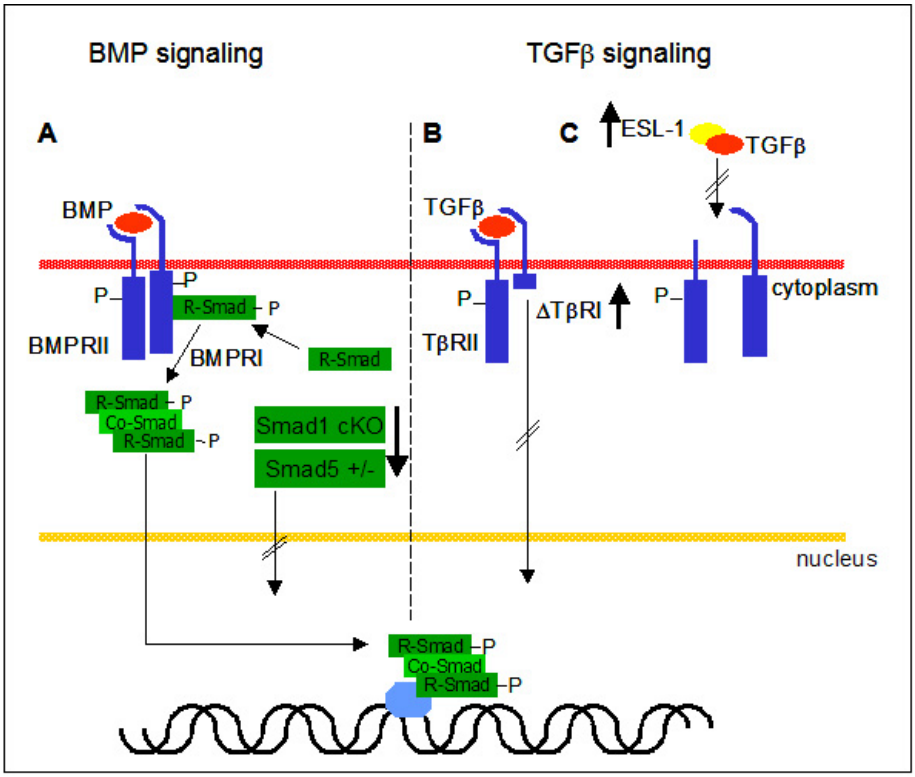

Figure 60: Mouse models used to study the disruption of TGFβ and BMP signaling in proliferating chondrocytes.

(A) The normal pathway of BMP/TGFβ signaling. After binding of the ligand, the signaling cascade via the Smad proteins commences and leads to either activation or repression of target genes in the nucleus. *Smad1* conditional mouse model with *Smad5* heterozygous background. (B) Transgenic mouse model overexpressing the dominant negative TβRI receptor. (C) Transgenic mouse model overexpressing Esl-1, a protein able to bind TGFβ ligands and represses binding of the TGFβ ligand to its specific receptor. Co-Smad, Common partner Smad; P, phosphate; R-Smad, receptor related Smad.

Smad1 deficiency in proliferating chondrocytes

Smad1 knockout mice die around E10.5 because they fail to form an umbilical connection to the placenta. The first morphological abnormalities seen in these mice are characteristic ruffles in the visceral endoderm overlying the distal extra embryonic region close to the primitive streak and a abnormal twisting of the epiblast and the newly formed mesoderm, which is evident at E7.0 (Tremblay et al. 2001).

To circumvent the lethality, a conditional *Smad1* knockout mouse model was used in this thesis. The conditional knock out animals were mated to transgenic mice carrying *Cre recombinase* under the control of the collagen type II promoter (*Col2-cre*) (Ovchinnikov et al.

2000) to study the loss of *Smad1* function during endochondral ossification. The tissue specific expression of *Cre recombinase* in the transgenic *Col2-cre* mice was first confirmed by mating these mice with Rosa26R reporter animals. These transgenic mice express *LacZ* only in tissues where *Cre recombinase*-mediated recombination occurs (Soriano 1999). All cartilaginous regions in newborn mice exhibited strong and specific staining (figure 10). The *Col2-cre* transgenic mice were therefore considered suitable to study loss of *Smad1* function specifically in the zone of proliferating chondrocytes of the growth plate.

The mutant transgenic mouse from this mating is clearly smaller than the wild type littermate (figure 12). Given that both animals are female; the size difference is not solely attributable to sex difference. Patterning defects were not discernable in these mice, but all cartilaginous and bony parts were shorter and more fragile. In multiple subsequent matings with comparable skeletal preparations this result could not be replicated and histological analyses of these additional matings did not reveal any gross differences either. An explanation for this discrepancy in findings is difficult. The limited severity of differences between the knock out mice and their wild type littermates might be attributable to their genetic background. Or it might be that a recombination event occurred in the first transgenic mice that led to the observed phenotype (positional effect of the transgene). Therefore the first described phenotype could not be observed in further breeding experiments.

Smad1 deficiency in proliferating chondrocytes with heterozygous *Smad5* background leads to a shortened growth plate

These data suggest that Smad1 might not play a uniquely pivotal role during skeletogenesis; another gene compensating for Smad1 might be functioning in this tissue. Most likely Smad5 might rescue the Smad1 phenotype given that both proteins share high identity (89.7%) at the protein level (figure 62).

This similarity as well as the fact that Smad1 and Smad5 seemed to be expressed in the same regions of the growth plate suggests that the two proteins might have similar or perhaps redundant functions in the development of the skeleton. Additionally, Smad5 null mice (like *Smad1* nulls) are embryonic lethal due to various embryonic and extraembryonic defects (Chang et al. 1999).

```
           1           15 16          30 31          45 46          60 61          75 76          90
1 gi|Smad1| ----MNVTSLFSFTS PAVKRLLGWKQGDEE EKWAEKAVDALVKKL KKKKGAMEELEKALS CPGQPSNCVTIPRSL DGRLQVSHRKGLPHV
2 gi|Smad5| ---MTSMASLFSFTS PAVKRLLGWKQGDEE EKWAEKAVDALVKKL KKKKGAMEELEKALS SPGQPSKCVTIPRSL DGRLQVSHRKGLPHV
           91         105 106         120 121         135 136         150 151         165 166         180
1 gi|Smad1| IYCRVWRWPDLQSHH ELKPLECCEFPFGSK QKEVCINPYHYKRVE SPVLPPVLVPRHSEY NPQHSLLAQFRNLGQ NEPHMPLNATFPDSF
2 gi|Smad5| IYCRVWRWPDLQSHH ELKPLDICEFPFGSK QKEVCINPYHYKRVE SPVLPPVLVPRHNEF NPQHSLLVQFRNLSH NEPHMPQNATFPDSF
           181         195 196         210 211         225 226         240 241         255 256         270
1 gi|Smad1| QQPNSHPFPHSPNSS YPNSPGGSSTYPHS PTSSDPGSPFQMPAD TPPPAYLPPEDPMAQ DGSQPMDTN-MMAPP LPAEISRGDVQAVAY
2 gi|Smad5| HQPNNAPFPLSPNSP YPPSP--ASSTYPNS PASSGPGSPFQLPAD TPPPAYMPPDDQMAP DNSQPMDTSSNMIPQ TMPSISSRDVQPVAY
           271         285 286         300 301         315 316         330 331         345 346         360
1 gi|Smad1| EEPKHWCSIVYYELN NRVGEAFHASSTSVL VDGFTDPSNNKNRFC LGLLSNVNRNSTIEN TRRHIGKGVHLYYVG GEVYAECLSDSSIFV
2 gi|Smad5| EEPKHWCSIVYYELN NRVGEAFHASSTSVL VDGFTDPSNNKSRFC LGLLSNVNRNSTIEN TRRHIGKGVHLYYVG GEVYAECLSDSSIFV
           361         375 376         390 391         405 406         420 421         435 436         450
1 gi|Smad1| QSRNCNYHHGFHPTT VCKIPSGCSLKIFNN QEFAQLLAQSVNHGF ETVYELTKMCTIRMS FVKGWGAEYHRQDVT STPCWIEIHLHGPLQ
2 gi|Smad5| QSRNCNFHHGFHPTT VCKIPSSCSLKIFNN QEFAQLLAQSVNHGF EAVYELTKMCTIRMS FVKGWGAEYHRQDVT STPCWIEIHLHGPLQ
           451         465 466
1 gi|Smad1| WLDKVLTQMGSPHNP ISSVS
2 gi|Smad5| WLDKVLTQMGSPLNP ISSVS
```

Figure 61: Homology between Smad1 and Smad5 proteins.

An approximate 90% homology between the murine proteins Smad1 (AAG41407) and Smad5 (AAC83580) has been observed. High homology is seen at both ends of the protein, which resembles the two Mad homology (MH) domains, while the linker region (shown in gray) is less homologous. The red letters indicate the identity between both proteins and black letters indicate divergence of both proteins. Protein sequences from NCBI Entrez Protein (http://www.ncbi.nlm.nih.gov/sites/entrez)

Conditional *Smad5* mice have previously been described. Ubiquitous *Cre recombinase* mediated deletion of *Smad5* showed that these mice phenocopy the conventional knockout of the gene (Umans et al. 2003). Unfortunately these mice were not available for further studies. To elucidate whether *Smad5* can rescue the *Smad1* loss of function phenotype, heterozygous Smad5 (*Smad5*$^{+/-}$) mice were considered as a good alternative for this study. Heterozygous *Smad5* null mice appear to be normal and fertile allowing for the conditional *Smad1* knockout mice to be crossed onto the heterozygous *Smad5* null background.

A weighing study was performed on mice from the above referenced crossing and it was expected that the *Smad1* conditional knock out mice, with and without the *Smad5* heterozygous background, should be lighter in weight, since the disrupted BMP signaling in the growth plate should lead to a shortening of skeletal elements. In males this assumption could not be confirmed at any of the three different weighting time points. In contrast the difference in the weight of females was as expected. One-day-old *Smad1* conditional knock out females with *Smad5* heterozygous background have been shown to be lighter in weight at statistically significant levels than their wild type littermates (figure 15). In three-week-old as well as seven-week-old females, the difference in weight was not statistically significant but the tendency for mutants to be lighter was still apparent (figure 17).

Weighing studies do not seem to represent an acceptable methodology for detecting gross phenotypic changes in these conditional knockout mice. The differences in the knockout

mice are less severe than expected and it would be necessary to do the weighing study with a considerable increase in the number of each phenotypic group to achieve statistical significance. Additionally hormonal influences potentially confound interpretation of the results.

In contrast to the results of the weighting study the histological analyses performed on one-day-old and eight-week-old mice are more consistent and importantly revealed the shortening of the growth plate in both females and males (figures 16 and 18). Analyses of eight-week-old animals not only confirmed shortening of the growth plate, but also that fewer cells were present and the growth plate of the mutant mice seemed to be disorganized when compared to wild type sections.

The shortening of the growth plate could either be due to a decrease in the proliferation of the chondrocytes or due to an increase in apoptotic processes in this tissue. To address this question, a proliferation assay was performed on hind limbs of one-day-old mice. In wild type control sections, more cells are stained compared to the conditional *Smad1* knockout mice with heterozygous *Smad5* background. A 5% increase in the number of proliferating cells was seen among the wild type control mice (figure 20). The proliferation rate in the knockout animals is therefore decreased, even more so with a *Smad5* heterozygous background, suggesting that the BMP signaling in proliferating chondrocytes plays a role in the regulation of proliferation. This has also been reported in conditional knock out mice for the receptors *Bmpr1a* and *Bmpr1b* (Yoon et al. 2005). The mice in this report also showed a decrease in the cell survival. Whether an increase in the rate of apoptosis also contributes to the shortening of the growth plate could unfortunately not be examined within the time frame of this work, but the observed decrease in proliferation appears most likely to be solely responsible for the slight reduction in size of the growth plate. If an increase in the rate of apoptosis would occur concurrently, one would expect to see an even more severe phenotype, e.g. more severe shortening and/or disorganization of the growth plate.

In order to gain further insights into these processes, *in situ* hybridization with the tissue specific probes *Ihh* and *Col10a1* was performed. *Ihh* is a specific marker for prehypertrophic chondrocytes, whereas *Col10a1* is a marker specifically for hypertrophic chondrocytes. These markers allow for independent assessment of observed changes in the growth plate, specifically the lengths of the prehypertrophic and the hypertrophic zones in mice that lack *Smad1* in proliferating chondrocytes, with and without *Smad5* heterozygous background and wild type mice, respectively. Both, the prehypertrophic as well as hypertrophic zones are

shortened in *Smad1* conditional knockout mice, with a slightly worse phenotype in mice on a *Smad5* heterozygous background (figure 21). The prehypertrophic zone appears to be more severely impaired reflected by the significant down-regulation of *Ihh* expression in these knockout mice. To quantify the *Ihh* and *Col10a1* expression levels in these hind limbs, quantitative real time PCR on cDNA derived from cartilage RNA would provide data at the level of transcription.

To gain further insight toward the molecular mechanism of the observed phenotype, Safranin O staining was performed to evaluate possible changes in the composition of the extracellular matrix as a consequence of reduced proliferation. Von Kossa staining was done to assess a possible delayed mineralization in *Smad1* conditional knockout mice with heterozygous *Smad5* background. No difference however was seen in either staining study of mutant mice compared to wild type controls (figure 22). It could be argued that the two staining methods are too crude to detect subtle differences or that the ECM composition and mineralization might be un-affected in the mutant mice studied in this work.

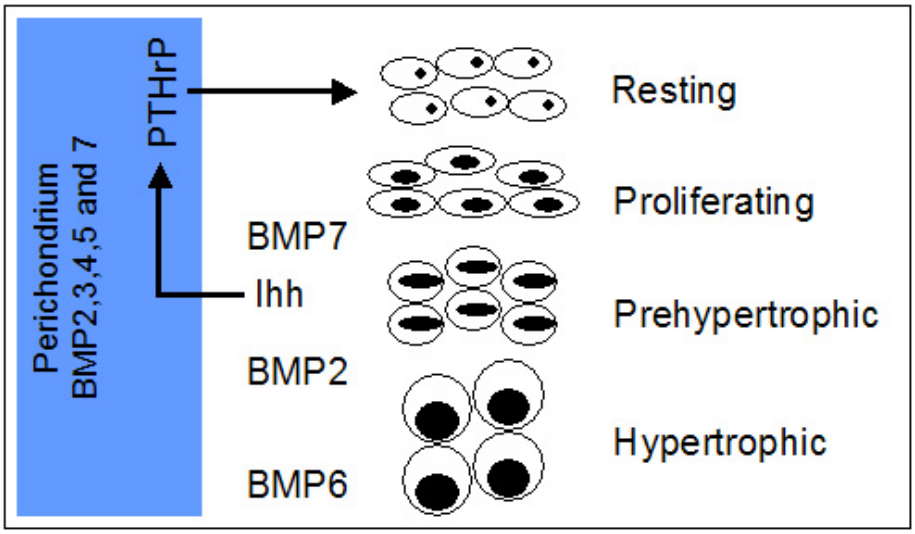

Figure 62: Normal expression and regulation of BMP and Ihh in the growth plate.

BMP2, 3, 4, 5 and BMP7 are highly expressed in the perichondrium. BMP7 is alone expressed in proliferating chondrocytes, where it probably promotes differentiation of proliferating chondrocytes to prehypertrophic chondrocytes. The prehypertrophic chondrocytes express Ihh, which promotes expression of PTHrP. PTHrP is predominantly expressed in the perichondrium and stimulates, via its receptor, which is expressed in the periarticular chondrocytes, proliferation (modified from Goldring et al. 2006).

BMP7 is the only ligand of the signaling pathway which is exclusively expressed in the zone of proliferating chondrocytes, while *BMPs 2*, *3*, *4*, *5* and *BMP7* are expressed in the perichondrium. It appears that BMP7 is promoting proliferation and differentiation to

prehypertrophic chondrocytes, which leads to the expression of *Ihh* in the prehypertrophic zone. Ihh then signals back via Ptc and Gli, leading to the expression of PTHrP, which in turn is able to promote proliferation (figure 62) (Minina et al. 2001; Goldring et al. 2006).

The data generated in this thesis suggest that the balance of BMP signaling is disrupted in proliferating chondrocytes in the *Smad1* mutant mice (both with and without a heterozygous *Smad5* null background), apparently leading to the inhibition of the differentiation from proliferating to prehypertrophic chondrocytes.
Less *Ihh* is expressed, in all likelihood due to the fact that fewer cells enter hypertrophy, resulting again in the down regulation of proliferation of chondrocytes, thus leading to the observed shortening of the growth plate (figure 63).

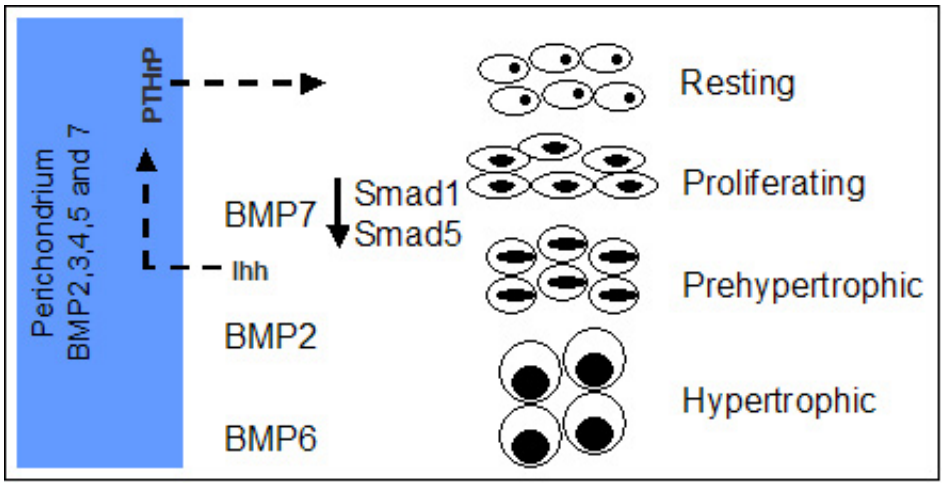

Figure 63: Impaired signaling pathway due to the partial disruption of BMP signaling in proliferating chondrocytes.

Disruption of BMP signaling in proliferating chondrocytes leads to down regulation of the proliferation rate in mutant animals. Prehypertrophic cell formation is impaired, thus leading to a shortened prehypertrophic zone with reduced expression of *Ihh*. The hypertrophic zone is shortened as well (modified from Goldring et al. 2006).

Craniofacial phenotype in *Smad1* conditional knock out mice on a heterozygous *Smad5* background

X-ray analyses was utilized to examine, whether the shortening of prehypertrophic and hypertrophic zones in the growth plate in addition to the diminished proliferation could be associated with hindrance in the growth or renewal of cartilage and bone in adult animals. If this would be the case this should lead to alterations in the bone density of the adult mutant animals. However, the mutant animals did not show any changes in bone density nor did the

length of the bones differ from controls. But the x-rays did reveal a craniofacial phenotype in mice lacking *Smad1* in proliferating chondrocytes and those on a *Smad5* heterozygous background. The mandibles, which were disarticulated from the skull for the x-ray analyses were normal but the nasal cartilage appeared to be disorganized and the nasal septum was absent. Additionally, the head of *Smad1* mutant mice (without the heterozygous *Smad5* null background) was overall smaller in size when compared to the wild type littermates. To verify these data and seek greater detail, Micro-CT was performed (figure 25) and corroborated the x-ray analyses but did not reveal additional findings nor provide further insights into the observed phenotype afforded by the x-ray study.

It is known that both BMP and TGF-β have distinct roles in the development of facial structures. Mutations of *Bmp5* lead to the naturally occurring short ear mutant (Kingsley et al. 1992). The knockout of *Bmps 2* and *4* are early embryonic lethal, but studies on the chick model gave some insights into the role of these ligands during the development of facial structures. The ectopic application of *Bmp2* and *4* results in activation of expression of *Msx*-1 and and *Msx*-2, which can result in the bifurcation of skeletal structures. The ectopic application of *Bmp2* can additionally increase the proliferation rate in the mandibular primordia, while haploinsufficiency of *Bmp4* in mice can result in the formation of shorter frontal and nasal bones and a unilateral curvature of the snout region, giving the appearance of a "boxer's nose" (Dunn et al. 1997). These published data suggest that both BMP2 as well as BMP4 may play a role in the outgrowth of the facial primordial and is consistent with the results of this study. The knockout of *Smad1* leads to a shortening of the snout region in mice. There are no data in the literature suggesting that *Smad1* and *Smad5* have a redundant function in the development of the skull. While the knockout of *Smad1* leads to a disorganized and shortened snout, a shortening of the snout in mice with additional haploinsufficiency of *Smad5* was not seen, but the disorganization of the cartilage is still evident. This feature suggests that on one hand, they might exert antagonistic effects during skull development, but on the other hand, have redundant functions during phases of long bone growth.

This leads to the question of why the phenotype of the mice that are mutant for the receptors are more severely affected than the mice that are null for the corresponding mediators of these receptor related signaling pathways. One weakness of the data presented here is certainly that the conditional knockout mouse for *Smad5* was not available for direct assessment of how

Smad1 functions in the growth plate. A complete loss of function for *Smad1* and *Smad5* in proliferating chondrocytes would in all probability have led to a more severe phenotype.

On the other hand, it is known that BMP signaling can occur independently of the Smad proteins as mediators, so that loss of function of BMP molecules or their specific receptors leads to a more severe phenotype, since SMADs mediate only part of these signals (figure 65).

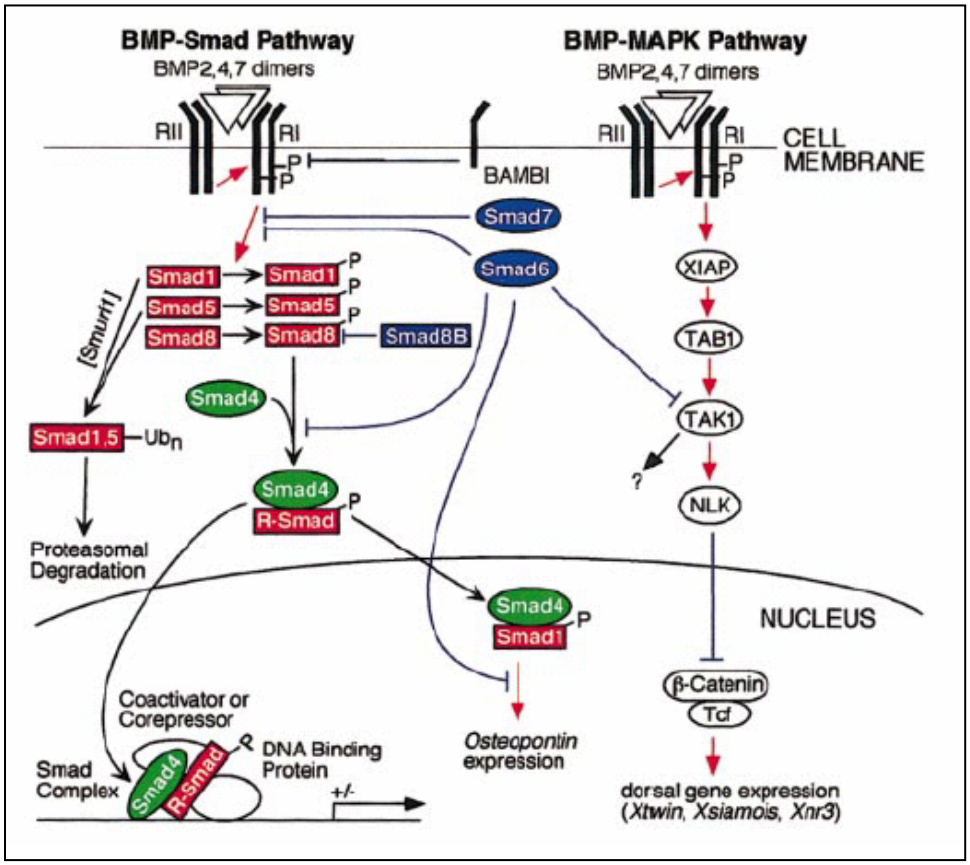

Figure 64: Alternative BMP-MAPK pathway.

The left side of the figure is the "canonical" BMP-Smad pathway. BMP2, BMP4 and BMP7 dimers bind to the type II receptors and this binding leads to the recruitment and phosphorylation of the type I receptor, which then phosphorylates the appropriate R-Smad (Smad1, Smad5 or Smad8). The phosphorylation of the R-Smads can be inhibited by the inhibitory or I-Smads Smad6 and Smad7. The pseudoreceptor BAMBI can inhibit the signal by binding to the Ligand/typeII receptor complex instead of the type I receptor. R-Smads following phosphorylation bind to the Co-Smad Smad4 and translocate into the nucleus. Here they activate or repress the expression of their target genes. Smurf and a splice variant of Smad8 are also able to regulate this signaling pathway. Smurf proteins can ubiquitinate phosphorylated R-Smads, which leads to proteasomal degradation, while Smad8B is able to inhibit the phosphorylation of Smad8 by binding to the receptor. The right side of the figure shows the alternative BMP-MAPK pathway. The activated BMP receptor might interact with XIAP, which in turn can activate the MAPKKK TAK1 via TAB1. TAK1 is afterwards able to activate NLK. NLK can inhibit the DNA binding ability of β-catenin/Tcf, which normally activates target genes of the Wnt pathway. NLK, NEMO-like kinase; RI, BMP receptor type I; RII, BMP receptor type II; R-Smad, Receptor-related Smad; TAB, TAK1-binding protein; TAK1, TGFβ-activating kinase; XIAP, Xenopus inhibitor of apoptosis protein; MAPKKK, mitogen activated protein kinase kinase kinase; XIAP, X-chromosome-linked inhibitor of apoptosis protein. (von Bubnoff and Cho 2001)

BMP signals are mediated not only by the Smad signaling pathway, but also via the mitogen-activated protein (MAP) kinase pathway. The signals are transduced via the X-chromosome linked inhibitor of apoptosis (XIAP). XIAP interacts with the adaptor molecule TAK1 binding protein 1 (TAB1) as well as with the BMP type I and type II receptor complex and acts most probably as an adaptor protein linking the receptor and TAB1 (Yamaguchi et al. 1999). TAB1 then binds to the TGFβ-activating kinase 1 (TAK1). TAK1 belongs to the MAP kinase kinase kinase (MAPKKK) family and it is also a key player in the BMP mediated MAP kinase cascade. Together with the adaptor molecule TAB1 TAK1 is able to activate MAP kinase resulting in the activation of JNK and p38 (Miyazono et al. 2001). Cell culture experiments with inhibitors of p38 in a ATDC5 chondrogenic cell line showed that the down-regulation of this pathway results in the suppression of chondrogenic differentiation by activation of growth and differentiation factor-5 (GDF5) (Nakamura et al. 1999; Watanabe et al. 2001). Whereas activation of p38 alone by using a constitutively active MKK6 induced the expression of the hypertrophic marker collagen type X (Seto et al. 2004).

All of these results suggest an important role for the mediators of the BMP signaling pathway in the development of the long bones and facial bone formation. The promoter used in this work was adequate, but the expression pattern of *Smad1* and *Smad5* and the expression of the receptor *Bmpr1a* in prehypertrophic and hypertrophic chondrocytes suggests that a conditional knockout model with *Cre recombinase* driven by a promoter specific for hypertrophic chondrocytes could provide valuable additional insight into the role of these TGFβ mediators in the growth plate.

4.2 Transgenic mouse studies to disrupt functional TGFβ signaling in proliferating chondrocytes

To better understand the individual and collective effects of the BMP and TGFβ signaling pathways in the growth plate, several transgenic mouse models were generated. The role of BMPs was previously evaluated by using a conditional knockout model of the mediators of this signaling pathway, however with difficulties in the execution of certain experiments and interpretation of their results. Since the conditional knockout model for *Smad1* had already been generated and tested as well as having been made available for the studies of this thesis, (Tremblay et al. 2001) the significant effort associated with creation of such a model was avoided. Nonetheless, mating schemes, experimental strategies and evaluations can represent a considerable if not uncertain investment.

Transgenic mouse models being easier and faster to generate, represent attractive alternatives for seminal investigations. The overexpression of inhibitors of TGFβ to down-regulate its signaling in proliferating chondrocytes was considered to be both an expeditious and appropriate first approach to inhibiting TGFβ signaling in this tissue.

It is also known, that TGFβ is expressed in the growth plate and that by inhibiting the signals at the initial steps of the pathway, the mediators of TGFβ could be studied. This is in direct contrast to knockout of the gene itself or other efforts at down-regulating these mediators.

Members of the TGFβ signaling pathway play an important role in embryonic and adult skeletal tissues. TGFβ1 and 3 are expressed in the perichondrium and periosteum of E13.5 mice and thereafter until birth. TGFβ2 and 3 are both expressed in chondrocytes. (Sandberg et al. 1988; Gatherer et al. 1990; Pelton et al. 1990; Millan et al. 1991; Pelton et al. 1991). The receptors for TGFβ (TβRI and TβRII) could be localized in perichondrium as well as in proliferating and maturing chondrocytes in the growth plate (Serra et al. 1999) (figure 65). This expression pattern is comparable to the expression of BMP receptors in developing cartilage. The BMP receptors BMPRI and BMPRII were also detected in proliferating and maturing chondrocytes, while the expression of the BMPRII extends more into the zone of mature chondrocytes (Sakou et al. 1999). This similar expression patterns of the BMP and TGFβ receptors and multiple *in vitro* as well as *in vivo* studies, suggest an antagonistic effect of BMP and TGF-β signaling in the developing growth plate.

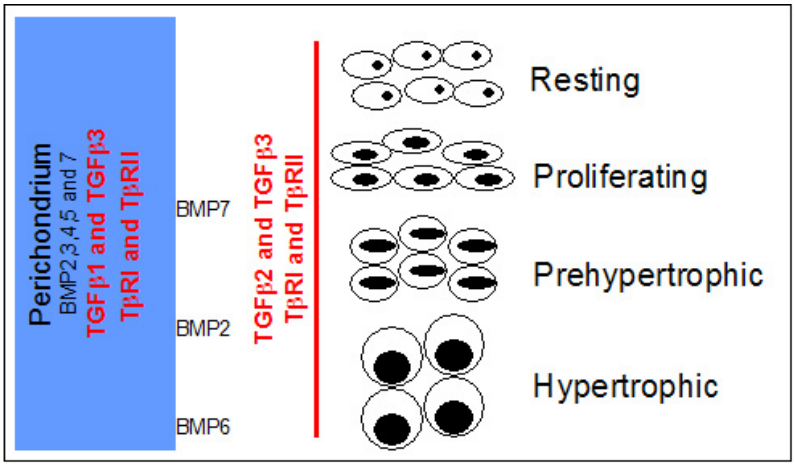

Figure 65: Expression pattern of TGFβ in the growth plate.

TGFβ1 is expressed in the perichondrium. TGFβ2 is expressed throughout the growth plate. TGFβ3 could be detected in all cell types of the growth plate as well as in the perichondrium.

Smad2 and Smad3 are known mediators of the TGF-β signaling pathway. *Smad2* null mice are, like *Smad1* and *Smad5* mutant mice, embryonic lethal. They die before E8.5 and are much smaller in size compared to wild type controls and show a pronounced reduction in the extraembryonic portion of the egg cylinder. At E7.5 most of the homozygous *Smad2* null mice were resorbed or did not form a distinguishable headfold or primitive streak. They also fail to form a mesoderm (Weinstein et al. 1998). A conditional knockout model for *Smad2* has recently been described (Liu et al. 2004).

Smad3 null mice are viable and survive into adulthood. They are smaller then their wild type littermates and show incomplete penetrance of joint formation abnormalities (Datto et al. 1999).

To further analyze the TGFβ signaling pathway it would be possible to mate mice carrying the *Smad2* conditional knockout allele combined with a *Smad3* null background as an alternative to the laborious approach to study the loss of function of TGFβ signaling mediators in proliferating chondrocytes using the transgenic mice carrying *Cre recombinase* under the control of the *col2a1* promoter. Since there are also Smad independent TGFβ signaling pathways, therefore transgenic mouse models were established in which TGFβ signaling was disrupted upstream of the signaling mediators and again specifically in proliferating chondrocytes, thus circumventing a putative compensation of the Smad dependent through the Smad independent TGFβ signaling pathway.

4.2.1 Overexpression of Esl-1 in proliferating chondrocytes

Esl-1 as a negative regulator for TGFβ pathway

E-selectin ligand 1 (Esl-1) is a highly conserved type I transmembrane sialoglycoprotein that was originally identified as the ligand for E-selectin in myeloid cells and a role in the regulation in leukocyte rolling was predicted (Steegmaier et al. 1995), because it could be co-purified with TGFβ1 in a large protein complex and it interacts also with FGF receptor *in vitro*. Generated *Esl-1* null mice showed no defects in the leukocyte rolling, but distinctive skeletal and growth defects were manifest. Newborn homozygous *Esl-1* null mice are 30-50 % smaller than their wild type littermates and demonstrate a narrowing of the chest. Skeletal preparation and subsequent alcian blue and alizarin red staining revealed a general shortening of all skeletal parts but without any obvious patterning defects. The histological analyses indicated a shortening of both the proliferating and hypertrophic zones. The proliferating zone in the *Esl-1* null mice has a decreased cell density and the chondrocytes seem to be moderately disorganized, suggesting that the synthesis and disposition of the extracellular matrix (ECM) occurs abnormally. A proliferation assay showed that the shortening of the growth plate is affected by a decrease in chondrocyte proliferation (Yang et al., unpublished data). Therefore ESL-1 might cause a pre- and postnatal skeletal dysplasia associated with decreased chondrocyte proliferation, which implies that ESL-1 plays a role in the regulation of skeletal development, growth and homeostasis.

Additionally, recent western blot studies showed that in the Esl-1 null mice a greater level of phosphorylated *Smad2* can be observed than in wild type controls (Yang et. al, unpublished data). Loss of function of Esl-1 leads to increased TGFβ signaling, but the mechanism of action has not yet been revealed. Cell culture studies also showed that secreted TGFβ is reduced in the presence of Esl-1, but it is not clear if this is a result of an increase in degradation of TGFβ or from decreased processing of TGFβ.

Generation and phenotypic characterization of the *col2-Esl-1* transgenic mice

Consistent with the aims of this thesis, mice overexpressing *Esl-1* in proliferating chondrocytes (*Col2-Esl1*) were generated to test the western blot studies in an *in vivo* mouse model. The hypothesis being that these mice would show a reverse phenotype: demonstrating an elongation of the growth plate as well as an increase in the chondrocytes proliferation rate.

The weighting studies of two-day-old and four-week-old adult mice showed no phenotypic differences between transgenics and wild type littermates. In addition, skeletal preparation with alcian blue and alizarin red staining showed no visible differences in the length of any of the skeletal elements. Neither the long bones, nor the rib cage in the transgenic mice showed any alteration nor could any patterning defects be observed (figure 29). The 14.5 fold overexpression of *Esl-1* in cartilage, which was established by quantitative real time PCR (figure 28), is perhaps insufficient to cause an obvious phenotype. However, histological analysis revealed an increased cell density at the junction of proliferating and hypertrophic chondrocytes (figure 30), but this does not result in an apparent elongated hypertrophic zone. The proliferation assay showed an up to 4% (figure 31) increase in the proliferation rate in transgenic mice. Multiple tissue sections of transgenic and wild type mice (n=2) were counted and the results are statistically significant. The *in situ* hybridization on hind limb sections indicate that the expression of *Ihh*, the marker for prehypertrophic chondrocytes, is strongly increased in the transgenic mice (figure 32), suggesting that the reduction in TGFβ signaling from overexpression of *Esl-1* in proliferating chondrocytes probably leads to an increased differentiation rate. The overexpression of *Ihh* was verified by qPCR. Additionally the qPCR showed, that *Col2a1*, the transcription factor *Sox9* and *PTHrP,* (markers for resting and proliferating chondrocytes respectively), are clearly downregulated in the transgenic animals. *Col10a1*, a marker for hypertrophic chondrocytes, is upregulated supporting the results of the *in situ* hybridization. The expression of the *PTH/PTHrP receptor* (*PPR)* is unchanged in transgenic animals compared to the wild type control (figure 26). These findings were consistent with the expectations based upon the qPCR results received by Dr. Yang on cDNA of ribcage cartilage from *Esl-1* null mice, which were directly opposite to these results obtained on transgenic mice overexpressing *Esl-1* in proliferating chondrocytes (Yang et al., unpublished data).

Taken together, these data suggest that Esl-1 is in fact inhibiting TGF-β signaling during development of the skeleton. Early studies revealed that TGF-β promotes the synthesis of extracellular matrix molecules during the condensation process, but thereafter it inhibits differentiation (Roark and Greer 1994). This would explain the phenotype observed in the *Col2-Esl-1* transgenic mouse. More cells proliferate, but the terminal differentiation of the chondrocytes is depleted.

4.3.2 Overexpression of the dominant negative TGF-β receptor 1

Another transgenic model with an impaired TGFβ signaling in proliferating chondrocytes was generated using a dominant negative TGFβ receptor 1 (ΔTβR1) under the control of the *Col2a1* regulatory element. Transgenic mice should overexpress a truncated protein, which lacks the serine/threonine kinase domain. This receptor is able to bind TGFβ ligands but the signaling is inhibited due to the lack of the kinase domain. Thus this truncated receptor is competing with the endogenous receptors for ligand binding and leads so to an overall down regulation of the TGFβ signaling in proliferating chondrocytes.
The plasmid containing the ΔTβR1 with a 3' Flag-tag (to distinguish between the endogenous TGFβ and the transgene) was a generous gift of Dr. Rick Derynck (UC San Francisco, USA). The *ΔTβR1-Flag* was cloned downstream of the 6 kb *Col2a1* regulatory fragment to direct its expression specifically to the zone of proliferating chondrocytes in the growth plate.

Not surprisingly, the *Col2a1-ΔTβR1* and the *Col2a1-Esl1* transgenic mice showed a similar phenotype. Earlier studies revealed that TGFβ has an antiproliferative function and therefore a longer growth plate. The increased proliferation rate and thus the increased expression of the prehypertrophic marker *Ihh* was expected.

The growth plate is longer due to a lengthening of the prehypertrophic and hypertrophic zones. While the histological analysis of the R1 generation of the transgenic *Col2-ΔTβR1* mice reveals that the longer growth plate is due to an enlargement of the cells itself (figure 36). But the analyses of the F1 generation of the same transgenic mice showed that the longer hypertrophic zone is a result of an increased number of cells that enter terminal differentiation (figure 43). Although more cells are entering hypertrophy, only a slight elongation of the hypertrophic zone can be observed. The proliferation assay showed an up to 4% increased proliferating rate (figure 45). Additionally, *in situ* hybridization with the prehypertrophic marker *Ihh* and the hypertrophic marker *Col10a1* showed that the expression of *Ihh* is strongly elevated, and the hypertrophic zone slightly elongated. Mineralization assay with von Kossa staining showed that a high expression of the transgene lead to an increased mineralization rate compared to wild type animals.

Mice that express a dominant negative TGFβ receptor type II (under the control of a metallothionein promoter) in skeletal tissues showed severe skeletal defects in transgenic

animals. Histological analyses of four-week-old transgenic animals showed a disorganized growth plate with a thicker hypertrophic zone; the cells of the hypertrophic zone were not organized in columns (figure 37). *In situ* hybridization studies of these mice also showed a stronger and broader expression of *Ihh* in the growth plate (Serra et al. 1997), which is comparable to the *Col2-ΔTβRI* transgenic mice, described in this work (figure 44).

While establishing two different lines of the *Col2-ΔTGFβ* transgenic mice the R2 x R2 mating produced mice that were severely shorter than some of their transgenic littermates. Multiple matings and phenotype distributions showed that these mice were born consistent with Mendelian ratios (1:2:1) suggesting that they are most likely homozygous for the transgenic allele, although the verification via qRT-PCR is still pending. Additionally, these mice exhibited a darker fur than their transgenic littermates indicating that these animals are presumptive homozygous mice. They exhibit a shortened stature with thinner long bones and craniofacial abnormalities including a shortened head, while their transgenic (heterozygous) littermates show no obvious differences to the wild type controls (figure 39).
Although these mice have indicated an increased proliferation rate, a longer prehypertrophic and hypertrophic zone and increased mineralization, they are severely smaller than the wild type controls. This may be attributable to the craniofacial phenotype. The heads of three weeks old homozygous are smaller (figure 39); the upper incisors are broken, perhaps due to a severe under bite. The mandible is more prominent in comparison to the wild type animals, while the snout region is shorter. It is likely that these mice have feeding problems, which would result in the smaller size of the animals. This is supported by the observations made in one-day-old animals that are only slightly shorter than controls, but in which a more prominent mandible is already obvious, while the skull seems to be only slightly shorter (figure 42). Observation of the mice until shortly before they stop lactating would be a means of confirming that the transgenic *Col2-ΔTGFβ* mice have feeding problems due to the craniofacial defects.

Micro-CT of the three-week-old mice showed a disorganized nasal cartilage, which might be due to mechanical stress. The craniofacial phenotype in one-day-old mice is not as severe as in three-week-old mice, suggesting that stress while biting the “hard” food may erode the cartilage. To test this hypothesis, comparable sections of heads of the ages of one-day-old, two- and three-week-old as well as adult mice would be helpful. It might be either that the cartilage formation is defective in the transgenic animals or the cartilage could be too soft due

to mineralization defects or altered extracellular matrix composition. This could be evaluated through Alcian blue, Safranin O and von Kossa staining on head section.

The flat bones of the skull and the clavicles are formed through intramembranous ossifaction (chapter 1.1), while parts of the mandibular as well as the occipital bone develop through endochondral ossification. In both mechanisms, TGFβ pathways play pivotal roles. Knockout of *Tgfβ-3* leads to the development of a cleft palate since it is specifically required for the fusion of the palatal shelves (Sun et al. 1998). The facial primordia as well as the palatal shelves themselves do not fail to form in these mice. *Tgfβ-1* knockout mice die before E10.5 due to defective haematopoiesis and vasculogenesis (Dickson et al. 1995). *Tgfβ-2* knockout mice displayed defects in maxillary and mandibular development and the palate fail to fuse only occasionally (Sanford et al. 1997).

TGFβ signaling regulates key aspects of embryonic and fetal development and it has been shown that TGFβ1 for example plays a role during all phases of the endochondral ossification. The role of TGFβ in the development of the mandible is described here as an example.

The first step in the development of the mandible is the migration of neural crest cells to their future site in skeletogenesis (Atchley and Hall 1991). Fibronectin is an extracellular molecule, which is induced by TGFβ and which is necessary for the migration of the cells. During migration, the cells begin to proliferate and generate extracellular matrix, which is promoted again by the expression of TGFβ (Itoh et al. 2000). Together with BMP2 and 4 as well as Msx-1 and tenascins, TGFβ controls the following epithelial-mesenchymal interactions (Hall and Miyake 2000). Progression to condensation is dependent on an enhanced mitotic activity of mesenchymal cells and the local changes of the extracellular matrix, which contains now more fibronectin. The production of fibronectin is influenced by TGFβ1 and fibronectin interacts in turn with TGFβ, this interaction is proposed to be a casual event in the establishment of the condensation phase (Newman and Frisch 1979). This hypothesis is supported by the observation that mice with defective fibronectin production fail to form limbs, likely due to inhibition of condensation (George et al. 1993). TGFβ also maintains chondrogenesis through the activity of p38, ERK-1 and JNK. This regulation of the mesenchymal progenitor cells includes the modulation of expression levels of N-Cadherin, which in turn controls cell-cell interactions and thus the event of chondrogenic

differentiation (Tuli et al. 2003). Studies on chick limbs implied that TGFβ promotes endochondral development including condensation. During subsequent differentiation TGFβ1 has inhibitory effects (Roark and Greer 1994; Kanaan and Kanaan 2006).

4.3 Antagonistic effects of BMP and TGFβ signals in proliferating chondrocytes

In this thesis three separate mouse models were utilized to study the role of TGFβ and BMP signaling during proliferation of chondrocytes in endochondral ossification. BMP signaling in proliferating chondrocytes was disrupted by knocking out *Smad1* as one mediator for the signaling pathway in this cell type. The *Smad5* null allele was crossed into these mice, since *Smad1* and *Smad5* are homologous and both expressed in the growth plate in a similar fashion. In addition it has been speculated that Smad5 might compensate for Smad1 loss of function but this has never been experimentally shown in the literature. And data presented in this work suggest, that Smad1 and Smad5 might have indeed different functions in the developing skeleton. The role of TGFβ signaling during endochondral ossification was studied using two different transgenic mouse models each inhibiting TGFβ signaling specifically in proliferating chondrocytes at different levels of the signaling cascade.

In both transgenic mouse models, the overexpression of Esl-1 and the overexpression of a dominant-negative TGFβ receptor type I lead to the partial disruption of TGFβ signaling in proliferating chondrocytes and the effects upon the growth plate were comparable between these two lines.

While disruption of BMP in proliferating chondrocytes leads to a shortening of the growth plate due to a decreased proliferation rate, the disruption of TGFβ signaling results in a increased proliferation rate and thus to an enlarged prehypertrophic zone with increased expression of the prehypertrophic marker *Ihh*. The results suggest that these two pathways play antagonistic roles in the growth plate (figure 66). Moreover, transgenic mice overexpressing the dominant-negative TGFβ receptor type I exhibit a craniofacial phenotype. This phenotype could be responsible for the feeding problems (in homozygous transgenic mice only) that manifested in a distinct size difference, evident at three weeks of age.

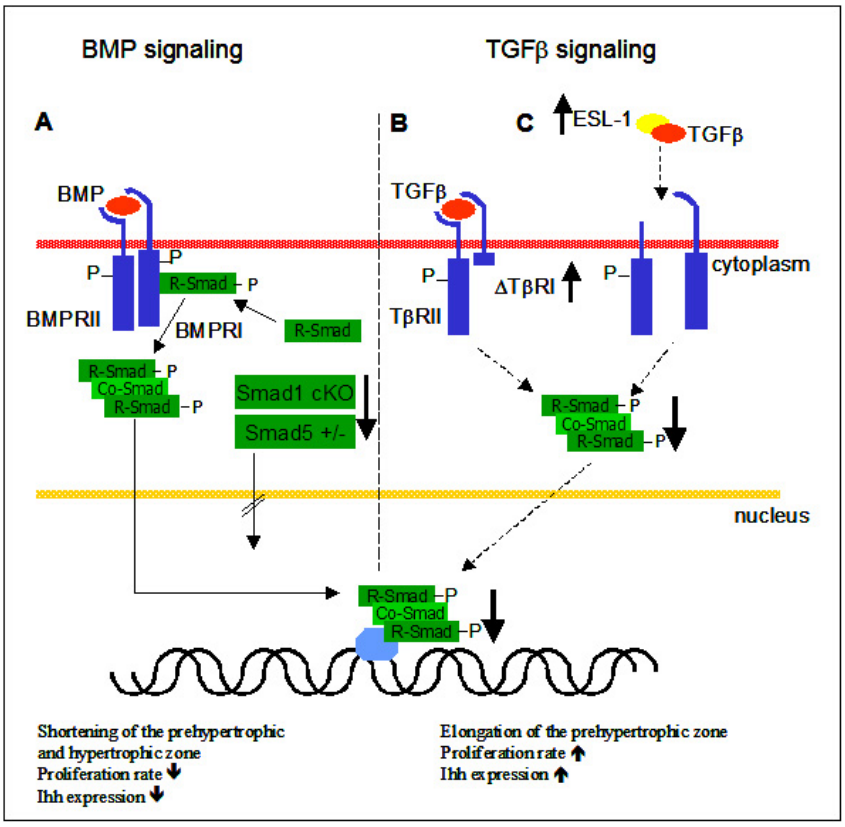

Figure 66: Overview of the different mouse models and the antagonistic effects of the two signaling pathways in the proliferating chondrocytes.

(A) The normal signaling pathway of BMP/TGFβ is shown in the left panel. The *Smad1* conditional mouse model on a *Smad5* heterozygous background leads to a complete knock out of *Smad1* in proliferating chondrocytes, but the pathway cannot be disrupted completely. Smad5 protein is still present, but the knock out mice (with and without Smad5+/- background) showed a shortening of the prehypertrophic and hypertrophic zones with a decreased proliferation rate and an decreased *Ihh* expression. (B) Transgenic mice carrying the dominant negative TβRI receptor allele and (C) the transgenic mouse model overexpressing Esl-1 both have an elongated prehypertrophic zone due to an increased proliferation rate as well as an increased *Ihh* expression. Co-Smad, Common partner Smad; Ihh, Indian hedgehog; P, phosphate; R-Smad, receptor related Smad.

4.4 *Cre Recombinase* expression under the control of the 10 kb collagen type X promoter

Thus far the role of different proteins belonging to the TGFβ or BMP pathway was identified by using knockout and transgenic mouse models specifically in proliferating chondrocytes. The well studied Collagen type II (Vikkula et al. 1992; Zhou et al. 1995; Lefebvre et al. 1996a; Lefebvre et al. 1996b; Zhou et al. 1998; Ovchinnikov et al. 2000) was therefore utilized. The expression pattern of the *Smads*, *BMPs* and *TGFβs* in the growth plate suggests an important role of these proteins not only in the proliferation of chondrocytes but also in the zone of hypertrophic chondrocytes as well. Therefore a reporter mouse line that would

express *Cre recombinase* or other transgenes of interest specifically in the hypertrophic chondrocytes would serve as a very valuable tool to the entire research community for the study of the function of relevant embryonically lethal genes in the hypertrophic zone of the growth plate. This would enable us to study not only the proliferation but also the maturation processes of the growth plate.

Type X collagen is a network forming collagen and it is the only known marker specific to hypertrophic chondrocytes. It is transiently expressed in hypertrophic cartilage in fetal and juvenile growth plates of long bones, ribs and vertebrae (Schmid et al. 1994). Mutations in *COL10A1* in humans are associated with Metaphyseal chondrodysplasia type Schmid (MCDS) (Warman et al. 1993) and the phenotype of mice deficient for *Col10a1* partially resembles MCDS (Kwan et al. 1997). The gene is located on murine chromosome 10 and human chromosome 6.

The murine *Col10a1* consists of 3 exons and encodes a 680 amino acid long protein. The gene and promoter structure is shown in figure 67.

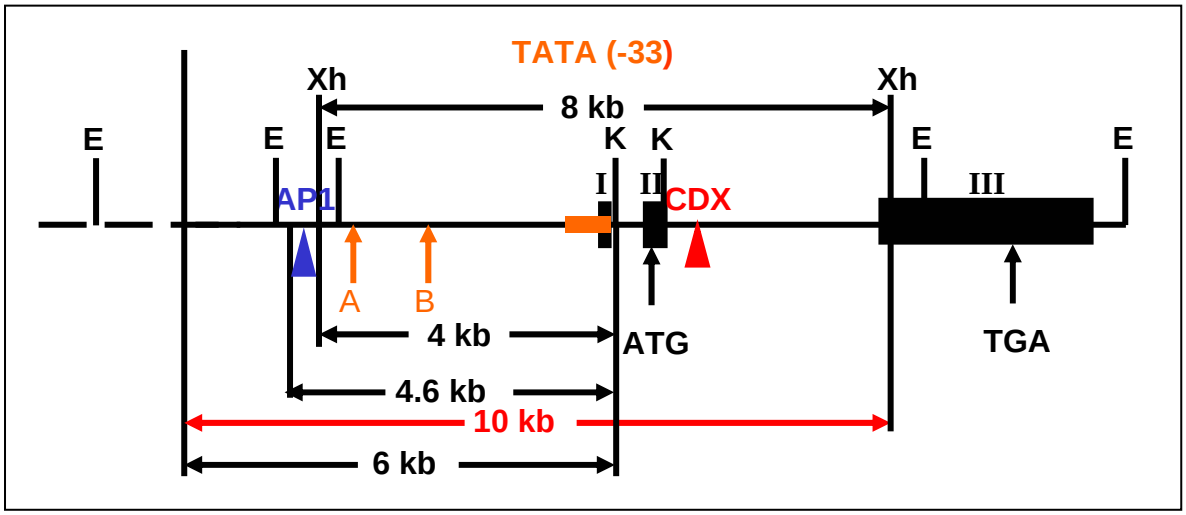

Figure 67: Restriction map and analyses of mouse type X collagen gene.

Col10a1 consists of three exons numbered I, II and III. The positions of the TATA box in the minimal promoter, ATG start codon, and TGA stop codon are indicated. Two conserved *Runx2* binding elements within the 4 kb *Col10a1* promoter are designated as A and B. Two additional conserved elements within both *Col10a1* distal promoter and second intron are indicated by red (CDX) and blue (AP1) triangles. The 4 kb, 4.6 kb, 6 kb, 8 kb and 10 kb *Col10a1* fragments used in transgenic mice studies are indicated by arrows. E: *EcoRI*, Xh: *XhoI*, K: *KpnI*. The 8 kb and 10 kb *Col10a1* elements with endogenous ATGs within exon II were mutated into ACGs for all transgenic mouse studies.

Upstream of exon1 are two putative Runx2 binding sites, as well as a putative AP1 binding site (indicated as A and B in figure 67). The highly conserved sequence in intron 2 exhibits high homology to a putative CDX binding site.

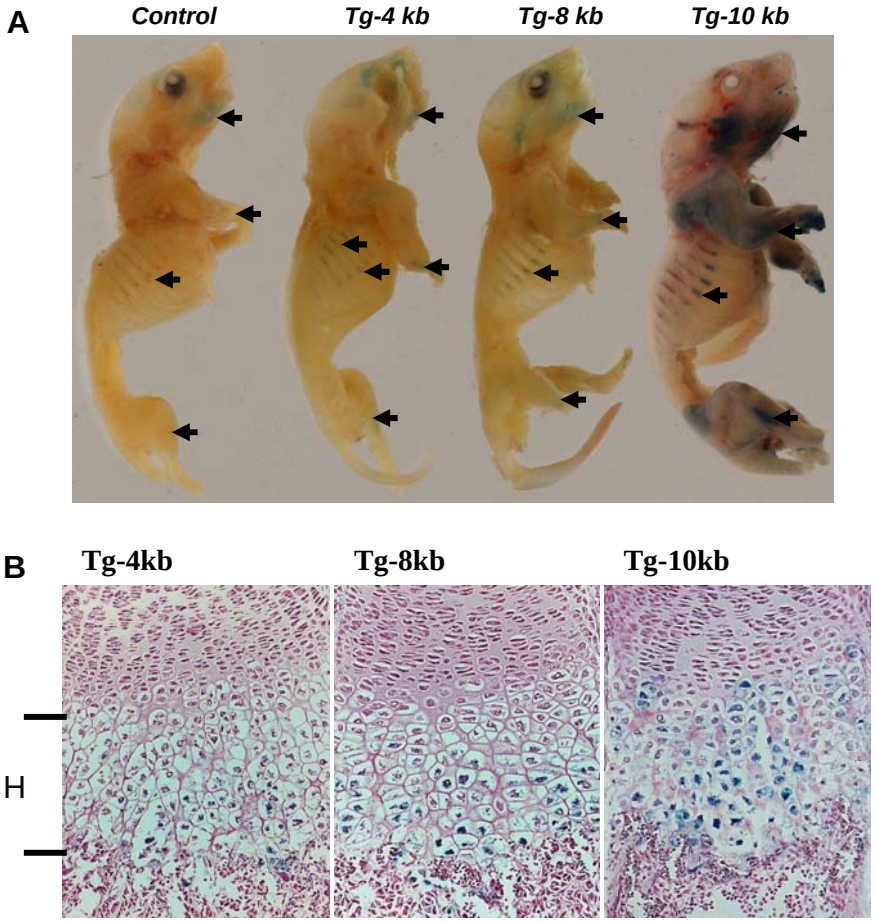

Figure 68: Analyses of *Col10a1*-4 kb, 8 kb and 10 kb transgenic one-day-old mice.

(A) Whole mount staining of *Col10a1*-4 kb, 8 kb and 10 kb transgenic P1 mice. X-gal staining of one-day-old transgenic mice using the 4 kb *Col10a1* element showed blue staining in the lower hypertrophic zone (***Tg-4 kb***, arrows). The wild-type littermate control showed no staining (***Control***). Background staining (probably due to endogenous β-galactosidase activity) was observed both in transgenic and control mouse embryos in the craniofacial region (***Tg-4 kb***, and ***Control***, arrows). A more specific blue staining was observed in 8 kb transgenic mice (***Tg-8 kb***, arrows). The 10 kb *Col10a1* regulatory element can direct high levels of tissue-specific expression of the transgene compared to the staining pattern of 8 kb transgenic mice (***Tg-10 kb***, arrows). **(B)** Paraffin embedded sections of one-day-old mice from *Col10a1* 4 kb, 8 kb and 10 kb transgenic mouse. Sagittal sections of distal ulna from ***Tg-4 kb*** line shows weak blue staining in the lower hypertrophic zone (left panel), while comparable sagittal sections from ***Tg-8 kb*** show a low level staining throughout the zone of hypertrophy (middle panel). Sagittal sections of distal ulna from ***Tg-10 kb*** line show stronger blue staining throughout the hypertrophic zone than that of the *Col10a1* 8 kb transgenic mice (right panel). *Tg*: transgenic mice, HZ: hypertrophic zone of the growth plate (from Zheng et al., 2003).

Earlier data obtained in cooperation with co-workers in the laboratory of Dr. Brendan Lee provided strong evidence that all of these elements are important for tissue specific and high

levels of expression of *Col10a1* in hypertrophic chondrocytes. Transgenic mouse lines expressing lacZ driven by a 4 kb long promoter, which includes only the two putative *Runx2*-binding sites showed only a very weak, but nonetheless a tissue specific staining of the lower hypertrophic zone (Zheng et al. 2003) (figure 68).

The promoter fragment containing the putative *AP-1*-binding site (*Tg-6 kb*) showed a stronger x-gal staining in whole embryos as well as in tissue sections, which were counterstained with Nuclear Fast Red. Since the 10 kb long promoter fragment (figure 68A) showed the strongest and most specific staining, in particular in the sections of the ulna, (figure 68B) therefore this promoter was used to generate mice expressing the *Cre recombinase* in hypertrophic chondrocytes.

Cloning strategy and characterization of the *10kb-Col10-cre* construct

Cre recombinase was placed under the control of the above described 10 kb regulatory element and the construct was injected in pronuclei of FVB/N zygotes. Positive founder mice were mated with Rosa26R reporter mice (R26R) to confirm the tissue specificity of the *Cre recombinase*.

The *Cre recombinase* gene expression in the offspring of the founders was different among the transgenic littermates (figure 50). Whereas one of the transgenic mice showed the expected expression pattern in all cartilaginous regions of the body, another littermate was stained completely blue, suggesting an ubiquitious expression of the transgenic allele most likely due to positional effects. To examine the specificity of *Cre recombinase* at the cellular level, limbs and ribs of mice that were deemed to be specific were further analyzed histologically (figure 51). Blue staining in regions of *Cre recombinase* activity can be appreciated not only in hypertrophic chondrocytes of the growth plate, but also in resting and proliferating chondrocytes. Bone marrow and connective tissue as well as some muscle tissue showed blue staining attributable to *Cre* activity. The expression is not only non-specific; but the strength of expression seems to increase in a proximal to distal direction.

The insertion site of a transgene is an important factor governing specific expression. Positional effects, resulting from the action of enhancers or repressors distant or in the vicinity of the inserted transgenic allele, may intensify, inhibit or completely alter the correct

expression of the transgene. Insulator sequences such as the HS4 β-globin chicken insulator may reduce the risk of an incorrect expression pattern since they are considered to protect the transgenic allele from positional effects (West et al. 2002). This way, positional effects may be reduced or even completely avoided. However, positional effects alone cannot explain the different expression pattern of the transgenic allele in different mice of the same litter. More likely, multiple insertion sites could be responsible for the different activities of *Cre recombinase* in the offspring of the same litter. Alternatively, the 10 kb *Col10a1* promoter fragment may not contain the all necessary regulatory elements responsible for tissue specific expression.

The *10kb-Col10-cre* construct with *Tyrosinase* cassette and HS4 insulator

To overcome the problem of positional effects in the generated transgenic mouse lines, the *10kb-col10-Cre* construct was subcloned into a vector, containing two copies of the HS4 β-globin chicken insulator at the 3' end as well as a *Tyrosinase* cassette under the control of the K14 (keratinocyte) promoter (Hsiao et al. 2004), also allowing for the visual genotyping of the newborn mice. Mice carrying the transgene express *Tyrosinase*, which in turn leads to a change in eye color from red to black in FVB/N mouse strain and as a reflection of the strength of expression (most likely due to multiple sites of insertion) to a change in the color of the fur as well (chapter 3.2). In contrast to the generation of the transgenic mouse lines, no WPRE (Donello et al. 1998; Zufferey et al. 1999; Mian et al. 2005) element was used to enhance the expression of the transgenic allele, because the expression of the *Cre recombinase* in the described transgenic mouse model is sufficiently strong without additional enhancement.

All founders were crossed with R26R reporter mice to confirm the specificity of the *Cre recombinase* activity. In contrast to the transgenic mice without the insulators, all newly generated transgenics exhibited a tissue specific expression of the *lacZ* gene as demonstrated by the blue staining in the hypertrophic chondrocytes. Expression strength varied between the offspring of the different founder mice and correlated well with the empirically observed strength of the expression of the *Tyrosinase* gene (figure 54).
Histological analyses of these mice confirmed the different expression levels of the *Cre recombinase* among the transgenics (figure 55). All mice reflect some expression of *Cre recombinase* in hypertrophic chondrocytes, but in addition, a more or less leaky activity of

Cre recombinase was observed in the bone marrow. Moreover, a high level of expression level was visible in the digits of all transgenic mice. One of the founders expressed *Cre recombinase* in parts of the proliferating zone of the growth plate as well as in the perichondrium and the surrounding soft tissue. A strong *Cre* expression in these mice seems to lead to greater non-specific *Cre* activity. The histological analyses also revealed a gradient of expression levels, from proximal to distal, also previously seen in transgenic mice generated without the *Tyrosinase* and insulator elements.
In contrast to the *10kb-Col10-cre* transgenic mouse generated in this thesis, Yang et al. used a construct driven by the 1 kb proximal promoter. The expression pattern in these mice is comparable to the *Cre recombinase* expression described in this work but is not completely restricted to hypertrophic chondrocytes. Also observed was a non-specific expression in the perichondrium, in bone marrow and bone trabeculae (in femur sections of P2 old mice) as well as in skin (Yang et al. 2005). The expression of *Cre recombinase* in these transgenic mice is relatively low compared to the expression of the *10kb-Col10-Cre* driven transgenic allele described here. These results as well as the transgenic mouse models with different promoter fragments suggest that 1 kb promoter fragment together with the basal *Col10a1* promoter is insufficient for strong and tissue specific expression of the *Cre recombinase*.

Recent transgenic mouse data indicate that a 300 bp element located approximately 4 kb upstream of exon 1 is necessary for a specific expression of *collagen type X* in hypertrophic chondrocytes (Gebhard et al. 2004) (figure 67). The staining of the transgenic mice generated with this element, show a strong and very specific expression in hypertrophic chondrocytes. The non-specific staining of resting chondrocytes, perichondrium and connective tissue that was seen in the 10 kb transgenic mouse line was not detected in these 4 x 300 bp transgenic mice (in cooperation with Dr. Qiping Zheng, unpublished data, figure 57).

Because of this strong and tissue specific expression, the 4 x 300 bp element with the basal promoter was chosen to drive the *Cre recombinase* expression in transgenic mice (figure 59). The basal promoter contains a sequence of seven bases (TATAAAA) called the TATA-Box. The TATA-Box of the *col10a1* gene is located 33 bp upstream of exon 1 (figure 67). While the construct has been injected, further study of the founders is beyond of the scope of this thesis. Preliminary data, however, are very encouraging and it appears likely that it will be possible to generate a reporter mouse line expressing *Cre recombinase* specifically in the hypertrophic chondrocyte zone in the very near future. This mouse line will constitute a

tremendously important research tool in the study of loss of function of genes that play a pivotal role during bone development in hypertrophic chondrocytes.

A different approach for generating mice that express *Cre recombinase* in hypertrophic chondrocytes would be to knock in the *Cre recombinase* cDNA into the endogenous *Col10a1* locus. This strategy was not considered since the disruption of the *Col10a1* gene in mice itself leads to phenotypic consequences, some of which partly resemble MCDS. Loss of *collagen X* in mutant mice leads to a change in the distribution of the matrix materials in the epiphyseal growth plate. Homozygous mutant *Col10a1* mice also display a significant reduction in the thickness of the resting zone, the articular cartilage as well as exhibiting altered trabecular structure. The mice develop *coxa vara*, which is one of the typical phenotypic changes in human MCDS patients (Kwan et al. 1997). Although heterozygous mice appeared normal (Kwan et al. 1997), a disruption of one allele in conjunction with the disruption of the gene of interest using the Cre/loxP system in hypertrophic chondrocytes necessarily confounds interpretation of phenotypic consequences. Another consideration would be to knock in the cDNA of *Cre recombinase* into the 3' region of the *Col10a1* gene using an IRES cassette for bidirectional expression. In this manner the *Cre recombinase* could be expressed in the endogenous *Col10a1* locus without disruption of the gene function.
It is not known, if there are additional regulatory elements in the 3' genomic region of the *Col10a1* gene but the study with the *Col10a1* enhancer elements suggests that this might be very unlikely.

Future directions

The signaling of TGF-β and the subfamily of BMP ligands plays a pivotal role in the development of the skeleton with apparently antagonistic functions. While TGF-β inhibitis proliferation and subsequently differentiation, the signaling of the ligands of the BMP family promotes proliferation, especially in cells in the proliferating zone. The disruption of BMP signaling therefore leads to shortened prehypertrophic and hypertrophic zones, due to the reduction in proliferation.
The influence of BMP signaling on terminal differentiation during endochondral ossification could not be studied in this thesis. Since it is known that *Smad1* and *Smad5* are both expressed in the zone of maturing chondrocytes and that both Smads, together with Runx2,

are likely able to bind to the *Col10a1* promoter to modulate its activity (Leboy et al. 2001), the loss of function of these two genes in hypertrophic chondrocytes in a conditional mouse model would be an interesting approach to study the role of these two BMP mediators in the terminal hypertrophy.

The generation of a reporter mouse expressing *Cre recombinase* in hypertrophic chondrocytes under the control of the *Col10a1* promoter is nearly complete. The mouse model still has to be tested by mating the newly born founders with Rosa26R reporter mice, but the preliminary data showed a strong and specific expression of the tested *Col10a1* promoter fragment (4x300bp), described in this thesis which should render the effort simply technical. This mouse line could be used to elucidate the role of *Smad1* and *Smad5* in hypertrophic chondrocytes and it should represent an attractive tool for the research community. The final demarcation of the *Col10a1* promoter would allow the generation of transgenic mice with a specific overexpression of *Esl-1* as well as the *ΔTβRI* in hypertrophic chondrocytes to facilitating the study of other functions of the TGFβ pathway in terminal differentiation.

5 Summary

TGF-β/BMP signaling is essential for normal developmental processes in almost all embryonic and extraembryonic tissues and it is also necessary for maintenance of homeostasis in adults. Ligands of this pathway are involved in the development of cartilage and bone at different stages. BMPs are important during early condensation of cartilaginous anlagen, proliferation and hypertrophy of chondrocytes. BMPs are able to induce ectopic bone development and the expression pattern of BMPs and their receptors in the growth plate suggest an important role of BMPs in this region. Knockout and conditional knockout mice of *Bmpr1a* and *Bmpr1b* developed a generalized chondrodysplasia. Smad1, Smad5 and Smad8 are mediators for the BMP signaling pathway. Since *Smad1* and *Smad5* are both expressed in the growth plate, the question arose, whether both have similar functions and if they could compensate the loss of one of the proteins. Therefore, to test this hypothesis, conditional *Smad1* knockout mice were crossed with transgenic mice that express *Cre recombinase* specifically in proliferating chondrocytes with and without a heterozygous *Smad5* background.

Mice lacking *Smad1* specifically in proliferating chondrocytes show only a slight shortening of the growth plate, while mice with an additional *Smad5* heterozygous background show a more severe phenotype with shorter prehypertrophic and hypertrophic zones and exhibit a diminished proliferation rate. *Ihh* expression in these mice is downregulated. Additionally, X-ray analyses revealed a disorganized snout region with an absence of the nasal septum. Both, mineralization and the extracellular matrix production were not seen to be affected.

In order to compare BMP and TGFβ signaling during endochondral ossification, mice with a disrupted TGFβ signaling in proliferating chondrocytes were generated as well. Two different transgenic mouse models were studied and showed similar phenotypes. Esl-1 is a TGFβ binding protein, which is reported to inhibit TGFβ signaling. *Esl-1* null mice have been demonstrated to be smaller compared to their wild type littermates and overexpression of *Esl-1* specifically in proliferating chondrocytes results in a longer growth plate and an enhanced proliferation rate. Cartilaginous markers like *Col2a1* and *Sox9* were shown to be downregulated while *Col10a1* and *Ihh* as marker for prehypertrophic and hypertrophic chondrocytes were upregulated, suggesting that more cells enter chondrocyte hypertrophy.

Mice that overexpress a dominant negative TGFβ receptor I (ΔTβRI) in proliferating chondrocytes showed an elongated growth plate with enhanced *Ihh* expression and an

increased proliferation rate. Separate from the phenotype in the growth plate in ΔTβRI transgenic mice, alterations were detected in the head of this mouse model, which led to a decreased size of homozygous mice, however most likely due to feeding problems.

It appears that in the development of the long bones and especially in the proliferating zone of their growth plates, that signaling via the BMP and TGFβ pathways has antagonistic effects. While disruption of BMP signaling leads to a shortening of the growth plate with fewer proliferating cells, impairment of TGFβ signaling results in an increase in the proliferation rate and thus a longer prehypertrophic and hypertrophic zone.

The second aim of this work was to generate mice that express *Cre recombinase* specifically in hypertrophic chondrocytes. *Col10a1* is a marker specific for hypertrophic chondrocytes. Extensive promoter studies have been performed during the course of this thesis. A 300 bp putative AP1 element approximately 4 kb upstream of the first exon has been shown to drive specific *lacZ* expression in transgenic animals. A construct was generated that contains four copies of this element together with the basal *Col10a1* promoter to drive specific *Cre recombinase* expression in prehypertrophic chondrocytes. Final experiments are forthcoming, but preliminary data suggests that a mouse line will indeed be generated exhibiting strong and specific expression of *Cre recombinase* only in hypertrophic chondrocytes.

6 References

Abremski, K., R. Hoess, and N. Sternberg. 1983. Studies on the properties of P1 site-specific recombination: evidence for topologically unlinked products following recombination. *Cell* **32**: 1301-11.

Aikawa, T., G.V. Segre, and K. Lee. 2001. Fibroblast growth factor inhibits chondrocytic growth through induction of p21 and subsequent inactivation of cyclin E-Cdk2. *J Biol Chem* **276**: 29347-52.

Annes, J.P., J.S. Munger, and D.B. Rifkin. 2003. Making sense of latent TGFbeta activation. *J Cell Sci* **116**: 217-24.

Ashique, A.M., K. Fu, and J.M. Richman. 2002. Signalling via type IA and type IB bone morphogenetic protein receptors (BMPR) regulates intramembranous bone formation, chondrogenesis and feather formation in the chicken embryo. *Int J Dev Biol* **46**: 243-53.

Atchley, W.R. and B.K. Hall. 1991. A model for development and evolution of complex morphological structures. *Biol Rev Camb Philos Soc* **66**: 101-57.

Baffi, M.O., E. Slattery, P. Sohn, H.L. Moses, A. Chytil, and R. Serra. 2004. Conditional deletion of the TGF-beta type II receptor in Col2a expressing cells results in defects in the axial skeleton without alterations in chondrocyte differentiation or embryonic development of long bones. *Dev Biol* **276**: 124-42.

Bai, S., X. Shi, X. Yang, and X. Cao. 2000. Smad6 as a transcriptional corepressor. *J Biol Chem* **275**: 8267-70.

Balemans, W. and W. Van Hul. 2002. Extracellular regulation of BMP signaling in vertebrates: a cocktail of modulators. *Dev Biol* **250**: 231-50.

Barna, M., P.P. Pandolfi, and L. Niswander. 2005. Gli3 and Plzf cooperate in proximal limb patterning at early stages of limb development. *Nature* **436**: 277-81.

Baur, S.T., J.J. Mai, and S.M. Dymecki. 2000. Combinatorial signaling through BMP receptor IB and GDF5: shaping of the distal mouse limb and the genetics of distal limb diversity. *Development* **127**: 605-19.

Beier, F., I. Eerola, E. Vuorio, P. Luvalle, E. Reichenberger, W. Bertling, K. von der Mark, and M.J. Lammi. 1996. Variability in the upstream promoter and intron sequences of the human, mouse and chick type X collagen genes. *Matrix Biol* **15**: 415-22.

Beier, F., S. Vornehm, E. Poschl, K. von der Mark, and M.J. Lammi. 1997. Localization of silencer and enhancer elements in the human type X collagen gene. *J Cell Biochem* **66**: 210-8.

Bi, W., J.M. Deng, Z. Zhang, R.R. Behringer, and B. de Crombrugghe. 1999. Sox9 is required for cartilage formation. *Nat Genet* **22**: 85-9.

Bicknell, L.S., T. Morgan, L. Bonafe, M.W. Wessels, M.G. Bialer, P.J. Willems, D.H. Cohn, D. Krakow, and S.P. Robertson. 2005. Mutations in FLNB cause boomerang dysplasia. *J Med Genet* **42**: e43.

Birnboim, H.C. and J. Doly. 1979. A rapid alkaline extraction procedure for screening recombinant plasmid DNA. *Nucleic Acids Res* **7**: 1513-23.

Bockamp, E., M. Maringer, C. Spangenberg, S. Fees, S. Fraser, L. Eshkind, F. Oesch, and B. Zabel. 2002. Of mice and models: improved animal models for biomedical research. *Physiol Genomics* **11**: 115-32.

Boulet, A.M., A.M. Moon, B.R. Arenkiel, and M.R. Capecchi. 2004. The roles of Fgf4 and Fgf8 in limb bud initiation and outgrowth. *Dev Biol* **273**: 361-72.

Brunet, L.J., J.A. McMahon, A.P. McMahon, and R.M. Harland. 1998. Noggin, cartilage morphogenesis, and joint formation in the mammalian skeleton. *Science* **280**: 1455-7.

Capdevila, J. and J.C. Izpisua Belmonte. 2001. Patterning mechanisms controlling vertebrate limb development. *Annu Rev Cell Dev Biol* **17**: 87-132.

Capdevila, J. and R.L. Johnson. 1998. Endogenous and ectopic expression of noggin suggests a conserved mechanism for regulation of BMP function during limb and somite patterning. *Dev Biol* **197**: 205-17.

Chacko, B.M., B.Y. Qin, A. Tiwari, G. Shi, S. Lam, L.J. Hayward, M. De Caestecker, and K. Lin. 2004. Structural basis of heteromeric smad protein assembly in TGF-beta signaling. *Mol Cell* **15**: 813-23.

Chang, H., D. Huylebroeck, K. Verschueren, Q. Guo, M.M. Matzuk, and A. Zwijsen. 1999. Smad5 knockout mice die at mid-gestation due to multiple embryonic and extraembryonic defects. *Development* **126**: 1631-42.

Chang, S.C., B. Hoang, J.T. Thomas, S. Vukicevic, F.P. Luyten, N.J. Ryba, C.A. Kozak, A.H. Reddi, and M. Moos, Jr. 1994. Cartilage-derived morphogenetic proteins. New members of the transforming growth factor-beta superfamily predominantly expressed in long bones during human embryonic development. *J Biol Chem* **269**: 28227-34.

Cheah, K.S., E.T. Lan, P.K. Au, and P.P. Tam. 1991. Expression of the mouse a1(II) collagen gene is not restricted to cartilage during development. *Development* **111**: 945-953.

Chen, D. and e. al. 2003. BMP signaling through the Smad1 pathway is required for normal postnatal bone formation. *J. Bone Miner. Res.* **18**: S6.

Chen, H., Y. Lun, D. Ovchinnikov, H. Kokubo, K.C. Oberg, C.V. Pepicelli, L. Gan, B. Lee, and R.L. Johnson. 1998. Limb and kidney defects in Lmx1b mutant mice suggest an involvement of LMX1B in human nail patella syndrome. *Nat Genet* **19**: 51-5.

Chen, L., C. Li, W. Qiao, X. Xu, and C. Deng. 2001. A Ser(365)-->Cys mutation of fibroblast growth factor receptor 3 in mouse downregulates Ihh/PTHrP signals and causes severe achondroplasia. *Hum Mol Genet* **10**: 457-65.

Chen, X., M.J. Rubock, and M. Whitman. 1996. A transcriptional partner for MAD proteins in TGF-beta signalling. *Nature* **383**: 691-6.

Chen, X., E. Weisberg, V. Fridmacher, M. Watanabe, G. Naco, and M. Whitman. 1997a. Smad4 and FAST-1 in the assembly of activin-responsive factor. *Nature* **389**: 85-9.

Chen, Y.G., F. Liu, and J. Massague. 1997b. Mechanism of TGFbeta receptor inhibition by FKBP12. *Embo J* **16**: 3866-76.

Chiang, C., Y. Litingtung, E. Lee, K.E. Young, J.L. Corden, H. Westphal, and P.A. Beachy. 1996. Cyclopia and defective axial patterning in mice lacking Sonic hedgehog gene function. *Nature* **383**: 407-13.

Colvin, J.S., B.A. Bohne, G.W. Harding, D.G. McEwen, and D.M. Ornitz. 1996. Skeletal overgrowth and deafness in mice lacking fibroblast growth factor receptor 3. *Nat Genet* **12**: 390-7.

Cox, K.H., B. Tabin, C.J. and V. Rosen. 2004. Absence of both Bmp2 and Bmp4 during skeletal development results in severe defects in osteoblasts but not in chondrocytes. *J. Bone Miner. Res.* **Res. 19**: S11.

Crossley, P.H., G. Minowada, C.A. MacArthur, and G.R. Martin. 1996. Roles for FGF8 in the induction, initiation, and maintenance of chick limb development. *Cell* **84**: 127-36.

Dailey, L., E. Laplantine, R. Priore, and C. Basilico. 2003. A network of transcriptional and signaling events is activated by FGF to induce chondrocyte growth arrest and differentiation. *J Cell Biol* **161**: 1053-66.

Daluiski, A., T. Engstrand, M.E. Bahamonde, L.W. Gamer, E. Agius, S.L. Stevenson, K. Cox, V. Rosen, and K.M. Lyons. 2001. Bone morphogenetic protein-3 is a negative regulator of bone density. *Nat Genet* **27**: 84-8.

Datta, P.K., A. Chytil, A.E. Gorska, and H.L. Moses. 1998. Identification of STRAP, a novel WD domain protein in transforming growth factor-beta signaling. *J Biol Chem* **273**: 34671-4.

Datto, M.B., J.P. Frederick, L. Pan, A.J. Borton, Y. Zhuang, and X.F. Wang. 1999. Targeted disruption of Smad3 reveals an essential role in transforming growth factor beta-mediated signal transduction. *Mol Cell Biol* **19**: 2495-504.

Deng, C., A. Wynshaw-Boris, F. Zhou, A. Kuo, and P. Leder. 1996. Fibroblast growth factor receptor 3 is a negative regulator of bone growth. *Cell* **84**: 911-21.

Derynck, R., W.M. Gelbart, R.M. Harland, C.H. Heldin, S.E. Kern, J. Massague, D.A. Melton, M. Mlodzik, R.W. Padgett, A.B. Roberts, J. Smith, G.H. Thomsen, B. Vogelstein, and X.F. Wang. 1996. Nomenclature: vertebrate mediators of TGFbeta family signals. *Cell* **87**: 173.

Derynck, R. and Y. Zhang. 1996. Intracellular signalling: the mad way to do it. *Curr Biol* **6**: 1226-9.

Dickson, M.C., J.S. Martin, F.M. Cousins, A.B. Kulkarni, S. Karlsson, and R.J. Akhurst. 1995. Defective haematopoiesis and vasculogenesis in transforming growth factor-beta 1 knock out mice. *Development* **121**: 1845-54.

Donello, J.E., J.E. Loeb, and T.J. Hope. 1998. Woodchuck hepatitis virus contains a tripartite posttranscriptional regulatory element. *J Virol* **72**: 5085-92.

Dong, C., Z. Li, R. Alvarez, Jr., X.H. Feng, and P.J. Goldschmidt-Clermont. 2000. Microtubule binding to Smads may regulate TGF beta activity. *Mol Cell* **5**: 27-34.

Dubois, C.M., M.-H. Laprise, F. Blanchette, and e. al. 1995. Processing of transforming growth factor beta1 precursor by human furin convertase. *J Biol Chem.* **270**: 10618–10624.

Dudley, A.T., K.M. Lyons, and E.J. Robertson. 1995. A requirement for bone morphogenetic protein-7 during development of the mammalian kidney and eye. *Genes Dev* **9**: 2795-807.

Dunn, N.R., G.E. Winnier, L.K. Hargett, J.J. Schrick, A.B. Fogo, and B.L. Hogan. 1997. Haploinsufficient phenotypes in Bmp4 heterozygous null mice and modification by mutations in Gli3 and Alx4. *Dev Biol* **188**: 235-47.

Feinberg, A.P. and B. Vogelstein. 1983. A technique for radiolabeling DNA restriction endonuclease fragments to high specific activity. *Anal Biochem* **132**: 6-13.

Francis-West, P., R. Ladher, A. Barlow, and A. Graveson. 1998. Signalling interactions during facial development. *Mech Dev* **75**: 3-28.

Gatherer, D., P. Ten Dijke, D.T. Baird, and R.J. Akhurst. 1990. Expression of TGF-beta isoforms during first trimester human embryogenesis. *Development* **110**: 445-60.

Gebhard, S., E. Poschl, S. Riemer, E. Bauer, T. Hattori, H. Eberspaecher, Z. Zhang, V. Lefebvre, B. de Crombrugghe, and K. von der Mark. 2004. A highly conserved enhancer in mammalian type X collagen genes drives high levels of tissue-specific expression in hypertrophic cartilage in vitro and in vivo. *Matrix Biol* **23**: 309-22.

George, E.L., E.N. Georges-Labouesse, R.S. Patel-King, H. Rayburn, and R.O. Hynes. 1993. Defects in mesoderm, neural tube and vascular development in mouse embryos lacking fibronectin. *Development* **119**: 1079-91.

Goldring, M.B., K. Tsuchimochi, and K. Ijiri. 2006. The control of chondrogenesis. *J Cell Biochem* **97**: 33-44.

Grant, W.T., G.J. Wang, and G. Balian. 1987. Type X collagen synthesis during endochondral ossification in fracture repair. *J Biol Chem* **262**: 9844-9.

Guo, D. and e. al. 2004. Bmp4 is necessary for bone formation: conditional Bmp4 knock-out using the 3.6 kb and 2.3 kb collagen 1a1 promoter-Cre and Bmp4-floxed mice. *J. Bone Miner. Res.* **19**: S14.

Guo, X., T.F. Day, X. Jiang, L. Garrett-Beal, L. Topol, and Y. Yang. 2004. Wnt/beta-catenin signaling is sufficient and necessary for synovial joint formation. *Genes Dev* **18**: 2404-17.

Haas, A.R. and R.S. Tuan. 1999. Chondrogenic differentiation of murine C3H10T1/2 multipotential mesenchymal cells: II. Stimulation by bone morphogenetic protein-2 requires modulation of N-cadherin expression and function. *Differentiation* **64**: 77-89.

Hall, B.K. 1988. The embryonic development of bone. *Am. Sci.* **76**: 174-181.

Hall, B.K. and T. Miyake. 2000. All for one and one for all: condensations and the initiation of skeletal development. *Bioessays* **22**: 138-47.

Hata, A., G. Lagna, J. Massague, and A. Hemmati-Brivanlou. 1998. Smad6 inhibits BMP/Smad1 signaling by specifically competing with the Smad4 tumor suppressor. *Genes Dev* **12**: 186-97.

Hatakeyama, Y., J. Nguyen, X. Wang, G.H. Nuckolls, and L. Shum. 2003. Smad signaling in mesenchymal and chondroprogenitor cells. *J Bone Joint Surg Am* **85-A Suppl 3**: 13-8.

Hayashi, H., S. Abdollah, Y. Qiu, J. Cai, Y.Y. Xu, B.W. Grinnell, M.A. Richardson, J.N. Topper, M.A. Gimbrone, Jr., J.L. Wrana, and D. Falb. 1997. The MAD-related protein Smad7 associates with the TGFbeta receptor and functions as an antagonist of TGFbeta signaling. *Cell* **89**: 1165-73.

Hoodless, P.A., T. Haerry, S. Abdollah, M. Stapleton, M.B. O'Connor, L. Attisano, and J.L. Wrana. 1996. MADR1, a MAD-related protein that functions in BMP2 signaling pathways. *Cell* **85**: 489-500.

Horton, W., T. Miyashita, K. Kohno, J.R. Hassell, and Y. Yamada. 1987. Identification of a phenotype-specific enhancer in the first intron of the rat collagen II gene. *Proc. Nat. Acad. Sci. USA* **84**: 8864-8868.

Hsiao, Y.C., H.H. Chang, C.Y. Tsai, Y.J. Jong, L.S. Horng, S.F. Lin, and T.F. Tsai. 2004. Coat color-tagged green mouse with EGFP expressed from the RNA polymerase II promoter. *Genesis* **39**: 122-9.

Hyman, C.A., L. Bartholin, S.J. Newfeld, and D. Wotton. 2003. Drosophila TGIF proteins are transcriptional activators. *Mol Cell Biol* **23**: 9262-74.

Ikeda, T., H. Takahashi, A. Suzuki, N. Ueno, S. Yokose, A. Yamaguchi, and S. Yoshiki. 1996. Cloning of rat type I receptor cDNA for bone morphogenetic protein-2 and bone morphogenetic protein-4, and the localization compared with that of the ligands. *Dev Dyn* **206**: 318-29.

Imamura, T., M. Takase, A. Nishihara, E. Oeda, J. Hanai, M. Kawabata, and K. Miyazono. 1997. Smad6 inhibits signalling by the TGF-beta superfamily. *Nature* **389**: 622-6.

Inman, G.J. and C.S. Hill. 2002. Stoichiometry of active smad-transcription factor complexes on DNA. *J Biol Chem* **277**: 51008-16.

Itoh, S., F. Itoh, M.J. Goumans, and P. Ten Dijke. 2000. Signaling of transforming growth factor-beta family members through Smad proteins. *Eur J Biochem* **267**: 6954-67.

Janknecht, R., N.J. Wells, and T. Hunter. 1998. TGF-beta-stimulated cooperation of smad proteins with the coactivators CBP/p300. *Genes Dev* **12**: 2114-9.

Kanaan, R.A. and L.A. Kanaan. 2006. Transforming growth factor beta1, bone connection. *Med Sci Monit* **12**: RA164-9.

Karsenty, G. 2003. The complexities of skeletal biology. *Nature* **423**: 316-8.

Karsenty, G. and E.F. Wagner. 2002. Reaching a genetic and molecular understanding of skeletal development. *Dev Cell* **2**: 389-406.

Katagiri, T., A. Yamaguchi, M. Komaki, E. Abe, N. Takahashi, T. Ikeda, V. Rosen, J.M. Wozney, A. Fujisawa-Sehara, and T. Suda. 1994. Bone morphogenetic protein-2 converts the differentiation pathway of C2C12 myoblasts into the osteoblast lineage. *J Cell Biol* **127**: 1755-66.

Kato, H.D., Y. Terao, M. Ogawa, T. Matsuda, T. Arima, K. Kato, Z. Yong, and N. Wake. 2002. Growth-associated gene expression profiles by microarray analysis of trophoblast of molar pregnancies and normal villi. *Int J Gynecol Pathol* **21**: 255-60.

Kavsak, P., R.K. Rasmussen, C.G. Causing, S. Bonni, H. Zhu, G.H. Thomsen, and J.L. Wrana. 2000. Smad7 binds to Smurf2 to form an E3 ubiquitin ligase that targets the TGF beta receptor for degradation. *Mol Cell* **6**: 1365-75.

Kimura, N., R. Matsuo, H. Shibuya, K. Nakashima, and T. Taga. 2000. BMP2-induced apoptosis is mediated by activation of the TAK1-p38 kinase pathway that is negatively regulated by Smad6. *J Biol Chem* **275**: 17647-52.

Kingsley, D.M., A.E. Bland, J.M. Grubber, P.C. Marker, L.B. Russell, N.G. Copeland, and N.A. Jenkins. 1992. The mouse short ear skeletal morphogenesis locus is associated with defects in a bone morphogenetic member of the TGF beta superfamily. *Cell* **71**: 399-410.

Kinoshita, A., T. Saito, H. Tomita, Y. Makita, K. Yoshida, M. Ghadami, K. Yamada, S. Kondo, S. Ikegawa, G. Nishimura, Y. Fukushima, T. Nakagomi, H. Saito, T. Sugimoto, M. Kamegaya, K. Hisa, J.C. Murray, N. Taniguchi, N. Niikawa, and K. Yoshiura. 2000. Domain-specific mutations in TGFB1 result in Camurati-Engelmann disease. *Nat Genet* **26**: 19-20.

Kmita, M., B. Tarchini, J. Zakany, M. Logan, C.J. Tabin, and D. Duboule. 2005. Early developmental arrest of mammalian limbs lacking HoxA/HoxD gene function. *Nature* **435**: 1113-6.

Kobayashi, T., K.M. Lyons, A.P. McMahon, and H.M. Kronenberg. 2005. BMP signaling stimulates cellular differentiation at multiple steps during cartilage development. *Proc Natl Acad Sci U S A* **102**: 18023-7.

Komori, T., H. Yagi, S. Nomura, A. Yamaguchi, K. Sasaki, K. Deguchi, Y. Shimizu, R.T. Bronson, Y.H. Gao, M. Inada, M. Sato, R. Okamoto, Y. Kitamura, S. Yoshiki, and T. Kishimoto. 1997. Targeted disruption of Cbfa1 results in a complete lack of bone formation owing to maturational arrest of osteoblasts. *Cell* **89**: 755-64.

Kos, C.H. 2004. Cre/loxP system for generating tissue-specific knockout mouse models. *Nutr Rev* **62**: 243-6.

Krakow, D., S.P. Robertson, L.M. King, T. Morgan, E.T. Sebald, C. Bertolotto, S. Wachsmann-Hogiu, D. Acuna, S.S. Shapiro, T. Takafuta, S. Aftimos, C.A. Kim, H. Firth, C.E. Steiner, V. Cormier-Daire, A. Superti-Furga, L. Bonafe, J.M. Graham, Jr., A. Grix, C.A. Bacino, J. Allanson, M.G. Bialer, R.S. Lachman, D.L. Rimoin, and D.H. Cohn. 2004. Mutations in the gene encoding filamin B disrupt vertebral segmentation, joint formation and skeletogenesis. *Nat Genet* **36**: 405-10.

Kretzschmar, M., J. Doody, and J. Massague. 1997. Opposing BMP and EGF signalling pathways converge on the TGF-beta family mediator Smad1. *Nature* **389**: 618-22.

Kretzschmar, M., J. Doody, I. Timokhina, and J. Massague. 1999. A mechanism of repression of TGFbeta/ Smad signaling by oncogenic Ras. *Genes Dev* **13**: 804-16.

Kronenberg, H.M. 2003. Developmental regulation of the growth plate. *Nature* **423**: 332-6.

Kwan, K.M., M.K. Pang, S. Zhou, S.K. Cowan, R.Y. Kong, T. Pfordte, B.R. Olsen, D.O. Sillence, P.P. Tam, and K.S. Cheah. 1997. Abnormal compartmentalization of cartilage matrix components in mice lacking collagen X: implications for function. *J Cell Biol* **136**: 459-71.

Laufer, E., C.E. Nelson, R.L. Johnson, B.A. Morgan, and C. Tabin. 1994. Sonic hedgehog and Fgf-4 act through a signaling cascade and feedback loop to integrate growth and patterning of the developing limb bud. *Cell* **79**: 993-1003.

Leboy, P., G. Grasso-Knight, M. D'Angelo, S.W. Volk, J.V. Lian, H. Drissi, G.S. Stein, and S.L. Adams. 2001. Smad-Runx interactions during chondrocyte maturation. *J Bone Joint Surg Am* **83-A Suppl 1**: S15-22.

Lee, M.H., Y.J. Kim, H.J. Kim, H.D. Park, A.R. Kang, H.M. Kyung, J.H. Sung, J.M. Wozney, H.J. Kim, and H.M. Ryoo. 2003b. BMP-2-induced Runx2 expression is mediated by Dlx5, and TGF-beta 1 opposes the BMP-2-induced osteoblast differentiation by suppression of Dlx5 expression. *J Biol Chem* **278**: 34387-94.

Lee, M.H., T.G. Kwon, H.S. Park, J.M. Wozney, and H.M. Ryoo. 2003a. BMP-2-induced Osterix expression is mediated by Dlx5 but is independent of Runx2. *Biochem Biophys Res Commun* **309**: 689-94.

Lefebvre, V., K. Mukhopadhyay, G. Zhou, S. Garofalo, C. Smith, H. Eberspaecher, J.H. Kimura, and B. de Crombrugghe. 1996a. A 47-bp sequence of the first intron of the mouse pro alpha 1(II) collagen gene is sufficient to direct chondrocyte Expression. *Ann N Y Acad Sci* **785**: 284-7.

Lefebvre, V., G. Zhou, K. Mukhopadhyay, C.N. Smith, Z. Zhang, H. Eberspaecher, X. Zhou, S. Sinha, S.N. Maity, and B. de Crombrugghe. 1996b. An 18-base-pair sequence in the mouse proalpha1(II) collagen gene is sufficient for expression in cartilage and binds nuclear proteins that are selectively expressed in chondrocytes. *Mol Cell Biol* **16**: 4512-23.

Li, C., L. Chen, T. Iwata, M. Kitagawa, X.Y. Fu, and C.X. Deng. 1999. A Lys644Glu substitution in fibroblast growth factor receptor 3 (FGFR3) causes dwarfism in mice by activation of STATs and ink4 cell cycle inhibitors. *Hum Mol Genet* **8**: 35-44.

Liu, F., A. Hata, J.C. Baker, J. Doody, J. Carcamo, R.M. Harland, and J. Massague. 1996. A human Mad protein acting as a BMP-regulated transcriptional activator. *Nature* **381**: 620-3.

Liu, Y., M.H. Festing, M. Hester, J.C. Thompson, and M. Weinstein. 2004. Generation of novel conditional and hypomorphic alleles of the Smad2 gene. *Genesis* **40**: 118-123.

Lo, R.S. and J. Massague. 1999. Ubiquitin-dependent degradation of TGF-beta-activated smad2. *Nat Cell Biol* **1**: 472-8.

Logan, C.Y. and R. Nusse. 2004. The Wnt signaling pathway in development and disease. *Annu Rev Cell Dev Biol* **20**: 781-810.

Long, F., U.I. Chung, S. Ohba, J. McMahon, H.M. Kronenberg, and A.P. McMahon. 2004. Ihh signaling is directly required for the osteoblast lineage in the endochondral skeleton. *Development* **131**: 1309-18.

Loomis, C.A., E. Harris, J. Michaud, W. Wurst, M. Hanks, and A.L. Joyner. 1996. The mouse Engrailed-1 gene and ventral limb patterning. *Nature* **382**: 360-3.

Luo, G., C. Hofmann, A.L. Bronckers, M. Sohocki, A. Bradley, and G. Karsenty. 1995. BMP-7 is an inducer of nephrogenesis, and is also required for eye development and skeletal patterning. *Genes Dev* **9**: 2808-20.

Luo, K., S.L. Stroschein, W. Wang, D. Chen, E. Martens, S. Zhou, and Q. Zhou. 1999. The Ski oncoprotein interacts with the Smad proteins to repress TGFbeta signaling. *Genes Dev* **13**: 2196-206.

Lyons, K.M., B.L. Hogan, and E.J. Robertson. 1995. Colocalization of BMP 7 and BMP 2 RNAs suggests that these factors cooperatively mediate tissue interactions during murine development. *Mech Dev* **50**: 71-83.

Lyons, K.M., R.W. Pelton, and B.L. Hogan. 1990. Organogenesis and pattern formation in the mouse: RNA distribution patterns suggest a role for bone morphogenetic protein-2A (BMP-2A). *Development* **109**: 833-44.

Macias, D., Y. Ganan, T.K. Sampath, M.E. Piedra, M.A. Ros, and J.M. Hurle. 1997. Role of BMP-2 and OP-1 (BMP-7) in programmed cell death and skeletogenesis during chick limb development. *Development* **124**: 1109-17.

Mariani, F.V. and G.R. Martin. 2003. Deciphering skeletal patterning: clues from the limb. *Nature* **423**: 319-25.

Massague, J. and R.R. Gomis. 2006. The logic of TGFbeta signaling. *FEBS Lett* **580**: 2811-20.

Massague, J., J. Seoane, and D. Wotton. 2005. Smad transcription factors. *Genes Dev* **19**: 2783-810.

Massague, J. and D. Wotton. 2000. Transcriptional control by the TGF-beta/Smad signaling system. *Embo J* **19**: 1745-54.

Matsuura, I., N.G. Denissova, G. Wang, D. He, J. Long, and F. Liu. 2004. Cyclin-dependent kinases regulate the antiproliferative function of Smads. *Nature* **430**: 226-31.

Mian, A., M. Guenther, M. Finegold, P. Ng, J. Rodgers, and B. Lee. 2005. Toxicity and adaptive immune response to intracellular transgenes delivered by helper-dependent vs. first generation adenoviral vectors. *Mol Genet Metab* **84**: 278-88.

Mikic, B., M.C. van der Meulen, D.M. Kingsley, and D.R. Carter. 1995. Long bone geometry and strength in adult BMP-5 deficient mice. *Bone* **16**: 445-54.

Millan, F.A., F. Denhez, P. Kondaiah, and R.J. Akhurst. 1991. Embryonic gene expression patterns of TGF beta 1, beta 2 and beta 3 suggest different developmental functions in vivo. *Development* **111**: 131-43.

Minina, E., C. Kreschel, M.C. Naski, D.M. Ornitz, and A. Vortkamp. 2002. Interaction of FGF, Ihh/Pthlh, and BMP signaling integrates chondrocyte proliferation and hypertrophic differentiation. *Dev Cell* **3**: 439-49.

Minina, E., S. Schneider, M. Rosowski, R. Lauster, and A. Vortkamp. 2005. Expression of Fgf and Tgfbeta signaling related genes during embryonic endochondral ossification. *Gene Expr Patterns* **6**: 102-9.

Minina, E., H.M. Wenzel, C. Kreschel, S. Karp, W. Gaffield, A.P. McMahon, and A. Vortkamp. 2001. BMP and Ihh/PTHrP signaling interact to coordinate chondrocyte proliferation and differentiation. *Development* **128**: 4523-34.

Mishina, Y., A. Suzuki, N. Ueno, and R.R. Behringer. 1995. Bmpr encodes a type I bone morphogenetic protein receptor that is essential for gastrulation during mouse embryogenesis. *Genes Dev* **9**: 3027-37.

Miyazono, K., K. Kusanagi, and H. Inoue. 2001. Divergence and convergence of TGF-beta/BMP signaling. *J Cell Physiol* **187**: 265-76.

Moses, H.L. and R. Serra. 1996. Regulation of differentiation by TGF-beta. *Curr Opin Genet Dev* **6**: 581-6.

Murakami, G., T. Watabe, K. Takaoka, K. Miyazono, and T. Imamura. 2003. Cooperative inhibition of bone morphogenetic protein signaling by Smurf1 and inhibitory Smads. *Mol Biol Cell* **14**: 2809-17.

Murakami, S., G. Balmes, S. McKinney, Z. Zhang, D. Givol, and B. de Crombrugghe. 2004. Constitutive activation of MEK1 in chondrocytes causes Stat1-independent achondroplasia-like dwarfism and rescues the Fgfr3-deficient mouse phenotype. *Genes Dev* **18**: 290-305.

Nakamura, K., T. Shirai, S. Morishita, S. Uchida, K. Saeki-Miura, and F. Makishima. 1999. p38 mitogen-activated protein kinase functionally contributes to chondrogenesis induced by growth/differentiation factor-5 in ATDC5 cells. *Exp Cell Res* **250**: 351-63.

Nakao, A., M. Afrakhte, A. Moren, T. Nakayama, J.L. Christian, R. Heuchel, S. Itoh, M. Kawabata, N.E. Heldin, C.H. Heldin, and P. ten Dijke. 1997. Identification of Smad7, a TGFbeta-inducible antagonist of TGF-beta signalling. *Nature* **389**: 631-5.

Nakashima, K., X. Zhou, G. Kunkel, Z. Zhang, J.M. Deng, R.R. Behringer, and B. de Crombrugghe. 2002. The novel zinc finger-containing transcription factor osterix is required for osteoblast differentiation and bone formation. *Cell* **108**: 17-29.

Naski, M.C., J.S. Colvin, J.D. Coffin, and D.M. Ornitz. 1998. Repression of hedgehog signaling and BMP4 expression in growth plate cartilage by fibroblast growth factor receptor 3. *Development* **125**: 4977-88.

Neptune, E.R., P.A. Frischmeyer, D.E. Arking, L. Myers, T.E. Bunton, B. Gayraud, F. Ramirez, L.Y. Sakai, and H.C. Dietz. 2003. Dysregulation of TGF-beta activation contributes to pathogenesis in Marfan syndrome. *Nat Genet* **33**: 407-11.

Newman, S.A. and H.L. Frisch. 1979. Dynamics of skeletal pattern formation in developing chick limb. *Science* **205**: 662-8.

Niswander, L. 1996. Growth factor interactions in limb development. *Ann N Y Acad Sci* **785**: 23-6.

-. 2003. Pattern formation: old models out on a limb. *Nat Rev Genet* **4**: 133-43.

Niswander, L., S. Jeffrey, G.R. Martin, and C. Tickle. 1994. A positive feedback loop coordinates growth and patterning in the vertebrate limb. *Nature* **371**: 609-12.

Okamoto, M., J. Murai, H. Yoshikawa, and N. Tsumaki. 2006. Bone morphogenetic proteins in bone stimulate osteoclasts and osteoblasts during bone development. *J Bone Miner Res* **21**: 1022-33.

Olofsson, A., U. Hellman, P. Ten Dijke, S. Grimsby, H. Ichijo, A. Moren, K. Miyazono, and C.H. Heldin. 1997. Latent transforming growth factor-beta complex in Chinese hamster ovary cells contains the multifunctional cysteine-rich fibroblast growth factor receptor, also termed E-selectin-ligand or MG-160. *Biochem J* **324 (Pt 2)**: 427-34.

Olsen, B.R., A.M. Reginato, and W. Wang. 2000. Bone development. *Annu Rev Cell Dev Biol* **16**: 191-220.

Onichtchouk, D., Y.G. Chen, R. Dosch, V. Gawantka, H. Delius, J. Massague, and C. Niehrs. 1999. Silencing of TGF-beta signalling by the pseudoreceptor BAMBI. *Nature* **401**: 480-5.

Ornitz, D.M. and P.J. Marie. 2002. FGF signaling pathways in endochondral and intramembranous bone development and human genetic disease. *Genes Dev* **16**: 1446-65.

Otto, F., A.P. Thornell, T. Crompton, A. Denzel, K.C. Gilmour, I.R. Rosewell, G.W. Stamp, R.S. Beddington, S. Mundlos, B.R. Olsen, P.B. Selby, and M.J. Owen. 1997. Cbfa1, a candidate gene for cleidocranial dysplasia syndrome, is essential for osteoblast differentiation and bone development. *Cell* **89**: 765-71.

Ovchinnikov, D.A., J.M. Deng, G. Ogunrinu, and R.R. Behringer. 2000. Col2a1-directed expression of Cre recombinase in differentiating chondrocytes in transgenic mice. *Genesis* **26**: 145-6.

Parr, B.A. and A.P. McMahon. 1995. Dorsalizing signal Wnt-7a required for normal polarity of D-V and A-P axes of mouse limb. *Nature* **374**: 350-3.

Parr, B.A., M.J. Shea, G. Vassileva, and A.P. McMahon. 1993. Mouse Wnt genes exhibit discrete domains of expression in the early embryonic CNS and limb buds. *Development* **119**: 247-61.

Pathi, S., J.B. Rutenberg, R.L. Johnson, and A. Vortkamp. 1999. Interaction of Ihh and BMP/Noggin signaling during cartilage differentiation. *Dev Biol* **209**: 239-53.

Pearson, K.L., T. Hunter, and R. Janknecht. 1999. Activation of Smad1-mediated transcription by p300/CBP. *Biochim Biophys Acta* **1489**: 354-64.

Pelton, R.W., M.E. Dickinson, H.L. Moses, and B.L. Hogan. 1990. In situ hybridization analysis of TGF beta 3 RNA expression during mouse development: comparative studies with TGF beta 1 and beta 2. *Development* **110**: 609-20.

Pelton, R.W., B. Saxena, M. Jones, H.L. Moses, and L.I. Gold. 1991. Immunohistochemical localization of TGF beta 1, TGF beta 2, and TGF beta 3 in the mouse embryo: expression patterns suggest multiple roles during embryonic development. *J Cell Biol* **115**: 1091-105.

Phan, T.C., J. Xu, and M.H. Zheng. 2004. Interaction between osteoblast and osteoclast: impact in bone disease. *Histol Histopathol* **19**: 1325-44.

Pircher, R., P. Jullien, and D.A. Lawrence. 1986. Beta-transforming growth factor is stored in human blood platelets as a latent high molecular weight complex. *Biochem Biophys Res Commun* **136**: 30–37.

Pizette, S. and L. Niswander. 2000. BMPs are required at two steps of limb chondrogenesis: formation of prechondrogenic condensations and their differentiation into chondrocytes. *Dev Biol* **219**: 237-49.

Pogue, R. and K. Lyons. 2006. BMP signaling in the cartilage growth plate. *Curr Top Dev Biol* **76**: 1-48.

Qiao, B., S.R. Padilla, and P.D. Benya. 2005. Transforming growth factor (TGF)-beta-activated kinase 1 mimics and mediates TGF-beta-induced stimulation of type II collagen synthesis in chondrocytes independent of Col2a1 transcription and Smad3 signaling. *J Biol Chem* **280**: 17562-71.

Reilly, G.C., E.B. Golden, G. Grasso-Knight, and P.S. Leboy. 2005. Differential effects of ERK and p38 signaling in BMP-2 stimulated hypertrophy of cultured chick sternal chondrocytes. *Cell Commun Signal* **3**: 3.

Riddle, R.D., R.L. Johnson, E. Laufer, and C. Tabin. 1993. Sonic hedgehog mediates the polarizing activity of the ZPA. *Cell* **75**: 1401-16.

Riemer, S., S. Gebhard, F. Beier, E. Poschl, and K. von der Mark. 2002. Role of c-fos in the regulation of type X collagen gene expression by PTH and PTHrP: localization of a PTH/PTHrP-responsive region in the human COL10A1 enhancer. *J Cell Biochem* **86**: 688-99.

Roark, E.F. and K. Greer. 1994. Transforming growth factor-beta and bone morphogenetic protein-2 act by distinct mechanisms to promote chick limb cartilage differentiation in vitro. *Dev Dyn* **200**: 103-16.

Rodan, G.A. and T.J. Martin. 2000. Therapeutic approaches to bone diseases. *Science* **289**: 1508-14.

Rosenzweig, B.L., T. Imamura, T. Okadome, G.N. Cox, H. Yamashita, P. ten Dijke, C.H. Heldin, and K. Miyazono. 1995. Cloning and characterization of a human type II receptor for bone morphogenetic proteins. *Proc Natl Acad Sci U S A* **92**: 7632-6.

Rozenblatt-Rosen, O., E. Mosonego-Ornan, E. Sadot, L. Madar-Shapiro, Y. Sheinin, D. Ginsberg, and A. Yayon. 2002. Induction of chondrocyte growth arrest by FGF: transcriptional and cytoskeletal alterations. *J Cell Sci* **115**: 553-62.

Sahni, M., D.C. Ambrosetti, A. Mansukhani, R. Gertner, D. Levy, and C. Basilico. 1999. FGF signaling inhibits chondrocyte proliferation and regulates bone development through the STAT-1 pathway. *Genes Dev* **13**: 1361-6.

Sahni, M., R. Raz, J.D. Coffin, D. Levy, and C. Basilico. 2001. STAT1 mediates the increased apoptosis and reduced chondrocyte proliferation in mice overexpressing FGF2. *Development* **128**: 2119-29.

Sakou, T., T. Onishi, T. Yamamoto, T. Nagamine, T. Sampath, and P. Ten Dijke. 1999. Localization of Smads, the TGF-beta family intracellular signaling components during endochondral ossification. *J Bone Miner Res* **14**: 1145-52.

Sandberg, M., H. Autio-Harmainen, and E. Vuorio. 1988. Localization of the expression of types I, III, and IV collagen, TGF-beta 1 and c-fos genes in developing human calvarial bones. *Dev Biol* **130**: 324-34.

Sanford, L.P., I. Ormsby, A.C. Gittenberger-de Groot, H. Sariola, R. Friedman, G.P. Boivin, E.L. Cardell, and T. Doetschman. 1997. TGFbeta2 knockout mice have multiple developmental defects that are non-overlapping with other TGFbeta knockout phenotypes. *Development* **124**: 2659-70.

Sasaki, A., Y. Masuda, Y. Ohta, K. Ikeda, and K. Watanabe. 2001. Filamin associates with Smads and regulates transforming growth factor-beta signaling. *J Biol Chem* **276**: 17871-7.

Saunders, J.W. 1948. The proximo-distal sequence of origin of limb parts of the chick wing and the role of the ectoderm. *J. Exp. Zool.* **108**: 363-404.

Saunders, J.W. and M. Gasseling. 1968. Ectodermal-mesenchymal interaction in the origin of the limb. *Epithelial-mesenchymal interaction*: 78-97.

Schipani, E. 2002. Conditional gene inactivation using cre recombinase. *Calcif Tissue Int* **71**: 100-2.

Schmid, T.M., A.A. Cole, Q. Chen, D.K. Bonen, and L. Luchene. 1994. Assembly of type X collagen by hypertrophic chondrocytes. *In: Yurchenco, P., Birk, D., Mecham, R. (Eds.), Extracellular Matrix Assembly and Structure. Academic Press, pp. 171– 206.*

Seki, K. and A. Hata. 2004. Indian hedgehog gene is a target of the bone morphogenetic protein signaling pathway. *J Biol Chem* **279**: 18544-9.

Serra, R. and C. Chang. 2003. TGF-beta signaling in human skeletal and patterning disorders. *Birth Defects Res C Embryo Today* **69**: 333-51.

Serra, R., M. Johnson, E.H. Filvaroff, J. LaBorde, D.M. Sheehan, R. Derynck, and H.L. Moses. 1997. Expression of a truncated, kinase-defective TGF-beta type II receptor in mouse skeletal tissue promotes terminal chondrocyte differentiation and osteoarthritis. *J Cell Biol* **139**: 541-52.

Serra, R., A. Karaplis, and P. Sohn. 1999. Parathyroid hormone-related peptide (PTHrP)-dependent and -independent effects of transforming growth factor beta (TGF-beta) on endochondral bone formation. *J Cell Biol* **145**: 783-94.

Seto, H., S. Kamekura, T. Miura, A. Yamamoto, H. Chikuda, T. Ogata, H. Hiraoka, H. Oda, K. Nakamura, H. Kurosawa, U.I. Chug, H. Kawaguchi, and S. Tanaka. 2004. Distinct roles of Smad pathways and p38 pathways in cartilage-specific gene expression in synovial fibroblasts. *J Clin Invest* **113**: 718-26.

Shen, G. 2005. The role of type X collagen in facilitating and regulating endochondral ossification of articular cartilage. *Orthod Craniofac Res* **8**: 11-7.

Shi, Y. and J. Massague. 2003. Mechanisms of TGF-beta signaling from cell membrane to the nucleus. *Cell* **113**: 685-700.

Shi, Y., Y.F. Wang, L. Jayaraman, H. Yang, J. Massague, and N.P. Pavletich. 1998. Crystal structure of a Smad MH1 domain bound to DNA: insights on DNA binding in TGF-beta signaling. *Cell* **94**: 585-94.

Smits, P., P. Li, J. Mandel, Z. Zhang, J.M. Deng, R.R. Behringer, B. de Crombrugghe, and V. Lefebvre. 2001. The transcription factors L-Sox5 and Sox6 are essential for cartilage formation. *Dev Cell* **1**: 277-90.

Solloway, M.J., A.T. Dudley, E.K. Bikoff, K.M. Lyons, B.L. Hogan, and E.J. Robertson. 1998. Mice lacking Bmp6 function. *Dev Genet* **22**: 321-39.

Soriano, P. 1999. Generalized lacZ expression with the ROSA26 Cre reporter strain. *Nat Genet* **21**: 70-1.

Southern, E.M. 1975. Detection of specific sequences among DNA fragments separated by gel electrophoresis. *J Mol Biol* **98**: 503-517.

Steegmaier, M., A. Levinovitz, S. Isenmann, E. Borges, M. Lenter, H.P. Kocher, B. Kleuser, and D. Vestweber. 1995. The E-selectin-ligand ESL-1 is a variant of a receptor for fibroblast growth factor. *Nature* **373**: 615-20.

Stroschein, S.L., W. Wang, S. Zhou, Q. Zhou, and K. Luo. 1999. Negative feedback regulation of TGF-beta signaling by the SnoN oncoprotein. *Science* **286**: 771-4.

Suda, T., N. Udagawa, and N. Takahashi. 1996. Cells of bone: Osteoclast generation. Principles of bone biology. *Bilezikian, J.P., Raisz, L.G. and Rodan, G.A. (eds). Academic Press, San Diego.*: 87-102.

Summerbell, D. 1974. A quantitative analysis of the effect of excision of the AER from the chick limb-bud. *J Embryol Exp Morphol* **32**: 651-60.

Sun, D., C.R. Vanderburg, G.S. Odierna, and E.D. Hay. 1998. TGFbeta3 promotes transformation of chicken palate medial edge epithelium to mesenchyme in vitro. *Development* **125**: 95-105.

Sun, X., M. Lewandoski, E.N. Meyers, Y.H. Liu, R.E. Maxson, Jr., and G.R. Martin. 2000. Conditional inactivation of Fgf4 reveals complexity of signalling during limb bud development. *Nat Genet* **25**: 83-6.

Tang, Y., V. Katuri, A. Dillner, B. Mishra, C.X. Deng, and L. Mishra. 2003. Disruption of transforming growth factor-beta signaling in ELF beta-spectrin-deficient mice. *Science* **299**: 574-7.

ten Dijke, P. 2006. Bone morphogenetic protein signal transduction in bone. *Curr Med Res Opin* **22 Suppl 1**: 7-11.

ten Dijke, P., H. Yamashita, T.K. Sampath, A.H. Reddi, M. Estevez, D.L. Riddle, H. Ichijo, C.H. Heldin, and K. Miyazono. 1994. Identification of type I receptors for osteogenic protein-1 and bone morphogenetic protein-4. *J Biol Chem* **269**: 16985-8.

Tickle, C. 2000. Limb development: an international model for vertebrate pattern formation. *Int J Dev Biol* **44**: 101-8.

-. 2003. Patterning systems--from one end of the limb to the other. *Dev Cell* **4**: 449-58.

Tickle, C. and A. Munsterberg. 2001. Vertebrate limb development--the early stages in chick and mouse. *Curr Opin Genet Dev* **11**: 476-81.

Topping, R.E., M.E. Bolander, and G. Balian. 1994. Type X collagen in fracture callus and the effects of experimental diabetes. *Clin Orthop Relat Res*: 220-8.

Tremblay, K.D., N.R. Dunn, and E.J. Robertson. 2001. Mouse embryos lacking Smad1 signals display defects in extra-embryonic tissues and germ cell formation. *Development* **128**: 3609-21.

Tsukazaki, T., T.A. Chiang, A.F. Davison, L. Attisano, and J.L. Wrana. 1998. SARA, a FYVE domain protein that recruits Smad2 to the TGFbeta receptor. *Cell* **95**: 779-91.

Tuli, R., S. Tuli, S. Nandi, X. Huang, P.A. Manner, W.J. Hozack, K.G. Danielson, D.J. Hall, and R.S. Tuan. 2003. Transforming growth factor-beta-mediated chondrogenesis of human mesenchymal progenitor cells involves N-cadherin and mitogen-activated protein kinase and Wnt signaling cross-talk. *J Biol Chem* **278**: 41227-36.

Umans, L., L. Vermeire, A. Francis, H. Chang, D. Huylebroeck, and A. Zwijsen. 2003. Generation of a floxed allele of Smad5 for cre-mediated conditional knockout in the mouse. *Genesis* **37**: 5-11.

Urist, M.R. 1965. Bone: formation by autoinduction. *Science* **150**: 893-9.

Verschueren, K., J.E. Remacle, C. Collart, H. Kraft, B.S. Baker, P. Tylzanowski, L. Nelles, G. Wuytens, M.T. Su, R. Bodmer, J.C. Smith, and D. Huylebroeck. 1999. SIP1, a novel zinc finger/homeodomain repressor, interacts with Smad proteins and binds to 5'-CACCT sequences in candidate target genes. *J Biol Chem* **274**: 20489-98.

Vikkula, M., M. Metsaranta, A.C. Syvanen, L. Ala-Kokko, E. Vuorio, and L. Peltonen. 1992. Structural analysis of the regulatory elements of the type-II procollagen gene. Conservation of promoter and first intron sequences between human and mouse. *Biochem J* **285 (Pt 1)**: 287-94.

von Bubnoff, A. and K.W. Cho. 2001. Intracellular BMP signaling regulation in vertebrates: pathway or network? *Dev Biol* **239**: 1-14.

von der Mark, K., T. Kirsch, A. Nerlich, A. Kuss, G. Weseloh, K. Gluckert, and H. Stoss. 1992. Type X collagen synthesis in human osteoarthritic cartilage. Indication of chondrocyte hypertrophy. *Arthritis Rheum* **35**: 806-11.

Wakefield, L.M., D.M. Smith, K.C. Flanders, and M.B. Sporn. 1988. Latent transforming growth factor-beta from human platelets. A high molecular weight complex containing precursor sequences. *J Biol Chem.* **263**: 7646–7654.

Walker, D.G. 1975a. Bone resorption restored in osteopetrotic mice by transplants of normal bone marrow and spleen cells. *Science*: 784-785.

-. 1975b. Spleen cells transmit osteopetrosis in mice. *Science* **190**.

Wan, M. and X. Cao. 2005. BMP signaling in skeletal development. *Biochem Biophys Res Commun* **328**: 651-7.

Warman, M.L., M. Abbott, S.S. Apte, T. Hefferon, I. McIntosh, D.H. Cohn, J.T. Hecht, B.R. Olsen, and C.A. Francomano. 1993. A type X collagen mutation causes Schmid metaphyseal chondrodysplasia. *Nat Genet* **5**: 79-82.

Watanabe, H., M.P. de Caestecker, and Y. Yamada. 2001. Transcriptional cross-talk between Smad, ERK1/2, and p38 mitogen-activated protein kinase pathways regulates transforming growth factor-beta-induced aggrecan gene expression in chondrogenic ATDC5 cells. *J Biol Chem* **276**: 14466-73.

Watanabe, M., N. Masuyama, M. Fukuda, and E. Nishida. 2000. Regulation of intracellular dynamics of Smad4 by its leucine-rich nuclear export signal. *EMBO Rep* **1**: 176-82.

Weinstein, M., X. Yang, C. Li, X. Xu, J. Gotay, and C.X. Deng. 1998. Failure of egg cylinder elongation and mesoderm induction in mouse embryos lacking the tumor suppressor smad2. *Proc Natl Acad Sci U S A* **95**: 9378-83.

West, A.G., M. Gaszner, and G. Felsenfeld. 2002. Insulators: many functions, many mechanisms. *Genes Dev* **16**: 271-88.

Wilkie, A.O., S.J. Patey, S.H. Kan, A.M. van den Ouweland, and B.C. Hamel. 2002. FGFs, their receptors, and human limb malformations: clinical and molecular correlations. *Am J Med Genet* **112**: 266-78.

Winnier, G., M. Blessing, P.A. Labosky, and B.L. Hogan. 1995. Bone morphogenetic protein-4 is required for mesoderm formation and patterning in the mouse. *Genes Dev* **9**: 2105-16.

Wotton, D., R.S. Lo, S. Lee, and J. Massague. 1999. A Smad transcriptional corepressor. *Cell* **97**: 29-39.

Wrana, J.L. 2000. Regulation of Smad activity. *Cell* **100**: 189-92.

Wu, J.W., M. Hu, J. Chai, J. Seoane, M. Huse, C. Li, D.J. Rigotti, S. Kyin, T.W. Muir, R. Fairman, J. Massague, and Y. Shi. 2001. Crystal structure of a phosphorylated Smad2. Recognition of phosphoserine by the MH2 domain and insights on Smad function in TGF-beta signaling. *Mol Cell* **8**: 1277-89.

Wu, J.W., A.R. Krawitz, J. Chai, W. Li, F. Zhang, K. Luo, and Y. Shi. 2002. Structural mechanism of Smad4 recognition by the nuclear oncoprotein Ski: insights on Ski-mediated repression of TGF-beta signaling. *Cell* **111**: 357-67.

Yamaguchi, K., S. Nagai, J. Ninomiya-Tsuji, M. Nishita, K. Tamai, K. Irie, N. Ueno, E. Nishida, H. Shibuya, and K. Matsumoto. 1999. XIAP, a cellular member of the inhibitor of apoptosis protein family, links the receptors to TAB1-TAK1 in the BMP signaling pathway. *Embo J* **18**: 179-87.

Yang, G., F. Cui, N. Hou, X. Cheng, J. Zhang, Y. Wang, N. Jiang, X. Gao, and X. Yang. 2005. Transgenic mice that express Cre recombinase in hypertrophic chondrocytes. *Genesis* **42**: 33-6.

Yi, S.E., A. Daluiski, R. Pederson, V. Rosen, and K.M. Lyons. 2000. The type I BMP receptor BMPRIB is required for chondrogenesis in the mouse limb. *Development* **127**: 621-30.

Yoon, B.S. and K.M. Lyons. 2004. Multiple functions of BMPs in chondrogenesis. *J Cell Biochem* **93**: 93-103.

Yoon, B.S., D.A. Ovchinnikov, I. Yoshii, Y. Mishina, R.R. Behringer, and K.M. Lyons. 2005. Bmpr1a and Bmpr1b have overlapping functions and are essential for chondrogenesis in vivo. *Proc Natl Acad Sci U S A* **102**: 5062-7.

Yoon, B.S., R. Pogue, D.A. Ovchinnikov, I. Yoshii, Y. Mishina, R.R. Behringer, and K.M. Lyons. 2006. BMPs regulate multiple aspects of growth-plate chondrogenesis through opposing actions on FGF pathways. *Development*.

Zhang, D., E.M. Schwarz, R.N. Rosier, M.J. Zuscik, J.E. Puzas, and R.J. O'Keefe. 2003. ALK2 functions as a BMP type I receptor and induces Indian hedgehog in chondrocytes during skeletal development. *J Bone Miner Res* **18**: 1593-604.

Zhang, H. and A. Bradley. 1996. Mice deficient for BMP2 are nonviable and have defects in amnion/chorion and cardiac development. *Development* **122**: 2977-86.

Zhang, R., S. Murakami, F. Coustry, Y. Wang, and B. de Crombrugghe. 2006. Constitutive activation of MKK6 in chondrocytes of transgenic mice inhibits proliferation and delays endochondral bone formation. *Proc Natl Acad Sci U S A* **103**: 365-70.

Zheng, Q., G. Zhou, R. Morello, Y. Chen, X. Garcia-Rojas, and B. Lee. 2003. Type X collagen gene regulation by Runx2 contributes directly to its hypertrophic chondrocyte-specific expression in vivo. *J Cell Biol* **162**: 833-42.

Zhou, G., S. Garofalo, K. Mukhopadhyay, V. Lefebvre, C.N. Smith, H. Eberspaecher, and B. de Crombrugghe. 1995. A 182 bp fragment of the mouse pro alpha 1(II) collagen gene is sufficient to direct chondrocyte expression in transgenic mice. *J Cell Sci* **108 (Pt 12)**: 3677-84.

Zhou, G., V. Lefebvre, Z. Zhang, H. Eberspaecher, and B. de Crombrugghe. 1998. Three high mobility group-like sequences within a 48-base pair enhancer of the Col2a1 gene are required for cartilage-specific expression in vivo. *J Biol Chem* **273**: 14989-97.

Zhu, H., P. Kavsak, S. Abdollah, J.L. Wrana, and G.H. Thomsen. 1999. A SMAD ubiquitin ligase targets the BMP pathway and affects embryonic pattern formation. *Nature* **400**: 687-93.

Zou, H., R. Wieser, J. Massague, and L. Niswander. 1997. Distinct roles of type I bone morphogenetic protein receptors in the formation and differentiation of cartilage. *Genes Dev* **11**: 2191-203.

Zufferey, R., J.E. Donello, D. Trono, and T.J. Hope. 1999. Woodchuck hepatitis virus posttranscriptional regulatory element enhances expression of transgenes delivered by retroviral vectors. *J Virol* **73**: 2886-92.

Zuzarte-Luis, V., J.A. Montero, J. Rodriguez-Leon, R. Merino, J.C. Rodriguez-Rey, and J.M. Hurle. 2004. A new role for BMP5 during limb development acting through the synergic activation of Smad and MAPK pathways. *Dev Biol* **272**: 39-52.

7 Acknowledgments

8 Appendix

8.1 Abbreviations

#	number
A	Adenin
abs	absolute
Ac	acetate
AER	apical ectodermal ridge
bp	base pair
BMP	Bone morphogenetic proteins
BSA	bovine serum albumin
C	cytosine
ºC	degree Celsius
cDNA	complementary DNA
CEN	centromere on episomal plasmid
Ci	Curie
Co-Smad	common partner Smad
dATP	deoxyadenosine triphosphate
dCTP	deoxycytidine triphosphate
dGTP	deoxyguanosine triphosphate
dNTPs	deoxynucleotide triphosphates
	(a mixture of dATP, dTTP, dCTP, dGTP 1:1:1:1)
DNA	deoxynucleic acid
dpc	days post conception
DTT	dithiothritol
dTTP	deoxytymidine triphosphate
E	embryonic day (of embryonic mouse development)
E. coli	*Escherichia coli*
EDTA	ethylenediamine tetracetic acid
e.g.	exempli gratia (for example)
EtOH	ethanol
FGF	*Fibroblast Growth Factor*

g	acceleration of gravity
G	guanine
h	hour
H & E	Hematoxylin and Eosin
hrs	hours
Ihh	*Indian hedgehog*
I-Smad	inhibitory Smad
ko	knockout
LB-medium	Luria-Bertani medium
Lmx1b	*LIM homeobox gene 1 b*
µ	micro
M	molar
MCDS	Metaphyseal Chondrodysplasia type Schmid
MEM	minimal essential medium
min	minute(s)
miRNA	micro RNA
ml	mililiter
MTN	multiple tissue Northern Blot
n	nano
NCBI	National Center for Biotechnology Information
NLS	nuclear localization signal
NTE	sodium-tris-EDTA buffer
OD	optical density
ORF	open reading frame
PAA	polyacrylamide
PBS	phosphate buffered saline
PCR	polymerase chain reaction
PFA	paraformaldehyde
PNK	polynucleotide kinase
PZ	progress zone
RNA	ribonucleic acid
rpm	revolutions per minute
R-Smad	receptor-related Smad
rt	room temperature

RT-PCR	reverse transcriptase polymerase chain reaction
Runx2	*Runt homoebox gene 2*
s	second(s)
SMCD	Schmid metaphyseal chondrodysplasia
SD	standard deviation
SDS	sodium dodecyl sulfate
Shh	*Sonic hedgehog*
SNP	single nucleotide polymorphism
SSC	standard-saline-citrate buffer
T	thymine
Tab	Table
TAE	tris-acetic-EDTA buffer
Taq	Thermophilus aquaticus DNA polymerase I
TBE	tris-borate-EDTA buffer
TE	tris-EDTA buffer
TEMED	N,N,N',N'-tetramethylethylendiamine
TGFβ	*Transforming growth factor β*
Tris	Tris(hydoxymethyle)aminomethane
U	units
USA	United States of America
UTR	untranslated region
vs.	versus
wt	wild type
X-gal	5-bromo-4-chloro-indolyl-β-D-galactoside
ZPA	zone of polarizing activity

8.2 Curriculum vitae

8.3 Publications

Poster presentations:

Characterization of cis elements and transcriptional determinants that confer tissue-specific expression of type X collagen gene during chondrogenesis in vivo. Q. Zheng, G. Zhou, R. Morello, D. Napierala, Y. Chen, B. Keller, X. Garcia-Rojas, and B. Lee. ASHG 53th annual meeting, Los Angeles, California, November 4 - 8, 2003

Identification of the Tissue-specific Enancer Element Responsible for Mouse TypeX Collagen Gene Expression *In vivo*. Q. Zheng, B. Keller, G. Zhou, D. Napierala, Y. Chen, A. Parker, and B. Lee. ASHG 54th annual meeting, Toronto, Canada, October 26 – 30, 2004

Generation of a mouse model to analyze the role of Adamts-5 in the pathogenesis of Osteoarthritis. J. Busch, C. Spangenberg, B. Keller, B. Lee, B. Zabel and C. Stelzer. OASI 9th annual world conference. Chicago, Illinois, December 02 – 05, 2004

A 300 bp of mouse Col10A1 distal promoter element is sufficient to mediate its high-level tissue-Specific expression in hypertrophic chondrocytes *in vivo*. Q. Zheng, B. Keller, G. Zhou, D. Napierala, Y. Chen, A. Parker and B. Lee.
ASBMR 27th annual meeting, Nashville, Tennessee, September 23 - 27, 2005

E-Selectin Ligand 1 Negatively Regulates TGFβ in the Golgi during Skeletogenesis.
T. Yang, R. Mendoza-Londono, H. Lu, K. Li, B. Keller, M. Jiang, Y. Chen, B. Dabovic, D. B. Rifkin, J. Hicks, A. L. Beaudet, B. Lee.
ASBMR 28th annual meeting, Philadelphia, Pennsylvania, September 15 - 19, 2006

Tissue-specific Expression of Type X Collagen in Hypertrophic Chondrocytes is Specified by a 150 bp *Col10a1* Distal Promoter Element. Q. Zheng, B. Keller, G. Zhou, D. Napierala, Y. Chen, A. Parker, and B. Lee.
ASHG 56th annual meeting, New Orleans, Louisiana, October, 9-13, 2006
ASBMR 28th annual meeting, Philadelphia, Pennsylvania, September 15 - 19, 2006

Redundant function of Smad1 and Smad5 during chondrogenesis. B. Keller, P. Hermanns, B. Zabel and B. Lee. ASHG 56th annual meeting, New Orleans, Louisiana, October, 9-13, 2006

Oral presentations

Identification of the Tissue-specific Enhancer Element Responsible for Mouse Type X Collagen Gene Expression *In vivo.* Q. Zheng, B. Keller, G. Zhou, D. Napierala, Y. Chen, A. Parker, and B. Lee.
ASBMR 26th annual meeting, Seattle, Washington, October 1 – 5, 2004